Trinity College Dublin
Coláiste na Tríonóide, Baile Átha Cliath
The University of Dublin

# REGULATION OF BOVINE β-DEFENSIN EXPRESSION

**THIS THESIS IS SUBMITTED TO THE UNIVERSITY OF DUBLIN FOR THE DEGREE OF DOCTOR OF PHILOSOPHY**

**2017**

**ANNE BARRY-REIDY**

**SCHOOL OF BIOCHEMISTRY & IMMUNOLOGY**

**TRINITY COLLEGE DUBLIN**

**SUPERVISORS: PROF. CLIONA O'FARRELLY & DR. KIERAN MEADE**

# TABLE OF CONTENTS

## DECLARATION

I declare that this thesis has not been submitted as an exercise for a degree at this or any other university and it is entirely my own work, except where stated:

- Estrus cycle staging of female reproductive tracts collected for β-defensin quantitative PCR within individual tissues:

  Dr Aspinas Chapwanya, Department of Clinical Sciences, Ross University, Basseterre, St. Kitts, West Indies.

- Quantitative PCR for BoHV-1 and BoHV-4 DNA within endometrial tissue samples used for primary stromal cell isolation:

  Dr. Eoin Ryan and staff at the Virology Division, DAFM Central Veterinary Research Laboratory, Backweston, Co. Kildare.

I agree to deposit this thesis in the University's open access institutional repository or allow the library to do so on my behalf, subject to Irish copyright legislation and Trinity College Library conditions of use and acknowledgement.

_____

Anne Barry-Reidy

August 2017

## ACKNOWLEDGEMENTS

Firstly, I would like to thank my academic supervisors. Thanks to Cliona O'Farrelly for believing in me and for bringing such imagination and energy to the project. Thanks to Kieran Meade for matching that with never-ending focus and persistence.

To the β-defensin grant collaborators- Pat Lonergan, Sean Fair and Emma Finlay: thanks for sitting through all those meetings and for having an interest in all that immunology and bioinformatics! Ronan and Bea- It was fantastic to have you both going through the whole process side-by-side with me and your support was so valuable. Fernando- I couldn't have inherited the β-defensin project mantle from a more knowledgeable, diligent and helpful person. My sincerest thanks to all the staff at Kildare Chilling Factory, especially Robert Walsh and Paul Delaney. This project wouldn't have been possible without you welcoming us in week after week and constantly going above and beyond to help with such patience and good humour. Thanks to Aspinas Chapwanya and Eoin Ryan for being so helpful with the relevant technical aspects of the project. To my Team Bovine endometrial cell buddies- thanks Amy for being a calm counterpoint to all the COF lab wackiness and giant thanks to Paul for keeping it all going and keeping me sane. Mag- you keep the show on the road every day and have always been willing to lend an ear, we would all be lost without you. To all the past and present members of the O'Farrelly and Meade labs- the lunchtimes, chats, laughter, trips to Tesco/Kennedys/for donuts are so deeply appreciated. Thanks to the Bowie lab for technical (and life) advice and to the Sheedy lab for bringing the banter. I would also like to acknowledge the Walsh Fellowship Programme and the Department of Agriculture, Food and the Marine for funding my stipend and consumables respectively.

Lots of kind and patient people out in the real world kept me motivated, made me laugh and picked me up when I needed picking up. Thank you, thank you, thank you, your support has meant more than I can say.

## ABBREVIATIONS

| | |
|---|---|
| 1,25D | 1α,25-dihydroxyvitamin D3 |
| 25D | 25-hydroxyvitamin D2 |
| AMP | Antimicrobial peptide |
| AP-1 | Activator protein 1 |
| AP-2 | Activating enhancer-binding protein 2 |
| AR | Androgen receptor |
| AUC | Area under the curve |
| BSA | Bovine serum albumin |
| CCL | Chemokine (c-c motif) ligand |
| CD | Cluster of differentiation |
| CDXA | Caudal-related homeobox protein |
| CE | Cytological endometritis |
| CEBPD | CCAAT enhancer binding protein delta |
| cGAS | Cyclic guanosine monophosphate-adenosine monophosphate synthase |
| ChIP-Seq | Chromatin-immunoprecipitation sequencing |
| CREB | Cyclic adenosine monophosphate response element binding protein |
| CRM | Cis-regulatory module |
| CTCF | CCCTC-binding factor |
| CYP | Cytochrome P450 |
| DAMP | Danger-associated molecular patterns |
| DC | Dendritic cell |
| DPP | Days post-partum |
| EBD | Enteric β-defensin |
| ECR | Evolutionarily-conserved region |
| EN1 | Homeobox protein engrailed 1 |
| ERABP | Epididymal retinoic acid binding protein |
| ERK | Extracellular regulated protein kinase |

| | |
|---|---|
| Ets | E twenty-six |
| FRT | Female reproductive tract |
| GM-CSF | Granulocyte macrophage colony-stimulating factor |
| GR | Glucocorticoid receptor |
| HBD | Human β-defensin |
| HB-EGF | Heparin-binding EGF-like growth factor |
| HBSS | Hank's balanced salt solution |
| HDAC | Histone deacetylase |
| HDP | Host defence peptide |
| HIF1α | Hypoxia inducible factor |
| HNF1β | Hepatocyte nuclear factor 1β |
| HNF4 | Hepatocyte nuclear factor |
| HNP | Human neutrophil peptide |
| HPV16 | Human papilloma virus |
| HSV1 | Herpes simplex virus 1 |
| IFI | Interferon-inducible |
| IFNAR | Interferon-α/β receptor |
| IL | Interleukin |
| iNOS | Inducible nitric oxide synthase |
| INSM1 | Insulinoma-associated protein 1 |
| IRF | Interferon regulatory factor |
| ISG | Interferon-stimulated gene |
| ITS-X | Insulin, transferrin, selenium supplement with ethanolamine |
| IκB-α | Nuclear factor of kappa light polypeptide gene enhancer in B-cells inhibitor, alpha |
| JDP | Jun dimerization protein |
| JNK | c-Jun N-terminal kinase |
| KLF7 | Krüppel-like factor 7 |
| LAP | Lingual antimicrobial peptide |
| LCN5 | Lipocalin 5 |

| | |
|---|---|
| LXRα-RXRα | Liver X receptor α- retinoid X receptor α heterodimer |
| MAPK | Mitogen-activated protein kinase |
| MAVS | Mitochondrion-associated antiviral signalling protein |
| MCP | Monocyte chemoattractant protein |
| MDA5 | Melanoma differentiation-associated protein 5 |
| mDC | Myeloid dendritic cell |
| MEF | Myeloid ELF-like factor |
| miRNA | Micro RNA |
| MSX | Msh homeobox |
| NCBI | National Center for Biotechnology Information |
| NFAT | Nuclear factor of activated T cells |
| NFIL3 | Nuclear factor interleukin 3 regulated protein |
| NF-κB | Nuclear factor kappa-light-chain-enhancer of activated B cells |
| NOD2 | Nucleotide oligomerization domain 2 |
| OSR | Odd-skipped related |
| PAX | Paired box |
| PBM | Protein-binding microarray |
| PBMC | Peripheral blood mononuclear cell |
| PBS | Phosphate-buffered saline |
| PCR | Polymerase chain reaction |
| pDC | Plasmacytoid dendritic cell |
| PMN | Polymorphonuclear cells |
| PTPRC | Protein tyrosine phosphatase, receptor type C |
| PWM | Position-weight matrix |
| RAR | Retinoic acid receptor |
| RARα | Retinoic acid receptor α |
| REST | RE1-silencing transcription factor |
| RFX | Regulatory factor X |
| RIG-I | Retinoic acid inducible gene I |

| | |
|---|---|
| RLR | RIG-like receptor |
| ROC | Receiver operating characteristic |
| RPMI | Roswell Park Memorial Institute medium |
| RSV | Respiratory syncytial virus |
| RXR | Retinoid X receptor |
| RXRα | Retinoid X receptor α |
| SLPI | Secretory leukocyte protease inhibitor |
| SOX | SRY-related HMG box |
| SP | Specificity protein |
| SPZ1 | Spermatogenic leucine zipper 1 |
| SREBF1 | Sterol regulatory element binding transcription factor 1 |
| SRF | Serum response factor |
| STAT | Signal transducer and activator of transcription |
| STING | Stimulator of interferon genes |
| T3Rα | Thyroid hormone receptor α |
| TAP | Tracheal antimicrobial peptide |
| TBP | TATA-binding protein |
| TCF3 | Transcription factor 3 |
| TEAD | Transcriptional enhancer factor |
| TF | Transcription factor |
| TFBS | Transcription factor binding site |
| TIMP | Tissue inhibitor of metalloproteinase |
| TNFα | Tumour necrosis factor α |
| TRAF | Tumour necrosis factor receptor-associated factor |
| VDR | Vitamin D receptor |
| VDRE | Vitamin D response element |
| ZBTB | Zinc finger and BTB domain-containing protein |
| ZFP | Zinc finger protein |
| ZSCAN4 | Zinc finger and SCAN domain-containing protein 4 |

## LIST OF FIGURES

CHAPTER 1



CHAPTER 2



CHAPTER 3

CHAPTER 4

CHAPTER 5



APPENDICES

## LIST OF TABLES

CHAPTER 5



APPENDICES

## ABSTRACT

β-defensins are a class of host defence peptides with antibacterial, antiviral and immunomodulatory roles. The bovine genome contains up to 57 putative β-defensin genes in four syntenic clusters on different chromosomes. The regulation of expression of these pleiotropic molecules is still poorly explored. As β-defensins are involved in bovine fertility, the overall aim of this project was to investigate the regulation of expression of β-defensins in this context.

We have bioinformatically analysed the proximal promoter regions of chromosome 13 β-defensin genes from the bovine and other mammals to identify potential regulators of gene transcription for further investigation. Transcription factor binding site over-representation analysis of a β-defensin cluster which is highly expressed in the male reproductive tract indicates enrichment of DNA binding sites for transcription factors important in regulating gene expression at this site. These include androgen receptor, glucocorticoid receptor and retinoic acid receptor. Alignment of over 300kb of this β-defensin gene region from five distantly-related mammals highlighted three putative intergenic enhancers within the cluster. A candidate enhancer proximal to *DEFB126*, which is associated with male fertility, contains binding sites for androgen receptor and AP-2α, a chromatin-opening transcription factor known to co-operate with androgen receptor in the murine epididymis. We hypothesise that these potential enhancers may act as distal regulatory elements to control expression of one or more male reproductive tract-specific β-defensins.

β-defensin 3, encoded by the gene *DEFB103*, has been attributed roles in direct antimicrobial defence, immunomodulation and wound healing. As this gene is associated with an inflammatory gene signature in the post-partum bovine uterus, in which endometritis is both prevalent and economically important, we were interested in identifying stimuli driving *DEFB103* expression. Application of our transcription factor binding site over-representation approach to the promoters of *DEFB103* orthologs indicates AP-1 regulation of this gene at the transcriptional level. AP-1 mediates the response to a number of inflammatory stimuli and regulates *DEFB103* in some human cell types. Therefore we investigated inflammation-driven β-defensin expression in a bovine reproductive tract-derived primary cell culture model. Cultured primary endometrial stromal cells isolated from reproductive tracts of recently slaughtered cows constitutively

express *DEFB103*. A primer set targeting the ruminant expansion of *DEFB4A* (e*DEFB4A*), consisting of eight chromosome 27 β-defensins with high sequence similarity, revealed expression of at least one of these genes in stromal cells. As IL-1β and IL-17A are implicated as drivers of human β-defensin expression, they were used to stimulate bovine endometrial stromal cells. IL-1β upregulated expression of *DEFB103* and e*DEFB4A*. IL-17A also upregulates *DEFB103*. Upregulation of β-defensins by pro-inflammatory cytokines may be an important link between post-partum inflammation and β-defensin expression.

Viral infection of the cow reproductive tract contributes to prolonged post-partum inflammation, with associated economic and welfare implications. Here, we profile nucleic acid-mediated β-defensin expression in endometrial stromal cells. The dsRNA molecule poly(I:C) upregulates *DEFB103* (*n*=6; p=0.0041), while e*DEFB4A* is downregulated (p=0.0139). Similarly, poly(dA:dT) is a synthetic dsDNA analog which upregulates transcription of *DEFB103* (*n*=6; p=0.0001) but not e*DEFB4A*. Thus, viral infection may prolong inflammation in the post-partum uterus.

As a dietary hormone with the ability to modulate HDP expression, 1,25-dihydroxyvitamin D (1,25D) is a candidate therapeutic immunomodulator. In the endometrial stromal cell model, 1,25D induces expression of e*DEFB4A* (*n*=6; 25.51±11.48 fold, p=0.0005). To investigate whether 1,25D could modulate the viral-mediated differential regulation of β-defensins, stromal cells were stimulated with viral ligands in the presence of 1,25D. 1,25D blunts poly(dA:dT)-induced *DEFB103* expression. Conversely, 1,25D reverses poly(I:C)-mediated downregulation of e*DEFB4A*.

In conclusion, we have used computational and primary cell culture techniques to identify multiple potential regulatory mechanisms driving fertility-related β-defensin expression. As stromal cells of the endometrium experience both systemic inflammatory signals and local infection, induction of these pleiotropic β-defensins in response to such stimuli may be a key driver of pathological inflammation in the post-partum uterus. In addition, hormonally-active vitamin D can modulate β-defensin expression, which is of potential therapeutic relevance in the context of endometritis.

# Chapter 1 Introduction

## 1.1 Antimicrobial/Host-defence peptides

Antimicrobial peptides (AMPs) are a large and diverse group of short amphipathic peptides, less than 100 amino acids in length (Lehrer and Ganz, 1999; Mansour et al., 2014). First discovered in cereal plants (De Caleya et al., 1972), the existence of AMPs in animal species was confirmed by two separate lines of enquiry. The isolation of bacteria-lysing peptides called cecropins from insect hemolymph (Hultmark et al., 1980) was followed by the discovery that granulocytes from the peritoneal exudates of rabbits injected with *E. coli* contain cationic peptides with bactericidal activity against several strains of bacteria (Selsted et al., 1984).

In the intervening years, more than 1200 AMPs have been discovered in diverse species from insects to humans, molluscs to cattle (Steinstraesser et al., 2011). In addition to the originally described antimicrobial activity, many of these peptides have immunoregulatory roles, with chemoattraction, adjuvant properties, modulation of tumour immunity and wound healing properties having also been demonstrated (Steinstraesser et al., 2011). This has led to the renaming of the group as host-defence peptides (HDPs) (Hancock and Sahl, 2006). Due to their prevalence in the human, mouse and important agricultural species such as the bovine and chicken, particular focus has been dedicated to a group of HDPs named defensins.

## 1.2 Defensins

The isolation of AMPs from the granulocytes of rabbits was closely followed by similar work on human neutrophils. Three peptides, named human neutrophil peptides (HNP) 1-3, were extracted and formally classified as defensins due to their antimicrobial activity against *P. aeruginosa*, *E. coli*, *S. aureus* and herpes simplex virus 1 (HSV1) (Selsted et al., 1985). The first bovine defensin was isolated from the trachea (Diamond

et al., 1991). Named tracheal antimicrobial peptide (TAP), it contains six cysteine residues which form three disulfide bonds. The length, cationic nature and antimicrobial activity led the authors to conclude this peptide belonged to the antimicrobial peptide family. Particularly, it was most similar to the defensins identified by that point. However TAP did not share the high level of sequence similarity and canonical cysteine spacing observed among the other defensins. It is now known that there are three classes of defensins, with the HNPs being α-defensins and TAP being the first β-defensin to be characterised.

The three classes of defensins share several properties. All are less than 60 amino acids in length and have a net cationic charge. Six cysteine residues form three disulfide bonds, leading to a β-sheet secondary structure (Selsted and Ouellette, 2005). All defensins are initially synthesised as a prepropeptide, consisting of a conserved signal sequence which is removed to leave a propeptide, which is in turn enzymatically cleaved to leave an active mature peptide (Wilson et al., 1999), which is generally the most variable in amino acid sequence.

The three groups can be distinguished by their secondary structure and cysteine pairing (Figure 1.1). α-defensins are characterised by disulfide bonding between cysteines 1-6, 2-4 and 3-5. While these peptides first evolved before the split between marsupials and placental mammals (Lynn and Bradley, 2007), the group was subsequently lost in several mammalian lineages. The horse is the only Laurasiatherian species currently known to have functional α-defensins (Bruhn et al., 2009). Humans have five α-defensin genes (Lehrer and Lu, 2012). Four are expressed exclusively by polymorphonuclear cells (PMN) while the other is expressed by the Paneth cells within intestinal crypts and by various epithelial cells (Zasloff, 2002). *In silico* analysis of the bovine genome indicates α-defensins have been lost from this lineage (Fjell et al., 2008).

θ-defensins have a homodimeric structure formed from natural backbone cyclisation of α-defensin-like peptides (Tang et al., 1999). They are found only in non-human primates (Lehrer and Lu, 2012).

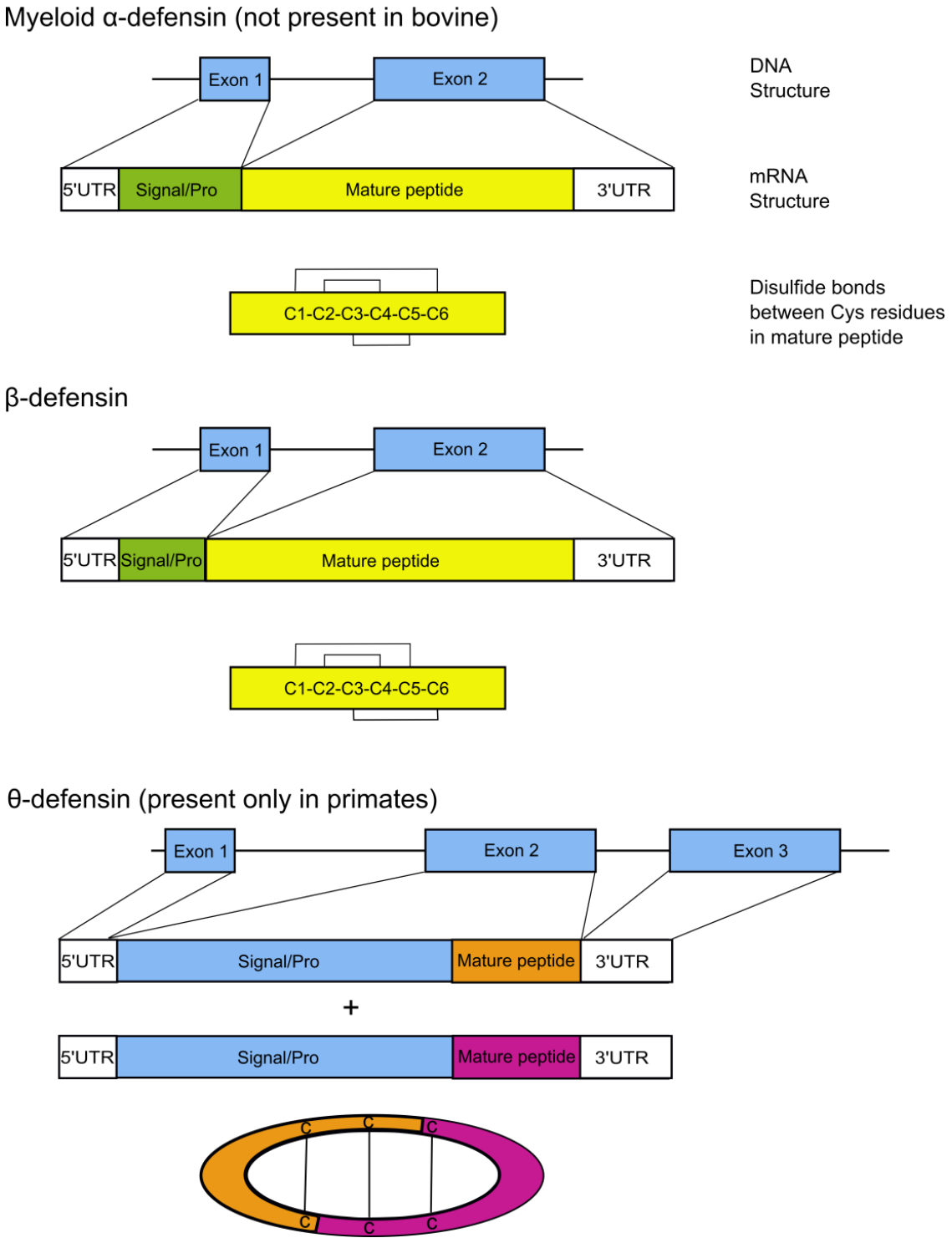


**Figure 1.1 DNA, mRNA and peptide structure of mammalian defensins.**
Defensin genes consist of 2-3 exons, coding for a peptide with a signal sequence, pro-peptide and mature peptide which is released by enzymatic cleavage. All defensins contain 6 conserved cysteines, the disulfide boding pattern between which defines the classes. θ-defensins, which exist only in primates, form homodimers which are stabilised by disulfide bonds. Bovines and most other Laurasiatherian species do not have α-defensin genes. Modified from (Selsted and Ouellette, 2005).

## 1.3 β-defensins

β-defensins are characterised by a 1-5, 2-4 and 3-6 disulfide bonding of conserved cysteine residues (Selsted et al., 1993). Present in teleost fish (Zou et al., 2007) and birds (van Dijk et al., 2008), β-defensins are the most ancient group of defensins, being the prototype defensin molecule from which the other classes subsequently evolved (Liu et al., 1997). The β-defensin repertoire is spread across four gene clusters, each located on a different chromosome (Figure 1.2) (Patil, 2005; reviewed in Meade et al., 2013). Bioinformatics analysis conducted by our group indicates the bovine genome contains an expanded repertoire of up to 57 β-defensin genes (Cormican et al., 2008), though the annotation and exact number of β-defensin genes in the human and particularly the bovine genome differs between genome assemblies.

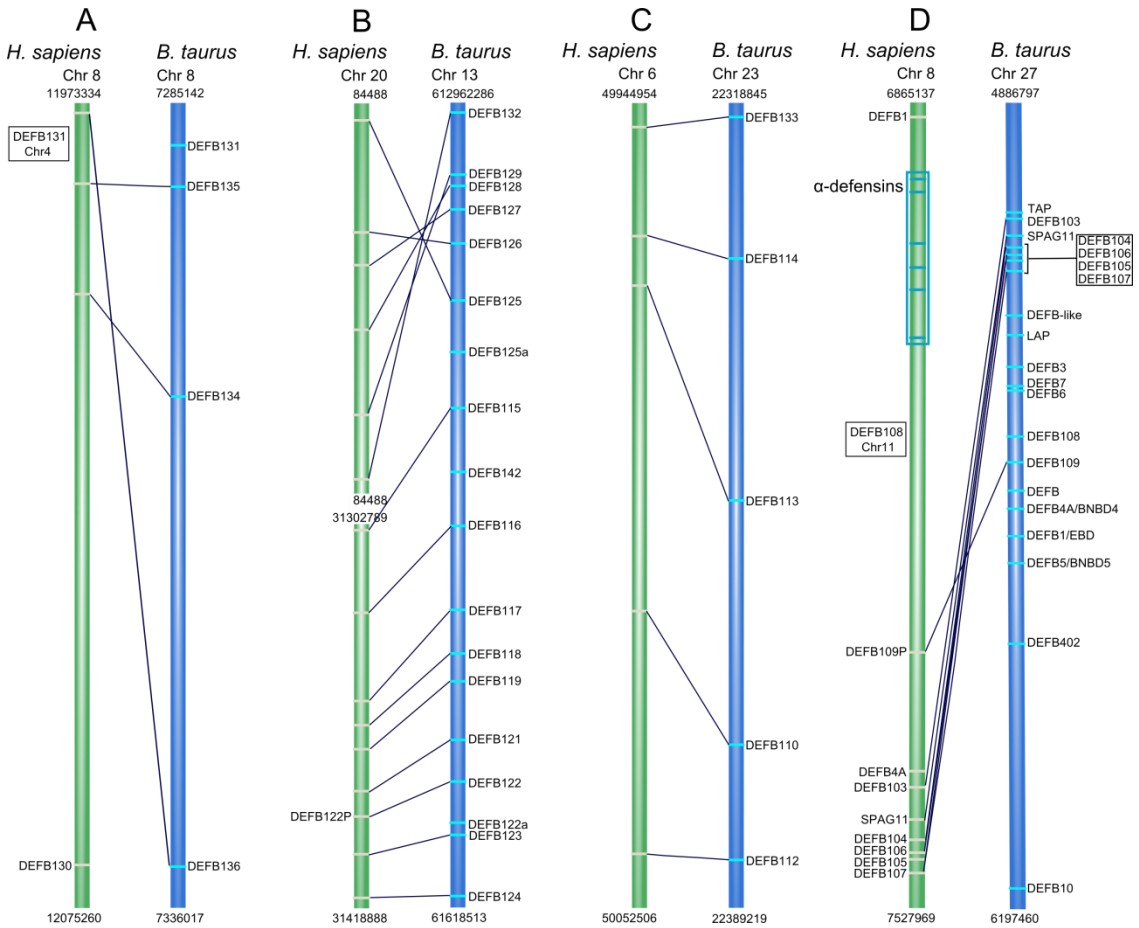


**Figure 1.2 Syntenic map of β-defensin genes in the bovine and human genomes.**
β-defensins are located in four clusters, each found on a different chromosome in the bovine, with clusters A and D both on chromosome 8 in the human genome. Human genes *DEFB108* and *DEFB131* are located on separate chromosomes as indicated. Joining lines indicate orthology, i.e., two genes which have been separated by a speciation event. The numbers at the top and bottom are chromosomal co-ordinates. The total gene number on bovine chromosome 27 is controversial and differs between genome assemblies. Only genes with two complete exons in the most recent bovine genome assembly (UMD3.1.1/BosTau8) are annotated here. The human genome assembly used was hg38. P indicates a gene is pseudogenised.

β-defensins from syntenic cluster D are expressed by non-immune cells throughout the mammalian body (Jarczak et al., 2013). They are also expressed by granulocytes in species without α-defensins, including bovine (Selsted et al., 1993). In contrast, the genes located in syntenic cluster B are predominantly or solely expressed in the male reproductive tract (Com et al., 2003; Narciandi et al., 2011; Rodríguez-Jiménez et al., 2003). Little is known about the expression pattern or function of the genes in syntenic clusters A and C.

Expression of β-defensin genes can be constitutive or inducible. Human β-defensin (hBD) 1, the peptide encoded by the gene *DEFB1*, is constitutively expressed by epithelial cells of the colon and other organs but is not upregulated in colonic epithelial

cell lines infected with *Salmonella* (O'Neil et al., 1999). Conversely, *DEFB4A*, encoding hBD-2 peptide, is not constitutively expressed by the same cell lines but is upregulated by *Salmonella* exposure through nuclear factor kappa-light-chain-enhancer of activated B cells (NF-κB) binding to the *DEFB4A* promoter. Similarly, hBD-2 levels are massively increased in keratinocytes from psoriatic lesions relative to those from healthy skin. Tumour necrosis factor α (TNFα) treatment increases hBD-2, but not hBD-1 secretion from keratinocytes (Harder et al., 1997). *DEFB103* is constitutively expressed in a number of human tissues, particularly the skin, trachea and tonsils, but is also induced by bacterial stimulation of keratinocytes and bronchial epithelial cells (Harder et al., 2001).

### 1.3.1 Antimicrobial properties

An extensive body of work has demonstrated many β-defensins possess direct antimicrobial effector abilities. As is to be expected from its microbially-induced expression pattern, hBD-2 has been implicated as an important component of the immune response in several disease models. hBD-2 produced by keratinocytes from psoriatic lesions is active against *Candida albicans* and *Staphylococcus aureus* (Harder et al., 1997). hBD-2 peptide is also detectable in bronchoalveolar lavage fluid and exhibits potent antimicrobial activity against the cystic fibrosis-associated pathogen *Pseudomonas aeruginosa* (Singh et al., 1998). In addition, hBD-2 is expressed by human extraplacental membranes, where it kills *Streptococcus spp*. associated with neonatal sepsis (Boldenow et al., 2013). hBD-1 (Schroeder et al., 2011) hBD-3 (Harder et al., 2001), hBD-4 (García et al., 2001b) and hBD-6 (Xin et al., 2014) all have antimicrobial activity against a variety of pathogens.

The human β-defensin 2 gene has several bovine orthologs. Phylogenetic analysis by our group indicates at least ten bovine β-defensin genes are more similar in sequence to canine β-defensin 2 then they are to the most closely-related bovine paralog (Meade et al., 2013). Selsted et al. (1993) have shown that bovine granulocytes contain up to 13 different peptides with highly similar amino acid sequence which would fall within this group. Each of these peptides inhibits the growth of *S. aureus* and *E. coli* in radial diffusion assays. TAP and the highly similar lingual antimicrobial peptide (LAP), also

fall within this phylogenetic group and are antimicrobial against a variety of bacterial and fungal species (Diamond et al., 1991; Schonwetter et al., 1995; Tomasinsig et al., 2012).

Several male reproductive tract-specific β-defensins have demonstrable antimicrobial activity. Survival of *S. aureus*, *E.coli* and *C. albicans* is reduced by 20-100μg/mL human DEFB126 peptide (Liu et al., 2013). Human DEFB114 is predominantly expressed in the epididymis and has microbicidal capability towards the same species (Yu et al., 2013). Our group has shown that bovine DEFB123 exhibits antimicrobial activity against several Gram-negative and Gram-positive bacteria (Cormican et al., 2008), while DEFB118 is active against *E.coli* (Yenugu et al., 2004).

The antimicrobial potential of β-defensins is dependent on a number of factors. Antimicrobial activity is highly pathogen strain selective, with the minimum inhibitory concentration for two strains of the same species differing by up to two orders of magnitude within the μg/mL range. This indicates that different cell membrane compositions or virulence factors modulate β-defensin effectiveness. Broadly, hBD-2 and hBD-3 are more highly antimicrobial against aerobes than anaerobes in an *in vitro* setting in which the antimicrobial assay is carried out under oxygen concentrations appropriate for each group (Joly et al., 2004). The disulfide bridges have been shown to be essential in some experiments (Schroeder et al., 2011), but not others (Wu et al., 2003).

However, a variety of environmental factors modulate the antimicrobial potential of these molecules *in vivo*. Reduction of hBD-1 vastly improves antimicrobial activity, indicating this peptide may be much more potent under the low oxygen conditions within the large intestine, where *DEFB1* is highly expressed (Schroeder et al., 2011). In contrast, physiological salt concentrations attenuate the antimicrobial activity of most β-defensins (e.g. Veldhuizen et al., 2008). The μg/mL concentrations needed for antimicrobial activity *in vitro* are likely only achieved *in vivo* in selected situations, such as at the bottom of intestinal crypts or immediately after leukocyte degranulation (Hancock et al., 2016). Nevertheless, β-defensin expression is associated with *in vivo* defence. Reduced *DEFB1* and *DEFB103* expression in human skin increases the likelihood of persistent *S. aureus* nasal carriage (Nurjadi et al., 2013).

A variety of mechanisms have been proposed to explain the antimicrobial action of β-defensins and other HDPs. The earliest of these are reviewed by Brodgen et al.,

(2005) and suggest the peptides form pores in the bacterial membrane. More recent research points to disruption of a host of essential macromolecule synthesis and trafficking functions. hBD-2 interacts with the cell wall of *Enterococcus faecalis* at discrete anionic lipid microdomains, disrupting the localisation of proteins which are key to the proper secretion and extracellular attachment of virulence factors (Kandaswamy et al., 2013). Sass et al (2010) have used *in vitro* preparations of bacterial cell walls to investigate the effect of hBD-3 on cell wall biosynthesis. Enzymatic reactions which use localised domains of lipid II as a substrate are inhibited, probably due to the binding of hBD-3 to lipid II. This results in cytoplasmic accumulation of soluble cell wall component precursors and formation of small lesions in the cell wall.

In addition to these antibacterial and antifungal properties, β-defensins also have antiviral capabilities. Exposure of HIV-1 isolates to hBD-2 or hBD-3, but not hBD-1, decreases retroviral activity (Quiñones-Mateu et al., 2003). hBD-3, but not hBD-1 or hBD-2, blocks HSV1 from binding to and penetrating cervical epithelial cells (Hazrati et al., 2006). In addition, hBD-1 and hBD-2 inhibit the ability of influenza virus to infect MDCK kidney epithelial cells (Doss et al., 2009).

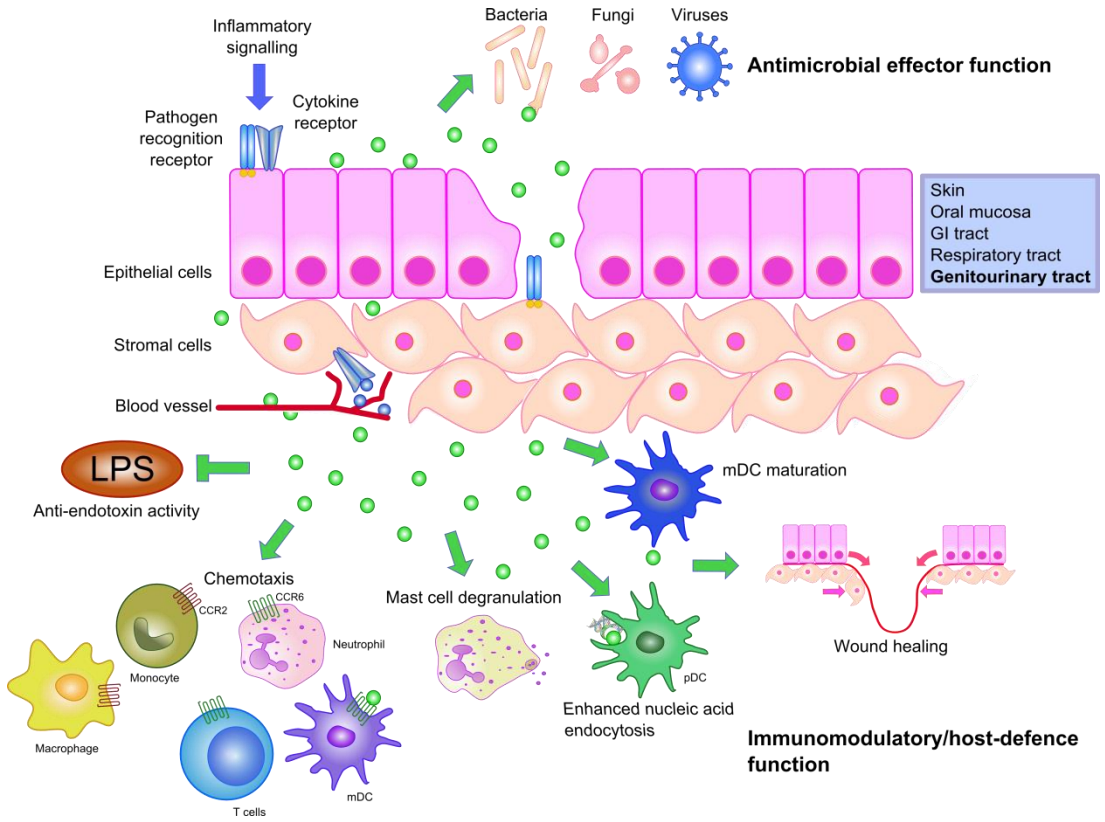


**Figure 1.3 Functions of β-defensins.**
β-defensins are produced by a variety of cell types, including epithelial cells and the underlying stromal cells, in response to a wide range of stimuli. Both direct and indirect inflammatory signals are particularly important and may come from the external environment or from the blood. The reported functions of β-defensins include altering extracellular sensing, cellular chemotaxis and maturation and wound healing.

### 1.3.2 Immunomodulatory properties

The immunomodulatory properties of β-defensins depend on their ability to chemoattract cells, to bind pathogens and their products extracellularly, to modulate binding of those pathogens to host cells and to alter intracellular signalling (Harvey et al., 2013; Figure 1.3). The effects can be wide ranging, with transcriptomic analyses indicating thousands of genes are differentially regulated by β-defensin stimulation (Hancock et al., 2016). The existing literature is at times contradictory, with the cell type, β-defensin concentration and co-stimulus apparently determining the end result.

The similarity of structure and function shared by chemokines and defensins has been evident since the discovery of the latter. The first isolation of α-defensins from rabbit neutrophils also yielded monocyte chemoattractant proteins (MCP) 1 and 2, with all six

peptides being antimicrobial, having three disulfide bonds and being highly similar in sequence (Selsted et al., 1984).

Human dendritic cells (DCs) and memory T cells migrate towards 0.1-1μg/mL hBD-2, with CC chemokine receptor (CCR) 6 and other CCRs being necessary for this function (Yang et al., 1999). hBD-2, hBD-3, mBD-4 and mBD-14 are all chemotactic for monocytes through CCR2 (Röhrl et al., 2010a), while mBD-4 is chemotactic for murine resident peritoneal cells through CCR6 (Röhrl et al., 2010b). Neutrophils express CCR6 and are chemoattracted to hBD-2 (Niyonsaba et al., 2004). Human DEFB124 is chemotactic for THP-1 monocytes (Kim et al., 2014b).

The chemotactic properties of β-defensins may underlie their ability to stimulate wound healing through enhanced migration of epithelial cells. hBD-2 increases HT-29 intestinal epithelial cell migration and rate of gap closure in confluent monolayers through CCR6 (Otte et al., 2008). hBD-2 and -3 both increase human keratinocyte migration (Niyonsaba et al., 2006). β-defensins also have demonstrable wound healing capability *in vivo*: infection of porcine epidermal wounds with a hBD-3-expressing adenovirus also increases wound healing (Hirsch et al., 2009).

Chemokine receptor engagement also mediates β-defensin-driven modulation of the myeloid cell response via other mechanisms. hBD-3 decreases the rate of neutrophil apoptosis and induces neutrophil migration via CCR6 (Nagaoka et al., 2008). hBD-2, but not hBD-1, induces histamine, prostaglandin D2 and arachidonic acid release by mast cells in a G-protein coupled receptor-dependent manner (Niyonsaba et al., 2001).

Several studies indicate β-defensins induce maturation of myeloid cells. Treatment of bone marrow-derived immature dendritic cells with mBD-2 led to a TLR4-mediated increase in the number of cells expressing maturity markers cluster of differentiation (CD) 11c, CD40 and B7.2. These mature DCs increased expression of interleukin (IL)-1α, IL-1β and IL-12p40, suggesting a Th1 polarizing ability (Biragyn et al., 2002). Incubation of peripheral blood mononuclear cells (PBMCs) with recombinant hBD-3 drives increased expression of CD80, CD86 and CD40 surface costimulatory molecules on myeloid DCs (mDCs) but not plasmacytoid DCs (pDCs) (Funderburg et al., 2007). A similar effect was seen in monocytes but not lymphocytes, with this mechanism

being TLR1/2 dependent. hBD-3 potentiates induction of CD86 expression on monocytes by the danger-associated molecular pattern (DAMP) extracellular ATP (Lioi et al., 2015).

There is less agreement in the literature regarding the ability of β-defensins to modulate cytokine production. β-defensins can both increase and decrease TNF-α release from LPS-stimulated macrophages (Barabas et al., 2013; Semple et al., 2010), with extracellular LPS binding activity and entry of the β-defensin into the macrophage having been demonstrated separately (Scott et al., 2000; Semple et al., 2011). In contrast, the available data indicate β-defensins exacerbate nucleic acid-mediated inflammation. hBDs -2 and -3 interact with human genomic DNA and bacterial DNA, condensing it into structures that are more easily endocytosed by pDCs and sensed via TLR9 (Lande et al., 2015; McGlasson et al., 2017). The addition of hBD-3 to nucleic acid also means it is detected by the cytoplasmic sensor melanoma differentiation-associated 5 (MDA-5) rather than TLR3, with interferon production being potentiated in the process (Semple et al., 2015).

β-defensins modulate the cytokine response in several disease models. Periodontitis is an inflammatory condition of the oral cavity during which recruitment of leukocytes and release of proinflammatory cytokines damages the tooth-supporting gingival tissue. hBD-3 attenuates LPS induction of several proinflammatory cytokines in a 3D co-culture model of gingival epithelial cells and fibroblasts (Bedran et al., 2014), indicating this β-defensin may be a useful treatment for periodontitis. Similarly, CD3/CD28-stimulated T cells increase IFN-γ, TNF-α, IL-1β, IL-6, IL-10 and IL-22 and decrease IL-17 secretion when treated with hBD-2 (Kanda et al., 2011). This ability to shape the T cell response indicates β-defensins truly link the innate and adaptive immune responses.

### 1.3.3 β-defensin 3

β-defensin 3, encoded by the *DEFB103* gene, is one of the most studied human β-defensin peptides and is a good example of both the pleiotropic nature of these molecules and of the conflicted data that exists as to their function. As much of the data presented in this thesis pertains to *DEFB103*, a brief discussion on this molecule in particular is worthwhile.

As neither hBD-1 nor hBD-2 were effective against *S. aureus*, a major cause of skin infections, retrieval of *S. aureus*-bound proteins from skin extracts led to the discovery of hBD-3. hBD-3 is active against a variety of Gram-positive and -negative bacteria, with 15μg/mL completely attenuating bacterial growth. Unlike the other β-defensin peptides studied by that point, hBD-3 is functional at physiological salt concentrations (Harder et al., 2001). *DEFB103* was simultaneously discovered in the same year by a second research group who demonstrated that the hBD-3 peptide is chemotactic for macrophages (García et al., 2001a). hBD-3 is antimicrobial against a wider array of bacteria and fungi than hBD-2 (Joly et al., 2004), possibly due to an increased positive charge and ability to dimerise (Schibli et al., 2002). The native disulfide bridging of hBD-3 is necessary for chemotactic abilities but not antimicrobial activity (Wu et al., 2003).

The immunomodulatory properties of hBD-3, and indeed most of the β-defensins which have been studied, are highly concentration dependent. Of hBDs 1-4, hBD-3 is the most potent immunomodulator in human keratinocytes, with 30μg/mL for 6 hours inducing IL-6, RANTES, MCP-1 and IL-10 (Niyonsaba et al., 2006). In contrast, 1μg/mL hBD-3 for 24 hours attenuates IL-6 expression driven by the *P. gingivalis* adhesion molecule HagB (Pingel et al., 2008). Similarly contradictory results have been obtained from human macrophage models, with hBD-3 both downregulating (Lyu et al., 2017; Semple et al., 2010) and upregulating (Jin et al., 2010) IL-6 and TNFα.

To address the contradictory nature of the available *in vitro* data, a functional proteomics model was built based on published data on DC response and signalling. This model predicted a 10:1 molar ratio of hBD-3 to HagB would attenuate HagB-induced inflammation, while a 10000:1 ratio would potentiate inflammation (Harvey et al., 2013). Subsequent *in vitro* experiments using a range of hBD-3 concentrations and time points

indicated the relative timing of both stimuli is important. Prior mixing of the β-defensin with HagB attenuates inflammation, but separate addition of hBD-3 before, with or after HagB generally potentiates inflammation. 0.2μM or 2.0μM hBD-3 concentrations dampens inflammation while 20μM β-defensin is proinflammatory. Some cytokines, including TNFα, showed one trend at 2 hours and the opposite at 16 hours. This study highlights the importance of using a range of time points and β-defensin concentrations for *in vitro* work. In addition, the dramatic difference in response after differing concentrations indicate tight regulation of β-defensin expression is likely to be critical *in vivo*.

hBD-3 is implicated in the pathogenesis of several conditions. It is over-expressed in oral carcinoma *in situ* lesions relative to healthy oral epithelium, possibly due to overexpression of epidermal growth factor receptor (EGFR) which induces hBD-3 expression in this cell type. *In vitro* data indicate hBD-3 is responsible for the recruitment of macrophages to these lesions, where they create a favourable microenvironment for tumour growth (Kawsar et al., 2009). hBD-3 is over-expressed in oropharyngeal cancer biopsies positive for human papilloma virus 16 (HPV-16) as the HPV-16 protein E6 drives hBD-3 expression by an as yet unspecified mechanism (DasGupta et al., 2016). In osteoarthritis patients, hBD-3 expression is induced in the articular cartilage. *In vitro* experiments indicate the disease-associated cytokines IL-1β and TNF-α drive β-defensin expression, with hBD-3 then inducing several matrix metalloproteinases and downregulating several tissue inhibitor of metalloproteinase (TIMP) genes. Thus, hBD-3 is involved in the pathogenic articular cartilage remodelling which occurs in osteoarthritis (Varoga et al., 2005).

Dysregulation of β-defensin production is observed in a wide variety of conditions, however the exact mechanisms underlying this are generally poorly understood. With several β-defensins having been discovered in the context of psoriasis, research into this condition illustrates the contribution of β-defensin function and regulation to disease. Psoriasis is a Th1/Th17 cell-mediated inflammatory disease characterised by scaly plaque-like lesions resulting from keratinocyte over-proliferation (Baliwag et al., 2015). β-defensin expression is upregulated in these lesions (de Jongh et al., 2005; Ong et al., 2002). β-defensin copy number is associated with psoriasis risk (Hollox et al., 2008), with *DEFB4A* being a potential biomarker (Kolbinger et al., 2017).

A proposed mechanism for β-defensins in psoriasis suggests cellular damage induced by infection or trauma releases self-DNA (Morizane and Gallo, 2012). Self-DNA forms complexes with hBD-2 and hBD-3, which are taken up by DCs leading to TLR9 activation and IFN-α production (Lande et al., 2007). hBD-3 also induces maturation of skin-derived dendritic cells which then induce IFN-γ production by T cells (Ferris et al., 2013). The classic Th1/Th17 cytokines associated with psoriasis include IFN-γ, TNF-α, IL-17A and IL-22 (Baliwag et al., 2015) which are all known β-defensin inducers. Thus, a positive feedback loop is initiated, with the cytokine environment driving β-defensin expression which in turn potentiates keratinocyte over-proliferation, chemokine production etc. (Niyonsaba et al., 2006). Interestingly, psoriasis patients experience a decreased rate of skin infections (Henseler and Christophers, 1995). Therefore, this example highlights the duality of β-defensins, with their pleiotropic nature simultaneously contributing to both health and disease in the one context.

### 1.3.4 β-defensins in reproduction

Evidence from several species also supports a direct role for β-defensins in reproduction, to date focusing on the male reproductive tract. The β-defensin genes in syntenic cluster B (Figure 1.2) are highly expressed in the male reproductive tract, particularly the epididymis. Quantification of syntenic cluster B gene mRNA across a panel of tissues from both cow and bull reproductive tracts indicated that all nineteen genes are expressed in the male reproductive tract, particularly the epididymis (Narciandi et al., 2011). In the human, syntenic cluster B genes *DEFB126* and *DEFB129*, as well as the cluster D gene *DEFB106*, are differentially regulated in the epididymis of infertile men (Dubé et al., 2008).

Several studies have elucidated the function of DEFB126 in the macaque male reproductive tract (Tollner et al., 2012). This gene is expressed by epithelial cells of the epididymal mid-region and the peptide is consequently present on the surface of ejaculated sperm (Yudin et al., 2003). Glycosylation of the elongated DEFB126 C-terminus confers a negative charge to the sperm surface, allowing progressive movement through the negatively-charged cervical mucus to reach the uterus (Tollner et al., 2008a).

The peptide then mediates attachment of sperm to the oviductal epithelium (Tollner et al., 2008b). Up to this point, DEFB126 helps mask the foreign proteins of the sperm from immune recognition (Yudin et al., 2005). After ovulation, biochemical changes in the uterine lumen cleave the sialic acid residues anchoring DEFB126 to the sperm surface, allowing the now fully mature sperm to migrate toward and fertilise the ovum (Tollner et al., 2004).

DEFB126 is also important in human male fertility. A frameshift mutation has been identified which impairs sperm penetration of cervical mucus and significantly reduces pregnancy rate in affected couples (Tollner et al., 2011). Another similar frameshift mutation leads to the absence of peptide on ejaculated sperm and reduced sperm motility, although the effect of this mutation on pregnancy outcome was not tested (Duan et al., 2015).

hBD-1 also binds to the surface of the human sperm, though in this case attachment is via the CCR6 receptor. Reduced hBD-1 on sperm is observed in a number of subfertility-associated conditions. Addition of recombinant hBD-1 restores several essential parameters such as motility and egg-binding ability through CCR6-mediated $Ca^{2+}$ influx (Diao et al., 2014).

Rodent studies similarly indicate a crucial role for β-defensins in male fertility. *Defb15* knockdown in mature male rats before mating reduces sperm motility, increases embryo development failure and reduces numbers of live offspring (Zhao et al., 2011). In mice, *Defb15* and eight other β-defensin genes in same syntenic cluster have been simultaneously knocked down, resulting in sterility of male, but not female mice (Zhou et al., 2013). Therefore, β-defensin function extends beyond defence, with at least some genes being essential for fertility.

## 1.4 Regulation of β-defensins

### 1.4.1 Regulation of syntenic cluster D β-defensins

As β-defensin function is concentration dependent, understanding how each gene is regulated in a given context is key to using β-defensins to improve health and disease. Most individual studies have measured either mRNA or protein, though the few that have measured both indicate that induction of transcription is mirrored by protein production (Jin et al., 2010; Joly et al., 2005).

Regulation of β-defensin expression is highly cell type-specific. This was illustrated elegantly by a study which applied a variety of stimuli to human primary keratinocytes, immortalised monocytes and colonic epithelial cells. *DEFB4A* was induced by phorbol 12-myristate 13-acetate and IL-1α in keratinocytes, by butyrate in colonic epithelium and by butyrate and *Streptococcus spp.* in monocytes (Schauber et al., 2006). Another study showed *Fusobacterium nucleatum* induced *DEFB1* in DCs but not gingival epithelial cells (Yin et al., 2010). Cytokine induction was also markedly different between the two cell types. hBD-2 induced GRO, IL-8 and MCP-1, while hBD-3 induced TIMP-2 in DCs. Therefore, the mechanisms regulating β-defensins in one cell type do not automatically apply to another.

Unsurprisingly given its antimicrobial properties, several pro-inflammmatory stimuli regulate *DEFB4A* expression. Pathogen-mediated *DEFB4A* induction in oesophageal (Steubesand et al., 2009) and colonic epithelium (O'Neil et al., 1999) occurs via NF-κB. Nucleotide oligomerization domain 2 (NOD2) mediates induction in middle ear epithelium in response to *Hemophilus influenzae* (Woo et al., 2014). In contrast, activation of mitogen-activated protein kinase (MAPK), not NF-κB, is essential for *DEFB4A* expression in primary gingival cells exposed to the oral bacterium *Fusobacterium nucleatum* (Krisanaprakornkit et al., 2002). Several cytokines also regulate *DEFB4A* expression. IL-17A drives *DEFB4A* through MAPK signalling in keratinocytes (Sørensen et al., 2005), but via NF-κB in bronchial epithelium (Kao et al., 2008). IL-22 upregulates *DEFB4A* and *DEFB103* in keratinocytes, possibly via signal transducer and activator of transcription (STAT)3 (Wolk et al., 2004).

While *DEFB4A* is inducible in response to a range of bacteria, *DEFB1*, encoding the peptide HBD-1, is mainly constitutive in expression (O'Neil et al., 1999). Expression of this gene in the hypoxic (oxygen-deprived) environment of the colon is mediated by binding of hypoxia inducible factor α (HIF1α) to a response element in the *DEFB1* promoter (Kelly et al., 2013). HIF1α also upregulates *DEFB4A* in *Mycobacterium tuberculosis*-infected macrophages (Nickel et al., 2012). Hypoxia occurs in a variety of settings, being increased in colitic lesions (Karhausen et al., 2004) and in the postpartum uterus (Yoshii et al., 2014). The interplay between hypoxia and inflammation is increasingly appreciated, with NF-κB upregulating the transcription factor CCAAT enhancer binding protein δ (CEBPD) which then binds to the promoter of *HIF1A*, generating so-called inflammatory hypoxia (Yamaguchi et al., 2015). This suggests the role of hypoxia in β-defensin gene regulation in an inflammatory context may be much greater than is known at present.

Both pathogens and cytokines regulate *DEFB103*. The human gene is driven by IL-1β, IL-17, IL-22 and TNFα in various cell types (Dixon et al., 2016; King et al., 2007). HIV infection also stimulates expression (Quiñones-Mateu et al., 2003). Bacterial stimuli drive epidermal growth factor receptor (EGFR) activation and *DEFB103* induction in keratinocytes (Sørensen et al., 2005), oral carcinoma (Shuyi et al., 2011) and gastric carcinoma cell lines (Muhammad et al., 2016). EGFR has a number of endogenous ligands and initiates several intracellular signalling pathways (Holcmann and Sibilia, 2015). In an *ex vivo* model of sterile skin injury, membrane-bound heparin-binding EGF-like growth factor (HB-EGF) is cleaved from the keratinocyte cell surface, allowing it to bind EGFR and induce *DEFB103* expression (Roupé et al., 2010). Given that hBD-3 has been shown to promote skin healing (Hirsch et al., 2009), EGFR-mediated detection of keratinocyte injury may be crucial in promoting healing via *DEFB103*. However, EGFR is particularly active in the skin and in cancer cells (Lichtenberger et al., 2013), therefore it may not play such a direct role in *DEFB103* induction in other cell types.

Several steroid hormones regulate expression of β-defensin genes. Cortisol, a member of the glucocorticoid class of steroids, downregulates murine *Defb3*, the ortholog of human *DEFB4A*, in response to psychological stress (Aberg et al., 2007). *DEFB4A* expression by colonic epithelium in response to IL-1β and TNFα is heightened by dexamethasone, a synthetic corticosteroid (Witthöft et al., 2005). In contrast, bronchial

epithelium downregulates *DEFB103* expression, with dexamethasone having no effect on *DEFB1* or *DEFB4A* (Duits et al., 2001).

Sex steroids are important β-defensin regulators, particularly in the reproductive tract. Human uterine lining, known as the endometrium, expresses at least four β-defensins and the expression pattern of each varies across the menstrual cycle. *DEFB1* and *DEFB103* are most highly expressed in the progesterone-dominant secretory phase, *DEFB104* is maximally expressed during the oestrogen-dominant proliferative phase and the cortisol-dominant menstrual phase predominantly drives *DEFB4A* expression (King et al., 2003). Similarly, uterine expression of murine β-defensins peaks before ovulation, possibly to clear pathogens from the tract in anticipation of pregnancy, then declines in later phases of the estrus cycle, which the authors posit may be to facilitate tolerance of the allogenic sperm and embryo (Hickey et al., 2013). Androgens can also drive β-defensin expression. Several murine syntenic cluster D β-defensins are fully or partially responsive to androgen in the epididymis (Hu et al., 2014). Rat *Defb15*, a rodent-specific gene, is regulated by androgen, as evidenced by a decline in mRNA levels following castration which is rescued by androgen supplementation (Zhao et al., 2011).

Vitamin D, a steroid hormone obtained through sun exposure and dietary intake, modulates both innate and adaptive immune responses (Prietl et al., 2013). Studies investigating vitamin D regulation of β-defensin expression are conflicting. Calcipotriol, a vitamin D analog used topically to treat psoriasis, downregulates *DEFB4A* and *DEFB103* expression as measured from biopsy punches before and after treatment. This was mediated by downregulation of IL-17A and upregulation of nuclear factor of kappa light polypeptide gene enhancer in B-cells inhibitor, alpha, (IκB-α) which blocks NF-κB signalling (Peric et al., 2009). In contrast, another *in vitro* study using primary keratinocytes found vitamin D increased *DEFB4A* expression through upregulation of NOD2 (Wang et al., 2010). Vitamin D receptor (VDR) mRNA positively correlates with *DEFB4A* and *DEFB103* mRNA in oral mucosa of people who have been exposed to HIV-1 but remain uninfected, who also have higher VDR mRNA in PBMCs versus HIV-positive individuals (Aguilar-Jiménez et al., 2013). Despite opposing results, it does appear that vitamin D can modulate β-defensin expression via a number of mechanisms.

Several of the factors known to stimulate expression of human syntenic cluster D genes have also been investigated in the bovine, though again these data pertain to a small subset of the total gene repertoire. The gene encoding HBD-2/β-defensin 2 appears to have undergone a gene expansion in the bovine. The canine ortholog, called *CBD102* here, clusters with 10 bovine β-defensin genes: *DEFB5*, *DEFB4A*, *BNBD11* (bovine neutrophil β-defensin), *BBD403*, *LAP*, *TAP*, *BNBD7*, *BNBD10*, *BNBD10A* and *EBD* (enteric β-defensin), also known as *DEFB* (Figure 1.4). Studies investigating regulation of bovine syntenic cluster D genes, which are found on bovine chromosome 27, relate mainly to these genes and suggest mechanisms of regulation are similar to what has been observed for human *DEFB4A*.

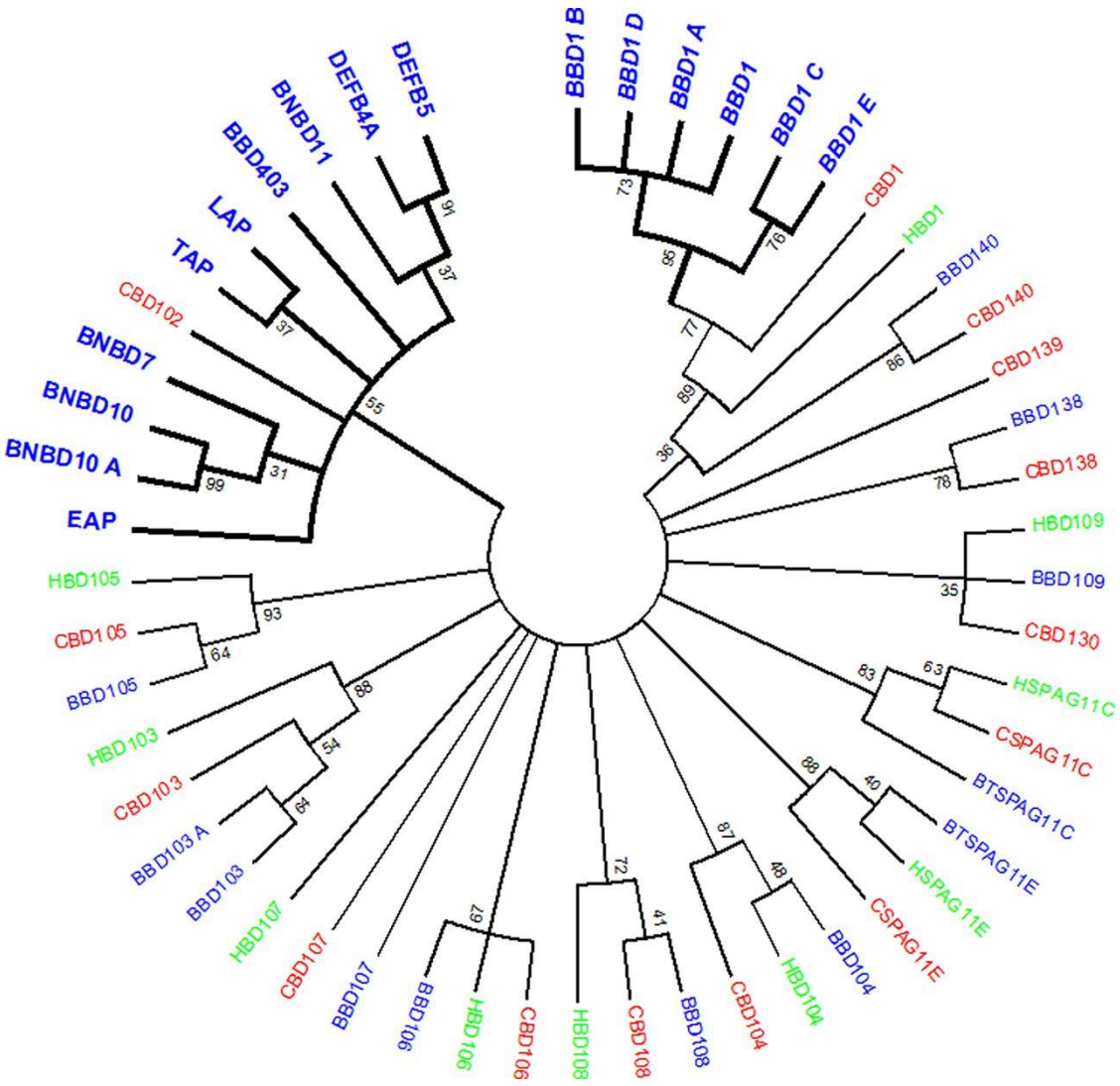


**Figure 1.4 Phylogenetic tree including syntenic cluster D β-defensin genes from bovine, human and dog.**
Bovine genes are coloured in blue, human in green and dog in red. Numbers at nodes indicate percentage bootstrap support. β-defensin 2 has undergone a gene expansion in the bovine, with 10 genes clustering with the canine ortholog CBD102. The human ortholog, *DEFB4A*, has not been included. DEFB1/HBD-1 is also expanded in the bovine, with several gene copies, of non-identical sequence, as indicated by lettering. Sequences were obtained from GenBank. Taken from Meade et al. (2013).

Genes within this expansion respond to pathogenic-derived stimuli in some contexts. *TAP* expression is upregulated in primary bovine tracheal epithelial cells in response to LPS, TNFα and IL-1β. An NF-κB binding site in the proximal promoter modulates this response (Diamond et al., 2000). However, LPS had no effect on *TAP* expression in lung alveolar macrophages (Ryan et al., 1998). Similar to *DEFB4A*, *LAP* expression is increased by IL-17 in tracheal epithelial cells (Berghuis et al., 2014). *LAP* and *TAP* are both upregulated in primary endometrial stromal and epithelial cells by LPS

(Davies et al., 2008) and *E. coli* (Chapwanya et al., 2013). Expression of *EBD* in intestinal epithelial cells is increased in animals infected with the parasite *Cryptosporidium parvum* (Tarver et al., 1998).

While there is no data on sex steroid regulation of bovine β-defensins, a little more is known about vitamin D. Several β-defensins are expressed in monocytes in response to a combination of LPS and vitamin D, though inclusion of an inhibitor of protein translation blocked expression of β-defensin mRNA, suggesting the effect of vitamin D of β-defensin expression was indirect (Merriman et al., 2015). Chromosome 27 β-defensins are similarly upregulated by vitamin D, either with or without LPS, in primary mammary epithelial cells (Téllez-Pérez et al., 2012).

### 1.4.2 Regulation of syntenic cluster B β-defensins

Though the regulation of this group of genes has received far less attention, the existing data indicate androgens are at least partly responsible. This is not surprising given the male reproductive tract is the main site of expression. A murine model of castration followed by testosterone supplementation indicated *Defb20* (*DEFB128* ortholog) and *Defb19 (DEFB117* ortholog) were fully responsive to androgen, *Defb22* (*DEFB126*) was partially responsive to androgen, while *Defb29* (*DEFB116*) was unresponsive (Hu et al., 2014). *Defb21*, *Defb24*, *Defb27* and *Defb36* are rat orthologs of *DEFB118*, *DEFB119*, *DEFB122* and *DEFB123* respectively. Castration reduces but does not eliminate epididymal expression of these genes (Yenugu et al., 2004). In contrast, expression of these same genes in caput epididymis is increased by LPS treatment despite a corresponding decline in serum testosterone (Biswas and Yenugu, 2011). Blocking of NF-κB signalling ameliorates this effect (Biswas and Yenugu, 2013). This is not surprising as DEFB118 exhibits antimicrobial properties *in vitro* (Yenugu et al., 2004).

Regulation of bovine syntenic cluster B genes, expressed on chromosome 13, has not yet been investigated. At least some of these genes are likely to be regulated by androgen in the male reproductive tract, as *DEFB132-DEFB125A* are not expressed in the reproductive tract of the sexually-immature male (Narciandi et al., 2011). While this cluster is expressed outside the male reproductive tract (Narciandi et al., 2011; Rodríguez-

Jiménez et al., 2003), the regulatory mechanisms operating in the context of other tissues have also yet to be explored.

### 1.4.3 The non-coding genome and regulation of β-defensins

As β-defensins are highly pleiotropic peptides which may have both pro-inflammatory and anti-inflammatory properties depending on the concentration, regulation of the level of expression may be the difference between an appropriate immune response to a detected pathogen and pathological inflammation. As gene regulation at the transcriptional level is exerted by the binding of transcription factors to both gene-proximal and distal non-coding DNA in a context-specific manner, understanding of how this process controls the expression of β-defensin genes could help identify individuals who are more likely to suffer from such pathological inflammation.

LPS-mediated *DEFB4A* expression in intestinal epithelium involves transcription factor recruitment to specific NF-κB and activator protein 1 (AP-1) sites in the proximal promoter (Vora et al., 2004). In contrast, macrophages require two NF-κB sites in order to activate LPS-mediated expression of *DEFB4A* (Tsutsumi-Ishii and Nagaoka, 2002). In this cell model, the AP-1 site in the promoter does not appear to be essential for promoter activity. Serial deletions of the human *DEFB4A* promoter, followed by site-directed mutagenesis, pinpoint a vitamin D response element ~1000bp upstream of the transcription start site as being key to vitamin D-mediated gene expression (Wang et al., 2004). Myeloid ELF-like factor 1 (MEF) drives *DEFB4A* in unstimulated epithelial cells by binding to an E twenty-six (Ets)-binding site in the promoter (Lu et al., 2004). Thus, transcription factor usage and regulation of β-defensin expression is somewhat cell-type specific.

SNPs in the *DEFB1* promoter have been linked to a variety of conditions. *DEFB1* expression is decreased in ulcerative colitis lesions. There is a statistically significant link between a *DEFB1* promoter SNP located 44bp upstream of the translation initiation codon, which affects *DEFB1* expression level, and the incidence of ulcerative colitis (Peyrin-Biroulet et al., 2010). This same SNP, rs1800972, affects expression of *DEFB1*, but also *DEFB103*, in oral keratinocytes and is correlated with antimicrobial activity of

keratinocyte extracts (Kalus et al., 2009). This SNP has been associated with chronic obstructive pulmonary disorder, HIV transmission, levels of *Candida albicans* in the oral cavity and atopic dermatitis.

Three SNPs in the *DEFB1* promoter, including rs1800972, form a haplotype associated with dental caries risk (Ozturk et al., 2010). Two of these three are associated with differential salivary HBD-1 peptide concentrations (Polesello et al., 2015). The high caries-associated haplotype is also associated with persistent nasal *Staphylococcus aureus* carriage due to lowered *DEFB1* expression in keratinocytes (Nurjadi et al., 2013). It is not yet known what transcription factors may be responsible for this effect.

Flores Saiffe Farías et al. (2015) have attempted to bridge this gap using a computational analysis pipeline which identifies known disease-associated SNPs in human gene promoters. SNPs whose locations overlap with open DNA regions annotated in public databases are subjected to transcription factor binding site prediction. The intended outcome is identification of SNPs predicted to alter binding of transcription factors known to be involved in the given disease. When *DEFB1* was analysed in this manner, promoter SNPs putatively affecting binding of key transcription factors were highlighted, including NF-κB for tuberculosis and CCAAT enhancer binding protein for HIV-1. While comprehensive, this method is currently applicable only to human. Given the demonstrated link between non-coding DNA polymorphisms, β-defensin gene expression level and disease, identification of regulatory elements which modulate gene expression will improve our ability to harness the properties of β-defensins for the improvement of bovine health.

## 1.5 A potential role for bovine β-defensins in fertility

### 1.5.1 Fertility in Irish beef and dairy herds

Ireland's beef and dairy industries operate on a low-cost seasonal-based grazing system. In order to ensure continued synchronicity between calving season and the period of optimal grass growth in spring, the average number of days between successive calvings, or calving interval, needs to be as close as possible to 365 days. This requires a high rate of conception to first service and a timely return to fertility after parturition. In the 2016 calving season, the average calving interval for Irish dairy cows was 389 days and for beef cows was 399 days (ICBF, 2016). Conception to first service can be as low as 50% (Berry et al., 2011), but can fall much lower when low fertility bulls are used. Cumulative costs associated with such reproductive inefficiency in dairy systems are €52/cow (Shalloo et al., 2014). Given there are over 1.2 million dairy cows in Ireland, the economic implications are significant and unsustainable. In fact, fertility has been identified by Irish animal health experts as the single most detrimental issue facing the industry (More et al., 2010).

Both bull and cow fertility issues are contributing to this problem. Understanding of the factors contributing to male fertility is relatively poor (Berry et al., 2011). Predictive fertility assessment of bulls currently relies on physical examination of the animal coupled with analysis of sperm parameters such as shape and progressive motility (Kastelic and Thundathil, 2008). However, the relationship between these traits and field pregnancy rate is inconsistent (Parkinson, 2004). A greater understanding of the genetic basis of bull fertility, and indeed a predictive genetic test, would greatly improve sire selection and improve the rate of genetic gain.

Until the 1990s, international cattle breeding programmes focused solely on terminal production-related traits such as milk yield and muscle mass, with a resulting genetics-driven decline in cow reproductive performance. Incorporation of reproductive performance goals into breeding programmes has partially reversed this trend in dairy, but not beef, cows (Berry et al., 2014). Even though the heritability of cow reproductive performance is relatively low, combination of a genetics-focused breeding programme

with a farm-level personalised management plan considering individual genotype and phenotype, has huge potential to improve cow reproductive performance and welfare (Berry et al., 2016). Understanding of both genetic and environmental factors driving both outcomes needs to drastically improve in order to realise this goal.

Prolonged post-partum uterine inflammation is a key driver of cow reproductive performance, though the genetic basis underlying this is currently poorly understood (Berry et al., 2014). It is believed that persistent post-partum uterine disease represents a failure to cycle between a range of polarised immune states in the peri-partum to post-partum periods (LeBlanc, 2012). A necessary quiescent immune state during pregnancy is followed by a productive pro-inflammatory state in the early post-partum period during which PMN assist in uterine involution and wound repair and cytokines and effector molecules respond to bacterial infection. Transcriptomic analysis of beef cow uterine biopsies 15 days post-partum (DPP) indicates a significant upregulation of inflammatory gene expression, with T cell signalling and cytokine-cytokine receptor interaction pathways being enriched (Foley et al., 2012).

If these mechanisms do not resolve this infection, or are excessive in severity or duration, the resumption of homeostasis necessary for conception is not achieved by the beginning of breeding season, typically 6-8 weeks after the first calving in a herd. Up to 40% of cows develop acute clinical uterine inflammation, known as metritis, within a week of parturition (Sheldon et al., 2009a). By three weeks post-partum, 30% will have chronic inflammation of the inner mucosal lining of the uterus, known as the endometrium, with a massive influx of neutrophils to this site. *Fusobacteriaceae* and *Porphyromonadaceae* species are significantly more abundant in metritic versus healthy animals (Knudsen et al., 2016), while the contribution of viruses to uterine inflammation and infertility is an emerging concept (Chastant-Maillard, 2015; Sheldon et al., 2009a).

Cows with endometritis take up to 27% longer to get pregnant than healthy animals (LeBlanc et al., 2002). There are a variety of mechanisms, both proposed and experimentally-demonstrated, by which prolonged uterine inflammation is thought to impact fertility (LeBlanc, 2012; Sheldon et al., 2009a). The size of the first post-partum dominant ovarian follicle is reduced in animals with a high uterine pathogen burden, as is circulating oestradiol concentration (Williams et al., 2007).

Currently, understanding of the factors leading to this inappropriate response is poor. Polymorphisms in immune genes, the species profile and quantity of invading bacteria, the level of physical injury and an energy deficit (negative energy balance) post-partum may all contribute to the outcome. Given the implications for fertility, there is an economic incentive to elucidate the processes underlying this condition.

### 1.5.2 β-defensins in bull fertility and uterine disease

Data from several studies indicate β-defensins may be involved in both bull and cow fertility. Cormican et al. (2008) bioinformatically predicted a cluster of bovine β-defensin genes on chromosome 13. Detailed transcriptional profiling of these genes in the reproductive tract tissues of both the sexually immature and mature bull and in the cow indicated that each of the genes is highly expressed throughout the male reproductive tract (Narciandi et al., 2011). In addition, 7 genes were found to be exclusively expressed in the sexually mature bull. This cluster is syntenic with the human chromosome 20 β-defensins. Rodríguez-Jiménez et al. (2003) showed these human orthologs were also predominantly expressed in the male reproductive tract, though they did detect expression of some of the genes in the liver, lung, heart and brain. *DEFB126* is located within this cluster. As discussed, DEFB126 peptide is found on the sperm and plays an important role in facilitating transit of the sperm through the female reproductive tract (Tollner et al., 2012). Bovine β-defensin 126 is similarly bound to the head and tail of ejaculated spermatozoa and contributes to sperm motility, but not oocyte fertilisation (Fernandez-Fuertes et al., 2016).

Sequencing of these genes in several cattle detected 17 SNPs (Narciandi, 2013). Seven of these were non-synonymous, amino-acid changing polymorphisms, six were synonymous, three were located in the promoter region and one was intronic. The latter non-coding SNPs may fall within gene regulatory regions and therefore may affect the context and extent of gene expression. Interestingly, four SNPs were found to significantly differ in allele frequency between Holstein-Friesian and Norwegian red animals, the former having been bred for high milk production and the latter for high fertility. The *BBD115* and *BBD117* SNPs were non-synonymous, the *BBD121* SNP was

located in the intron, while the last SNP, in *BBD122,* was synonymous (Narciandi et al., 2011).

While genotyping of another cohort of bulls with proven AI outcomes indicated there was no association between the presence of a particular allele and pregnancy rate, a SNP in *BBD117* which obliterates the stop codon was associated with reduced ability of sperm to swim through a cervical mucus mimic *in vitro*. There was no significant difference in allele frequency of this SNP between the Holstein-Friesian and Norwegian Red animals sequenced (Narciandi, 2013).

These data indicate that β-defensins play a functional role in the male reproductive tract. The observed genetic variation within these genes may contribute to observed differences in fertility between cattle breeds.

The implications of prolonged post-partum uterine inflammation on cow fertility has motivated the search for greater understanding of the role of β-defensins in this context. β-defensins are differentially expressed in the post-partum uterus. Healthy cows have increased uterine expression of *DEFB6* at 15DPP relative to 30 days (Foley et al., 2012). In a separate study, *DEFB*, *DEFB103B* and *DEFB5* were found to be up-regulated in uterine biopsies taken 7DPP relative to 21DPP (Foley et al., 2015). The same study also found *LAP*, *DEFB5* and *DEFB7* were significantly up-regulated in endometritic animals relative to healthy cows 21 DPP. Given the multitude of antimicrobial and immunomodulatory properties ascribed to β-defensins based on human and murine studies, the potential roles for these genes in this complex condition are numerous and warrant further investigation.

## 1.6 Aims and objectives

The overall aim of this project was to explore mechanisms regulating expression of bovine β-defensin genes. To this end, a number of approaches were used:

1. Identification of non-coding regions of the genome which may act as regulatory elements for bovine β-defensin gene expression.

2. Profiling of β-defensin expression in an expanded panel of female reproductive tract tissues.

3. Development of a primary culture model to allow hypothesis testing.

4. Quantification of β-defensin expression in primary cells in response to cytokines and viral ligands.

# Chapter 2 Materials and Methods

## 2.1 Bioinformatics analysis

### 2.1.1 Generation of β-defensin ortholog promoter sequence sets.

ENSEMBL genome browser, accessible at www.ensembl.org, was used to search for the human ortholog of each DEFB gene. Within the gene information page, the "Orthologs" menu was selected. This contains a list of species for which there is a designated ortholog of the target gene. This list was downloaded into Excel. This process was repeated for syntenic cluster B genes *DEFB132*, *DEFB129*, *DEFB128*, *DEFB127*, *DEFB126*, *DEFB125*, *DEFB124*, *DEFB123*, *DEFB121*, *DEFB119*, *DEFB118*, *DEFB116* and *DEFB11*. As human *DEFB122* is pseudogenised, there are no orthologs listed in ENSEMBL, so the *Bos taurus* gene was used as the basis for the ortholog search. *DEFB117* has one entry in ENSEMBL, the human gene, with no listed orthologs. This gene was omitted from the analysis, as were *DEFB122A*, *DEFB125A* and *DEFB142* as these genes are bovine specific.

A list of seventeen mammalian species was selected for inclusion in this analysis. While there are several primates genomes available, three species were chosen (human, gibbon and Rhesus macaque) to avoid biasing the dataset towards this order, since we are primarily interested in building hypotheses to be tested in a bovine model. Three additional Cetartiodactyls, one Perissodactyl, two carnivores, two bats, two rodents, the rabbit, elephant and armadillo were included to span the mammalian phylogenetic tree. The list of species chosen and the genome assemblies used are provided in Table A.1.

Having thus compiled a list of available β-defensin gene orthologs, the ENSEMBL IDs for which are given in Table A.2, the BIOMART feature of EMSEMBL was used to download promoter nucleotide sequences. As the 5'UTR has not been experimentally investigated for most of these genes, the 5000bp upstream of the translation initiation codon was selected as follows:

Dataset menu:

Choose database= ENSEMBL genes 83

Choose dataset= Select the genome assembly of each included species in turn

Filters menu (Gene):

Input external references ID list= List of DEFB gene ENSEMBL IDs pasted in

Attributes menu (Sequences):

Flank coding region (Gene)- Upstream flank =5000

The bovine genome assembly used by ENSEMBL is UMD3.1. There are large differences in the incidence of assembly errors between bovine genome assemblies (Zimin et al., 2012) and annotation of bovine β-defensin genes differs between each (Adelson et al., 2014). Therefore, the most recent assembly (UMD3.1.1/bosTau8) has been used in this project. This genome assembly is available in University of Santa Cruz (UCSC) Genome Browser, accessible at http://genome.ucsc.edu/. The bovine syntenic cluster B β-defensin region was downloaded from the UCSC Genome Browser, as follows:

Genomes menu:

Group= Mammal

Genome= Cow

Assembly= Jun. 2014 (Bos_taurus_UMD_3.1.1/bosTau8)

Position= chr13:61,292,225-61,620,456 (Submit)

View menu (DNA):

Sequence formatting options= All upper case

Extended DNA case/colour options

Cow mRNAs = Toggle case (Submit)

This generated a sequence file with coding exons indicated by case. This was pasted into an instance of the program A plasmid Editor (downloaded at http://biologylabs.utah.edu/jorgensen/wayned/ape/). Five thousand base pairs upstream of the translation initiation codon was manually selected and extracted for the analysis, using Sequence Massager, accessed at http://www.attotron.com/cybertory/analysis/seqMassager.htm, to generate the reverse complement where the gene is located on the reverse strand. This process was repeated for the chromosome 27 syntenic cluster D region, taking the region between

chr27:4,886,797-6,197,460. The chromosomal co-ordinates of the resulting promoter nucleotide sequences are compiled in Table A.3.

A pool of randomly-selected human gene promoter sequences to use as a background/control nucleotide set was generated using ENSEMBL BIOMART as before, with the following changes:

Dataset menu:

Choose dataset= Homo sapiens genes (GrCh38.p5)

Filters menu (Gene):

Limit to genes (external references)…= With RefSeq protein ID(s) (Only)

This resulted in a panel of 20,952 potential background sequences.

### 2.1.2 Transcription factor binding site over-representation analysis- JASPAR, oPOSSUM3

The JASPAR database, accessible at http://jaspar.genereg.net/, is a manually curated collection of non-redundant transcription factor (TF) position weight matrices (PWMs). Data are gathered from publicly available transcription factor chromatin-immunoprecipitation sequencing (ChIP-Seq) datasets. Version 4.0, released in 2010, is based on data collected from published papers (Portales-Casamar et al., 2010), while 2014 and 2016 releases have included data from multi-centre collaborations carrying out genome-wide ChIP-Seq assays to identify functional regulatory elements in a number of model species (Mathelier et al., 2013). These include human and mouse ENCODE projects and the modENCODE project focusing on *Drososphila melanogaster* and *Caenorhabditis elegans*. PWMs compiled from the above sources are contained in the CORE collection. The PBM collection contains PWMs assembled from the UniPROBE database of results from protein-binding microarray (PBM) experiments using mouse DNA. A DNA sequence can be uploaded within JASPAR in order to search against selected PWMs to identify putative transcription factor binding sites within the sequence that meet a user-selected similarity cut-off.

oPOSSUM3, accessible at http://oPOSSUM3.cisreg.ca/oPOSSUM3/, is a software tool built by the curators of JASPAR to identify transcription factor binding sites (TFBSs) which are over-represented in a set of nucleotide sequences versus a selected background set (Kwon et al., 2012). Specific versions exist for a number of model species, including human and mouse. A sequence-based input method exists for analysis of genes from non-model organisms. oPOSSUM3 uses PWMs from the JASPAR 4.0 database, released in 2010. In addition to CORE and PBM collections, a small number of PWMs which were not finished for the JASPAR 4.0 release were included in a Pending collection as they were of scientific interest to the authors. All three collections can be segregated into vertebrate, insect, nematode and fungi PWMs, leaving a panel of 291 vertebrate PWMs across the three collections. A small number of TFs are represented by two PWMs as they have been shown to bind more than one distinct DNA motif.

It is important that the relative GC nucleotide content of the input and background sequences are equal to avoid a bias towards TFBSs with higher or lower GC content (Kwon et al., 2012). oPOSSUM3 allows the user to submit files containing the intended foreground sequences and a panel of length-matched background sequences. Once the desired foreground:background ratio is specified, oPOSSUM3 selects the appropriate number of genes with the exact percentage GC content as each of the input gene set.

When selecting the PWMs to search for in the sequences, the minimum information content can be specified. Information content is a number summarising the length and complexity of the PWM, and provides an estimate how informative the PWM is. Specification of a minimum information content value means only PWMs with high specificity are used.

The matrix match threshold defines a cut-off of percentage similarity between a PWM and a possible site in the input sequence. The default 85% is recommended initially, with the possibility to lower to 75 or 70% if the involvement of a particular transcription factor is suspected, e.g. if indicated by experimental data. Results are evaluated by three tests. The Z score compares the rate of occurrence of putative TFBSs in a target gene set to the rate expected by chance, as computed from the background gene set (Figure 2.1), since these genes have been randomly selected and are not expected to have any overall commonality of regulation. This results in a number which represents the likelihood that

the number of TFBSs detected in the input gene set is significant compared to the number detected in the background set, expressed in units of magnitude of the standard deviation (Kwon et al., 2012). A relatively high number of sites in each of a subset of the target sequences may lead to a TFBS being considered over-represented by this method. The Z score method is particularly good at detecting common sites.

The Fisher one-tailed probability test computes the probability that the number of sequences with at least one TFBS hit versus the number of sequences with no hit in the input sequence set could have occurred by random chance based on the proportions for the background set, expressed as negative natural logarithm of the probabilities. Presence or absence of a site in each sequence is considered but occurrence of more than one site per sequence is not taken into account (Figure 2.1). Therefore the Fisher score is good for detecting relatively rare sites.

The Kolmogorof-Smirnoff centrality test compares the observed distribution of TFBS locations between input and background sequence sets. This is particularly suited to ChIP-Seq datasets.

The developers of the oPOSSUM3 suite of tools have found that TFBSs detected as over-represented by both Z and Fisher scores are most likely to be biologically functional (Kwon et al., 2012). An applied threshold takes into account the size of the foreground sequence set and is recommended by Kwon et al. (2012) as follows:

Z score applied threshold= mean score + (standard deviation x 2)

Fisher score applied threshold=mean score + (standard deviation x 1)

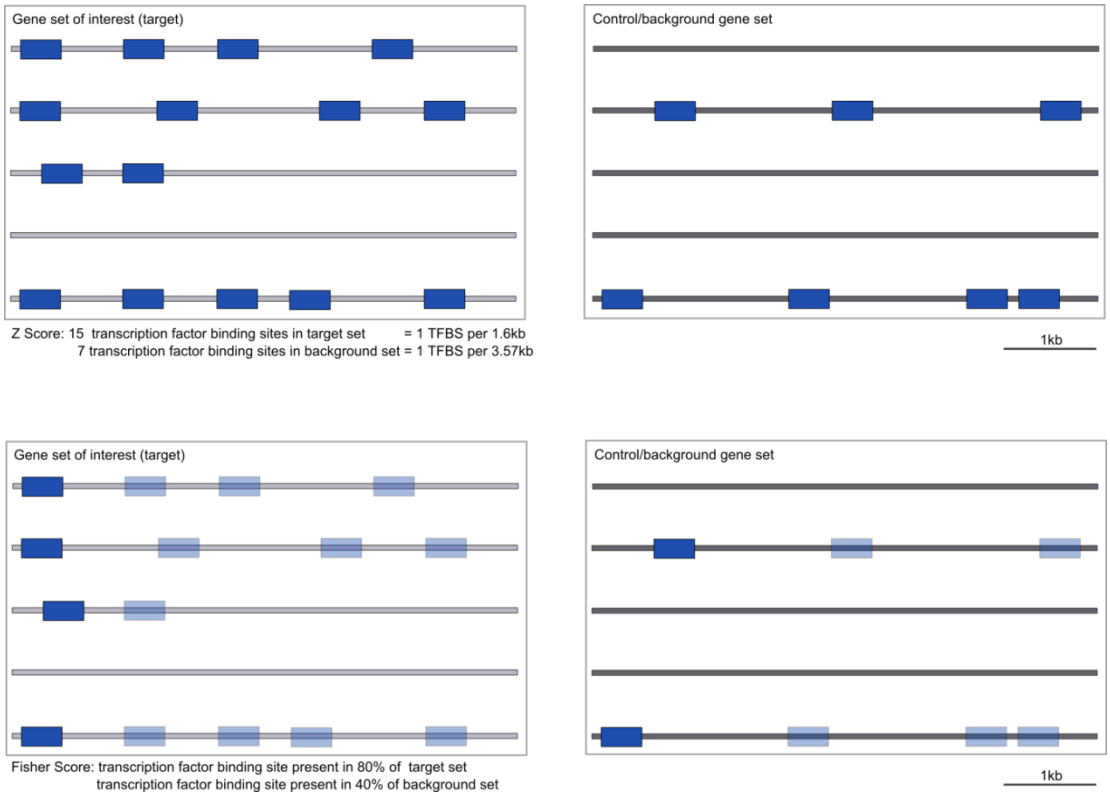


**Figure 2.1 Types of transcription factor binding site over-representation computed by oPOSSUM3 software.**

For a given input consisting of a target gene set and background gene set, Z score considers the total number of TFBSs in each set. A small subset of target genes containing a large number of sites can lead to a TFBS being considered over-represented by Z score. Fisher score considers only the presence or absence of a TFBS in a gene promoter, total number of sites is not considered.

The single-site, sequence-based analysis function was used here. Running a separate query for each β-defensin gene set, a GC-matched background nucleotide set with a ratio of 100 background sequences for every foreground sequence was generated using the in-built function in oPOSSUM3. Vertebrate PWMs from the CORE, PBM and Pending collections with minimum information content of 8 bits were used. The matrix match threshold was set to 85%. Results were saved in a csv format file and uploaded to RStudio (https://www.rstudio.com/) where the Z scores for each TF were plotted against Fisher scores and the recommended applied threshold was calculated.

To visualise the predicted binding site locations for the over-represented TFs, as provided by oPOSSUM3, β-defensin promoter nucleotide sequences were uploaded into the genome sequence navigation and visualisation software GenePalette (http://www.genepalette.org). TFBS motifs were added as features to the promoter

nucleotide sequences. The vector graphics program Inkscape (https://inkscape.org/en/) was used to compile the R- and GenePalette outputs into figures.

### 2.1.3 Detection of conserved motifs- DREME and TOMTOM (MEME suite)

MEME suite 4.11.1, accessible at http://alternate.meme-suite.org/, is a web-hosted set of motif-based sequence analysis tools. The MEME algorithm is designed to identify short-ungapped DNA motifs which are enriched within a set of DNA or protein sequences. As it does not depend on transcription factor binding site prediction by comparison to a PWM database, it can also be used to discover motifs describing other types of DNA signals. MEME does not constrain the length of the identified motifs, but the MEME web-server does not allow inputs of the size of the 5kb β-defensin promoter ortholog and control nucleotide sequence sets. For this reason the alternative tool DREME was used. This is a less computationally-intensive algorithm as only motifs up to 8 bases in length are identified and it was therefore possible to use the same nucleotide sets as in the oPOSSUM3 analysis. Statistical analysis of the DREME results includes the E-value, a Fisher's Exact Test for enrichment of a motif in the β-defensin promoter set, multiplied by the number of candidate motifs analysed as a form of multiple testing correction. As DREME performs best on short sequences, the EMBOSS Splitter tool (http://www.bioinformatics.nl/emboss-explorer/) was used to fragment the 5kb sequences into 100bp portions with a 10bp overlap. A DREME E-value cut-off of <0.05 is recommended by the MEME suite team and was used in this analysis.

The DREME results page allows every motif to be compared to the JASPAR 2016 vertebrate CORE collection of PWMs via the TOMTOM program within the MEME Suite. A cut-off E-value of 0.05 was used.

### 2.1.4 Prediction of conserved non-coding sequences- MULAN multi-species alignment

MULAN, accessed at http://mulan.dcode.org/, is part of the National Center for Biotechnology Information (NCBI)-hosted DCODE suite of tools which aim to exploit the increasing availability of whole genomes to identify key regulatory elements in the genome. It uses the MULTIZ threaded blockset alignment algorithm to generate a multispecies local alignment by creating a number of pairwise alignments based on the evolutionary relationships set out in a supplied phylogenetic tree. The alignment is split into blocks of orthology whose order does not vary between species, interspersed with non-conserved regions of variable length. This generates an alignment which does not change based on which species is set as the reference to which all others are compared. DNA duplications and inversions are addressed and evolutionarily-conserved regions (ECRs) are graphically represented.

The genomic region containing β-defensin syntenic cluster B was downloaded for five species including bovine, dog, little brown bat and rabbit. Sequences were obtained from the UCSC genome browser and loaded in ApE as described above. Coding exons were annotated as features within the ApE sequence files. Since syntenic cluster B has been split into two on chromosome 20 in the human (Figure 1.2) and the MULAN tool can only accommodate sequences up to 100kb in length, the alignment was carried out in five separate blocks, concatenated into two for the purposes of illustration. The first contains *DEFB132* to *DEFB125* (*DEFB125*a in bovine) and was aligned in two portions and the second includes *DEFB115* to *DEFB124* and was aligned in three segments (Table A.4).

The tba aligner option for finished sequences was selected. Gene annotation files were compiled from ApE. The relationship specified for phylogenetic tree construction was:

((Rabbit Human) (Bat (Cow Dog)))

Within the dynamic visualisation dialog in standard-stacked pairwise format, ECRs were initially determined using the default cut-off of 70% similarity across ≥100bp, in all

four pairwise alignments. Following (Ovcharenko et al., 2004), an increased cut-off of 77% similarity across ≥350bp was also applied. There were no ECRs meeting this criteria across all four pairwise alignments, but there were three common to the bovine-dog, bovine-bat and bovine-human alignments. The relevant sequences were extracted for further analysis by clicking on the ECR within the visualisation and copying the nucleotide sequences.

### 2.1.5 Modelling of transcription factor binding site features within conserved non-coding regions- CLARE

The NCBI DCODE suite contains a tool for the identification of important transcription factors in putative regulatory elements called CLARE (http://clare.dcode.org/). CLARE builds a linear binary classification model, or classifier, of TFBSs that best separates the input from control datasets. Three length- and GC composition-matched sequences are selected for each input sequence from a pool of random human non-coding sequences. The first step is to transform each sequence into a linear vector composed of identified motifs from a pool of 711 features. This includes the JASPAR and TRANSFAC databases of transcription factor PWMs and the top ten *de novo* motifs identified by the PRIORITY algorithm from the input set. Linear regression is used to apply a weight to each feature, with the aim of minimising the number of motifs with a non-zero weight, since most motifs will not be truly important in a given regulatory element. Features irrelevant to the classifier receive a zero weight and those associated receive a non-zero positive or negative weight. The performance of this classifier is assessed by the receiver operating characteristic (ROC). The false positive rate (specificity) is plotted against the true positive rate (sensitivity) i.e., the proportion of true positives versus false positives for a given discrimination threshold (Taher et al., 2012). The area under the curve (AUC) gives an idea of the relationship between false positives and true positives- if the false positive rate is low for a high true positive rate, the area under the curve approaches 1 and the classifier is capable of distinguishing positives from negatives. A random classifier with a diagonal ROC has an AUC of 0.5. CLARE operates

with a false positive rate of 0.05, so the true positive rate at this operating point and the AUC are reported.

It is important to note that the initial TFBS analysis is performed using an optimised cut-off for each TFBS. This means the cut-off is different for each TFBS and is selected to produce no more than one match every 10,000 base pairs on a 1,000,000 base pair random sequence composed from multiple random short fragments from the human genome. In addition, a sample size of 5 sequences is less than would probably be optimal for such tools.

The extracted ECRs, with gaps deleted, were submitted as target sequences, selecting the option to generate 3 length and GC-matched controls per sequence. Under "TFBS Matrices and Species", vertebrate TRANSFAC and JASPAR matrices were specified.

Binding sites for the identified TFs were located using the oPOSSUM3 sequence-based single site analysis tool. The PRIORITY and TRANSFAC PWMs were run using the "custom profiles" option, the TRANSFAC PWMs being downloaded from the TRANSFAC 7.0 public database at http://www.gene-regulation.com/cgi-bin/pub/databases/transfac/search.cgi. An 85% matrix match threshold was used, except in the case of androgen receptor and serum-response factor, where a 75% threshold was used. The PWMs used by CLARE for PIT-1 and GZF1 were from the TRANSFAC Professional database, which can only be accessed by subscription, therefore they were not included in this initial search. The identified binding sites were plotted within the ECR sequences using GenePalette as above.

### 2.1.6 Prediction of transcription factors binding conserved motifs in intergenic evolutionarily-conserved regions

Where PRIORITY motifs were included in the CLARE-generated model, potential TFBSs matching these were analysed by TOMTOM as previously described. STAMP, an alternative program to motif alignment and database comparison was accessed at http://www.benoslab.pitt.edu/stamp/ and run with default settings.

## 2.2 Collection of female reproductive tract tissue samples

Female reproductive tracts (FRTs) from post-pubertal, non-pregnant Holstein-Friesian cows were collected within 30 minutes of slaughter. Four cows in each of the two estrus cycles phases, follicular and luteal, were chosen. Veterinary examination of reproductive tracts identified animals which had been previously pregnant, confirmed the absence of visible disease or pregnancy, and determined whether the cow was in the follicular or luteal phase of the estrus cycle, based on examination of the ovaries. Cows in the follicular phase had no developing or mature corpus lutea and had a developing pre-ovulatory follicle on the ovaries. Cows in the luteal phase had a mature corpus luteum. Vaginal samples were taken from the anterior, or upper, vagina. Cervical samples were collected from the endocervix, which is next to the uterine opening. Endometrial samples were collected from between visible caruncles, within the ipsilateral horn on the same side as the developing follicle/corpus luteum. Oviduct samples were taken from the ampulla, which was located based on intermediate distance from either end of the oviduct. The ovary was sampled by avoiding developing follicles or corpus lutea. Scissors and forceps were used to dissect away portions of each tissue, which were then stored in 2mL cryovials and snap-frozen in a liquid nitrogen-charged dry shipper (List of materials used given in Table 2.2). Duplicate samples were also stored in 10% neutral-buffered saline for future histological analysis if necessary (List of reagents used given in Table 2.2).

## 2.3 List of reagents, materials and equipment used

**Table 2.1 Table of reagents used with manufacturer details**

| Reagent | Company | Location |
|---|---|---|
| **Primary Cell Isolation and Culture** | | |
| 10% Neutral-buffered formalin | Sigma-Aldrich | Poole, UK |
| 1α,25-dihydroxyvitamin D3 | Sigma-Aldrich | Poole, UK |
| Accutase Cell Detachment Solution | Biolegend | San Diego, CA, USA |
| Amphotericin B solution | Sigma-Aldrich | Poole, UK |
| Bovine Serum Albumin | Sigma-Aldrich | Poole, UK |
| Collagenase II | Sigma-Aldrich | Poole, UK |
| Distilled, sterile, nuclease-free water | Gibco (Thermo Fisher Scientific) | Paisley, UK |
| DNAse I | Sigma-Aldrich | Poole, UK |
| Fetal Bovine Serum | Gibco (Thermo Fisher Scientific) | Paisley, UK |
| Hank's balanced saline solution | Gibco (Thermo Fisher Scientific) | Madison, WI, UK |
| IL-17A, human, recombinant | Peprotech EC Ltd. | London, UK |
| IL-1β, bovine, recombinant | Thermo Fisher Scientific | Paisley, UK |
| IL-22, human, recombinant | Peprotech EC Ltd. | London, UK |
| Insulin-Transferrin-Selenium-Ethanolamine (ITS-X) | Gibco (Thermo Fisher Scientific) | Paisley, UK |
| Lipofectamine 2000 | Invitrogen (Thermo Fisher Scientific) | Paisley, UK |
| Opti-MEM | Gibco (Thermo Fisher Scientific) | Paisley, UK |
| Penicillin-Streptomycin 100X | Gibco (Thermo Fisher Scientific) | Paisley, UK |
| Phosphate-buffered saline (PBS) | Gibco (Thermo Fisher Scientific) | Paisley, UK |
| Poly(deoxyadenylic-thymidylic) acid-Poly(dA:dT) | Sigma-Aldrich | Poole, UK |
| Poly(inosinic:cytidylic) acid, low molecular weight | InvivoGen | San Diego, CA, USA |
| RNA Later | Ambion (Thermo Fisher Scientific) | Paisley, UK |
| RPMI 1640 + Glutamax | Gibco (Thermo Fisher Scientific) | Paisley, UK |
| Trypan blue | Sigma-Aldrich | Poole, UK |
| Trypsin 0.5% EDTA | Sigma-Aldrich | Poole, UK |
| **Molecular Biology** | | |
| 100bp DNA Ladder | Invitrogen (Thermo Fisher Scientific) | Paisley, UK |
| Agarose | Sigma-Aldrich | Poole, UK |
| Chloroform | Sigma-Aldrich | Poole, UK |
| Ethanol, molecular grade | Sigma-Aldrich | Poole, UK |
| Glycogen from blue mussel | Sigma-Aldrich | Poole, UK |
| GoTaq qPCR master mix | Promega | Madison, WI, UK |
| HotStar Taq Plus DNA Polymerase | Qiagen | Crawley, UK |
| Isopropanol/2-propanol | Sigma-Aldrich | Poole, UK |
| Oligo-dT Primers | Qiagen | Crawley, UK |
| Omniscript cDNA synthesis kit | Qiagen | Crawley, UK |
| PCR clean-up kit | Promega | Madison, WI, UK |
| PowerUp SYBR Green Master Mix | Applied Biosystems (Thermo Fisher Scientific) | Paisley, UK |
| SybrSafe DNA Gel Stain 10000X | Invitrogen (Thermo Fisher Scientific) | Paisley, UK |
| TRIzol | Ambion (Thermo Fisher Scientific) | Paisley, UK |

| | | |
|---|---|---|
| **Immunofluorescent staining of endometrial stromal cell cytoskeletal proteins** | | |
| 4',6-diamidino-2-phenylindole (DAPI) | Sigma-Aldrich | Poole, UK |
| Goat polyclonal anti-mouse secondary antibody (FITC) | Abcam | Cambridge, UK |
| Murine anti-human cytokeratin, clone F7.2.38 | Dako (Agilent Technologies) | Santa Clara, CA, USA |
| Murine anti-human vimentin, clone V1 | Sigma-Aldrich | Poole, UK |
| Murine IgG1 isotype control, clone MOPC 21 | Sigma-Aldrich | Poole, UK |
| **Histological processing of endometrial samples** | | |
| Haemotoxylin | Leica Biosystems | Newcastle, UK |
| Histoclear | National Diagnostics | Atlanta, GA, USA |
| Magnesium sulfate | Sigma-Aldrich | Poole, UK |
| Sodium bicarbonate | Sigma-Aldrich | Poole, UK |
| Surgipath mounting medium | Leica Biosystems | Newcastle, UK |

**Table 2.2 List of materials used, with manufacturer details**

| Reagent | Company | Location |
|---|---|---|
| **Primary Cell Isolation and Culture** | | |
| 0.2-µm mesh syringe filter | Sartorius | Göttingen, Germany |
| 15/50mL centrifuge tubes | Greiner Bio-One | Kremsmünster, Austria |
| 2mL cryovials | Thermo Fisher Scientific | Paisley, UK |
| 3.5mL transfer pastettes | Sarstedt | Nümbrecht, Germany |
| 40-µm mesh cell strainer | Becton Dickinson | Flintshire, United Kingdom |
| 5/10/25mL serological pipettes | Greiner Bio-One | Kremsmünster, Austria |
| 6/24-well flat bottom tissue culture plates | Greiner Bio-One | Kremsmünster, Austria |
| 70-µm mesh cell strainer (pluriStrainer) | pluriSelect Life Science | Leipzig, Germany |
| Falcon brand 50mL centrifuge tubes | Becton Dickinson | Flintshire, United Kingdom |
| Petri dishes | Greiner Bio-One | Kremsmünster, Austria |
| Scalpels | Swann Morton | Sheffield, UK |
| 75/175cm$^2$ tissue culture flasks | Greiner Bio-One | Kremsmünster, Austria |
| **Molecular Biology** | | |
| 0.2mL nuclease-free microcentrifuge tubes | Sarstedt | Nümbrecht, Germany |
| 1.5/2.0mL nuclease-free, sterile microcentrifuge tubes | Thermo Fisher Scientific | Paisley, UK |
| 96-well plates | Thermo Fisher Scientific | Paisley, UK |
| Optical adhesive film | Applied Biosystems (Thermo Fisher Scientific) | Paisley, UK |
| P10/20/200/1000 sterile, nuclease-free filtered pipette tips | Thermo Fisher Scientific | Paisley, UK |
| Stainless steel beads 3mm | Qiagen | Crawley, UK |
| **Histological processing of endometrial samples** | | |
| Surgipath casettes | Leica Biosystems | Newcastle, UK |

**Table 2.3 List of equipment and proprietary software used**

| Equipment/Software | Company | Location |
|---|---|---|
| Graphpad Prism 7.02 for Windows | GraphPad Software, Inc | San Diego, CA, USA |
| Mx3000P qPCR system | Stratagene Corporation | La Jolla, CA, USA |
| Gel Logic 200 Imaging System | Kodak | Rochester, NY, USA |
| MxPro v4.10 | Stratagene Corporation | La Jolla, CA, USA |
| NanoDrop Spectrophotometer | Thermo Fisher Scientific | Paisley, UK |
| Olympus IX81 upright microscope | Leica Biosystems | Newcastle, UK |
| Olympus BX51 inverted microscope | Leica Biosystems | Newcastle, UK |
| StepOne Software v2.3 | Applied Biosystems (Thermo Fisher Scientific) | Paisley, UK |
| StepOnePlus Real-Time PCR system | Applied Biosystems (Thermo Fisher Scientific) | Paisley, UK |
| Techne Prime Thermocycler | Bibby Scientific | Staffordshire, UK |
| Tissue Lyser II | Qiagen | Crawley, UK |

## 2.4 Primary endometrial stromal cell culture

### 2.4.1 Generation of primary endometrial stromal cell cultures

Reproductive tracts from non-pregnant, post-pubertal cows free of visible disease were collected at the abattoir within 30 minutes of slaughter. Only tracts in the early luteal stage of estrus were used, as determined by the presence of a stage 1 corpus luteum on one ovary. This is because progesterone levels are basal at this time (Ireland et al., 1980), ensuring consistency between experiments.

Collection of endometrial tissue was performed immediately at the abattoir. The outside of the tract was rinsed with 70% ethanol before being opened with sterile scissors at the base of the uterine horn beside the ovary with the corpus luteum (ipsilateral horn). The endometrial surface was rinsed with phosphate-buffered saline (PBS) without $Ca^{2+}$ and $Mg^{2+}$ ions supplemented with 50IU penicillin, 50µg/mL streptomycin and 2.5µg/mL amphotericin B. A sterile scissors and forceps were used to remove the endometrial surface from the ipsilateral uterine horn, collecting the tissue into a 50mL centrifuge tube containing 20mL of Roswell Park Memorial Institute medium (RPMI) 1640 supplemented with antibiotics as above. A section of un-sampled endometrium was stored in 10% neutral-buffered formalin. Another sample was stored in RNA Later for bovine herpesvirus DNA PCR. Samples were transported to the laboratory at room temperature within 90 minutes of collection. The tissue was rinsed twice in room temperature Hank's balanced salt solution (HBSS) supplemented with antibiotics as previously. A sterile scalpel was used to chop the tissue down to 1-3$mm^3$, before placing it in a Falcon brand 50mL centrifuge tube with 10mL antibiotic-supplemented HBSS and incubating at 37°C for 10 minutes. A sterile transfer pastette was used to remove as much HBSS as possible, before adding 10mL digestive solution pre-warmed to 37°C. 100mL digestive solution consisted of 375 BAEE units of trypsin-EDTA, 50mg collagenase II, 100mg bovine serum albumin (BSA) and 10mg DNase I, made up to 100mL with HBSS and 0.2µm sterile filtered. Samples were placed in a 37°C shaking incubator at 150rpm for 1 hour. The resulting mixture was filtered through a 70µm nylon mesh strainer, collecting the filtrate in a Falcon brand 50mL centrifuge tube containing 20mL HBSS with 10% fetal

bovine serum. This cell suspension was then filtered through a 40μm nylon mesh cell strainer. The filtrate from the 40μm filter contained stromal cells and was collected in one tube. The cells were pelleted by centrifugation at 400 x *g* for 10 minutes. Red blood cells were lysed by resuspending the pellet in 1mL sterile water and tapping the tube gently for 5 seconds before addition of 10mL complete growth medium. This consisted of RPMI 1640 supplemented with antibiotics as above, 10% fetal bovine serum and 1X insulin, transferrin, selenium supplement with ethanolamine (ITS-X). The cells were pelleted as before and red blood cell lysis repeated if necessary. The stromal cell suspension was split between two 175 $cm^2$ flasks with complete growth medium. These were stored in a 37°C incubator in 5% $CO_2$ in air for 24 hours, to allow stromal cells to adhere. The growth media was changed to remove any debris and was changed every 48 hours thereafter until the cells were 70% confluent. Visual examination of cell morphology under the light microscope was used to check purity of cultures.

### 2.4.2 Quantification of bovine herpesvirus DNA in endometrial tissue samples

RNA Later-preserved endometrial samples collected from uteri used for primary cell isolation were sent to the Virology Division of the Department of Agriculture, Food and the Marine Central Veterinary Research Laboratory. DNA was extracted and quantitative PCR for bovine herpesvirus (BoHV-)1 and -4 carried out. β-actin was quantified as a control. Both tests are accredited by the Irish National Accreditation Body to ISO17025. One sample tested positive for BoHV-4 and one was inconclusive for BoHV-1.

### 2.4.3 Immunofluorescent staining of endometrial cell cytoskeletal proteins

$2x10^4$ were seeded into 24-well tissue culture plates in complete growth medium, allowing one well each for vimentin staining (expressed by stromal cells), cytokeratin staining (expressed by epithelial cells) and an IgG1 isotype control, and allowed to settle for 12 hours. Growth medium was removed, the cell monolayer was rinsed three times with PBS and fixed with 10% neutral-buffered formalin at room temperature for 1 hour.

Formalin was removed and the cells washed three times with PBS before the primary antibody was added. Mouse anti-human vimentin antibody, mouse anti-human cytokeratin or IgG1 isotype control were applied as appropriate using 400µL per well of a 1:100 dilution in PBS. Cells were incubated at 4°C with rocking overnight. A FITC-conjugated polyclonal goat anti-mouse secondary antibody was applied to all wells in a 1:250 dilution, incubating at 37°C for 1 hour. After rinsing, DAPI stain for nuclei detection was applied in a 1:250 dilution for 10 minutes at 37°C. An Olympus IX81 inverted microscope was used to detect immunofluorescence, with positive vimentin staining in the absence of cytokeratin staining taken to indicate a pure endometrial stromal cell culture (List of equipment used in Table 2.3).

### 2.4.4 Detection of leukocyte contamination of primary endometrial cell cultures via *PTPRC* polymerase chain reaction (PCR)

The HotStar Master Mix PCR kit was used to carry out a PCR reaction to detect transcription of the protein tyrosine phosphatase, receptor type C (PTPRC) gene, encoding the pan-leukocyte marker CD45, within endometrial cell cultures. A 10µL reaction volume contained 0.3µL endometrial stromal cell cDNA, 1X CoralLoad reaction buffer, 200µM dNTP solution, 0.3µL HotStar Taq polymerase enzyme and 300nM *PTPRC*-specific primers (Integrated DNA Technologies, Leuven, Belgium; sequences obtained from Herath et al., (2006)), with nuclease-free water making up the remainder. cDNA prepared from bovine PBMCs was used as a positive control for *PRPTC* amplification. The constitutively-expressed gene ribosomal protein S6 (*RPS9*) (see Table A.7 for primer sequence) was amplified from all samples to ensure poor cDNA quality did not account for a lack of amplification. A non-template control without cDNA was run for both gene assays. The PCR reaction was carried in a Techne Prime thermocycler using the following thermocycling conditions: 95°C for 5 min and 40 cycles of 95°C for 30 sec, 60°C for 1 min, 72°C for 1 min. Results were assessed by presence or absence of a DNA product of expected size on a 2% agarose gel after electrophoresis.

### 2.4.5 Histological processing of endometrial samples

Endometrial biopsies were removed from formalin and immersed in 70% ethanol for 24 hours before overnight paraffin wax embedding in Surgipath cassettes. Embedded biopsies were sectioned at 3μm, dewaxed by Histoclear and rehydrated with 100%, 90%, 80% and 75% alcohol immersion steps. Haematoxylin was applied to the tissue sections for 10 minutes before immersion in Scott's tap water (30g magnesium sulfate and 2g sodium bicarbonate in 3L tap water) for 5 minutes. Tissue sections were progressively dehydrated by a reversal of the ethanol immersion steps used previously and mounted with Surgipath mounting medium. Slides were examined using an Olympus BX51 upright microscope.

### 2.4.6 Stimulation of cells

Primary endometrial stromal cells were plated after first passage, using Accutase cell dissociation reagent to detach the cells from the flasks. $1x10^5$ cells were plated into 6-well plates, allowing 1 well per treatment, and left to adhere for 12 hours before stimulation. The relevant stimuli were applied at a range of concentrations and left for 6, 12, 18 or 24 hours.

Where poly(I:C) or poly(dA:dT) were transfected into cells, the transfection reagent Lipofectamine 2000 was used. Lipofectamine-nucleic acid complexes were formed in Opti-MEM reduced serum medium as per manufacturer's instructions, before being added to the cell culture medium. A mock transfection treatment of Lipofectamine 2000 only was included in these experiments. As 1α,25-dihydroxyvitamin D3 (1,25D) stock solutions were prepared in ethanol, these experiments also included an ethanol-only vehicle control.

For 1,25D-nucleic acid combination experiments, cells were treated with 100nM 1,25D or the corresponding volume of ethanol for 12 hours, before the culture medium was changed and fresh 1,25D/ethanol was added with or without untransfected poly(I:C) or transfected poly(dA:dT). Cell were harvested after 24 hours.

In all cases, the cells were harvested using 1mL TRIzol per well and the suspensions stored at -80°C until processed.

## 2.5 Quantitative PCR (PCR)

### 2.5.1 RNA extraction

Total RNA was extracted using a phenol-chloroform extraction protocol. FRT tissue samples (~50mg per extraction) were disrupted by placing the tissue in a 2mL microcentrifuge tube with 1mL of TRIzol and a 3mm stainless steel bead. The tubes were loaded into the Tissue Lyser II which was run at full speed for 1.5-2.5 minutes, until the sample was completely broken down. Frozen TRIzol cell suspensions were allowed to defrost and remain at room temperature for 5 minutes. All tubes were centrifuged at 12,000 x *g* for 10 minutes at 4ºC to precipitate cell debris (and stainless steel bead). The supernatant was transferred to a clean tube and 200µL of chloroform added. The tubes were vigorously mixed for 15 seconds and incubated for 3 minutes at room temperature before centrifugation at 12,000 x *g* for 15 minutes at 4ºC. At this point, the samples had separated into 3 phases: an upper aqueous phase containing RNA and some DNA, an interphase containing DNA and an organic phase containing proteins and lipids. 600µL of the upper aqueous phase were transferred into a new tube containing 500µL of isopropanol/2-propanol. 1µL of molecular grade glycogen from blue mussel was added to endometrial stromal cell extractions to increase precipitation of RNA. Samples were then vortexed for 30 seconds and incubated at -20ºC, leaving FRT isolations for 1 hour and endometrial stromal cell isolations for 4 hours. After incubation, samples were centrifuged at 12,000 x *g* for 10 minutes at 4ºC. The supernatant was removed and discarded without disturbing the white gel-like RNA pellet. This was resuspended in 1mL of 75% ethanol, prepared with nuclease-free water. The samples were centrifuged at 7,600 x *g* for 5 minutes at 4ºC. The supernatant was removed and a second ethanol wash performed. The remaining pellet was air dried for 2 minutes to evaporate residual ethanol before being dissolved in 35µL nuclease-free water. Samples were then incubated at 55ºC for 5 minutes to dissolve RNA and stored at -80ºC. RNA quantity was determined by measurement of absorbance at 260nm using a NanoDrop spectrophotometer. A260/280nm and A260/230nm ratios were checked to assess presence of non-nucleic acid contaminants. RNA quality was evaluated by 2% agarose gel electrophoresis with Sybr SAFE staining, where the presence of 28S and 18S ribosomal RNAs as discrete

bands, with minimal smearing indicative of RNA degradation, or high molecular weight products, indicative of DNA contamination, was assessed.

### 2.5.2 cDNA synthesis

300ng of endometrial stromal cell RNA, or 1000ng of FRT tissue RNA per sample was reversed transcribed using the Omniscript RT kit and oligo dT primers for mRNA priming. A 20µL total reaction volume contained 1X reaction buffer, 16ng Oligo dT, 1µM dNTP solution, 1µL of Omniscript reverse transcriptase enzyme and 300/1000ng RNA, with nuclease-free water making up the remainder. Required RNA quantities were calculated using the RNA quantity determined by the NanoDrop. The reaction was carried out in a Techne Prime thermocycler, incubating at 37°C for 1 hour before a 5 minute 95°C phase to denature the enzyme. FRT cDNA solutions were diluted 1:10 in nuclease-free water, while endometrial stromal cell cDNA solutions were diluted 1:6 before storage at -20°C.

### 2.5.3 Quantitative PCR primer design

Where fully-annotated GenBank records existed for a gene, Primer-BLAST (http://www.ncbi.nlm.nih.gov/tools/primer-blast/) was used to design qPCR primers, supplying the GenBank accession number and specifying a product of between 70 and 250bp in length, which spanned an exon-exon junction to avoid amplification of any contaminating genomic DNA and was gene-specific as determined by comparison with the bovine nr database. Alternately, junction-spanning primers were picked manually, using Beacon Designer (http://www.premierbiosoft.com/qOligo/Oligo.jsp?PID=1) to ensure similarity of melting point and low primer-dimerising potential. *CYP24A1* primer sequences were taken from Merriman et al., (2015) All primers were synthesised by Integrated DNA Technologies in lyophilised form and resuspended in the lab in nuclease-free water. Primer solutions were aliquoted into working stocks to avoid excessive freeze-thaw.

### 2.5.4 Quantitative PCR

The GoTaq qPCR Master Mix Kit and Mx3000P qPCR system with MxPro v4.10 software was used for the FRT study (See Table 2.3 for a list of all proprietary software used). A 20µL reaction volume contained 10µL pre-made qPCR master mix, the desired concentration of gene-specific primers (varied during optimisation, or see Table A.7 for optimal concentrations) and 2µL cDNA, with nuclease-free water making up the remainder. As the above qPCR machine was replaced during this project, PowerUp SYBR Green Master Mix and StepOnePlus Real-time PCR System with StepOne Software v2.3 was used for endometrial stromal cell experiments. A 10µL reaction volume contained 8µL pre-made qPCR master mix, primers (see Table A.8 for optimal concentrations), 2µL cDNA and nuclease-free water. A non-template control was included in each gene assay to detect molecular contamination. All reactions were carried out in triplicate. The thermocycling program for the FRT study with the GoTaq qPCR master mix was: 10 min polymerase activation at 95°C, 40 cycles of 95°C for 30 sec, primer-specific annealing temperature for 1 min, 72°C for 30 sec; dissociation curve analysis at 95°C for 1 min, 55°C for 30 sec and 95°C for 30 sec.

The program for the endometrial stromal cell experiments with the PowerUp master mix was: 2 min at 50°C, 2 min at 95°C, 40 cycles of 95°C for 3 sec and primer-specific annealing temperature for 30 sec; dissociation curve analysis at 95°C for 15 sec, 60°C for 30 sec and 95°C for 15 sec.

After all qPCR assays, the absence of an amplification product within the non-template control was confirmed by absence of a plate $C_q$ value and dissociation curves were checked for absence of non-specific amplification as determined by the presence of a single amplification peak.

### 2.5.5 Quantitative PCR assay optimisation

A cDNA sample with high expression of the targeted gene was used to optimise the qPCR assay conditions. For the FRT study, the optimal primer annealing temperature was determined by running a PCR reaction on the Techne Prime thermocycler, using the qPCR reaction master mix with a 300nM primer concentration. The thermocycling conditions given above for the GoTaq master mix were used, except the primer annealing phase consisted of a 55-65°C temperature gradient. Dissociation curve analysis was performed by subsequently running the same plate in the Mx3000P qPCR machine using just the dissociation curve phase of the thermocycling program. For the endometrial stromal cell study, the StepOnePlus machine was used to run a temperature gradient qPCR with annealing phase temperatures of 55-65°C. The optimal temperature was assessed via examination of dissociation curves for a single peak and via 2% gel electrophoresis, choosing a temperature which resulted in the brightest band of expected size.

Optimal primer concentration was determined by titration. The concentration which achieved the lowest $C_q$ value while still generating a single product (single band after gel electrophoresis, single peak on dissociation curve) was selected.

The efficiency of each primer set with the specified reaction conditions was determined by running a reaction with 5 point 5-fold or 2-fold serial dilutions of the positive control cDNA, using the 2-fold series where the positive control $C_q$ values were in high twenties and upwards. The standard curves were represented as the semi-log regression line plot of $C_q$ value vs. log of the relative input cDNA concentration. The efficiencies were calculated using formula:

$E = 10^{(-1/Slope)}-1;$

$\%E=(10^{(-1/Slope)}-1) \times 100$

Efficiencies between 85% and 110% were considered acceptable. Where an efficiency of >100% was found, a 100% efficiency was used in calculations. The specificity of each primer set was determined by Sanger sequencing (GATC Biotech, Konstanz, Germany) of PCR products, examining electropherograms for single peaks at each position to confirm a single amplicon and running the returned sequence through

BLAST (http://blast.ncbi.nlm.nih.gov/Blast.cgi) to ensure the desired gene target was amplified.

### 2.5.6 qPCR data processing

$C_q$ data was analysed using the method described by Hellemans et al. (2007). For the FRT study, transcript abundance relative to a reference gene panel was calculated. Logarithmic Cq values were transformed into linear relative quantities using the formula:

$$RQ = E^{(Cq\ (sample) - Cq\ (sample\ with\ lowest\ Cq\ for\ that\ gene))}$$

For the endometrial stromal cell experiments, fold change in gene expression in a stimulated sample relative to an unstimulated control sample was calculated. In this case, relative quantities were obtained using the formula:

$$RQ = E^{(Cq\ (unstimulated\ control) - Cq\ (stimulated\ sample))}$$

This results in each unstimulated control value being set to 1, with stimulated samples expressed as fold changes relative to this unstimulated control.

RQ values for five potential reference genes amplified in poly(I:C)-stimulated stromal cell cDNA from three animals or from FRT samples from four animals were entered into Genorm analysis software (https://genorm.cmgg.be/). These genes were *RPS9*, *MRPS6*, *SF3A1*, *TUBA1B* and *RPL13A*. Genorm calculated the average expression stability (M) value for all five genes. The three genes with the lowest M values were the most stably-expressed and were chosen to form the reference gene panel. A normalisation factor was calculated for each sample as follows:

$$Normalisation\ Factor = Geometric\ mean\ (RQ_{Ref\ Gene\ 1}, RQ_{Ref.\ Gene\ 2}, RQ_{Ref\ Gene\ 3})$$

The normalised relative quantity, i.e., final relative abundance or fold change relative to unstimulated control: NRQ=RQ/Normalisation Factor

### 2.5.7 Statistical Analysis

Statistical analysis was carried out using GraphPad Prism 7 software.

For endometrial stromal cell experiments with one stimulus concentration and multiple time points or multiple stimuli/concentrations at one time point, a Friedman's one-way non-parametric, repeated-measures ANOVA was used. This was followed by Dunn's post hoc comparison of each stimulated sample to the unstimulated control.

For endometrial stromal cell experiments with multiple concentrations of a stimulus and multiple time points, a repeated-measures, two-way ANOVA was used, with time and concentration as factors. This was followed by Dunnett's post hoc multiple testing correction, comparing each concentration to the unstimulated control within the same time point.

For the FRT study, an ordinary two-way ANOVA was used, including tissue and stage of estrus cycle as factors. As this detected no significant differences, no post hoc testing was performed.

# Chapter 3 *In-silico* prediction of transcriptional regulation mechanisms of β-defensin genes

## 3.1 Introduction

### 3.1.1 Computational analysis of gene regulation

As the body of genome-wide association studies identifying disease-associated variants in non-coding regions grows (Hindorff et al., 2009), so too does interest in understanding the function of these regions in the regulation of gene expression. The Encyclopedia of DNA Elements (ENCODE) project has confirmed that the majority of disease-causing genetic variants lie in non-coding regions and has utilised a high-throughput approach to identify the spatio-temporal context in which many of these regions may be active (ENCODE Consortium, 2012). However, researchers working on non-human species or on tissue types not currently well represented in the ENCODE data are largely unable to use this wealth of data to their advantage. The types of biochemical assays being carried out within ENCODE are technically difficult and expensive for non-specialist labs (Blatti et al., 2015). In light of this, it is not surprising that the concept of using a bioinformatics approach to identify a subset of likely DNA regulatory elements for experimental validation has received considerable attention over the past number of years (reviewed by Kellis et al., 2014, Hardison and Taylor, 2012).

The increasing availability of whole genome assemblies means a comparative genomics approach has been integral in attempts to computationally identify regulatory elements in the non-coding genome. Phylogenetic footprinting, a term first coined by Tagle et al. in 1988, (reviewed by Ureta-Vidal et al., (2003)), refers to the identification of putative regulatory elements in non-coding DNA regions through cross-species comparison, working on the assumption that functional elements are relatively conserved over the course of evolution compared to the surrounding non-functional DNA.

Such approaches usually attempt to identify likely binding sites for transcription factors (TFs). These proteins represent the terminal stage of a transcription-regulating cell

signalling pathway, and their binding to accessible nuclear DNA in a sequence-specific manner initiates or blocks transcription through interaction with the basal transcriptional machinery (Mitchell and Tjian, 1989). DNA affinity- and ChIP assays, including the high-throughput ChIP-Seq approach, have facilitated empirical identification of the short DNA motifs to which these TFs bind. This information has been compiled in position weight matrices (PWMs) (Figure 3.1). Several databases of such PWMs have been compiled, including open-source JASPAR and proprietary TRANSFAC. These databases facilitate computational analysis of candidate DNA regulatory regions to identify putative transcription factor binding sites (TFBSs).

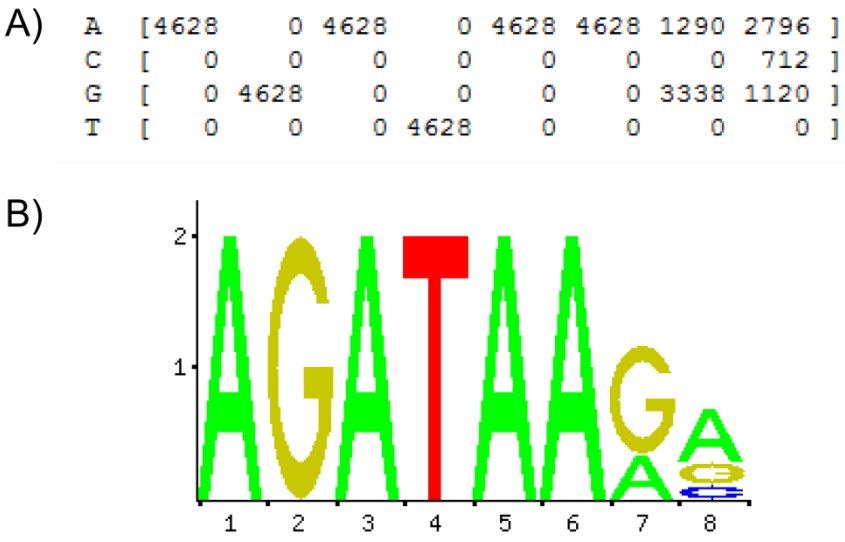


**Figure 3.1 Position-weight matrix and sequence logo for the transcription factor GATA3**
A) The GATA3 PWM was compiled from ChIP-Seq experiments carried out in human cells in which a GATA3-specific antibody was used to isolate DNA motifs bound by GATA3 across the entire human genome. Compilation of the sequenced motifs indicates the nucleotides at positions 1-6, indicated on the horizontal axis, are constrained, while those at 7 and 8 are more variable. B) This is represented visually by the sequence logo shown. This PWM (ID MA0037.2) is part of the JASPAR 2016 open-source database, which contains 519 vertebrate transcription factor PWMs. Accessed at [1].

Spatio-temporal specificity of transcription is conferred by the binding of several transcription factors in concert to sites whose proximity is constrained to a cis-regulatory module (CRM) of up to 1000bp in length. Identification of these CRMs is a core goal in computational identification of candidate regulatory regions (Hardison and Taylor, 2012).

[1] http://jaspar.genereg.net/cgi-bin/jaspar_db.pl

These modules are located in gene promoters, introns or intergenic enhancers or insulators.

The promoter of a gene is located immediately upstream of the transcription start site and is composed of core and proximal regions (Juven-Gershon and Kadonaga, 2010). The core promoter occupies the first ~50bp upstream and binds the essential transcription factors involved in the RNA Pol II complex, though it is now recognised that there is no one defining feature common to all eukaryotic core promoters. The proximal promoter is more difficult to define but is at least several hundred base pairs long, with 1kb being commonly used in experimental analyses and 5kb being common in computational analysis.

Leung et al. (2000) used a phylogenetic footprinting approach to map regions of the promoter of the *TNF* gene, encoding the TNFα protein, that were conserved among the human and seven other non-human primates. They found a 69bp CRM which was highly conserved between species and contained binding sites for three transcription factors driving *TNF* expression in B and T cells.

While promoter regions are undoubtedly important in controlling gene expression, regulatory elements also occur in 3'UTR, intronic and intergenic regions (Hindorff et al., 2009). The second intron of the *IL4* gene, encoding interleukin 4 (IL-4), contains binding sites for several transcription factors and mutations in each affect gene expression in mast cells (Hural et al., 2000).

Intergenic regulatory elements can be up to 1 Mb from the gene(s) they regulate and are defined as enhancers which activate transcription or insulators which suppress transcription (Hardison and Taylor, 2012). Such elements contact gene promoters by DNA looping or DNA diffusion (reviewed by Marsman and Horsfield, 2012). Alignment of 1 Mb of DNA containing 20 genes, including the interleukins *IL4*, *IL5* and *IL13*, between mouse and human, identified a number of regions which were conserved with >70% identity across at least 100bp, including one previously validated intergenic enhancer (Loots et al., 2000). The largest unvalidated putative regulatory element was conserved to greater than 80% identity across 5 mammals, despite the conservation of the surrounding interleukin genes being lower than this. When the function of this element was tested, deletion of the element led to fewer IL-4 and IL-13 producing $T_H2$ cells and

IL-5 expression was reduced (Loots et al., 2000). Thus, genes can be regulated by more distal elements, with conservation of sequences aiding in identification of these elements.

### 3.1.2 Transcriptional regulation of β-defensins

The broad expression of β-defensins as a group, coupled with the apparent pleiotropic nature of their function, suggests the mechanisms underlying their regulation may be similarly complex. A conservation-based *in silico* approach may aid the identification of putative regulatory elements without *a priori* bias towards particular transcription factors and known biological processes. This is appropriate given that the current body of work investigating the role of these genes has focused on a small number of genes, with the function of genes on syntenic clusters A, B and C being relatively understudied.

A computational approach has been used to identify TFs whose binding sites were conserved among whole families of HDPs (Brahmachary et al., 2006). A pool of 76 gene promoters from human, mouse and rat, across 22 HDP families was compiled. Thirteen β-defensin genes were included: two human and three murine genes from syntenic cluster B and three human, four murine and one rat gene from syntenic cluster D. An in-house motif identification program identified short motifs common within each HDP gene family and compared these to the TRANSFAC database of PWMs, identifying 78 transcription factors. TFs for which binding sites were identified within the β-defensin promoters included the nuclear hormone receptors glucocorticoid receptor (GR), androgen receptor (AR), vitamin D receptor (VDR), retinoid X receptor α (RXRα), retinoic acid receptor α (RARα), liver X receptor α- retinoid X receptor α heterodimer (LXRα-RXRα), thyroid hormone receptor α (T3Rα) and the homeo transcription factors Meis-1a and Meis-1b. Nuclear hormone receptors were one of the most frequently identified families across all HDP families, along with nervous system- and liver-specific transcription factors.

This study included a small number of genes and grouped all the β-defensins together, although existing expression data suggest syntenic clusters B and D differ in their characteristic location of expression and possibly function. Additional mammalian

genome assemblies and more comprehensive data on TFs and their binding sites available today means the application of *in silico* approaches toward understanding the regulation of β-defensin genes is well worth revisiting in a more focused manner. The fact that these genes are a paralogous group forming several clusters suggests the possibility of regulation via intergenic elements within the cluster, as has been shown for the $T_H2$ interleukins (Loots et al., 2000), warrants investigation.

Syntenic clusters B and D are both of interest to this group. However, the orthology of syntenic cluster D between bovine and the wider mammalian phylogenetic tree is more complicated than for syntenic cluster B. In humans, β-defensin syntenic cluster D is located on chromosome 8 and has been duplicated at two distinct loci within the chromosome. This cluster contains human β-defensin genes *DEFB1*, *DEFB4A* and *DEFB103* to *DEFB109*, with the region from *DEFB4A* to *DEFB107* being copy number variable as a single block (Groth et al., 2008; Hardwick et al., 2011). The number of copies of this block at each locus varies between individuals, with total β-defensin block copy numbers ranging from 1 to 12 per diploid genome.

Phylogenetic analysis previously carried out in our lab (Meade et al., 2013, see Figure 1.1) indicates *DEFB1* and *DEFB4A* have been expanded within the bovine genome, with each having several potential bovine orthologs. This probably represents a combination of genuine gene expansion, copy number variation and genome assembly error. Thirteen peptides of highly similar sequence have been extracted from the neutrophil granules of a single animal (Selsted et al., 1993), indicating genuine gene expansion/copy number variation. However ongoing issues with assembly of the bovine genome complicate the annotation of the cluster D β-defensin gene region. Comparison between the two independent assemblies indicates that a high proportion of the regions annotated as segmental duplications are actually assembly errors (Zimin et al., 2012). Particularly, there is a cluster of duplications within the β-defensin syntenic cluster D region that do not agree between both assemblies (Adelson et al., 2014). Current attempts to improve the genome annotation in this region may make bioinformatics analysis more viable in the near future (Andersson et al., 2015).

The current bovine genome assembly indicates *DEFB103* to *DEFB109* are in one-to-one orthology between bovine and human, however expression of most of these genes

has never been demonstrated in the bovine. *DEFB103* is expressed in a wide range of bovine tissues (Mirabzadeh-Ardakani et al., 2014) and is upregulated 7 DPP in the endometrium of cows whose uterine inflammation has resolved by 21 DPP (Foley et al., 2015). *DEFB106* is expressed in the caput epididymis in humans (Yamaguchi et al., 2002) and the human peptide has antimicrobial properties (Xin et al., 2014). Therefore, it is particularly interesting in the context of male fertility. However, the regulation of *DEFB106* has not been investigated.

In contrast, experimental evidence indicates activator protein 1 (AP-1) regulates *DEFB103* in some human cell types, with AP-1 but not NF-κB sites predicted in the human *DEFB103* promoter (Peng Jia et al., 2001). *C. albicans* (Steubesand et al., 2009), histamine (Ishikawa et al., 2009) and prostaglandin (Kanda et al., 2010) all induce MAPK signalling and *DEFB103* expression in human keratinocytes, though AP-1 involvement was not demonstrated in every case. AP-1 is necessary for *DEFB103* induction in human pulmonary epithelial cells exposed to *Moraxella catarrhalis* and *Legionella pneumonia* bacteria (Haarmann et al., 2015; Scharf et al., 2010).

Regulation of bovine *DEFB103* may or may not be similar. For instance, the existing data on transcriptional regulation of the host defence peptide gene cathelicidin indicates there are broad differences between rodents and primates. Murine bronchial epithelium and macrophages upregulate cathelicidin expression in response to *M. tuberculosis* infection (Castañeda-Delgado et al., 2010), while human PBMCs downregulate expression in response to the same stimulus (Martineau et al., 2007). In contrast, induction by vitamin D is specific to primates (Dimitrov and White, 2016). This is due to insertion of a vitamin D response element-containing transposable element within primate cathelicidin genes (Gombart et al., 2009).

A comparative genomics approach is still worth applying as the existing data indicates a broadly similar pattern of expression for syntenic cluster B genes. The results for *DEFB103* can be compared to the existing experimental data for this gene, thus indicating whether *DEFB103* is similarly regulated in different mammals. With a relative

paucity of data on regulation of β-defensin genes compared to other immune gene families, particularly in non-model species, the *in silico* analysis proposed here is a first step in understanding how to manipulate these pleiotropic molecules to best effect.

## 3.2 Hypothesis and specific aims

*We hypothesise that regulation of β-defensin gene expression is mediated by specific conserved regulatory elements in the non-coding genome.*

**Specific aims:**

1. To identify putative regulatory regions in the proximal promoters of β-defensin gene orthologs through:

    i) Over-representation analysis of transcription factor binding sites;

    ii) Identification of short conserved DNA motifs.

2. To identify transcription factors which may interact with these conserved regions.

3. To identify conserved DNA regions across the β-defensin syntenic cluster B through multi-species alignment.

## 3.3 Results

### 3.3.1 TFBS over-representation analysis of syntenic cluster B β-defensin promoters

TFBS over-representation analysis can be used to detect binding sites which have been conserved in sequence among orthologs of a given gene due to their role in transcriptional regulation of that gene. To this end, datasets consisting of the 5kb promoters for several mammalian orthologs of each β-defensin gene have been compiled. For each dataset, a GC- and length-matched background set of 100 randomly selected human promoters for each β-defensin promoter was also compiled (p31).

Due to their short length, TFBSs will be predicted randomly in any given DNA sequence. There are several approaches that apply the information contained in a PWM database to identify which sites are most likely to have function *in vivo*. The oPOSSUM3 suite compares the target gene set to a randomly-selected background set, calculating two statistics for each PWM- the Z and Fisher scores (p33).

From a database of 291 PWMs (the number of unique transcription factors will be slightly less than this as a small number of TFs are represented by several PWMs), 53 TFs in total were over-represented by both Z and Fisher scores in the β-defensin ortholog promoters, relative to randomly-selected background genes (Table 3.1). Three to eight transcription factors are over-represented in each promoter set (Figure 3.3 to Figure 3.16).

Grouping these TFs by structural family (Table 3.1) indicates several families were over-represented: nuclear hormone receptor, beta-beta-alpha zinc finger, homeo and helix-loop-helix. Each family contains at least 5 transcription factors that have been identified as over-represented in the promoters of at least one β-defensin ortholog set.

The nuclear hormone group includes androgen receptor (AR) which was over-represented in the promoters of *DEFB115* and *DEFB124* and glucocorticoid receptor (GR) which was over-represented in the *DEFB132*, *DEFB127* and *DEFB124* promoters. Retinoid X receptor (RXR) was over-represented paired with both retinoic acid receptor (RAR) and the liver X receptor, rationally named as nuclear receptor subfamily 1, group H, member 2 (NR1H2).

The beta-beta-alpha zinc finger family includes Krüppel-like factor 7 (KLF7) which was over-represented in *DEFB132*, *DEFB126* and *DEFB125*. CCCTC-binding factor (CTCF) was also over-represented in several promoter sets, occurring in *DEFB128*, *DEFB123* and *DEFB116*. The zinc finger proteins 143, 187, 281 and 423 (ZNF143, ZFP187, ZFP281 and ZFP423) and zinc finger and BTB domain-containing proteins 3 and 12 (ZBTB3, ZBTB12) also fall within this group. Paired box 5 (PAX5) and hepatocyte nuclear factor 1β (HNF1β) are both homeo family transcription factors. PAX5 was over-represented in the promoters of *DEFB129*, *DEFB125*, *DEFB116* and *DEFB118* while HNF1β sites were detected in the *DEFB128*, *DEFB118* and *DEFB119* ortholog promoter sets.

The helix-loop-helix family members transcription factor 3 (TCF3) and zinc finger and SCAN domain-containing protein 4 (ZSCAN4) were over-represented in the *DEFB132* and *DEFB116* and *DEFB126*, *DEFB125* and *DEFB115* promoters respectively. Activating enhancer-binding protein 2 (AP-2) family member binding sites were highlighted in the promoters of *DEFB126*, *DEFB116* and *DEFB123*.

It is possible that due to similarity of protein structure and therefore underlying target nucleotide sequence, the software has predicted binding sites for several TFs of the same family in a single location. Indeed, a given nucleotide site can often bind several transcription factors and competition between several transcription factors for a given site is a described method of gene regulation. Plotting the predicted binding sites along the β-defensin gene promoter sequences indicates that bar three instances, predicted binding sites for TF family members do not overlap. Androgen receptor and glucocorticoid receptor binding sites overlap in the *DEFB124* promoters of several species, as do the interferon regulatory factor (IRF) 5 and IRF9 binding sites (Figure 3.16). The predicted binding sites for AP-2β, AP-2γ, AP-2ε overlap in the promoter of *DEFB126* (Figure 3.7), though the strong similarity in DNA binding site among members the AP-2 family proteins has been noted in the literature (Badis et al., 2009).

**Table 3.1 TFs whose binding sites were over-represented by both Z and Fisher scores**

| | Hormone nuclear receptor | Beta-beta-alpha zinc finger | GATA-binding protein | Glial cells missing | Loop-sheet helix | ARID | IRF | Forkhead | RFX | Homeo | Helix-loop-helix | Myb | MADS | NFY CAAT-binding | High mobility group | STAT | Ets |
|---|---|---|---|---|---|---|---|---|---|---|---|---|---|---|---|---|---|
| ***DEFB132*** | GR | KLF7, OSR | | | | | | | | | TCF3, Max | | | | | | |
| ***DEFB129*** | RAR-RXR_DR5 | ZNF143 | | | | | | | | PAX5 | | | | | | | |
| ***DEFB128*** | | CTCF, ZFP187, ZFP423 | GATA3 | | | | | FOXF2 | RFX3 | HNF1β | | | SRF | | | | |
| ***DEFB127*** | GR | ZFP281 | | | | | | | | | ZSCAN4 | | | | | | EWSR1-FLI1 |
| ***DEFB126*** | | KLF7 | | | | | IRF4 | | | | AP-2β, AP-2ε, AP-2γ | | | | | | |
| ***DEFB125*** | PPARG | KLF7, ZBTB12 | | | | | | | | PAX5, Six6 | ZSCAN4, BHLHB2 | | | | | | |
| ***DEFB115*** | AR, NR1H2-RXRA | ZBTB12 | | | | | | | | | ZSCAN4 | | | | | | |
| ***DEFB116*** | | CTCF | | | | | | | | PAX5 | Myc, AP-2β, TCF3 | | | NFYA | | | |
| ***DEFB118*** | | ZBTB3 | | | | | | | | PAX5, Hoxa3, Pou5f1, HNF1β | | | | | Sox30 | | GABPA |
| ***DEFB119*** | HNF4α | | GATA3 | | | ARID3a | | | | HNF1β, NKX3.1 | ZSCAN4 | | | | | STAT1 | |
| ***DEFB121*** | | | | | | | | | RFX3 | PAX4 | | | | | HBP | | ESE3 |
| ***DEFB122*** | | HIC1 | | GCM1 | | | | | | | ABF1 | MYBL1 | | | | | |
| ***DEFB123*** | | CTCF | | | P53 | | | | | | AP-2β | | | | | | |
| ***DEFB124*** | AR, GR, HNF4α | | | | | | IRF5, IRF9 | | RFX1 | | | | | | | | EWSR1-FLI1 |

The binding sites for the TFs listed in Table 3.1 are represented graphically in Figure 3.3 to Figure 3.16. The symbols used to represent binding sites for each transcription factor are given in Figure 3.2.


**Figure 3.2 Key to symbols used to represent TFBSs in subsequent figures**

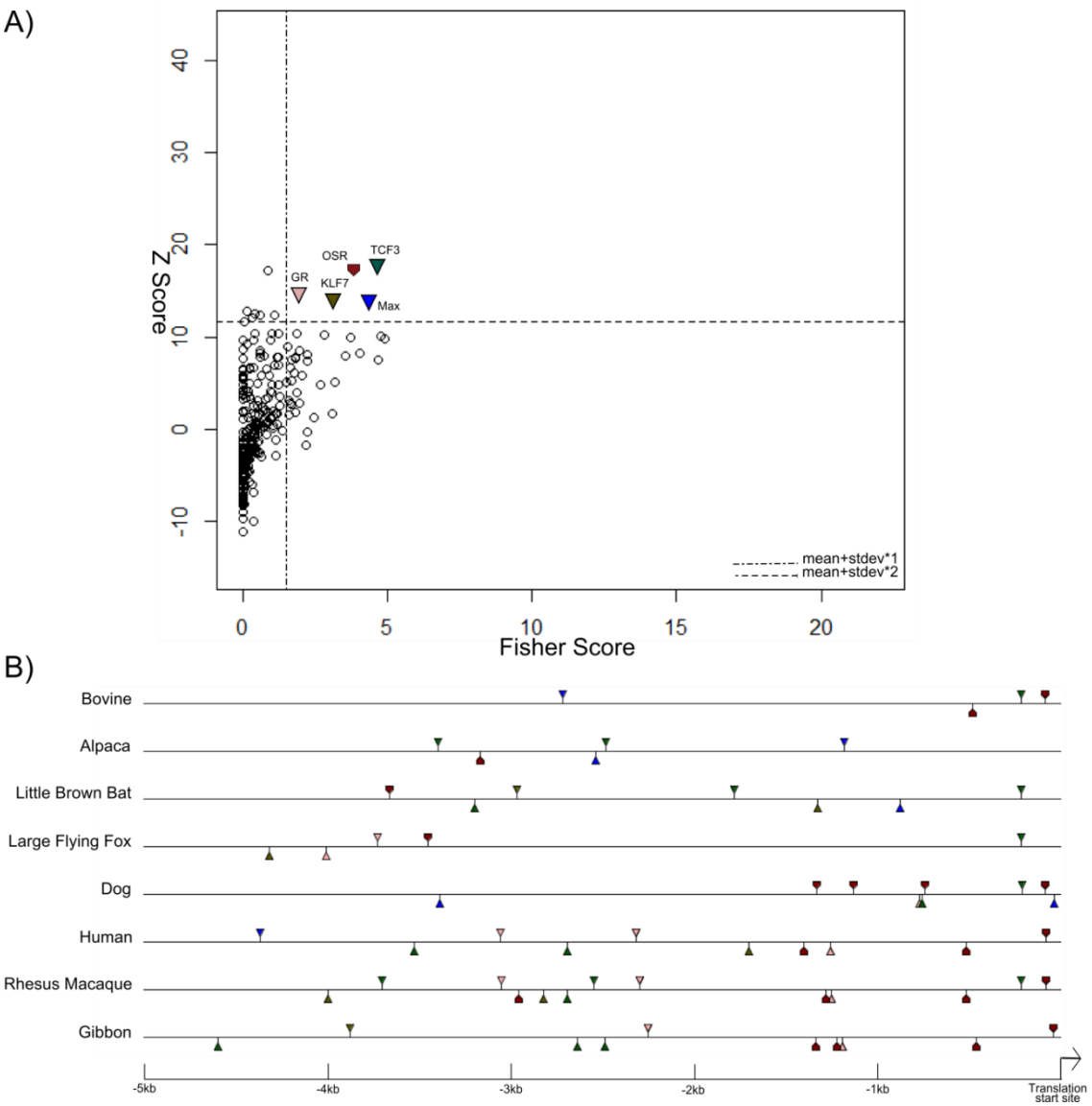


**Figure 3.3 *DEFB132*: oPOSSUM3 TFBS over-representation analysis of orthologs in eight species.** Five kb of nucleotide sequence upstream of the translation initiation codon for bovine *DEFB132* and seven orthologs was downloaded using ENSEMBL Biomart. The oPOSSUM3 sequence-based single site analysis software tool was used to determine which TFs were statistically overrepresented in the β-defensin promoters relative to a length- and GC-matched background set of human promoters. A 100:1 ratio of background to foreground sequences was used to ensure the background set was large enough to avoid skewing due to the presence of different subsets of genes. Two types of over-representation were assessed by Z score and Fisher score. A) Applied thresholds were used to identify TFs considered overrepresented by both measures as recommended by Kwon et al (2012). B) The positioning of individual TFBS within the promoter regions of eight *DEFB132* orthologs is indicated.

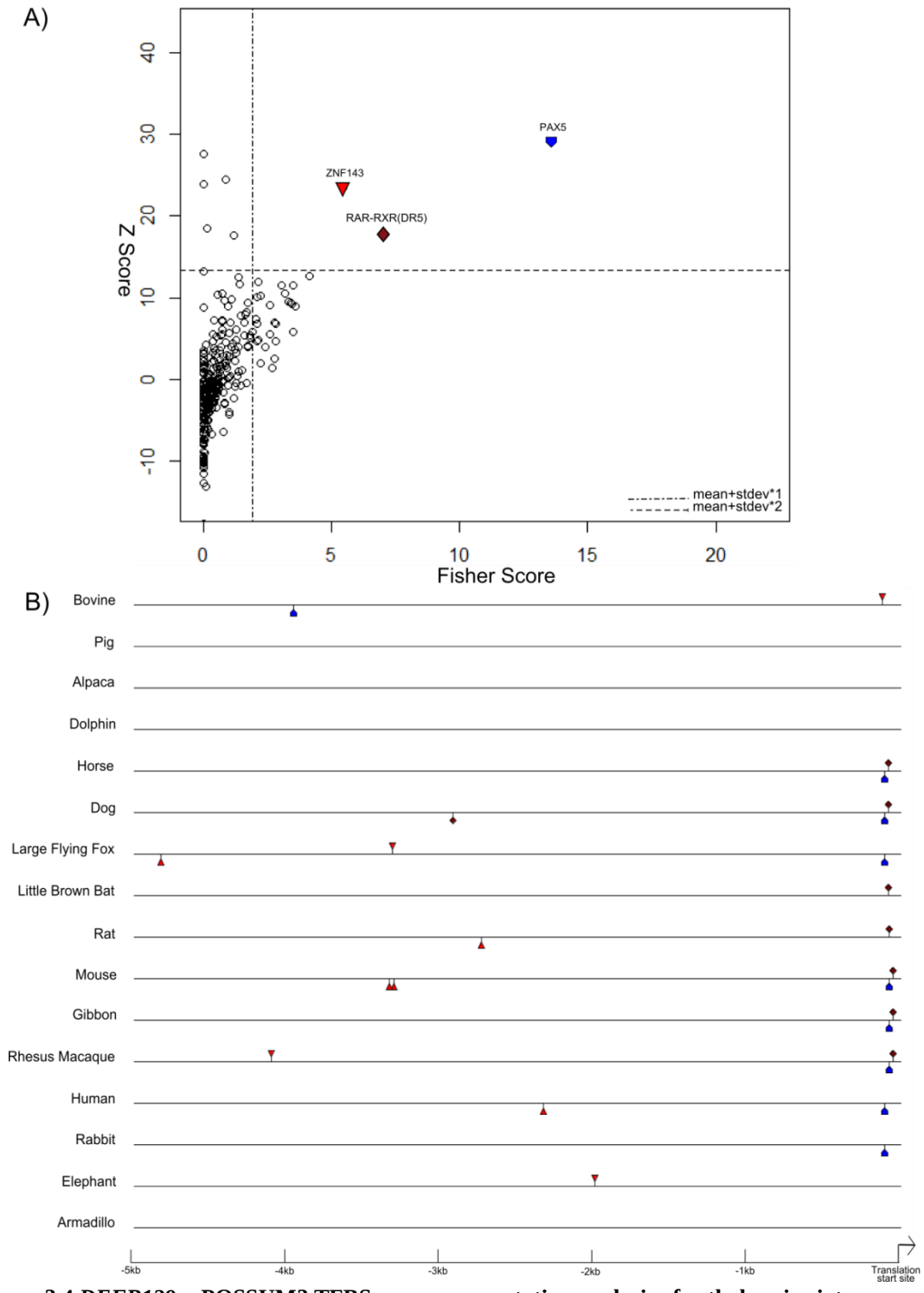


**Figure 3.4 *DEFB129*: oPOSSUM3 TFBS over-representation analysis of orthologs in sixteen species.** Five kb of nucleotide sequence upstream of the translation initiation codon for bovine *DEFB129* and fifteen orthologs was downloaded using ENSEMBL Biomart. The oPOSSUM3 sequence-based single site analysis software tool was used to determine which TFs were statistically overrepresented in the β-defensin promoters relative to a length- and GC-matched background set of human promoters. A 100:1 ratio of background to foreground sequences was used to ensure the background set was large enough to avoid skewing due to the presence of different subsets of genes. Two types of over-representation were assessed by Z score and Fisher score. A) Applied thresholds were used to identify TFs considered overrepresented by both measures as recommended by Kwon et al (2012). B) The positioning of individual TFBS within the promoter regions of sixteen *DEFB129* orthologs is indicated.

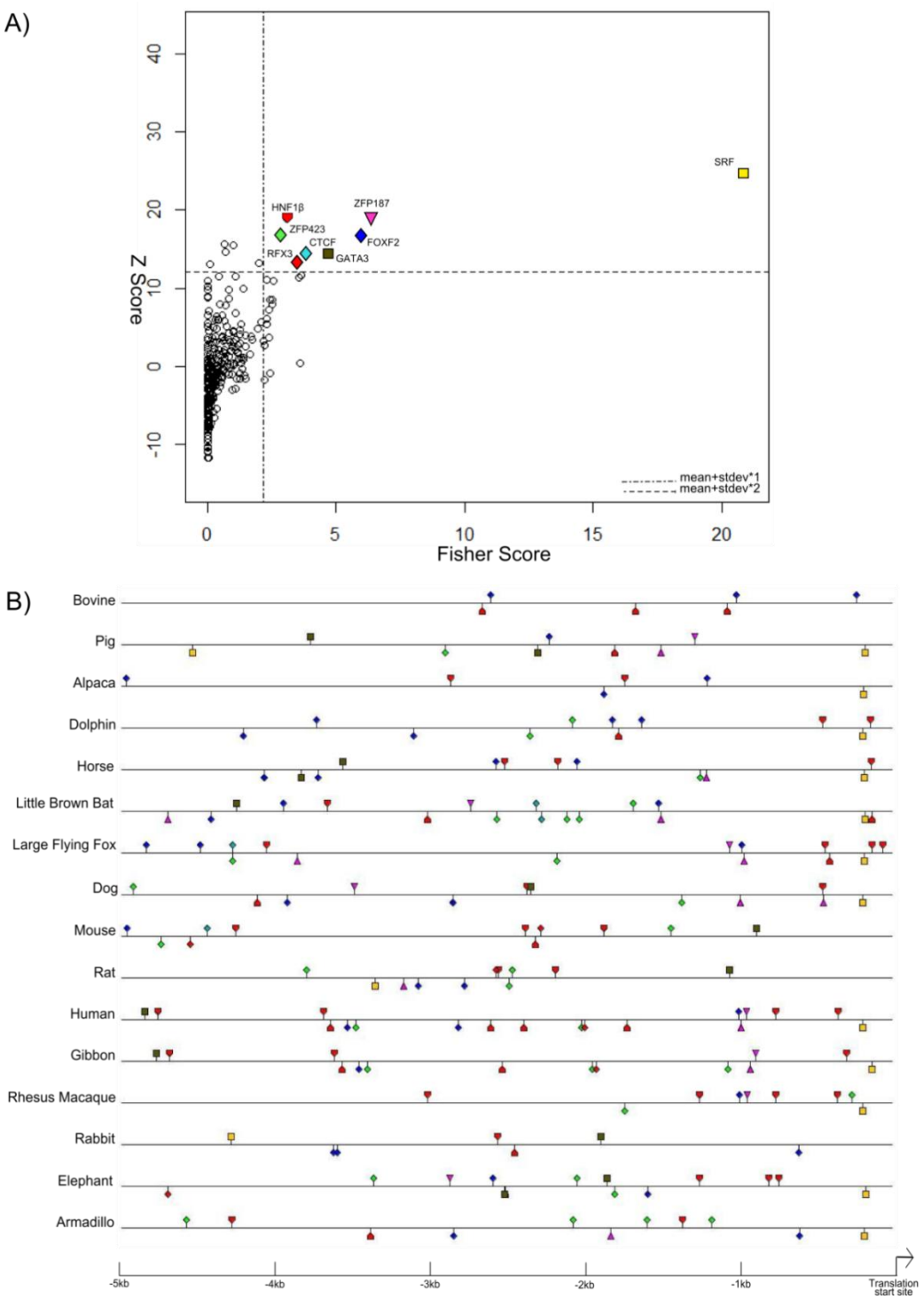


**Figure 3.5 *DEFB128*: oPOSSUM3 TFBS over-representation analysis of orthologs in sixteen species.** Five kb of nucleotide sequence upstream of the translation initiation codon for bovine *DEFB128* and fifteen orthologs was downloaded using ENSEMBL Biomart. The oPOSSUM3 sequence-based single site analysis software tool was used to determine which TFs were statistically overrepresented in the β-defensin promoters relative to a length- and GC-matched background set of human promoters. A 100:1 ratio of background to foreground sequences was used to ensure the background set was large enough to avoid skewing due to the presence of different subsets of genes. Two types of over-representation were assessed by Z score and Fisher score. A) Applied thresholds were used to identify TFs considered overrepresented by both measures as recommended by Kwon et al (2012). B) The positioning of individual TFBS within the promoter regions of sixteen *DEFB128* orthologs is indicated.

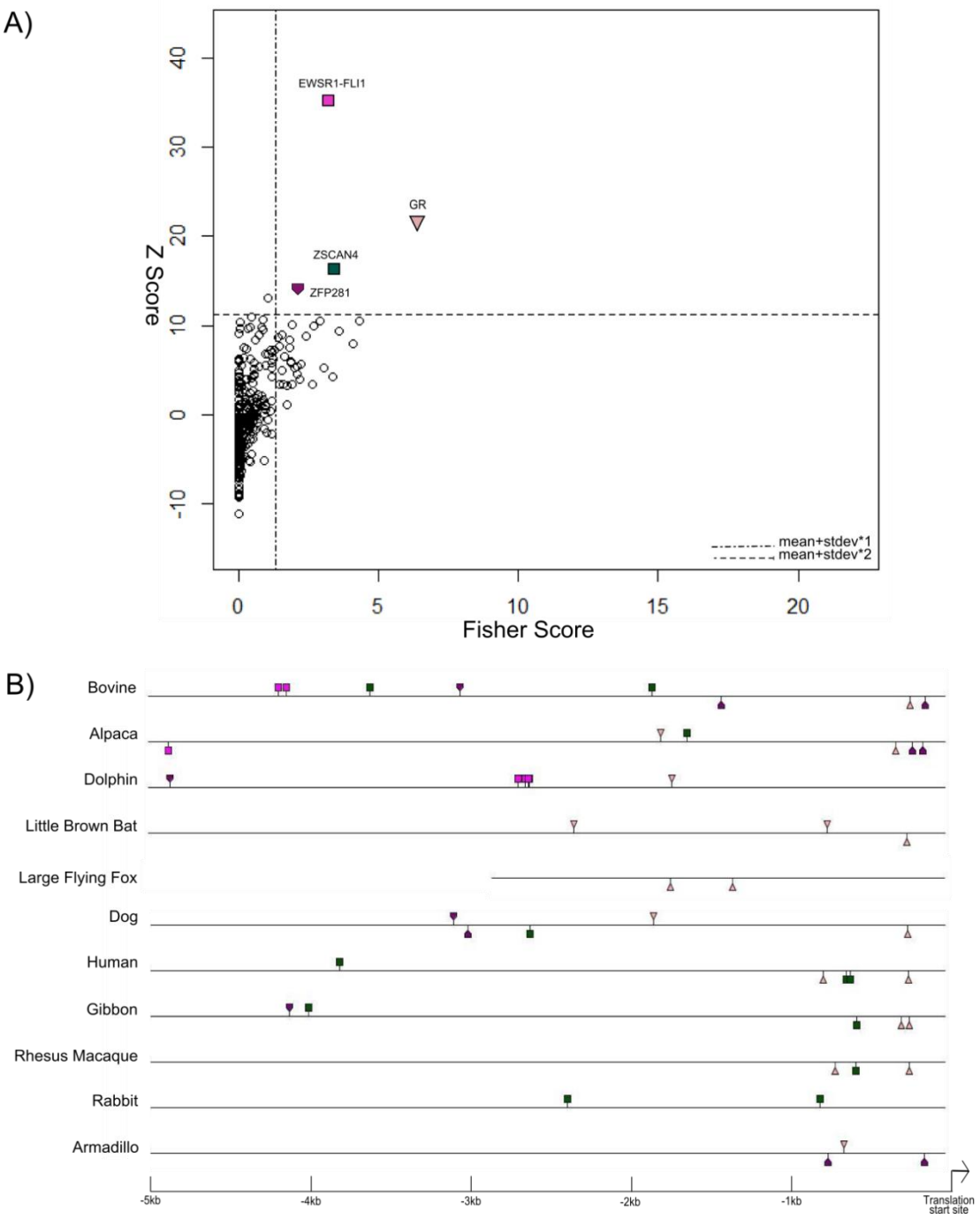


**Figure 3.6 *DEFB127*: oPOSSUM3 TFBS over-representation analysis of orthologs in eleven species.** Five kb of nucleotide sequence upstream of the translation initiation codon for bovine *DEFB127* and eleven orthologs was downloaded using ENSEMBL Biomart. The oPOSSUM3 sequence-based single site analysis software tool was used to determine which TFs were statistically overrepresented in the β-defensin promoters relative to a length- and GC-matched background set of human promoters. A 100:1 ratio of background to foreground sequences was used to ensure the background set was large enough to avoid skewing due to the presence of different subsets of genes. Two types of over-representation were assessed by Z score and Fisher score. A) Applied thresholds were used to identify TFs considered overrepresented by both measures as recommended by Kwon et al (2012). B) The positioning of individual TFBS within the promoter regions of eleven *DEFB127* orthologs is indicated.

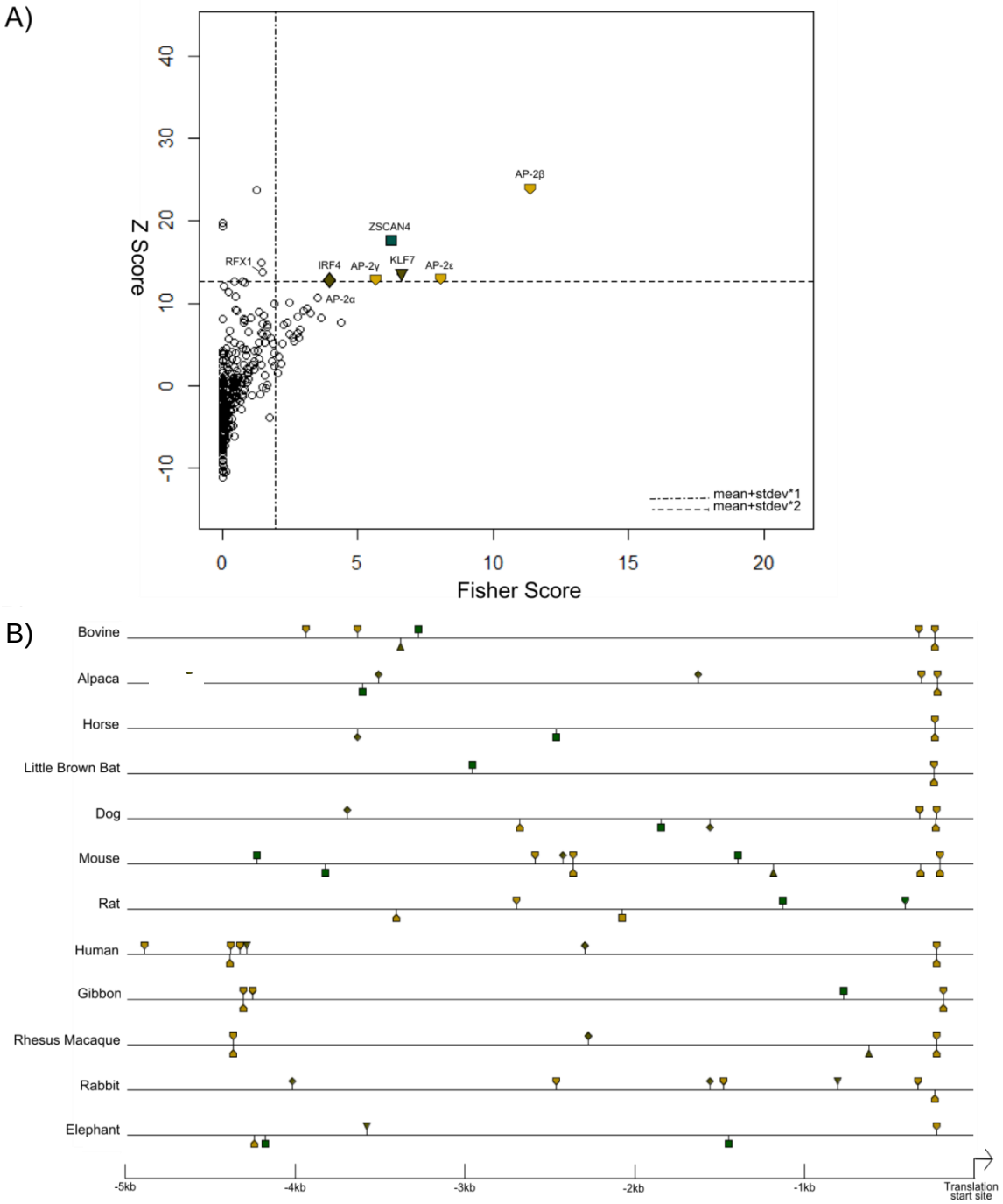


**Figure 3.7 *DEFB126*: oPOSSUM3 TFBS over-representation analysis of orthologs in twelve species.** Five kb of nucleotide sequence upstream of the translation initiation codon for bovine *DEFB126* and eleven orthologs was downloaded using ENSEMBL Biomart. The oPOSSUM3 sequence-based single site analysis software tool was used to determine which TFs were statistically overrepresented in the β-defensin promoters relative to a length- and GC-matched background set of human promoters. A 100:1 ratio of background to foreground sequences was used to ensure the background set was large enough to avoid skewing due to the presence of different subsets of genes. Two types of over-representation were assessed by Z score and Fisher score. A) Applied thresholds were used to identify TFs considered overrepresented by both measures as recommended by Kwon et al (2012). B) The positioning of individual TFBS within the promoter regions of twelve *DEFB126* orthologs is indicated.

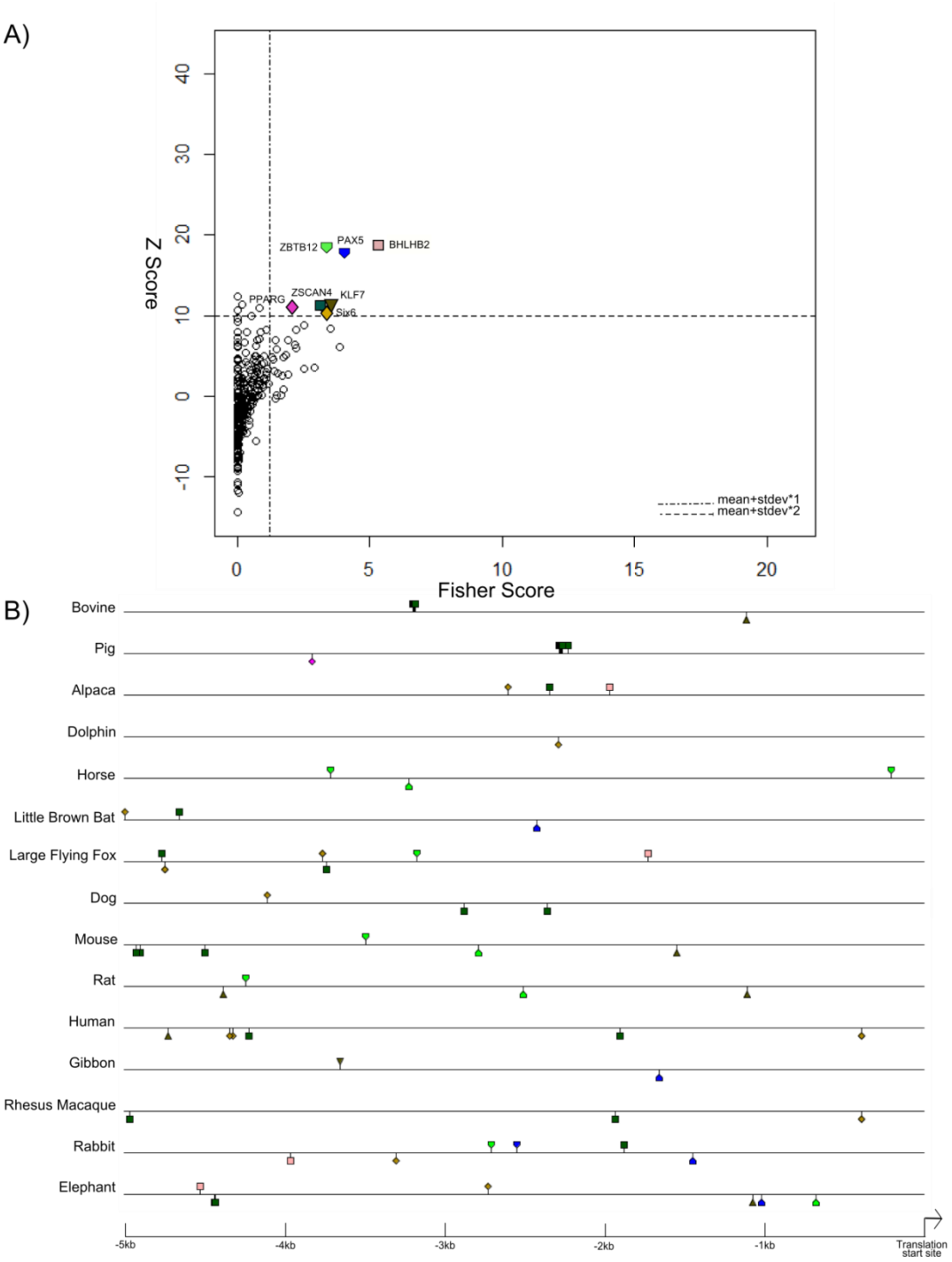


**Figure 3.8 *DEFB125*: oPOSSUM3 TFBS over-representation analysis of orthologs in fifteen species.** Five kb of nucleotide sequence upstream of the translation initiation codon for bovine *DEFB125* and fourteen orthologs was downloaded using ENSEMBL Biomart. The oPOSSUM3 sequence-based single site analysis software tool was used to determine which TFs were statistically overrepresented in the β-defensin promoters relative to a length- and GC-matched background set of human promoters. A 100:1 ratio of background to foreground sequences was used to ensure the background set was large enough to avoid skewing due to the presence of different subsets of genes. Two types of over-representation were assessed by Z score and Fisher score. A) Applied thresholds were used to identify TFs considered overrepresented by both measures as recommended by Kwon et al (2012). B) The positioning of individual TFBS within the promoter regions of fifteen *DEFB125* orthologs is indicated.

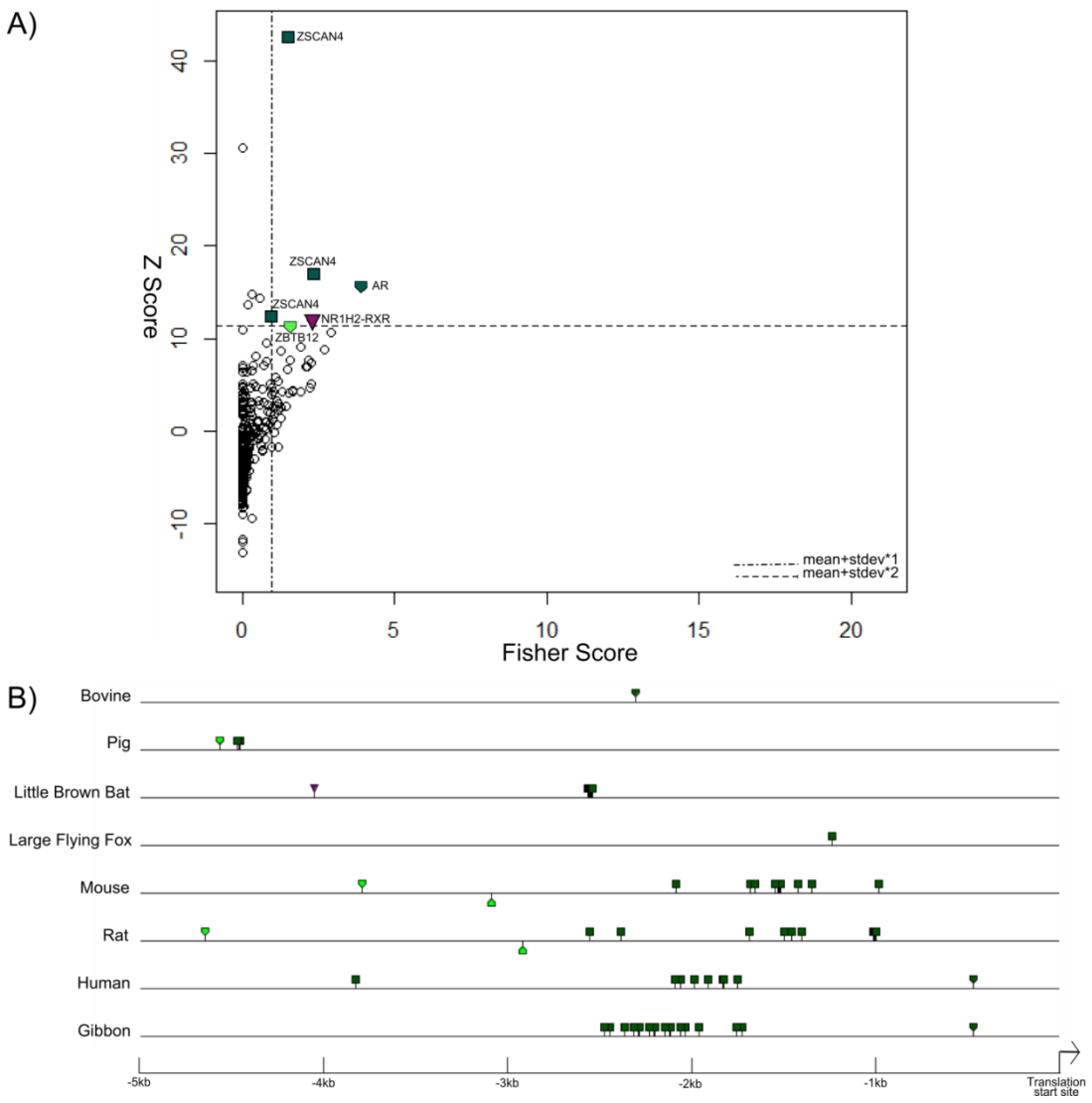


**Figure 3.9 *DEFB115*: oPOSSUM3 TFBS over-representation analysis of orthologs in nine species.** Five kb of nucleotide sequence upstream of the translation initiation codon for bovine *DEFB115* and eight orthologs was downloaded using ENSEMBL Biomart. The oPOSSUM3 sequence-based single site analysis software tool was used to determine which TFs were statistically overrepresented in the β-defensin promoters relative to a length- and GC-matched background set of human promoters. A 100:1 ratio of background to foreground sequences was used to ensure the background set was large enough to avoid skewing due to the presence of different subsets of genes. Two types of over-representation were assessed by Z score and Fisher score. A) Applied thresholds were used to identify TFs considered overrepresented by both measures as recommended by Kwon et al (2012). B) The positioning of individual TFBS within the promoter regions of nine *DEFB115* orthologs is indicated.

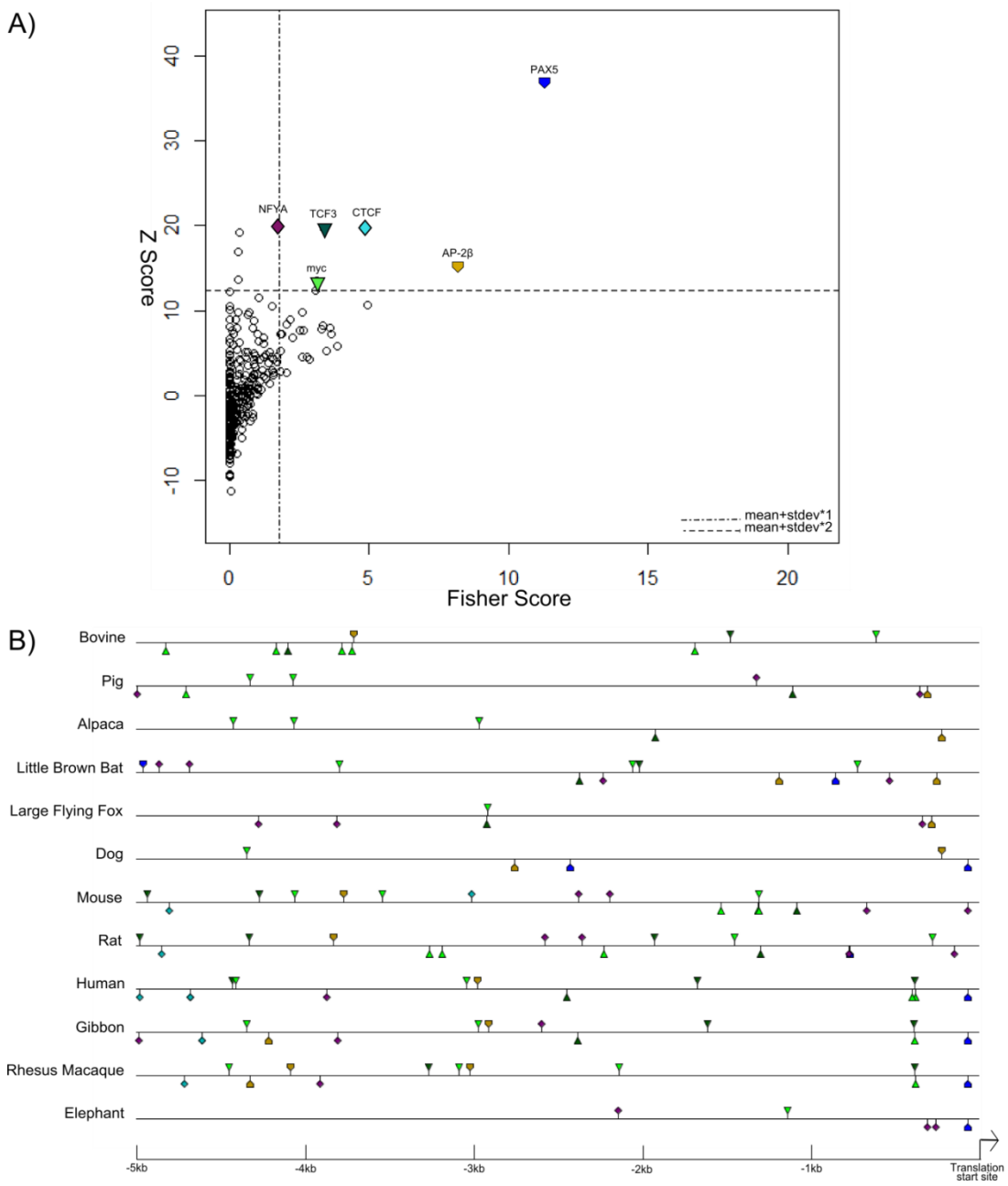


**Figure 3.10 *DEFB116*: oPOSSUM3 TFBS over-representation analysis of orthologs in twelve species.** Five kb of nucleotide sequence upstream of the translation initiation codon for bovine *DEFB116* and eleven orthologs was downloaded using ENSEMBL Biomart. The oPOSSUM3 sequence-based single site analysis software tool was used to determine which TFs were statistically overrepresented in the β-defensin promoters relative to a length- and GC-matched background set of human promoters. A 100:1 ratio of background to foreground sequences was used to ensure the background set was large enough to avoid skewing due to the presence of different subsets of genes. Two types of over-representation were assessed by Z score and Fisher score. A) Applied thresholds were used to identify TFs considered overrepresented by both measures as recommended by Kwon et al (2012). B) The positioning of individual TFBS within the promoter regions of twelve *DEFB116* orthologs is indicated.

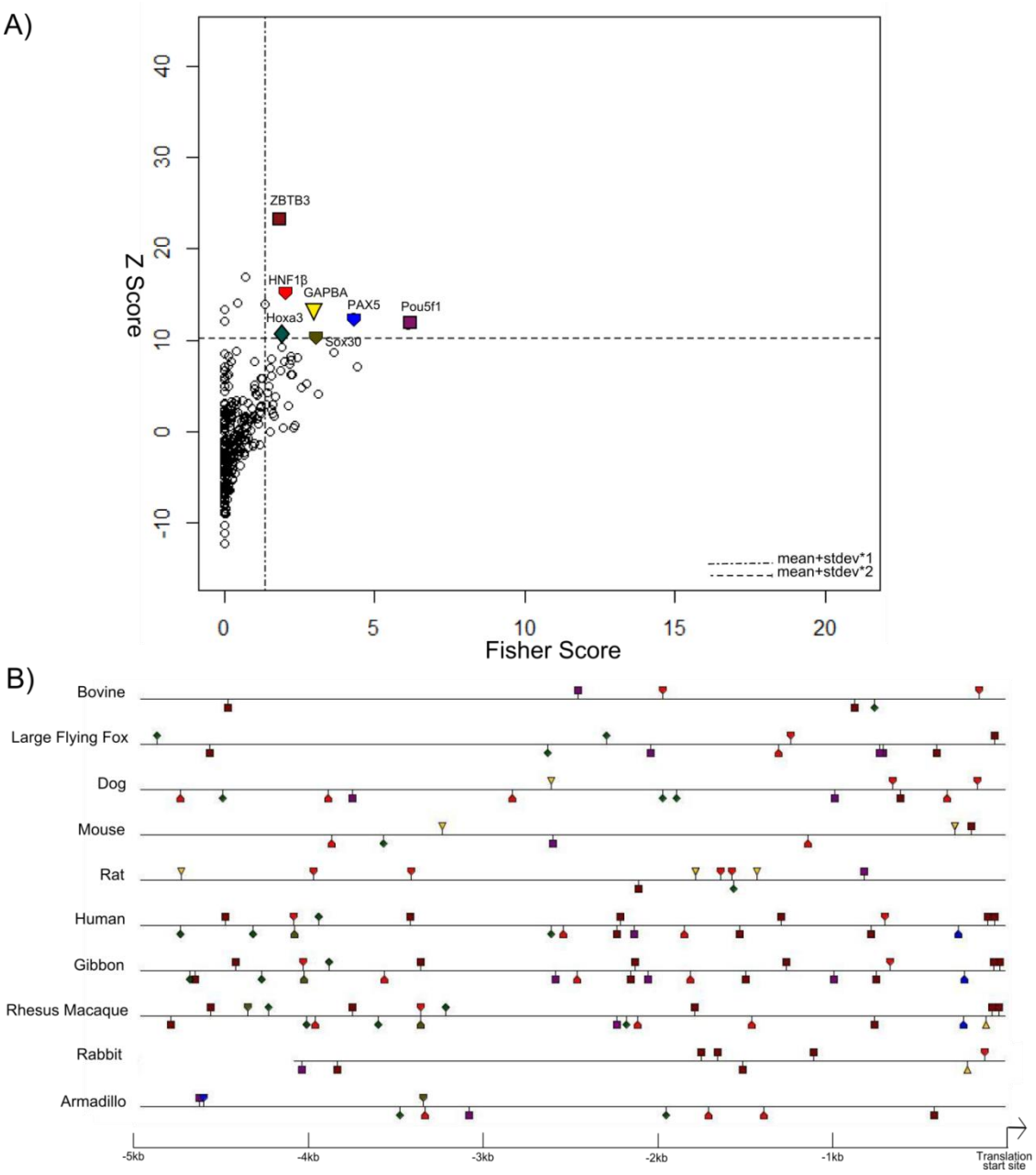


**Figure 3.11 *DEFB118*: oPOSSUM3 TFBS over-representation analysis of orthologs in ten species.** Five kb of nucleotide sequence upstream of the translation initiation codon for bovine *DEFB118* and nine orthologs was downloaded using ENSEMBL Biomart. The oPOSSUM3 sequence-based single site analysis software tool was used to determine which TFs were statistically overrepresented in the β-defensin promoters relative to a length- and GC-matched background set of human promoters. A 100:1 ratio of background to foreground sequences was used to ensure the background set was large enough to avoid skewing due to the presence of different subsets of genes. Two types of over-representation were assessed by Z score and Fisher score. A) Applied thresholds were used to identify TFs considered overrepresented by both measures as recommended by Kwon et al (2012). B) The positioning of individual TFBS within the promoter regions of ten *DEFB118* orthologs is indicated.

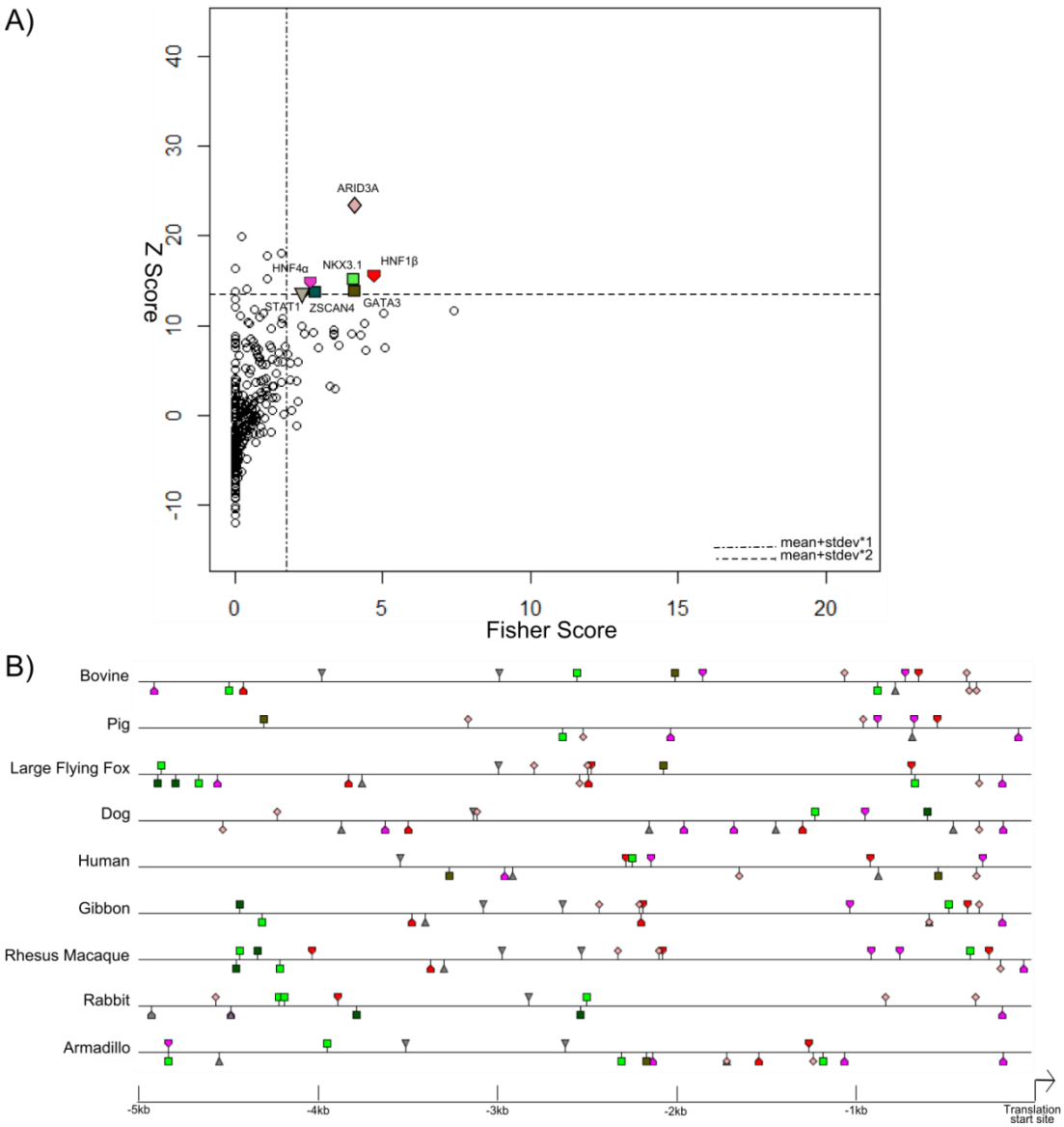


**Figure 3.12 *DEFB119*: oPOSSUM3 TFBS over-representation analysis of orthologs in nine species.** Five kb of nucleotide sequence upstream of the translation initiation codon for bovine *DEFB119* and eight orthologs was downloaded using ENSEMBL Biomart. The oPOSSUM3 sequence-based single site analysis software tool was used to determine which TFs were statistically overrepresented in the β-defensin promoters relative to a length- and GC-matched background set of human promoters. A 100:1 ratio of background to foreground sequences was used to ensure the background set was large enough to avoid skewing due to the presence of different subsets of genes. Two types of over-representation were assessed by Z score and Fisher score. A) Applied thresholds were used to identify TFs considered overrepresented by both measures as recommended by Kwon et al (2012). B) The positioning of individual TFBS within the promoter regions of nine *DEFB119* orthologs is indicated.

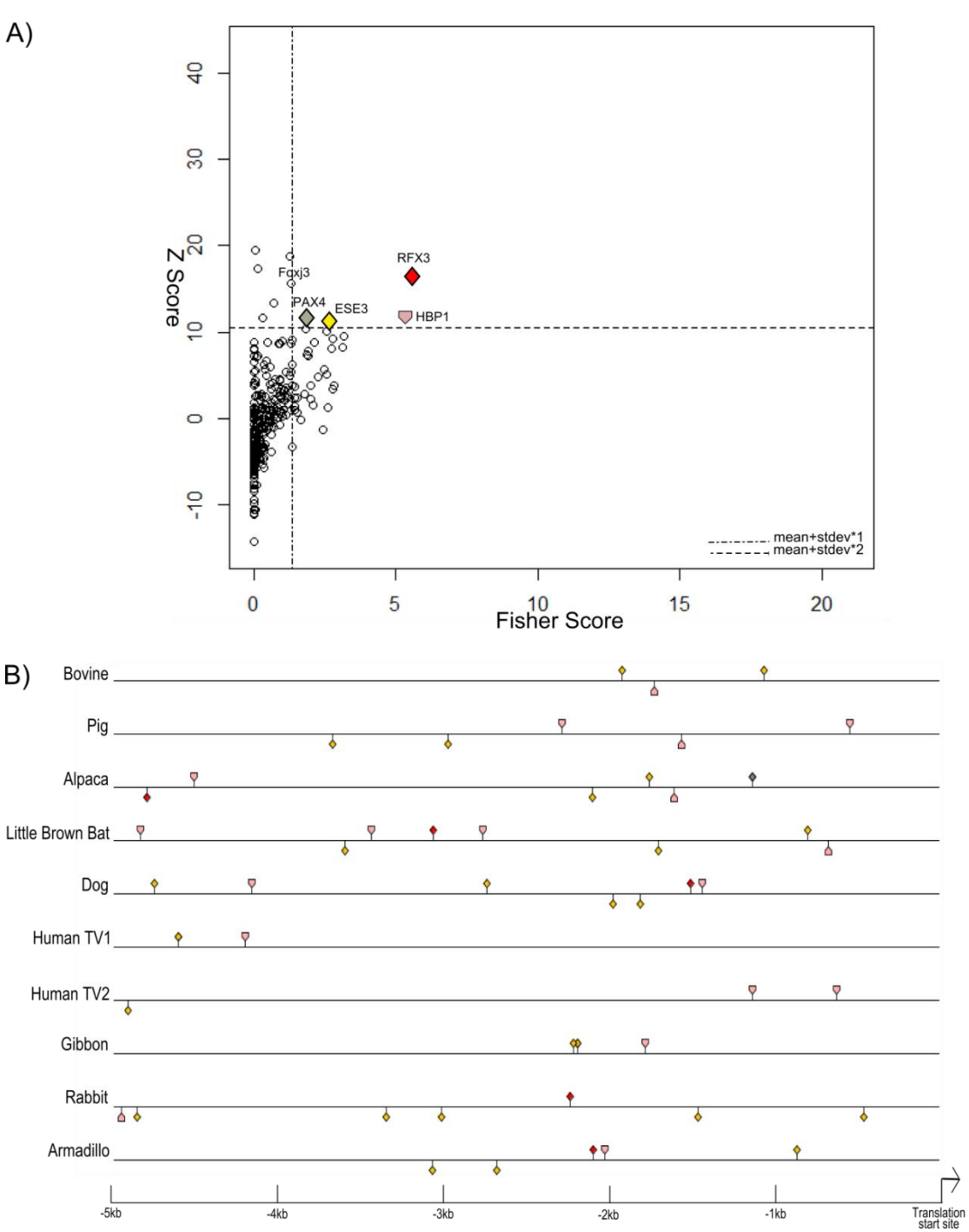


**Figure 3.13 *DEFB121*: oPOSSUM3 TFBS over-representation analysis of orthologs in nine species.** Five kb of nucleotide sequence upstream of the translation initiation codon for bovine *DEFB121* and eight orthologs was downloaded using ENSEMBL Biomart. Human *DEFB121* has two alternative splice variants with alternative promoters. TV= transcript variant. The oPOSSUM3 sequence-based single site analysis software tool was used to determine which TFs were statistically overrepresented in the β-defensin promoters relative to a length- and GC-matched background set of human promoters. A 100:1 ratio of background to foreground sequences was used to ensure the background set was large enough to avoid skewing due to the presence of different subsets of genes. Two types of over-representation were assessed by Z score and Fisher score. A) Applied thresholds were used to identify TFs considered overrepresented by both measures as recommended by Kwon et al (2012). B) The positioning of individual TFBS within the promoter regions of nine *DEFB121* orthologs is indicated.

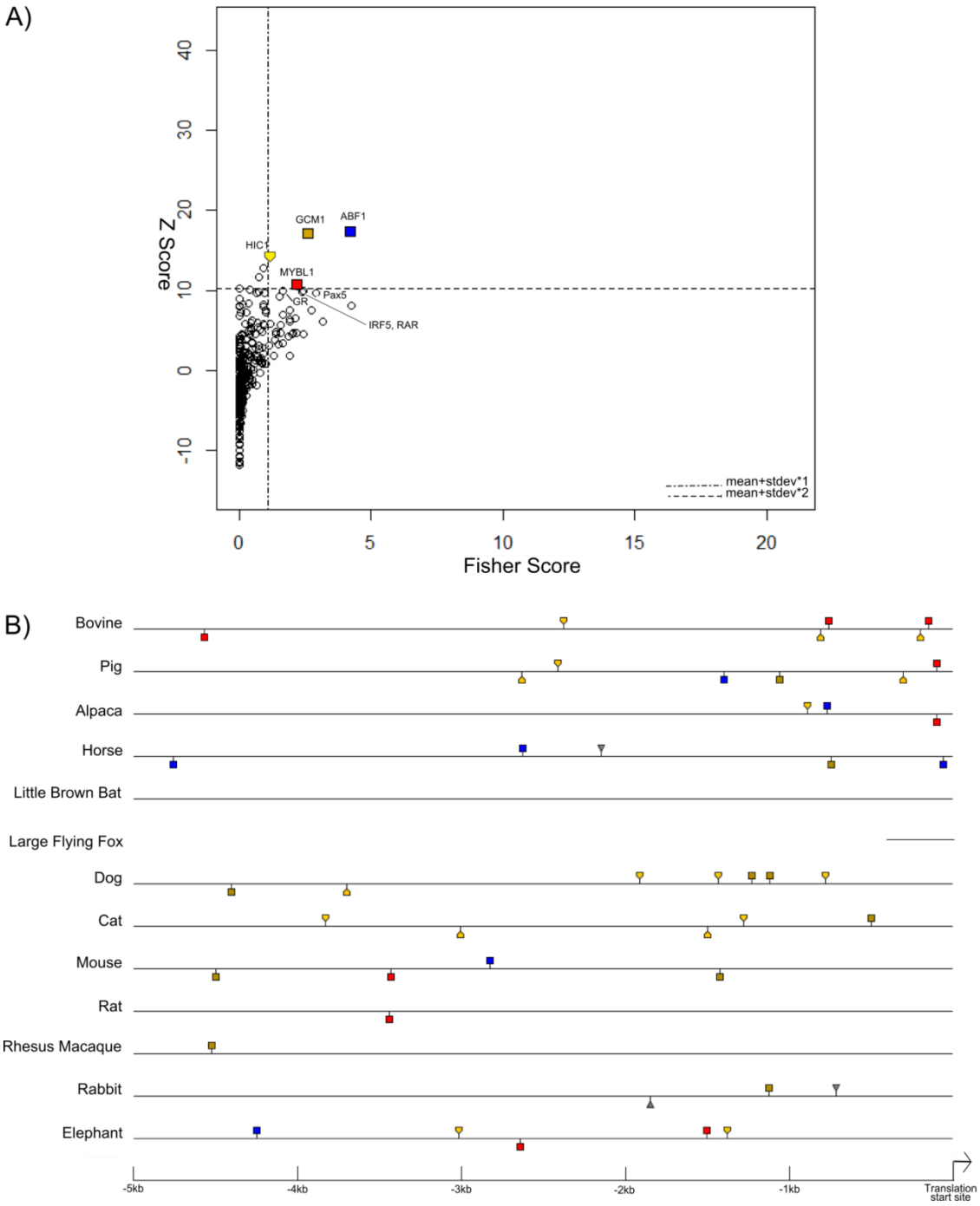


**Figure 3.14 *DEFB122*: oPOSSUM3 TFBS over-representation analysis of orthologs in thirteen species.**

Five kb of nucleotide sequence upstream of the translation initiation codon for bovine *DEFB132* and twelve orthologs was downloaded using ENSEMBL Biomart. The oPOSSUM3 sequence-based single site analysis software tool was used to determine which TFs were statistically overrepresented in the β-defensin promoters relative to a length- and GC-matched background set of human promoters. A 100:1 ratio of background to foreground sequences was used to ensure the background set was large enough to avoid skewing due to the presence of different subsets of genes. Two types of over-representation were assessed by Z score and Fisher score. A) Applied thresholds were used to identify TFs considered overrepresented by both measures as recommended by Kwon et al (2012). B) The positioning of individual TFBS within the promoter regions of thirteen *DEFB122* orthologs is indicated.

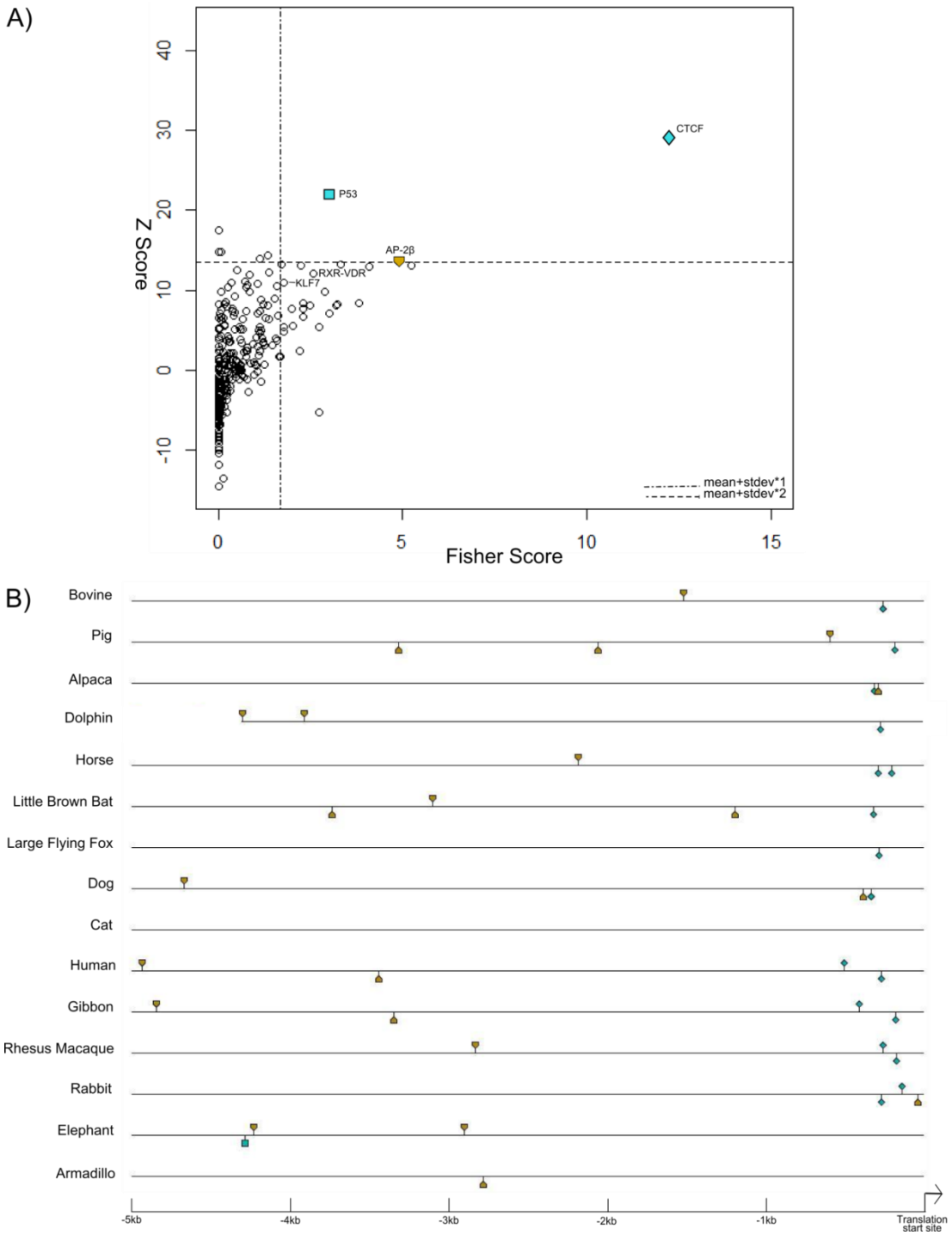


**Figure 3.15 *DEFB123*: oPOSSUM3 TFBS over-representation analysis of orthologs in fifteen species.** Five kb of nucleotide sequence upstream of the translation initiation codon for bovine *DEFB123* and fourteen orthologs was downloaded using ENSEMBL Biomart. The oPOSSUM3 sequence-based single site analysis software tool was used to determine which TFs were statistically overrepresented in the β-defensin promoters relative to a length- and GC-matched background set of human promoters. A 100:1 ratio of background to foreground sequences was used to ensure the background set was large enough to avoid skewing due to the presence of different subsets of genes. Two types of over-representation were assessed by Z score and Fisher score. A) Applied thresholds were used to identify TFs considered overrepresented by both measures as recommended by Kwon et al (2012). Green box indicates presence of TFBSs with conserved location. B) The positioning of individual TFBS within the promoter regions of fifteen *DEFB123* orthologs is indicated.

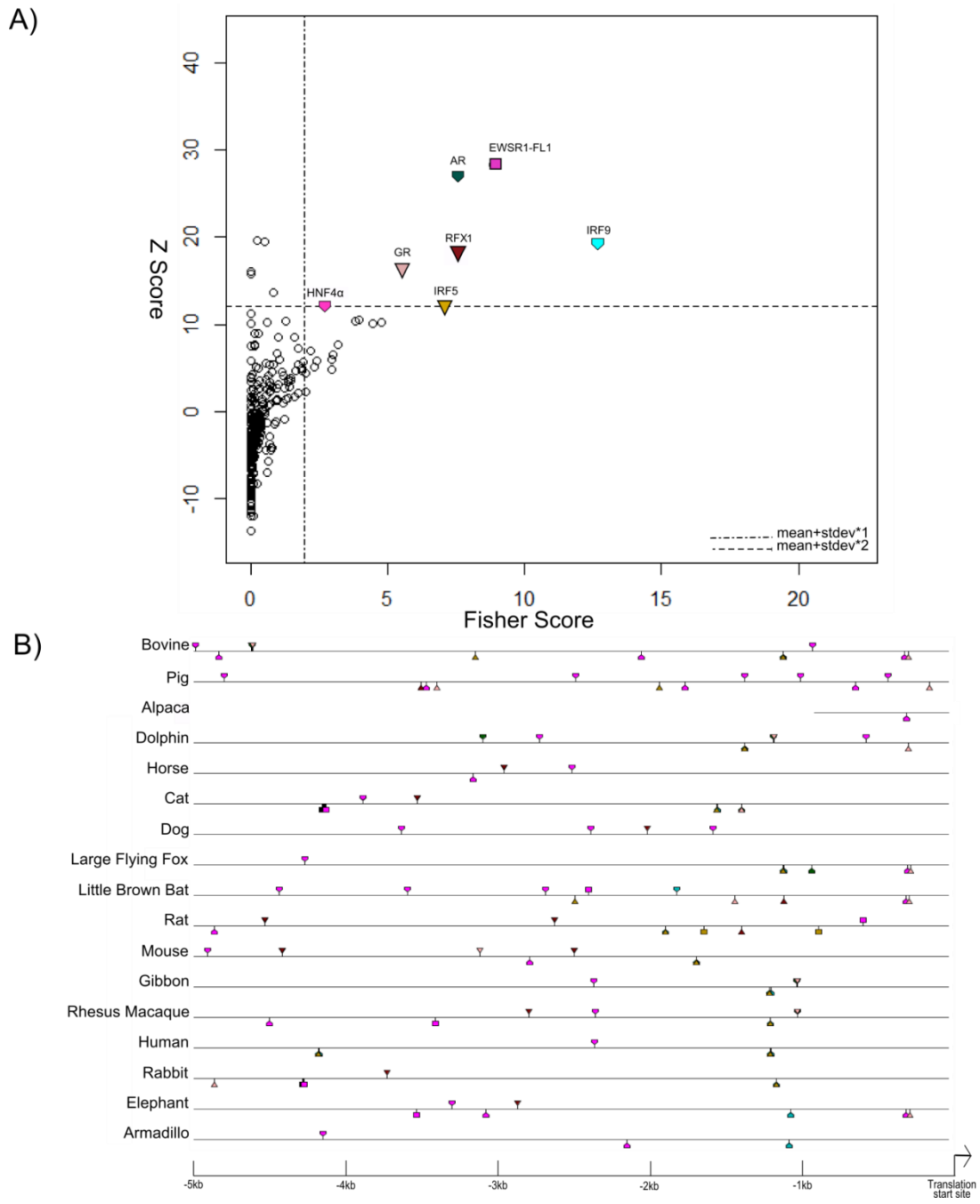


**Figure 3.16 *DEFB124*: oPOSSUM3 TFBS over-representation analysis of orthologs in seventeen species.**

Five kb of nucleotide sequence upstream of the translation initiation codon for bovine *DEFB124* and 16 orthologs was downloaded using ENSEMBL Biomart. The oPOSSUM3 sequence-based single site analysis software tool was used to determine which TFs were statistically overrepresented in the β-defensin promoters relative to a length- and GC-matched background set of human promoters. A 100:1 ratio of background to foreground sequences was used to ensure the background set was large enough to avoid skewing due to the presence of different subsets of genes. Two types of over-representation were assessed by Z score and Fisher score. A) Applied thresholds were used to identify TFs considered overrepresented by both measures as recommended by Kwon et al (2012). Green box indicates presence of TFBSs with conserved location. B) The positioning of individual TFBS within the promoter regions of seventeen *DEFB124* orthologs is indicated.

Examination of the location of the identified TFBSs reveals several interesting patterns. Strong similarity in the pattern of TFBSs and their locations was evident in the promoters of the three primate orthologs of several genes, namely *DEFB132*, *DEFB128*, *DEFB126*, *DEFB116* and *DEFB118* ( Figure 3.3, Figure 3.5, Figure 3.7, Figure 3.10, Figure 3.11). The two rodent species, mouse and rat, shared similarity of TFBS location in the *DEFB116* promoter (Figure 3.10). There was no similarity to the same extent between the bats or any of the Cetartiodactyl species analysed.

While all TFs whose binding site locations within the promoters have been determined were over-represented by both statistical measures used, the location patterning indicated some TFs have several binding sites in most promoters without precise conservation of location. Hepatocyte nuclear factor (HNF)1β in *DEFB128*, *DEFB118* and *DEFB119* promoters (Figure 3.5, Figure 3.11, Figure 3.12); Zinc finger and BTB domain-containing (ZBTB)12 in *DEFB125* and *DEFB115* promoters (Figure 3.8and Figure 3.9) and TCF3 in *DEFB132* and *DEFB116* promoter sets (Figure 3.3 and Figure 3.10) are good examples of this.

Binding sites for other TFs were less frequent in each individual promoter but the location was relatively conserved across the whole 5kb, usually occurring less than 500bp upstream of the translation initiation codon. In *DEFB132*, binding sites for TCF3 and odd-skipped related (OSR) were found in six of eight orthologs (Figure 3.3). A single serum response factor (SRF) binding site was found in twelve of sixteen *DEFB128* orthologs (Figure 3.5). Eleven of fifteen *DEFB123* ortholog promoters had at least one CTCF binding site within -130 to -330bp relative to the translation initiation codon (Figure 3.15). Retinoic acid heterodimer binding sites occurred within 100bp upstream of the translation initiation codon in seven of sixteen *DEFB129* orthologs (Figure 3.4). Eleven of twelve *DEFB126* ortholog promoters contained at least one AP-2 family binding site between -320 and -200bp, relative to the translation initiation codon (Figure 3.7). PAX5 binding sites were found in eight of sixteen *DEFB129* orthologs and five of twelve *DEFB116* orthologs (Figure 3.10). Eight of eleven *DEFB127* orthologs had a GR binding site within between 220 and 310bp of the translation initiation codon (Figure 3.6), while six of seventeen *DEFB124* ortholog promoters had a GR site within 120-260bp (Figure 3.16).

In the absence of validated information on the 5'UTRs for these genes, the DNA sequence chosen to represent the promoter region ends right before the translation initiation codon. This means that the chosen region likely contains 5'UTR, which would explain the apparent higher level of sequence conservation in these cases. In many of the above examples there was no corresponding binding site in the bovine ortholog with the 85% PWM match threshold used here. Kwon et al. (2012) recommend performing the initial over-representation analysis with a stringent matrix match threshold initially and decreasing stringency where there is a rationale for doing so, e.g. where experimental data indicate a given TF is important in the regulation of this gene. Taking relative conservation of location close to the translation initiation codon in a proportion of orthologs as a suggestion that that site may be functional, lowering of the matrix match cut-off in a number of test cases indicates the majority of the remaining orthologs also contain binding sites for the relevant TF in a comparable location.

Relaxing of the PWM similarity cut-off indicated the remaining eight *DEFB129* ortholog promoters also contained a PAX5 binding site with at least 80% similarity to the PWM within a 44bp range 100bp upstream of the translation initiation codon (Table 3.2).

**Table 3.2 PAX5 binding sites with a 75% matrix match threshold in *DEFB129* ortholog promoters**

| Species | % similarity | Location relative to translation start site | Orientation | Sequence |
|---|---|---|---|---|
| Bovine | 83.4 | -117 | - | TGAGCAGTCAAGTGCAGCCA |
| Pig | 84.1 | -89 | - | TGAGCAGTGAGGTGCAGCCA |
| Alpaca | 84 | -102 | - | TGAGCAGTGAAGTACAGCGA |
| Dolphin | 82.1 | -105 | - | TGAGCAGTAAAGTGCAGCCA |
| Horse | 86.7 | -105 | - | TGAGCAGTGAAGTGCAGCCA |
| Dog | 86.7 | -105 | - | TGAGCAGTGAAGTGCAGCCA |
| Megabat | 86.5 | -105 | - | TGATCAGTGAAGTATATCCA |
| Microbat | 81.7 | -105 | - | TGAGCAGTGAAGTGCACCAG |
| Rat | 84.5 | -103 | - | TAAGCAGTGAAGTGCGGCCA |
| Mouse | 86.7 | -73 | - | TGAGCAGTGAAGTGCAGCCA |
| Gibbon | 86.7 | -73 | - | TGAGCAGTGAAGTGCAGCCA |
| Macaque | 86.7 | -73 | - | TGAGCAGTGAAGTGCAGCCA |
| Human | 86.7 | -73 | - | TGAGCAGTGAAGTGCAGCCA |
| Rabbit | 85.2 | -103 | - | GGAGCACTGAAGTGCAGCCT |
| Elephant | 80.1 | -105 | - | TAGGCAATGAAGCACAGCTG |
| Armadillo | 82.2 | -103 | - | TAGGCAGTGAAGTGCAGCAA |

These additional sites are represented graphically in Figure 3.17.

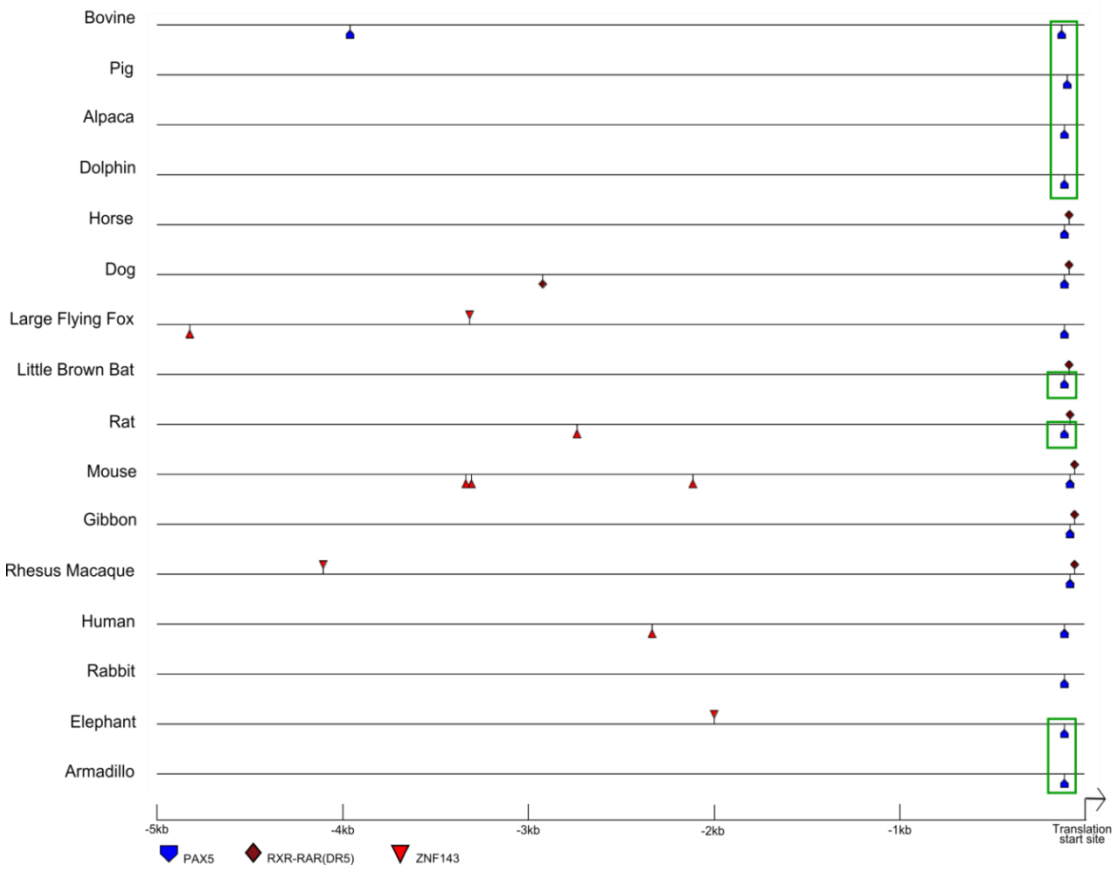


**Figure 3.17 Additional PAX5 sites in *DEFB129* ortholog promoters when a 75% matrix match threshold is applied.**

The 5kb promoters of *DEFB129* orthologs were analysed with oPOSSUM3 software using a 75% matrix match threshold. Eight additional PAX5 sites, all with >80% similarity to the PAX5 PWM, were identified with 70-120bp of the translation start site. These sites are indicated with a green box.

Similarly, nine additional orthologs contained GR binding sites within a 60bp range ~270bp from the translation initiation codon (Table 3.3 and Figure 3.18).

**Table 3.3 GR sites with a 75% matrix match threshold in *DEFB124* ortholog promoters**

| Species | % similarity | Location relative to translation start site | Orientation | Sequence |
|---|---|---|---|---|
| Bovine | 86.1 | -266 | - | GGGGACAGAATGTCTTGA |
| Pig | 75.7 | -210 | - | GGAGAGACCCAGTTCAAT |
| Alpaca | 83.3 | -262 | - | GGGGACAGAATTTTGTGA |
| Dolphin | 93 | -266 | - | GGGGACAGAATGTCCTGA |
| Horse | 83.9 | -257 | - | GGGGACAGGATTTCCTGA |
| Cat | 81 | -241 | + | CAGGAAATCCTGTCCGTA |
| Dog | No binding site within 200-300bp of translation start site | | | |
| Large Flying Fox | 88.5 | -246 | - | GGGGACAGAATTTCCTGA |
| Little Brown Bat | 86.1 | -257 | - | GGGGACAGAATCTCCTGA |
| Rat | No binding site within 200-300bp of translation start site | | | |
| Mouse | No binding site within 200-300bp of translation start site | | | |
| Gibbon | 77.8 | -252 | - | GGGGGTAGAATTTTCTGA |
| Rhesus Macaque | 78.5 | -250 | - | GGGGGTAGAATTTCCTGA |
| Human | 76.1 | -252 | - | GGAGGTAGAATTTTCTGA |
| Rabbit | 75.8 | -212 | + | CAGAAAATCCTGCCCGCA |
| Elephant | 87.2 | -255 | - | AGGGACAGAATTTTCTGA |
| Armadillo | 84.7 | -242 | - | GGGGGCAGAATTTCCTGA |

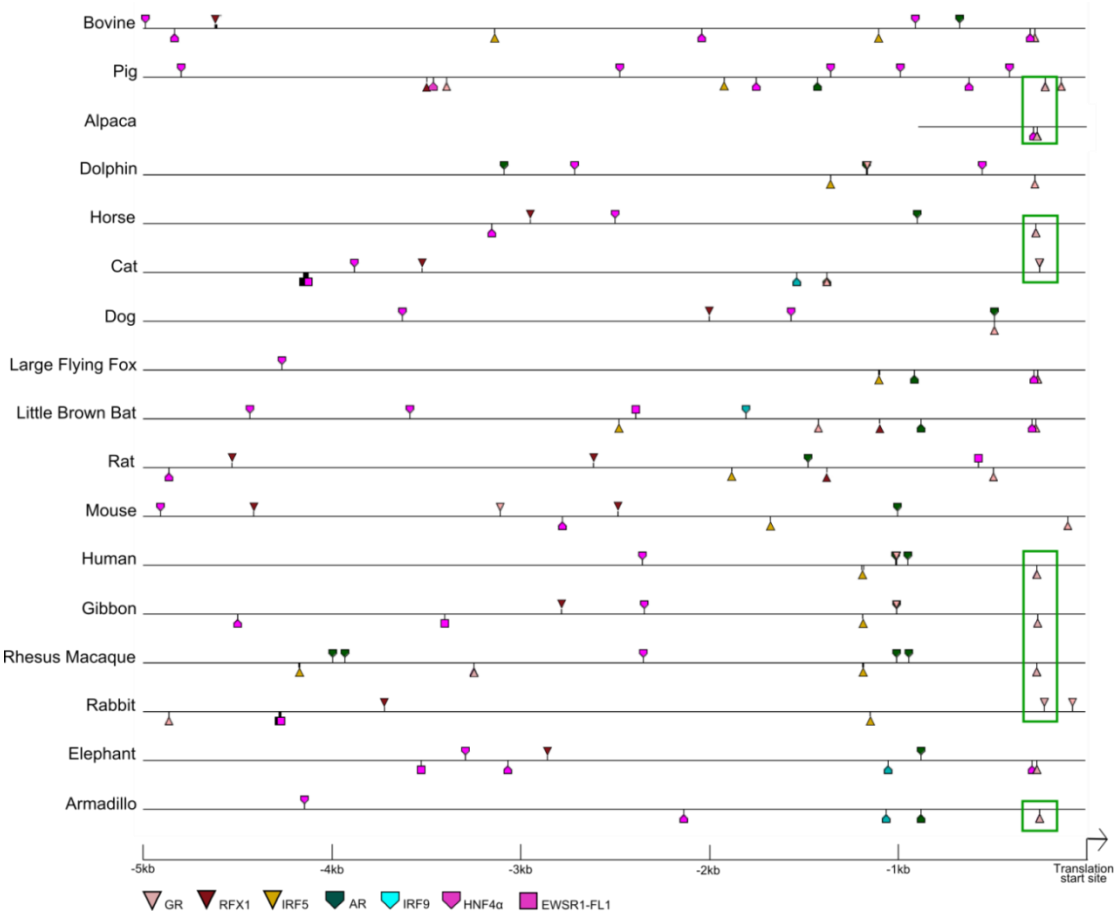


**Figure 3.18 Additional GR sites in *DEFB124* ortholog promoters when a 75% matrix match threshold is applied.**

The 5kb promoters of *DEFB124* orthologs were analysed with oPOSSUM3 using a 75% matrix match threshold. Ten additional GR sites, all with >75% score relative to the GR PWM, were identified within 200-300bp of the translation start site and are indicated with a green box.

### 3.3.2 DREME detection of conserved DNA motifs in syntenic cluster B β-defensin promoters

The oPOSSUM3 approach, and indeed any approach that involved searching against a PWM database, is limited by the content of that database. TFs may be missing from a database, or the DNA sequence they bind to in a given context may not match the PWM, for instance due to binding in conjunction with one or more partner TFs. In addition, non-coding regions many be conserved due to function in an alternative context. An alternative approach, focusing on searching for short motifs which are conserved among an input nucleotide sequence set, can potentially identify conserved regions in the promoters of β-defensin gene, without being constrained by comparison to a database of PWMs. The DREME tool was used to identify 8bp motifs enriched in the β-defensin promoter datasets relative to the same background used for the oPOSSUM3 analysis (p35).

There were a large number of short DNA motifs identified by DREME as being conserved among each β-defensin gene promoter set relative to the background (Table 3.4), which is the same GC- and length-matched background gene promoter set used for the oPOSSUM3 analysis. The number of motifs found ranged from 20 for *DEFB129* to 57 for *DEFB124*. This indicates there are non-coding regions within the promoters of diverse mammalian orthologs of each gene that have been conserved for some reason.

To compare these results to those from the oPOSSUM3 analysis, the motifs were compared to the JASPAR 2016 database of transcription factor binding motifs using the TOMTOM algorithm. Again, a corrected p-value, or E-value, was generated. The majority of conserved motifs did not match a TFBS PWM within the recommended E-value cut-off. This was probably due to the short length of the motifs, with most JASPAR profiles being longer than 8 nucleotides.

The motifs that were matched are given in Table 3.4, along with the TF identified and the corresponding E-value.

**Table 3.4 DREME search results with TOMTOM comparison to JASPAR 2016 database of TFBS profiles**

| Gene | Number of significant motifs (E-value<0.05) | Consensus motif | E-value of motif | TOMTOM-matched TF motif | Transcription factor family | E-value of TF motif |
|---|---|---|---|---|---|---|
| DEFB132 | 27 | ACAGGYGC | 0.00012 | Snail family zinc finger 2 (SNAI2) | Beta-beta-alpha zinc finger | 6.27E-05 |
| | | | | Inhibitor of DNA binding 4 (ID4) | Helix-loop-helix | 4.88E-02 |
| | | AACAWGGA | 0.021 | Forkhead box protein A1/Hepatocyte nuclear protein A3 (FOXA1) | Forkhead | 1.75E-02 |
| DEFB129 | 20 | GCKSS | 2.30E-25 | Myogenin/MyoD1-related protein (Myog) | Helix-loop-helix | 4.80E-02 |
| | | | | BHLHB2 | Helix-loop-helix | 4.80E-02 |
| | | TCTTGGCA | 2.70E-08 | NF-1A | SMAD/NF-1 DNA-binding domain factors | 4.22E-02 |
| DEFB128 | 33 | SGTAAACA | 0.00085 | Forkhead box protein I1 (FOXI1) | Forkhead | 4.47E-03 |
| | | | | Forkhead box protein O6 (FOXO6) | Forkhead | 8.83E-03 |
| | | | | Forkhead box protein O4 (FOXO4) | Forkhead | 2.84E-02 |
| DEFB127 | 20 | ATGGGATG | 7.70E-07 | Zinc finger protein 410 (ZNF410) | Beta-beta-alpha zinc finger | 0.0019849 |
| | | ATGTTTWC | 0.00064 | Forkhead box protein D1 (FOXD1) | Forkhead | 0.0270717 |
| | | TGACCTSA | 0.00085 | cAMP responsive element-binding protein 1 (CREB1) | Leucine zipper | 0.0436371 |
| DEFB126 | 28 | | | No TFs matched to motifs | | |
| DEFB125 | 24 | CACTGCAC | 0.00045 | SRY box 8 (SOX8) | High mobility group | 0.0142895 |
| DEFB115 | 20 | | | No TFs matched to motifs | | |
| DEFB116 | 30 | AATGTARA | 0.002 | Forkhead box protein K1 (FOXK1) | Forkhead | 0.0346261 |
| DEFB118 | 32 | CACTGCAC | 7.20E-18 | SOX8 | High mobility group | 0.0285791 |
| | | GATGAGWC | 0.032 | Nuclear factor, erythroid 2 (NFE2) | Leucine zipper | 0.0687393 |
| DEFB119 | 37 | RATTCAAA | 0.000011 | (Lin-54 homolog) LIN54 | CRC domain | 0.0373724 |
| DEFB121 | 26 | CACCAYG | 6.20E-15 | RE-silencing 1 (REST) | Beta-beta-alpha zinc finger | 0.0362724 |
| | | CACTSCAC | 3.80E-08 | SOX8 | High mobility group | 0.0188421 |
| DEFB122 | 21 | | | No TFs matched to motifs | | |
| DEFB123 | 25 | CCCTTGAY | 1.20E-10 | NR2F1 | Hormone nuclear receptor | 0.0499072 |
| DEFB124 | 56 | | | Regulatory factor X 1 (RFX1) | RFX | 6.03E-02 |

Regulatory factor X (RFX)1 matched one of the conserved motifs in the *DEFB124* set. This is in agreement with the oPOSSUM3 over-representation results (Figure 3.16), which indicated ten of seventeen orthologs contained a RFX1 binding site with >85% similarity to the RFX1 PWM.

The sole *DEFB128* motif with a TOMTOM-matched TF PWM is a potential forkhead box protein binding site, while the oPOSSUM3 analysis indicated every *DEFB128* ortholog contains 1-5 FOXF2 binding sites (Figure 3.5), though FOXF2 was not one of the three forkhead box proteins identified by TOMTOM. Both approaches indicated conservation of SRY-related HMG box (SOX) protein binding sites in *DEFB118* ortholog promoters, with SOX30 being identified by oPOSSUM3 (Figure

3.11) and SOX8 being identified by DREME/TOMTOM (Table 3.4). Helix-loop-helix and zinc finger proteins were similarly implicated by both techniques in the promoters of *DEFB132* (Figure 3.3) and *DEFB127* (Figure 3.6) respectively.

In addition to the constraints imposed by the size limit of DREME-detected motifs, a difference in the versions of JASPAR databases used may account for some of the differences in the TF families identified by the two methods. oPOSSUM3 works from the JASPAR 2010 database while TOMTOM accesses the most recent 2016 update. Nevertheless, this method has confirmed strong conservation of non-coding DNA motifs in the promoters of β-defensin genes and has implicated particular TF families as potentially binding these regions.

### 3.3.3 Multi-species alignment of syntenic cluster B β-defensin gene region and detection of evolutionarily-conserved regions

Assembly of the pre-initiation complex of general transcription factors takes place in the core promoter region and TFs conferring context-specificity of transcription can often bind to the proximal promoter region. However, consideration of only promoter regions ignores key components of the regulatory language of DNA. Introns bind essential TFs, while intergenic regions, possibly several kilobases or even megabases away from the genes they control, can act as enhancers or silencers of transcription.

With existing literature indicating syntenic cluster B β-defensin genes are preferentially expressed in the male reproductive tract, it is possible that tandem regulation via such intergenic elements within the gene cluster may contribute to this pattern. Multi-species alignment of large genome regions has proven useful in identifying conserved regions of the non-coding genome, the hypothesis being that these regions are conserved because they are functional. Indeed, function has been demonstrated for elements identified in this manner in several studies (Loots et al., 2000; Sakaguchi et al., 2015).

Over 300kb of the syntenic cluster B β-defensin region was downloaded from the UCSC Genome Browser for *Bos taurus*, *Homo sapiens*, *Canis lupus familiaris*, *Myotis lucifugus* and *Oryctolagus caniculus*. Threaded blockset alignment, as implemented by the open-source MULAN tool, identified evolutionarily-conserved regions (ECRs) common to each of the five species (p36). Basic ECRs are at least 100bp long and are conserved to ≥70% in each of the pairwise alignments, i.e. alignment between the bovine and each of dog, little brown bat, human and rabbit. A summary of the ECRs found within the cluster is provided in Figure 3.19. First exons were always conserved, with second exons, which encode the mature antimicrobial peptide, mostly, but not always surpassing the defined conservation cut-off. Second exons of *DEFB132*, *DEFB125*, and *DEFB119* were not defined as ECRs. Conversely, despite being annotated only in the bovine, both exons of DEFB125a and DEFB122a met these conservation criteria, though this does not mean that there is an open reading frame or that these genes are expressed in the other species. The regions just upstream, and in many cases just downstream of each gene were conserved. Given that the UTRs of most of these genes have not been empirically determined (those that are annotated in GenBank being coloured yellow in Figure 3.19) it is likely that such conserved regions correspond to 5'- and 3'UTRs.

There were several patterns of conservation observed in introns. The intronic region just proximal to the first exon may be conserved, e.g. *DEFB132* and *DEFB125*. Discrete bands of conservation along the whole intron were evident in *DEFB123* and *DEFB118*. In the case of *DEFB121* and *DEFB124*, the entire intron was conserved (Figure 3.20).

There were several intergenic ECRs, e.g. between *DEFB129* and *DEFB128* and either side of *DEFB124*. The region was also examined for ECRs meeting a more stringent cut-off of 77% conservation across a minimum of 350bp. This enhanced stringency has been shown to identify with increased confidence within inter-mammalian genome alignments, non-coding regions which are also conserved between the human and the more distantly-related pufferfish *Fugu rubripes* (Ovcharenko et al., 2004). This same study also showed the increased cut-off led to enrichment of enhancers with proven function within the resulting pool of ECRs, though not all of the functional enhancers met this level of conservation.

No ECRs met these criteria among all 5 species. However, 3 intergenic ECRs were conserved between bovine, dog, bat and human. These are represented as green bands and lie between *DEFB127-DEFB126*, *DEFB116*-DEFB117 and *DEFB123-DEFB124*.

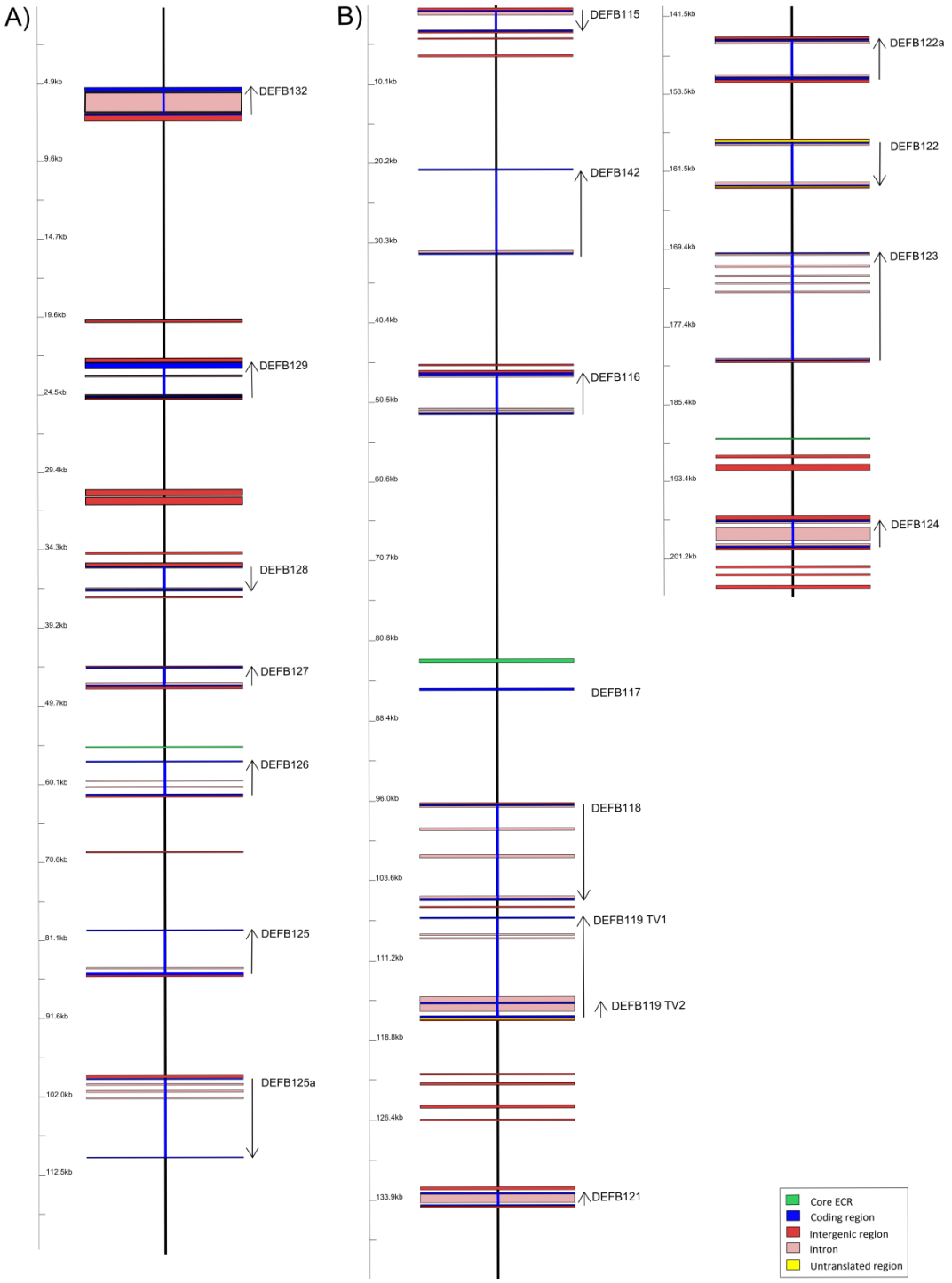


**Figure 3.19 Evolutionarily-conserved regions (ECRs) in β-defensin syntenic cluster B in a multi-species alignment including bovine, dog, little brown bat, human and rabbit.**
This cluster is separated into two in the human, so the alignment was done in two parts: A) genes *DEFB132* to *DEFB125* and B) genes *DEFB115* to *DEFB124*. Genomic sequences were downloaded from UCSC browser and aligned using a threaded blockset algorithm within the online MULAN software tool. The ECRs shown are regions of at least 100bp with a minimum of 70% conservation among the 5 species. Following Ovcharenko et al. (2004), an increased threshold of 350bp with >77% similarity was taken to be indicative of a core enhancer. Core enhancers have been shown to be highly conserved among vertebrates and are more likely to be functional. Intergenic regions with this level of conservation among 4 species are indicated in green.

Examination of pairwise alignments indicated a general agreement between length of ECRs and evolutionary distance. The conserved region was larger and the percentage conservation, as indicated by the height of the peak, greater between bovine and dog than between bovine and rabbit (see **Error! Reference source not found.** and REF _Ref479606223 \h **Error! Reference source not found.** for the full alignments; Figure 3.20 depicts the three core ECRs, extracted and displayed here for brevity).

It is not possible to know at the outset which species will be most informative for identification of functional regulatory elements. This depends on the rate of evolution of a given region and the genes contained within. While an alignment of the GATA3 gene and immediate proximal regions indicated all known functional elements were conserved in human-rodent, human-chicken and human-frog alignments, addition of a fish sequence recapitulated the coding exons but was only informative in terms of non-coding functional regulatory elements 50% of the time. Inclusion of such distantly-related species is only recommended when clear homology of a gene/genomic region can be established (Ovcharenko et al., 2005). While proteins such as TFs are evidently quite highly conserved, this cluster of β-defensin genes has been shown to have undergone positive selection since the rodent-primate split (Radhakrishnan et al., 2007). Accordingly, the pairwise alignments in Figure 3.20 indicate that conservation of protein-coding regions is not always high. For this reason we decided to proceed with the analysis of the intergenic enhancers meeting the higher conservation criteria, despite them not being conserved to this degree in the bovine-rabbit alignment.

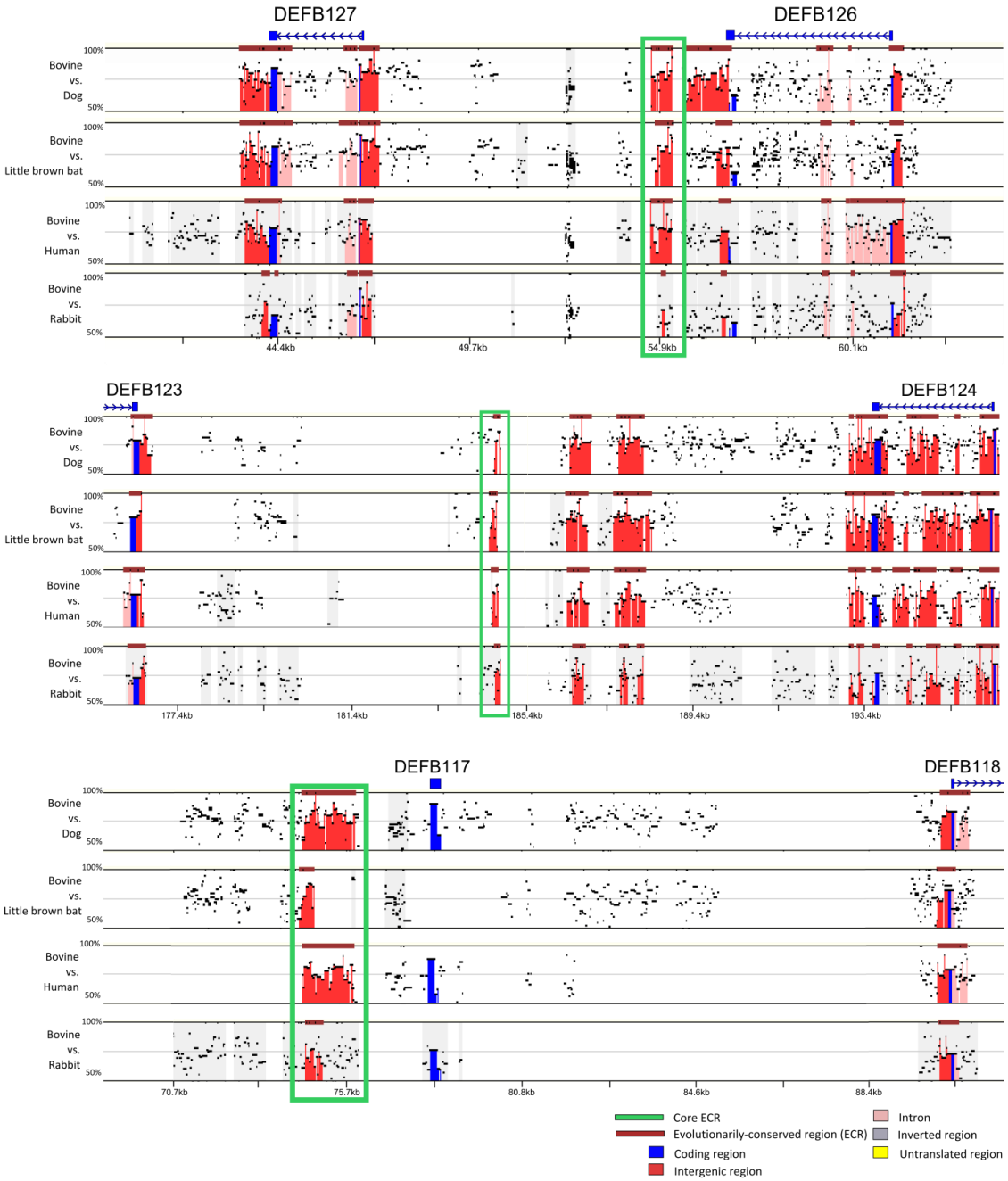


**Figure 3.20 ECRs from stacked pairwise alignment of β-defensin syntenic cluster B *DEFB124* between bovine and each of dog, little brown bat, human and rabbit.**

Genomic sequences were downloaded from UCSC browser and aligned using a threaded blockset algorithm within the online MULAN software tool. The full cluster alignment is shown in Appendix Figure A.1 and Figure A.2**Error! Reference source not found.** with key regions of the alignment being compiled here for brevity. The ECRs shown (red lines) are regions of at least 100bp with a minimum of 70% conservation among the 5 species. Following Ovcharenko et al. (2004), an increased threshold of 350bp with >77% similarity was taken to be indicative of a core enhancer. Core enhancers have been shown to be highly conserved among vertebrates and are more likely to be functional. Intergenic regions with this level of conservation among 4 species are indicated with a green box. The numbers underneath the alignment indicate position within the full syntenic cluster alignment.

### 3.3.4 TFBS modelling in the *DEFB127-DEFB126* intergenic ECR

To identify TFBSs within these core ECRs, the CLARE tool within the MULAN suite was used to build a linear classifier which distinguishes the ECR located between *DEFB127* and *DEFB126* (Figure 3.20) from a length- and GC-matched background generated within CLARE (Table 3.5; see p37 for method). The area under the curve (AUC) of 1 suggests the classifier is perfectly able to separate the β-defensin ECRs from the control sequences, though this is probably an overestimate due to the fact that the positive group is a small sample of sequences which have already been identified by alignment as being highly similar. AR is the top-weighted feature, with pituitary transcription factor 1 (PIT-1), SRF, AP-2α and the fourth, fifth and ninth motifs identified by PRIORITY from within the positive nucleotide sequences also being included in the classifier.

**Table 3.5 CLARE discriminative TFBS model of the *DEFB127-DEFB126* intergenic ECR**

| AUC | ROC operating point: | | Descriptive features of the model: | |
|---|---|---|---|---|
| | False positive rate | True positive rate | Transcription factor/motif | Weight |
| 1 | 0.05 | 0.55 | Androgen receptor (AR) | 354.93 |
| | | | Pituitary transcription factor 1 (PIT-1) | 188.91 |
| | | | Serum-response factor (SRF) | 75.33 |
| | | | PRIORITY motif 4 | 11.71 |
| | | | PRIORITY motif 5 | 6.7 |
| | | | AP-2α | 3.46 |
| | | | PRIORITY motif 9 | 2.23 |

As CLARE does not give nucleotide sequences for the returned transcription factor binding sites (with the exception of the PRIORITY motifs), binding sites for the named transcription factors were identified by searching the putative enhancer sequences using oPOSSUM3. There were two AP-2α binding sites in each sequence (Figure 3.21), while the AP-2 family was identified as being over-represented in the *DEFB126* promoters (Figure 3.7). Each sequence also contained one AR site and one of each of the three PRIORITY motifs. Despite not being conserved to the core ECR cut-off used in the MULAN analysis, the rabbit ECR contained five of the six motifs whose locations have been plotted in Figure 3.21.

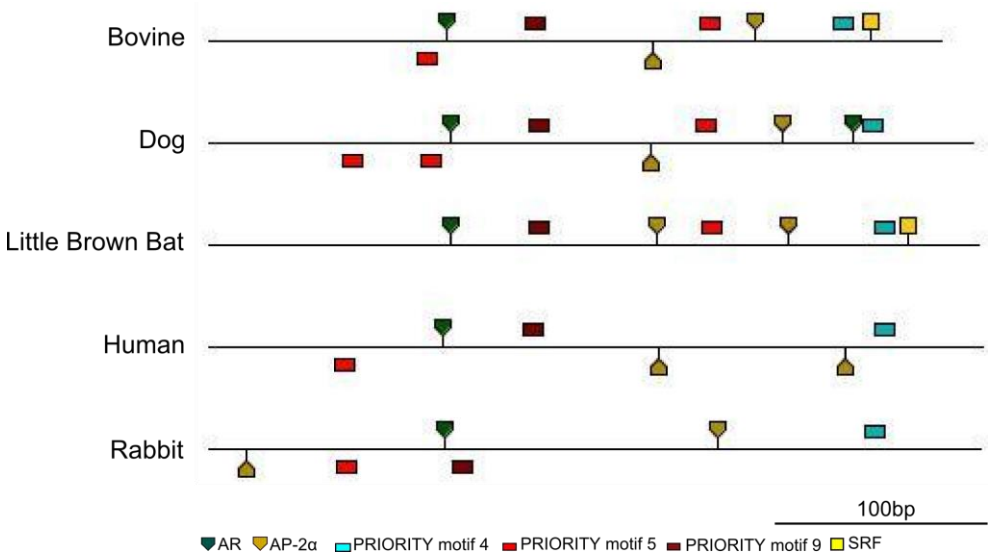


**Figure 3.21 *DEFB127-DEFB126* intergenic ECR: location of TFBSs identified by the CLARE discriminative model**
Nucleotide sequences corresponding to the core ECR between *DEFB127* and *DEFB126*, identified by MULAN within the genomes of five mammals, were analysed with oPOSSUM3 to identify individual binding sites for CLARE-implicated transcription factors. The sequence-based single site search function was used with an 85% similarity cut-off, except for AR and SRF for which a 75% cut-off was used as no sites were predicted with an 85% cut-off. The locations of these individual binding sites are represented graphically.

### 3.3.5 TFBS modelling in the *DEFB116-DEFB117* intergenic ECR

The classifier distinguishing the *DEFB116-DEFB117* cluster ECR from control sequences had a true positive rate of 0.46 and a AUC of 0.83 (Table 3.6). The β-defensin intergenic ECR was enriched for binding sites matching the LMO2COM PWM from the TRANSFAC database. The LMO2 complex is involved in the regulation of genes directing erythroid differentiation and is composed of a number of TFs, including GATA1, TAL1, E2A, LMO2 and LDB1 (Wadman et al., 1997). The PWM implicated here refers to the GATA1 half-site of this binding complex and nine of the ten unique LMO2COM binding sites were also identified as GATA1 sites using the JASPAR PWM with an 85% matrix match threshold, suggesting the GATA1 TF is involved here rather than the entire erythroid complex. A large number of caudal-related homeobox protein (CDXA) binding sites were also identified, as were TATA-binding protein (TBP) sites (Figure 3.22). RFX1 and oestrogen receptor 1 (ESR1, commonly referred to as ERα) were also identified by CLARE but binding sites for these factors were not identified in all sequences, even with a 75% cut-off. MIF1 refers to the PWM for the RFX1/myc-intron-binding polypeptide complex. All sites identified with this PWM were also identified by the RFX1 PWM and are represented in Figure 3.22 as RFX1 sites.

**Table 3.6 CLARE discriminative TFBS model of the *DEFB116-DEFB117* intergenic ECR**

| AUC | ROC operating point: False positive rate | ROC operating point: True positive rate | Descriptive features of the model: Transcription factor/motif | Descriptive features of the model: Weight |
|---|---|---|---|---|
| 0.83 | 0.05 | 0.46 | LMO2 complex (LMO2COM)/GATA1 | 1441.06 |
| | | | RFX1 | 191.34 |
| | | | CDXA | 141.29 |
| | | | TATA-binding protein (TBP) - motif 1 | 139.96 |
| | | | myc intron-binding protein (MIBP)/RFX1 complex (MIF1) | 62.5 |
| | | | Estrogen receptor 1 (ESR) | 55.62 |
| | | | PRIORITY motif 1 | 31.07 |
| | | | PRIORITY motif 4 | 8.38 |
| | | | TATA-binding protein (TBP )- motif 2 | 2.25 |

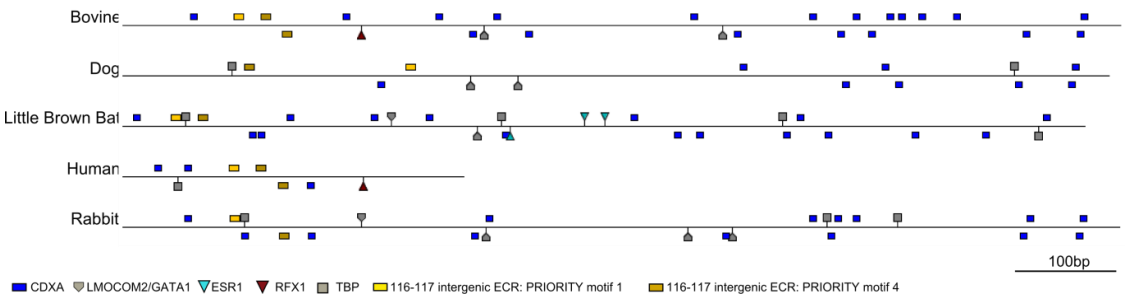


**Figure 3.22 *DEFB116-DEFB117* intergenic ECR: location of TFBSs identified by the CLARE discriminative model**

Nucleotide sequences corresponding to the core ECR between *DEFB116* and *DEFB116*, identified by MULAN within the genomes of five mammals, were analysed with oPOSSUM3 to identify individual binding sites for CLARE-implicated transcription factors. The sequence-based single site search function was used with an 85% similarity cut-off, except for AR and SRF for which a 75% cut-off was used as no sites were predicted with an 85% cut-off. The locations of these individual binding sites are represented graphically.

### 3.3.6 TFBS modelling in the *DEFB123-DEFB124* intergenic ECR

The model generated to characterise the *DEFB123-DEFB124* intergenic ECR had a true positive rate of 0.38 and an AUC of 0.87 (Table 3.7). The third and seventh motifs identified by the PRIORITY algorithm occurred once in each species. OCT1 and NFY motifs occurred in three of five sequences (Figure 3.23). GZF1 is specific to the TRANSFAC professional database and the PWM is not accessible.

**Table 3.7 CLARE discriminative TFBS model of the *DEFB123-DEFB124* intergenic ECR**

| AUC | ROC operating point: | | Descriptive features of the model: | |
|---|---|---|---|---|
| | False positive rate | True positive rate | Transcription factor/motif | Weight |
| 0.87 | 0.05 | 0.38 | PRIORITY motif 3 | 153.64 |
| | | | OCT | 66.58 |
| | | | NFY | 30.15 |
| | | | PRIORITY motif 7 | 27.95 |
| | | | OCT1 | 25.55 |
| | | | Glial cell line-derived neurotrophic factor inducible gene (GZF1) | 25.22 |

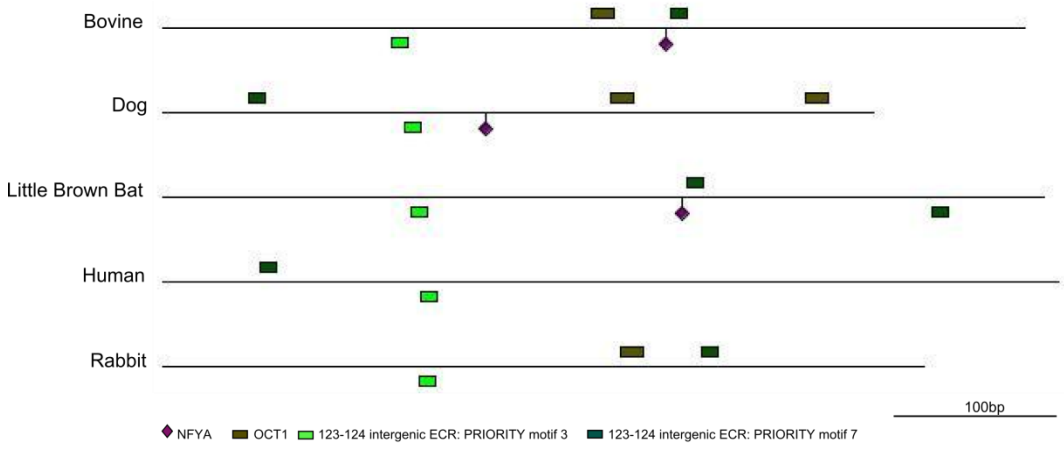


**Figure 3.23 *DEFB123-DEFB124* intergenic ECR: location of TFBSs identified by the CLARE discriminative model**
Nucleotide sequences corresponding to the core ECR between *DEFB123* and *DEFB124*, identified by MULAN within the genomes of five mammals, were analysed with oPOSSUM3 to identify individual binding sites for CLARE-implicated transcription factors. The sequence-based single site search function was used with an 85% similarity cut-off, except for AR and SRF for which a 75% cut-off was used as no sites were predicted with an 85% cut-off. The locations of these individual binding sites are represented graphically.

### 3.3.7 Prediction of TFs binding conserved motifs within ECRs

Within the ECR sequences, a number of PRIORITY-generated 10bp motifs distinguished these sequences from randomly-selected controls. To identify what TFs may be binding these motifs, TOMTOM was used to compare the motifs to the JASPAR 2016 database of TFBS PWMs. As there were only a small number of motifs to be analysed, the STAMP program, working from the JASPAR 2010 database, was also used (p38). Previous authors have found that STAMP and TOMTOM have complementary strengths and weaknesses and consideration of the two sets of results in tandem can produce the most accurate result (Zheng et al., 2014). A combined cut-off of TOMTOM $E<0.5$ with $E<1x10^{-5}$ for STAMP or $E<1$ for TOMTOM with STAMP $E<10^{-4}$ is recommended. $E<0.05$ is the cut-off recommended by the developers of TOMTOM when this tool is being used alone.

No TF PWMs were matched with high confidence by either tool to the three PRIORITY motifs in the *DEFB127-DEFB126* intergenic ECR or the fourth motif from the *DEFB116-DEFB117* enhancer.

A zinc finger protein may bind the first motif detected in the *DEFB116-DEFB117* enhancer (Table 3.8). While no PWM met the combined cut-off, the most similar PWMs were for C2H2 and beta-beta-alpha zinc fingers, with two different C2H2 transcription factors exceeding the $E<0.5$ TOMTOM cut-off.

**Table 3.8 TOMTOM and STAMP comparison of PRIORITY motifs from *DEFB116-DEFB117* ECR with JASPAR database**

| | **Transcription Factor Family** | **TOMTOM (E<1)** | **STAMP ($E<1x10^{-4}$)** |
|---|---|---|---|
| **PRIORITY motif 1** | | | |
| Zinc finger protein 740 (ZNF740) | C2H2 zinc finger | 2.44E-01 | |
| Specificity protein 1 (SP1) | C2H2 zinc finger | | 3.74E-05 |
| Specificity protein 2 (SP2) | C2H2 zinc finger | 4.04E-01 | |
| RE1-silencing transcription factor (REST) (Matrix 1) | Beta-beta-alpha zinc finger | | 4.95E-05 |
| REST (Matrix 2) | Beta-beta-alpha zinc finger | 7.84E-01 | 7.26E-05 |
| Sterol regulatory element binding transcription factor 1 (SREBF1) | Basic helix-loop-helix | 9.02E-01 | |
| Insulinoma-associated protein 1 (INSM1) | C2H2 zinc finger | | 3.68E-05 |
| **PRIORITY motif 4** | | | |
| No PWMs below cut-offs | | | |

The third motif identified by PRIORITY from the *DEFB123-DEFB124* intergenic ECR may bind a TEF-related factor. The highest TOMTOM match was to TEAD3 while STAMP returned TEAD1 (Table 3.8). Similarly, the most likely match to the seventh motif from both tools was an NFY TF. CLARE also identified NFY as enriched in this group of sequences (Table 3.7, Figure 3.23). While three of five orthologs contained the TRANSFAC NFY PWM, all five had binding sites for the seventh PRIORITY motif, suggesting this TF or one with a very similar structure may indeed bind to this putative regulatory region.

**Table 3.9 TOMTOM and STAMP comparison of PRIORITY motifs from *DEFB123-DEFB124* ECR with JASPAR database**

| | Transcription factor family | TOMTOM (E<1) | STAMP (E<1x10$^{-4}$) |
|---|---|---|---|
| **PRIORITY motif 3** | | | |
| Transcriptional enhancer factor TEF5 (TEAD3) | TEF1-related factor | 5.42E-01 | |
| Transcriptional enhancer factor TEF1 (TEAD1) | TEF1-related factor | | 9.58E-06 |
| Nuclear factor interleukin 3 regulated protein (NFIL3) | C/EBP-related factor | | 3.61E-05 |
| **PRIORITY motif 7** | | | |
| Nuclear transcription factor Y subunit β (NFYB) | Heterodimeric CCAAT-binding factor | 5.63E-01 | |
| Msh homeobox 1 (MSX1) | NK-related factor | 7.11E-01 | |
| Msh homeobox 3 (MSX3) | NK-related factor | 8.44E-01 | |
| Nuclear transcription factor Y subunit α (NFYA) | Heterodimeric CCAAT-binding factor | 8.70E-01 | 4.48E-05 |
| Homeobox protein engrailed 1 (EN1) | NK-related factor | 9.91E-01 | |

### 3.3.8 oPOSSUM3 TFBS over-representation analysis of identified ECRs

As the CLARE tool generates a relatively small background set consisting of 3 background sequences for each input sequence, oPOSSUM3 TFBS over-representation analysis was applied using a different background set. In this case, a set of human nucleotide sequences representing known open chromatin regions available within oPOSSUM3 was used to generate a GC-matched background of 100 background sequences for each ECR sequence. The sequence length varied between ECRs. The background sequences were 500bp long while the *DEFB127-DEFB126* ECRs were 368-394bp, the *DEFB116-DEFB117* ECR sequences were 353-1033bp long and the

*DEFB123-DEFB124* ECR sequences were 439-553bp long. The results generated for all three ECRs using an 85% PWM similarity cut-off are given in Table 3.10.

Within the *DEFB126-DEFB127* ECR, the AP2 family was over-represented, in agreement with the CLARE results for this ECR (Table 3.5). Spermatogenic leucine zipper 1 (SPZ1) was also over-represented. Androgen receptor binding was not identified as being over-represented based on a 85% similarity cut-off, however when this was lowered to 80%, androgen receptor was the most highly over-represented TF, with sex-determining region Y (SRY) the second most highly-over-represented.

oPOSSUM3 analysis with the more comprehensive background set indicated the *DEFB116-DEFB117* ECR was enriched for GATA5 and TBP binding sites. GATA1 and TBP were identified by the CLARE analysis of this ECR (Table 3.6). There was also agreement between the two analyses in respect of the *DEFB123-DEFB124* ECR, with NFYA and TEAD1 being identified by both (Table 3.7).

**Table 3.10 oPOSSUM3 analysis of ECRs using an 85% PWM similarity cut-off**

| | Z Score | Fisher Score | Number of species with ≥1 binding site |
|---|---|---|---|
| ***DEFB127-DEFB126* intergenic enhancer** | 6.524 (applied threshold) | 1.089 (applied threshold) | |
| AP2α | 29.736 | 6.431 | 5 |
| AP2γ | 20.232 | 7.786 | 5 |
| AP2ε | 17.467 | 5.201 | 4 |
| SPZ1 (Spermatogenic leucine zipper 1) | 14.256 | 2.686 | 3 |
| ZFP105 (Zinc finger protein 105) | 8.872 | 1.695 | 1 |
| OSR (Odd-skipped related) | 8.405 | 2.398 | 2 |
| ATF1 (cAMP-dependent transcription factor 1) | 8.285 | 1.792 | 1 |
| ***DEFB116-DEFB117* intergenic enhancer** | 8.473 (applied threshold) | 2.249 (applied threshold) | |
| MafB (musculoaponeurotic fibrosarcoma oncogene homolog B) | 17.595 | 5.302 | 2 |
| RXR-RAR(DR5) | 14.977 | 4.85 | 2 |
| HNF1A | 14.205 | 6.665 | 3 |
| NR2F2 (Nuclear receptor subfamily 2 group F member 2) | 12.684 | 6.262 | 4 |
| GATA5 | 12.341 | 5.64 | 3 |
| TBP | 11.76 | 2.384 | 4 |
| SMAD3 (SMAD family member 3) | 11.57 | 3.5 | 3 |
| ZSCAN4 | 11.476 | 4.446 | 4 |
| AP2α | 11.341 | 5.416 | 3 |
| KLF7 | 10.996 | 7.162 | 4 |
| PLAGL1 (PLAG1-like zinc finger protein 1) | 10.946 | 2.693 | 1 |
| ***DEFB123-DEFB124* intergenic enhancer** | 7.519 (applied threshold) | 1.291 (applied threshold) | |
| NFYA | 16.723 | 5.489 | 3 |
| TEAD1 | 14.304 | 4.127 | 3 |
| FOXQ1 | 9.688 | 1.329 | 4 |
| TFCP2L1 (Transcription factor CP2-like protein 1) | 8.812 | 3.643 | 3 |
| TCF3-HAND1 | 8.71 | 4.045 | 5 |
| CEBPA ( CCAAT/enhancer binding protein α) | 8.469 | 1.071 | 5 |

### *3.3.9* oPOSSUM3 TFBS over-representation analysis of syntenic cluster D genes *DEFB103* and *DEFB106*

Having used an *in silico* approach to generate a number of logical hypotheses relating to transcriptional regulation of syntenic cluster B β-defensin genes, we applied this approach to select syntenic cluster D genes.

Before carrying out TFBS analysis, the 5kb promoter regions of the two copies of *DEFB103* and *DEFB106* (named *DEFB103*/*106A* and *B*) annotated in the official human genome were aligned using MEGA6. The promoters of *DEFB103A* and *DEFB103B* were 100% identical. The *DEFB106A* and *DEFB106B* promoters were identical with the exception of a single extra nucleotide at different positions in each. In addition, EMSEMBL has assigned the same mammalian β-defensin gene records as being orthologs of each copy. Therefore, the B copy of each human gene was used and the annotated mammalian orthologs downloaded from ENSEMBL. The bovine promoters were taken from the most recent version of the bovine genome, accessible through the UCSC genome browser.

Binding sites for five transcription factors were over-represented in the promoters of *DEFB103* orthologs (Figure 3.24). The most highly over-represented was Jun dimerisation protein (JDP)2. JDP2 binding sites occurred in thirteen of fourteen *DEFB103* ortholog promoters, with a binding site occurring within -650 to-710bp relative to the translation start site. Notably, the four PWMs representing NF-κB components are under-represented in DEFB103 ortholog promoters relative to the randomly selected background set. The Z scores ranged from -8.526 to -15.043 and Fisher scores from 0 to 0.005, relative to the over-representation cut-offs of 10.420 and 1.168 respectively.

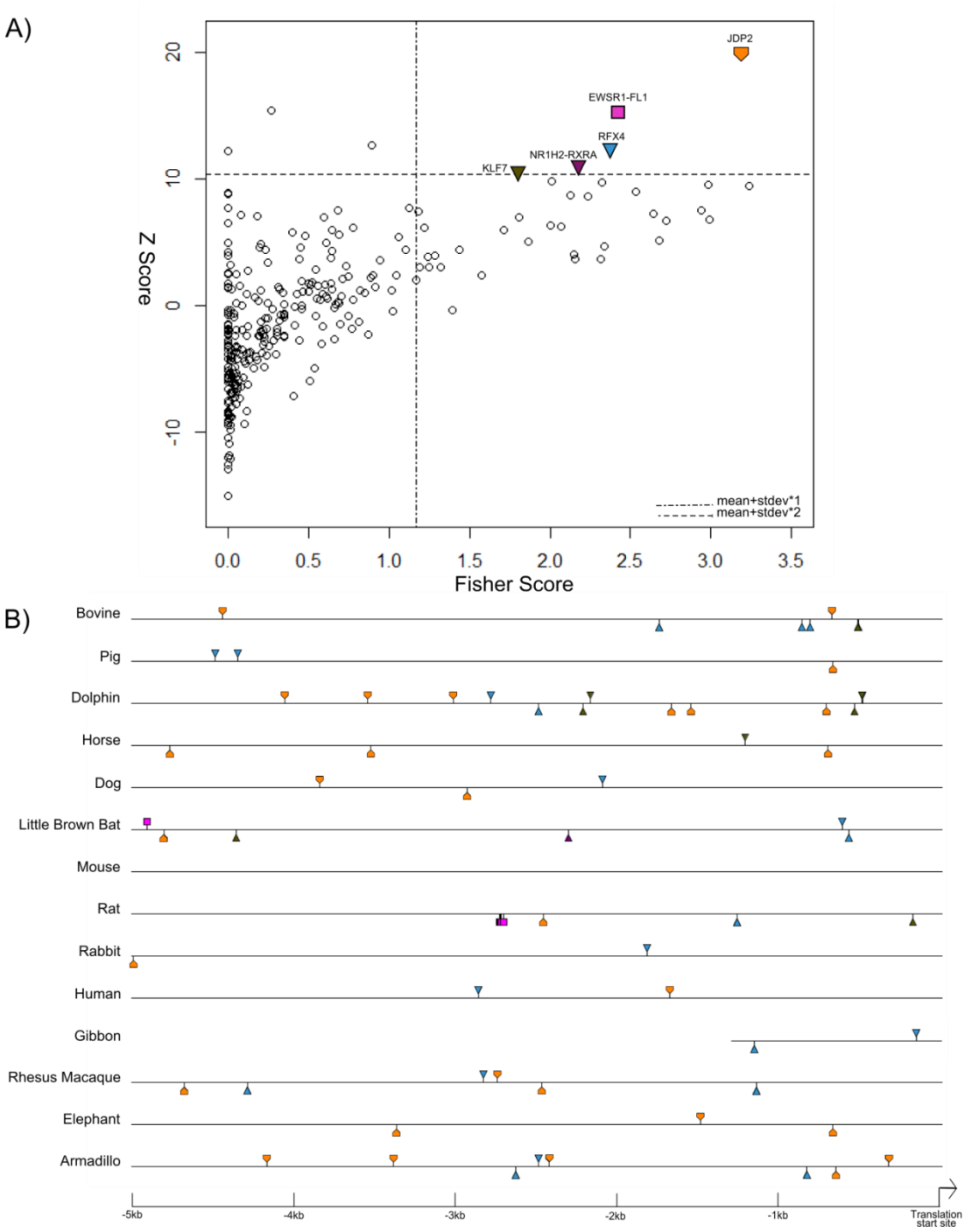


**Figure 3.24 *DEFB103*: oPOSSUM3 TFBS over-representation analysis of orthologs in fourteen species.**

Five kb of nucleotide sequence upstream of the translation initiation codon for bovine *DEFB103* and thirteen orthologs was downloaded using ENSEMBL Biomart. The oPOSSUM3 sequence-based single site analysis software tool was used to determine which TFs were statistically overrepresented in the β-defensin promoters relative to a length- and GC-matched background set of human promoters. A 100:1 ratio of background to foreground sequences was used to ensure the background set was large enough to avoid skewing due to the presence of different subsets of genes. Two types of over-representation were assessed by Z score and Fisher score. A) Applied thresholds were used to identify TFs considered overrepresented by both measures as recommended by Kwon et al (2012). B) The positioning of individual TFBS within the promoter regions of thirteen *DEFB103* orthologs is indicated.

Three transcription factors were over-represented in the promoters of *DEFB106* orthologs. PAX5 sites occurred in four of eight orthologs, with the site occurring within 110 to 140bp of the translation start site in each case (Figure 3.25).

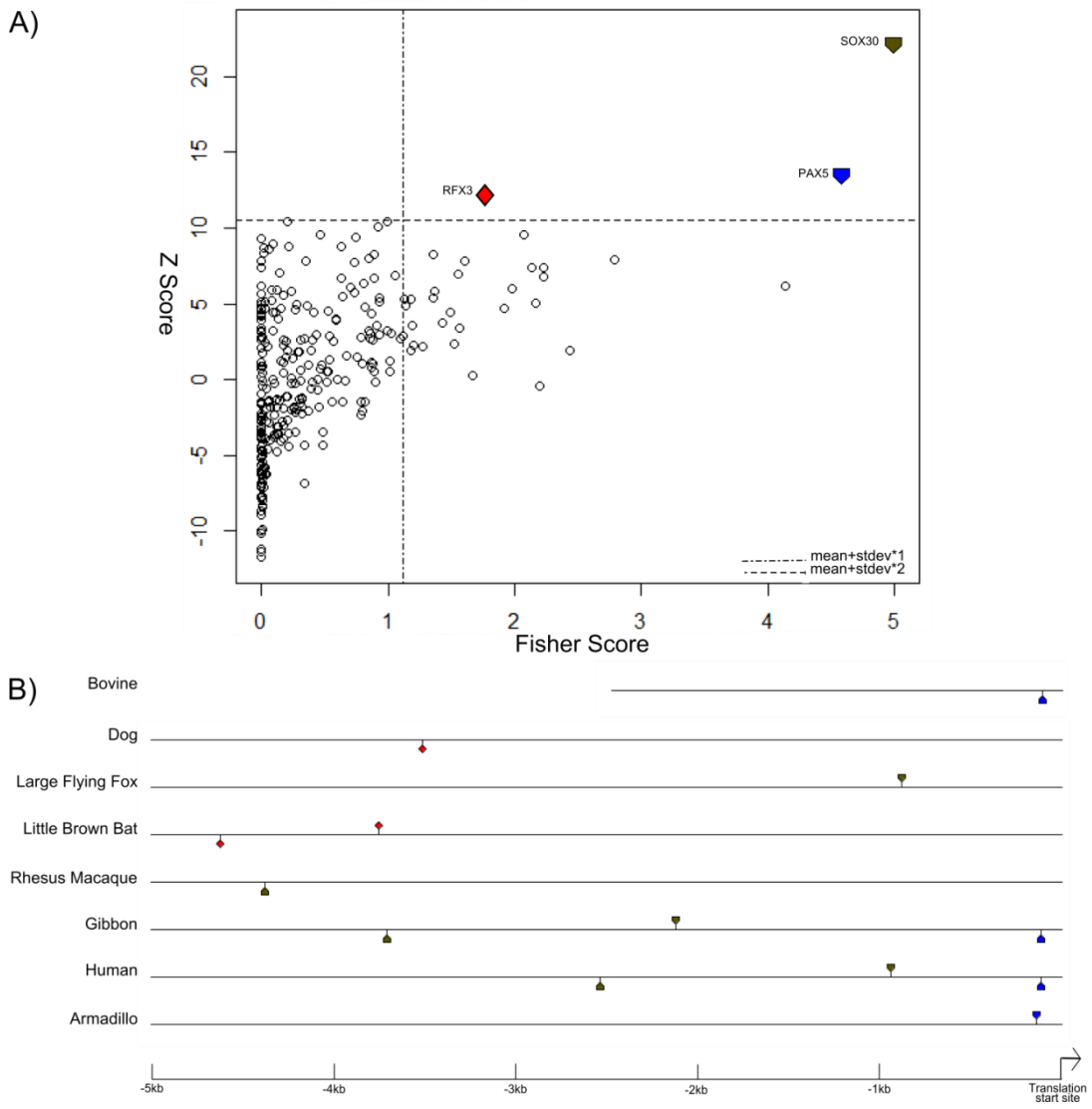


**Figure 3.25 *DEFB106*: oPOSSUM3 TFBS over-representation analysis of orthologs in eight species.** Five kb of nucleotide sequence upstream of the translation initiation codon for bovine *DEFB106* and seven orthologs was downloaded using ENSEMBL Biomart. The oPOSSUM3 sequence-based single site analysis software tool was used to determine which TFs were statistically overrepresented in the β-defensin promoters relative to a length- and GC-matched background set of human promoters. A 100:1 ratio of background to foreground sequences was used to ensure the background set was large enough to avoid skewing due to the presence of different subsets of genes. Two types of over-representation were assessed by Z score and Fisher score. A) Applied thresholds were used to identify TFs considered overrepresented by both measures as recommended by Kwon et al (2012). B) The positioning of individual TFBS within the promoter regions of seven *DEFB106* orthologs is indicated.

### 3.3.10 DREME detection of conserved DNA motifs in syntenic cluster D β-defensin promoters

DREME identified twenty nine conserved 8bp motifs in the *DEFB103* ortholog promoter set (Table 3.11); twelve were conserved in *DEFB106* promoters. Comparison of these motifs to the JASPAR 2016 database of transcription factor PWMs indicated three *DEFB103* motifs had matches. KLF1 was identified by TOMTOM from the JASPAR 2016 database, while KLF7 was identified by oPOSSUM3 from the JASPAR 2012 database. Another motif matched with binding sites for several AP-1 family binding sites, with the AP-1 family member JDP2 having been implicated by oPOSSUM3 (Figure 3.24).

**Table 3.11 DREME search results for *DEFB103* and *DEFB106* with TOMTOM comparison to JASPAR 2016 database of TFBS profiles**

| Gene | Number of significant motifs (E-value<0.05) | Consensus motif | E-value of motif | TOMTOM-matched TF motif | Transcription factor family | E-value of TF motif |
|---|---|---|---|---|---|---|
| *DEFB103* | 29 | CACASCCA | 6.70E-05 | Krüppel-like factor 1 (KLF1) | Beta-beta-alpha zinc finger | 4.77E-02 |
| | | GCAACASC | 9.90E-04 | Transcription factor 21 (TCF21) | Basic helix-loop-helix | 3.04E-02 |
| | | GTGACYCA | 1.00E-03 | Fos-related antigen 1 (FOSL1) | Basic leucine zipper | 2.54E-02 |
| | | | | Jun-D (JUND) | Basic leucine zipper | 4.17E-02 |
| | | | | FOS-Jun/AP-1 | Basic leucine zipper | 4.35E-02 |
| *DEFB106* | 12 | | | No TFs matched | | |

## 3.4 Discussion

Here we show that the syntenic cluster B β-defensin region contains several conserved non-coding regions. These occur within promoter, intronic and intergenic locations and we hypothesise that conservation among mammals indicates that these non-coding elements have regulatory function.

The results of our computational analysis broadly agree with some previous *in silico* work implicating a number of nuclear hormone receptors in β-defensin regulation. Computational analysis of a small number of human and rodent β-defensin promoters detected binding sites for androgen receptor (AR), glucocorticoid receptor (GR) and the retinoic acid receptors (Brahmachary et al., 2006). However, the work presented here extends this considerably and has generated interesting hypotheses as to how these innate immune genes might be regulated.

Twelve of sixteen *DEFB128* ortholog promoters contain a serum response factor (SRF) binding site within 500bp of the translation initiation codon. *DEFB128* is solely expressed in the male reproductive tract (Narciandi et al., 2011; Rodríguez-Jiménez et al., 2003) and epididymal expression of murine *DEFB128* is highly responsive to androgen through AR binding to the proximal promoter (Hu et al., 2014). Despite this, computational analysis of the AR-bound region detected no canonical AR-binding DNA motif (Hu et al., 2014). Similarly, the more comprehensive comparative genomics approach used here did not detect conservation of AR binding sites among mammals, but did highlight SRF. SRF is a ubiquitously-expressed transcription factor which is itself regulated by androgen (Prencipe et al., 2015). AR and SRF directly interact and bind to a serum response element (SRE) in the α-actin gene promoter to drive gene expression (Vlahopoulos et al., 2005). SRF is expressed in the testis and interacts with basic helix-loop-helix transcription factors at an SRE in the c-Fos promoter, resulting in expression of c-Fos in response to follicle-stimulating hormone. Androgen regulation of *DEFB128* may therefore be mediated by an SRF intermediate binding to its own canonical DNA binding site.

A similar pattern of conservation is seen in the *DEFB129* promoter, with conserved retinoic acid receptor (RAR)α- retinoid X receptor (RXR) heterodimer and paired box

(PAX)5 binding sites in close proximity to the translation initiation codon. The role of PAX5 in B cell function is well documented, and retinoic acid upregulates PAX5 expression in B cells (Chen et al., 2013). However, PAX5 is also expressed in the developing CNS and testis (Adams et al., 1992), though it's role in the testis remains unknown.

RAR and RXR genes are expressed by Sertoli cells of the testis (Vernet et al., 2006), as are the enzymes necessary to metabolise retinoic acid to its active form (Raverdeau et al., 2012). The importance of retinoic acid in spermatogenesis, the process by which diploid germ cells in the testis differentiate into haploid spermatocytes, has received much attention (reviewed by Hogarth and Griswold, 2010). Mice without retinoic acid activating enzymes in sperm-forming Sertoli cells experience arrested spermatogenesis (Raverdeau et al., 2012), demonstrating the importance of this dietary hormone in core testis function. While the cellular specificity of expression and the function of *DEFB129* within the testis are currently unknown, PAX5 and retinoic acid receptors may regulate expression of this gene in the male reproductive tract.

In contrast, the exact role of retinoic acid in the epididymis is still poorly understood. Mice without functional RARα expression in the epididymis are infertile due to thickening of the luminal fluid, implying large-scale changes in the proteins produced by the epithelium (Costa et al., 1997). Epididymal retinoic acid binding protein/lipocalin 5 (ERABP/LCN5) is one of the most abundant proteins in the epididymal fluid in both human (Newcomer and Ong, 1990) and bovine (Belleannée et al., 2011). The function of LCN5 has not yet been elucidated, however, it is posited to deliver retinoic acid to both the spermatozoa and the epithelium lining the tract (Ong et al., 2000). As LCN5 is itself regulated by androgen, particularly in the caput epididymis (Zwain et al., 1992), regulation of retinoic acid delivery by androgen may mediate the effects of androgen on *DEFB129* expression.

Previous analysis of androgen regulation of murine β-defensins showed the *DEFB126* ortholog was partially regulated by androgen, possibly via binding of AR to a motif located >9kb upstream of the gene (Hu et al., 2014). Our alignment of the β-defensin gene region in several mammals indicates the presence of a short ECR within a similar distance, though this has not been analysed for AR binding sites. AR binding of

the core ECR predicted within 2kb downstream of *DEFB126* was not detected in the mouse epididymis (Hu et al., 2014), despite our finding that this region was enriched for AR binding sites.

AP-2α binding sites have also been predicted within this ECR and within the *DEFB126* promoter, in close proximity to the translation initiation codon. A functional association between AR and the AP-2 family has been previously shown (Pihlajamaa et al., 2014). AR associates with hepatocyte nuclear factor (HNF4)α in the kidney and with AP-2α in the epididymis to differentially regulate expression of a number of genes in castrated mice with and without testosterone (Pihlajamaa et al., 2014). AP-2α was thought to act as a pioneer, opening chromatin where necessary to allow AR and probably other transcription factors to access necessary binding sites. A separate study also found AR ChIP-Seq peaks were enriched for AP-2 family binding sites (Hu et al., 2010). This suggests these two transcription factors may collaborate to regulate *DEFB126* expression (Figure 3.26). With Loots et al. (2000) demonstrating the ability of a single intergenic ECR to regulate several local paralogous genes in tandem, it is possible that this ECR may mediate androgen regulation of a number of androgen responsive β-defensin genes.

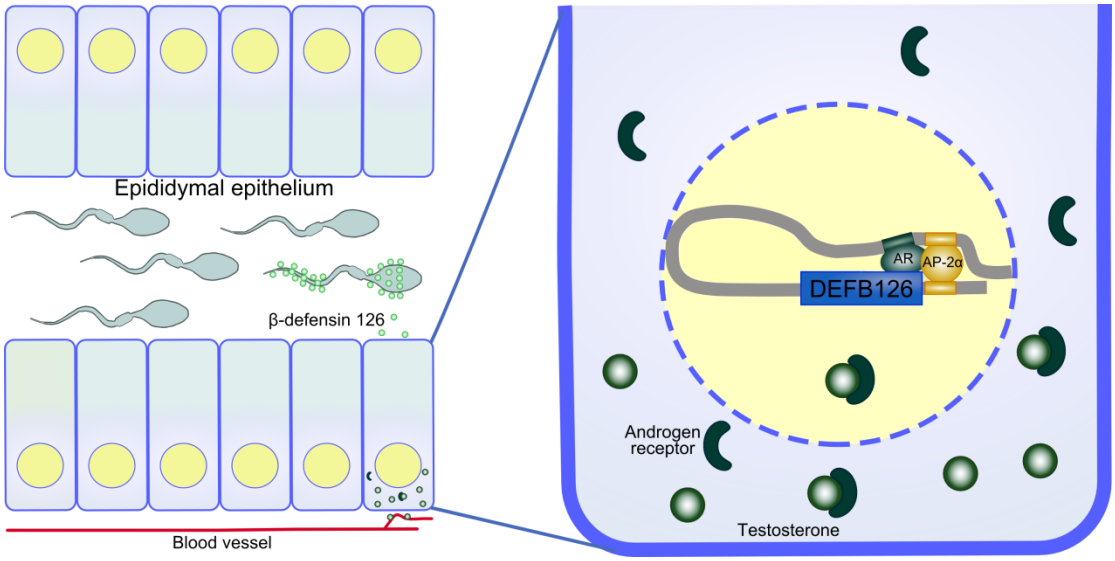


**Figure 3.26 Hypothesised regulation of *DEFB126* in the bovine epididymis**
When testosterone produced in the sexually-mature bull enters epididymal epithelial cells from the bloodstream and binds androgen receptor, AR translocates to the nucleus where it binds to the ECR downstream of *DEFB126*. AP-2α is also bound here and contact between this ECR and the *DEFB126* promoter, which could occur via a number of mechanisms, allows AP-2α to bind the promoter via the AP-2α binding site within. DEFB126 is released from the cells and binds to the sperm tail and post-acrosomal head where it promotes sperm motility.

The AP-2 family may also be involved in regulating *DEFB123*. Our analysis indicates both AP-2β and CTCF binding sites are over-represented in the *DEFB123* promoter, with the location of CTCF binding sites being relatively conserved close to the translation initiation codon. A high-throughput luciferase assay approach, testing for function of predicted CTCF sites in gene promoters in a number of cell types, showed only a small number of sites were functional in all cell types (Whitfield et al., 2012). This suggested CTCF may function with a variety of cell type-specific co-factors. Sites that were functional in all cell types were more likely to be conserved among mammals and be close to the transcription start site. These ubiquitously functioning sites co-occurred with binding sites for a number of other transcription factors, including the AP-2 family (Whitfield et al., 2012). Martin et al. (2011) also found that AP-2 binding sites were over-represented in close proximity to regions bound by CTCF across the cell types and species examined. Thus, the methodology applied here has yielded a number of viable hypotheses as to how syntenic cluster B β-defensin genes are regulated.

While AP-1 is known to regulate human *DEFB103* in keratinocytes and pulmonary epithelium, TFBS over-representation analysis suggests that AP-1 family

regulation of this gene has been conserved among mammals. AP-1 is a heterodimer of Fos and Jun family proteins. The Jun family includes c-Jun, JunB and JunD. Fos family members include c-Fos, FosB, FOSL1, and FOSL2 proteins. Activating transcription factor (ATFs) and cAMP response element binding protein (CREB) can also dimerise with jun proteins. The range of dimers that can result means a wide range of physiological and pathological processes converge on AP-1 activation (Eriksson et al., 2007) (Figure 3.27).

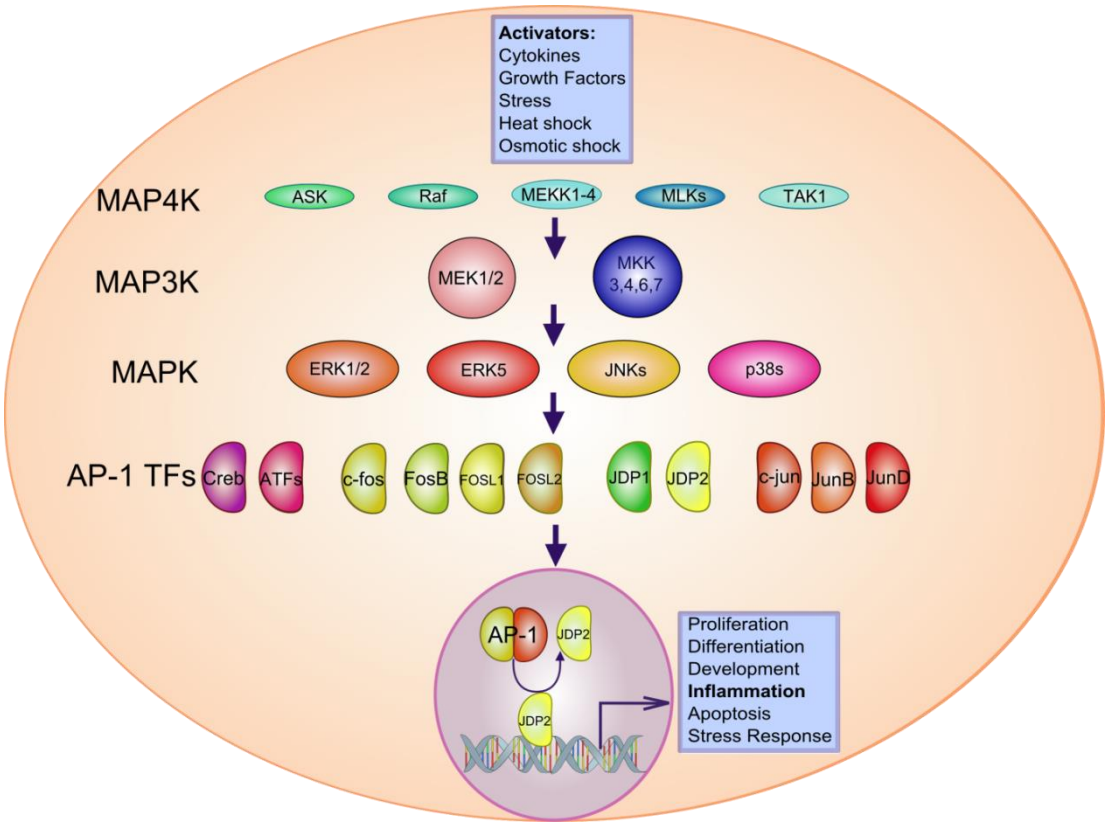


**Figure 3.27 MAPK signalling converges on AP-1 activation**
A diverse range of stimuli initiate a phosphorylation cascade culminating in dimerization and nuclear translocation of AP-1 family transcription factors. JDP2 constitutively binds DNA and represses the transcriptional activity of jun family proteins. Transcription of alternative jun binding partners displaces JDP2 and gene transcription is initiated. Based on (Aronheim et al., 1997; Eferl and Wagner, 2003; Zhang and Liu, 2002).

As AP-1 complexes bind DNA in unstimulated cells without initiating transcription, it was posited that such complexes included a repressor under baseline conditions. Screening for novel c-jun binding partners identified two proteins: Jun dimerization protein (JDP)1 and JDP2 (Aronheim et al., 1997). JDP2, but not JDP1, can

bind the AP-1 site alone. JDP2 represses transcriptional activation and is constitutively expressed, unlike c-fos. Under baseline conditions, jun predominantly associates with JDP2. Once fos expression is induced, fos-jun complexes dominate. Thus, JDP2 binding may limit *DEFB103* expression until cells are stimulated. The TFBS of JDP2 is very similar to, but slightly longer than, the canonical AP-1 binding site. This is probably why TFBS over-representation analysis has identified JDP2 rather than AP-1 itself. However, the literature indicates transcription-activating AP-1 complexes bind the same sites as JDP2.

AP-1 family proteins are activated by the mitogen-activated protein kinase (MAPK) pathway; a phosphorylation cascade including MAP4Ks, MAP3Ks and MAPKs. There are four groups of MAPKs: c-jun N-terminal kinases (JNKs), extracellular regulated protein kinases (ERKs) 1 and 2, ERK5 and p38s. All MAPKs can phosphorylate and activate AP-1 components under certain circumstances (Chang and Karin, 2001; Eriksson et al., 2007; Zhang and Liu, 2002). This means AP-1 signalling is activated by a wide range of stimuli, both immune-related and otherwise (Figure 3.27). Thus, while AP-1 binding sites are conserved in the *DEFB103* promoter, differences in receptor repertoire, intracellular signalling machinery and transcription factor co-operation between species and especially cell types may generate diversity in the stimuli that drive gene expression.

Searching for conserved DNA motifs within the β-defensin promoters independently of a transcription factor PWM database indicates there are several conserved motifs within each group of orthologs. This approach is important as new information emerges constantly on novel transcription factors and on the complexity of transcription factor-DNA interactions. Recent research indicates formation of transcription factor complexes can be mediated by DNA and can lead to binding to a novel DNA motif (Jolma et al., 2015).

Alternatively, several features within 5'UTRs control gene expression independent of transcription factor binding (Mignone et al., 2002). Secondary structures can be formed which control mRNA stability. Binding of various proteins allows mRNA decay or trafficking of mRNA to certain locations within the cell.

The 3'UTR is even more important in this regard, particularly as it is the primary site of regulatory non-coding RNA (ncRNA) binding (Kaikkonen et al., 2011). Micro RNAs (miRNAs) are the best characterised within this diverse group. miRNA binding of the mRNA 3'UTR is followed by recruitment of the RNA-induced silencing complex which can inhibit translation or destabilise the mRNA.

ncRNA regulation of β-defensins has not yet been investigated. However, detection of colon cancer-specific mutations in 3'UTRs of β-defensin genes indicates such regulatory mechanisms are important, given the expression of each gene is downregulated in malignant tissue (Semlali et al., 2015). The identification of conserved motifs upstream of coding exons, plus the conservation of 3' regions of syntenic cluster B genes detected in this analysis, could act as a starting point for future investigation of these mechanisms.

Epigenetic regulation, i.e., heritable change to DNA that does not affect the DNA sequence (Weinhold, 2006), is another important mechanism that has not been investigated here. Types of epigenetic change include methylation of cysteines within DNA and post-translational modifications of histone proteins within the tightly wound DNA-protein complex that composes chromatin. Both mechanisms regulate β-defensin expression. Histone deacetylase (HDAC) enzymes remove acetyl groups from N-terminal lysine residues of histones, opening chromatin to allow access for the transcriptional machinery. HDAC1 inhibition potentiates LPS induction of the rat orthologs of *DEFB118*, *DEFB119* and *DEFB122* (Biswas and Yenugu, 2014). HDAC1 also controls *DEFB1* expression in human lung epithelium, with inhibition increasing acetylation of histones at the *DEFB1* promoter which in turn increases transcriptional activity (Kallsen et al., 2012). Methylation of fourteen sites in the human *DEFB1* promoter decreases transcriptional activity in prostate cancer cells, with methylation of two particular sites being more frequent in tumour tissue than in non-tumour tissue from prostate cancer patients (Lee et al., 2016). HDAC activity also regulates human *DEFB4A* expression in response to bacteria (Yin and Chung, 2011) and yeast (Angrizano et al., 2013).

The agreement between the computational analyses for *DEFB103* and the existing experimental data indicates the comparative genomics approach used here does indeed generate meaningful predictions. These results allow us to direct our future experimental

work and add considerably to our understanding of how these multifunctional effector molecules are regulated.

# Chapter 4 Proinflammatory cytokines regulate β-defensin expression in primary endometrial stromal cells

## 4.1 Introduction

The bioinformatics approach used here suggests syntenic cluster B β-defensin genes are regulated by reproductive rather than immunological processes. In addition, there is a lack of validated *in vitro* male reproductive tract models to investigate these predictions in more detail. In contrast, both pro- and anti-inflammatory functions have been attributed to the proteins encoded by *DEFB4A* and *DEFB103*. AP-1 signalling has been identified as a potential regulator of *DEFB103* expression. Hence, the syntenic cluster D genes, found on bovine chromosome 27, were selected for further investigation. Our group has a strong interest in cow reproductive tract immunology, thus we decided to focus on regulation of β-defensin gene expression within this context.

The female reproductive tract (FRT) is routinely contaminated and must effectively defend against sexually-transmitted bacterial and viral pathogens. Parturition also results in an influx of a range of pathogens, while uterine involution requires repair of wide-spread tissue damage. Uniquely, the FRT must also remain tolerant of commensal bacteria and sperm while the role of uterine leukocytes in facilitating implantation of an allogenic trophoblast is increasingly recognised (Mor et al., 2011).

The antimicrobial and immunomodulatory properties of HDPs suggest that they may be involved in these functions. β-defensin expression throughout the FRT of human (Frew and Stock, 2011) and mouse (Hickey et al., 2013) has received much attention, with other animal models having been studied to a lesser extent. However, a limited number of the total repertoire of β-defensins have been studied in this context, namely the human syntenic cluster D genes *DEFB1*, *DEFB4A*, *DEFB103* and *DEFB104* and their murine orthologs.

The literature on sex steroid regulation of β-defensins suggests regulatory mechanisms are tissue specific. Murine β-defensins are more highly expressed in the vagina than the uterus, with uterine levels peaking during the oestrogen-dominant phase of the cycle (Hickey et al., 2013). Both estrogen and progesterone receptors interact with

activator protein 1 (AP-1) and AP-1 binding sites, (Bamberger et al., 1996; Webb et al., 1999), with our analysis finding that AP-1 binding sites are conserved in the promoters of *DEFB103* orthologs. In the human endometrium, *DEFB103* is most highly expressed during the progesterone-dominant secretory phase of the menstrual cycle, while *DEFB4A* expression is highest during the cortisol-dominant menstrual phase (King et al., 2003). However, oestrogen increases *DEFB4A* expression by primary human uterine epithelial cells *in vitro* (Fahey et al., 2008). In the ovine oviductal epithelium, *SBD1* expression is increased by oestrogen (Wen et al., 2012). However, oestrogen appears to have an opposing effect on *DEFB4A* regulation in the human vagina, with expression in epithelial cultures decreasing when oestrogen is used alone (Patel et al., 2013). A separate study indicates oestrogen increases LPS-driven *DEFB4A* expression in the same model, with progesterone decreasing it (Han et al., 2010).

The latter finding is particularly interesting as livestock, including cows, sheep and pigs, are less susceptible to uterine infection when progesterone levels are basal and more susceptible during the progesterone-dominant phase of the cycle. An exception to this is the immediate post-partum period when bacterial influx during labour leads to infection despite basal progesterone (Lewis, 2003). It is difficult to extrapolate from this body of work, if and how β-defensins may be regulated by sex steroids in the cow reproductive tract.

Pro-inflammatory signals also regulate β-defensin expression in the reproductive tract. IL-1β and TNFα drive expression of *DEFB4A* by primary human trophoblast cells (King et al., 2007) and *DEFB4A* (King et al., 2002) and *DEFB103* (King et al., 2003) in endometrial epithelial cells. These cytokines may mediate the observed innate immune response to pathogens detected in the FRT. Bacterial vaginosis drives an increase in secretion of hBD-2, the peptide encoded by *DEFB4A* (Fan et al., 2008). Similarly, *DEFB103* expression is increased in inflamed fetal membranes (Buhimschi et al., 2004). A range of HDPs, including hBD-1, are found in the cervical mucus plug and this pregnancy-generated structure exerts anti-microbial activity against a number of relevant pathogens (Hein et al., 2002). β-defensins may also mediate the anti-viral response in the FRT, as hBD-2 levels in the cervico-vaginal lavage fluid of HIV-positive women correlate with anti-HIV activity (Ghosh et al., 2010). In contrast, gammaherpesvirus infection of the murine cervix attenuates β-defensin expression, which may explain the

predisposition towards bacterial infection of the cervix observed in virally-infected animals (Racicot et al., 2013). Together, these studies indicate β-defensins are an important defence mechanism within the reproductive tract.

### 4.1.1 Inflammation within the cow reproductive tract

Inflammatory disorders of the cow reproductive tract, particularly in the post-partum period, negatively impact animal welfare and productivity. While uterine inflammation immediately post-partum is usually followed by a return to homeostasis (Chapwanya et al., 2012; Foley et al., 2015) persistence of an inflammatory state beyond 21 days post-partum (DPP) is pathological and has several implications.

Diagnosis of metritis, or uterine inflammation, is based on enlargement of the uterus along with discharge that is altered in both colour (due to the presence of pus, i.e. purulent discharge) and odour (fetid discharge). Metritis is often accompanied by systemic illness such as decreased milk yield and occurs within 21DPP (Sheldon et al., 2006). A meta-analysis indicates metritis is associated with increased time to first service, due to delayed return of uterine homeostasis, and a reduced conception rate after first service (Fourichon et al., 2000). More recent evidence indicates metritis remains a problem within dairy herds. Within 5,085 cows from a single US herd, an 18% incidence of metritis was associated with reduced conception rate and increased pregnancy loss (Ribeiro et al., 2016).

The presence of fetid or purulent discharge, in the absence of systemic illness, has been defined as clinical endometritis (Sheldon et al., 2006), with subclinical endometritis being defined by the proportion of polymorphonuclear cells (PMN) in uterine cytology samples, at or after 21 DPP. This has since been termed cytological endometritis (CE) (Dubuc et al., 2010). Several groups have determined the proportion of PMN within endometrial cytology which is indicative of pathological inflammation, as perceived due to a negative impact on pregnancy outcomes. This ranges from 6% (Dubuc et al., 2010) to 8% (Ricci et al., 2015) in the post-partum context.

Endometritis is prevalent in modern dairy farming, with incidences of between 13% and 25% being found in large multi-farm studies in the US and Canada (Cheong et al., 2011; Dubuc et al., 2011). Endometritis in beef cows is relatively understudied, however one study found that 30% of beef cows examined on six Italian farms had CE at 28-30 DPP, while 26% were still inflamed 49-68 DPP (Ricci et al., 2015). A negative impact on fertility was reported in each of these studies. Endometritis may also be important outside of the post-partum context, with Pascottini et al., (2016) finding an 8% incidence of CE at time of artificial insemination in dairy heifers who had never previously been pregnant. Notably, just 1% PMN perturbs fertility in this context.

While uterine inflammation has understandably received a lot of attention, inflammation of the lower reproductive tract is being increasing recognised as a separate but important phenomenon. Amongst 1000 dairy cows from six Canadian herds assessed for both purulent discharge and proportion of PMN in uterine cytology samples (CE), 14% had CE only, 9.4% had purulent discharge only and 6% had both (Dubuc et al., 2010). This led to the authors to conclude that diagnosis of clinical endometritis on the basis of purulent discharge alone was likely inappropriate and instead classified this as inflammation of the lower reproductive tract, when occurring in the absence of positive uterine cytology. Deguillaume et al., (2012) have extended this by collecting separate uterine and endocervical cytology from post-partum cows. They found 42% of cows examined before 35 days in milk had cervicitis, 45% had endometritis, and 32% had inflammation in both tissues. Cervicitis alone was associated with reduced risk of pregnancy, with inflammation in both sites increasing median time to conception over inflammation in one site alone. Purulent discharge is associated with a decreased risk of successful insemination in Irish cows (Aungier et al., 2014), however the presence or absence of uterine inflammation was not checked in this study. Gilbert (2016) notes that the source of purulent discharge found in the vagina is not always clear and in some cases may originate from inflammation of the vagina itself. Thus, as our appreciation of the prevalence and impact of lower reproductive tract inflammation increases, the need to improve understanding of the host immune response within this context is becoming clear.

It is important to note that an influx of PMN into the reproductive tract is not solely caused by bacterial infection. Ricci et al., (2015) found that 8% of animals have

cytological endometritis without bacteria present within the sample, 41% had bacteria present without surpassing the PMN cut-off and 22% had both bacteria and excessive PMN. Walker et al., (2015) reported no significant difference in bacteriology scores between endometritic and healthy cows. Therefore, other types of pathogen, such as viruses, may drive inflammation in some cases. In addition, a variety of soluble factors, including chemokines or β-defensins, may mediate this inflammation. To date, β-defensin expression within the lower cow reproductive tract has not been examined.

FRT inflammation, especially post-partum, must be considered in the context of the overall health status of the cow. Particularly, the period from three weeks pre-calving to three weeks post-calving is called the transition period and is a complex time both metabolically and immunologically. Within this timeframe, the cow experiences late gestation and the high energy demands of the fetus and associated membranes. Parturition is also energetically expensive and leads to tissue damage and influx of pathogens, followed by the onset of lactation and uterine involution (Drackley, 1999). Dry matter intake is insufficient to meet the resulting energy needs and the cow is said to be in a state of negative energy balance (Bell, 1995). Comparison of the immune response in mastectomised and intact cows after calving indicates the onset of lactation rather than calving itself induces systemic metabolic and inflammatory changes. Calcium (Goff et al., 2002) and IgG (Nonnecke et al., 2003) are mobilised for milk production, resulting in declining serum concentrations in the dam. This hypocalcemia drives a sharp increase in serum vitamin D the day before calving, which is maintained for the first three days of lactation (Goff et al., 2002). This may contribute to observed immunosuppression, with IgM and IFNγ secretion from PBMCs declining from 21 days before calving, reaching a nadir 0-4 days after calving, and returning to normal by three weeks post-partum.

After calving, a range of issues can drive a systemic inflammatory state. Negative energy balance necessitates the mobilisation of fat stores for energy, increasing circulating non-esterified fatty acid (NEFA) and β-hydroxybutyrate (BHBA) concentrations (Bell, 1995; Qu et al., 2014). These metabolites drive systemic inflammation through TLR4 activation and prostaglandin synthesis, among other mechanisms (reviewed in Sordillo et al., 2009). Mammary gland inflammation, known as mastitis, is driven by pathogen invasion of the teat canal and leads to increased circulating IL-1β, IL-6, TNFα (Shuster et al., 1993) and IL-17A (Usman et al., 2017). Lameness is a

prevalent post-partum condition with both infectious and non-infectious causes, which can further increase the elevated NEFA, BHBA, IL-6 and TNFα observed in cows (Zhang et al., 2015). In addition, uterine disease drives systemic inflammation. Complement gene expression is increased in the liver of endometritic animals, while *IL6* is increased in subcutaneous adipose tissue (Akbar et al., 2014). Kasimanickam et al., (2013) report increased serum TNFα, IL-1β and IL-6 in post-partum cows with uterine inflammation relative to healthy animals. Thus, the reproductive tract of the transition/post-partum cow is exposed to a complex cytokine milieu.

Cytokines are also produced by the uterus itself. Transcriptomic analysis of uterine biopsies indicates a significant upregulation of inflammatory gene expression 15 DPP in healthy beef cows, with T cell signalling and cytokine-cytokine receptor interaction pathways being enriched (Foley et al., 2012). *IL1B, IL6* and *IL17A* are upregulated in uterine biopsies of Holstein-Friesian cows with clinical endometritis at both 7 and 21 DPP versus healthy animals (Foley et al., 2015).

These same studies have detected differential β-defensin expression in the post-partum endometrium. RNA-Seq of Holstein-Friesian endometrial biopsies, followed by KEGG pathway analysis indicates a transition from a pro-inflammatory state at 7DPP to a more proliferative, wound-healing response by 21DPP (Foley et al., 2015). However, animals with CE experience a prolonged inflammatory state, with IL-1 and IL-17 signalling cascades remaining active. β-defensin expression is associated with this pro-inflammatory state: *DEFB, DEFB103B* and *DEFB5* are up-regulated in 7DPP uterine biopsies of healthy cows relative to 21DPP, while *LAP*, *DEFB5* and *DEFB7* are significantly up-regulated in cows with CE relative to healthy cows 21DPP (Figure 4.1). A separate study has also found *DEFB103, LAP*, *TAP*, *DEFB1* and *DEFB7* to be upregulated in biopsies from endometritic animals (Walker et al., 2015).

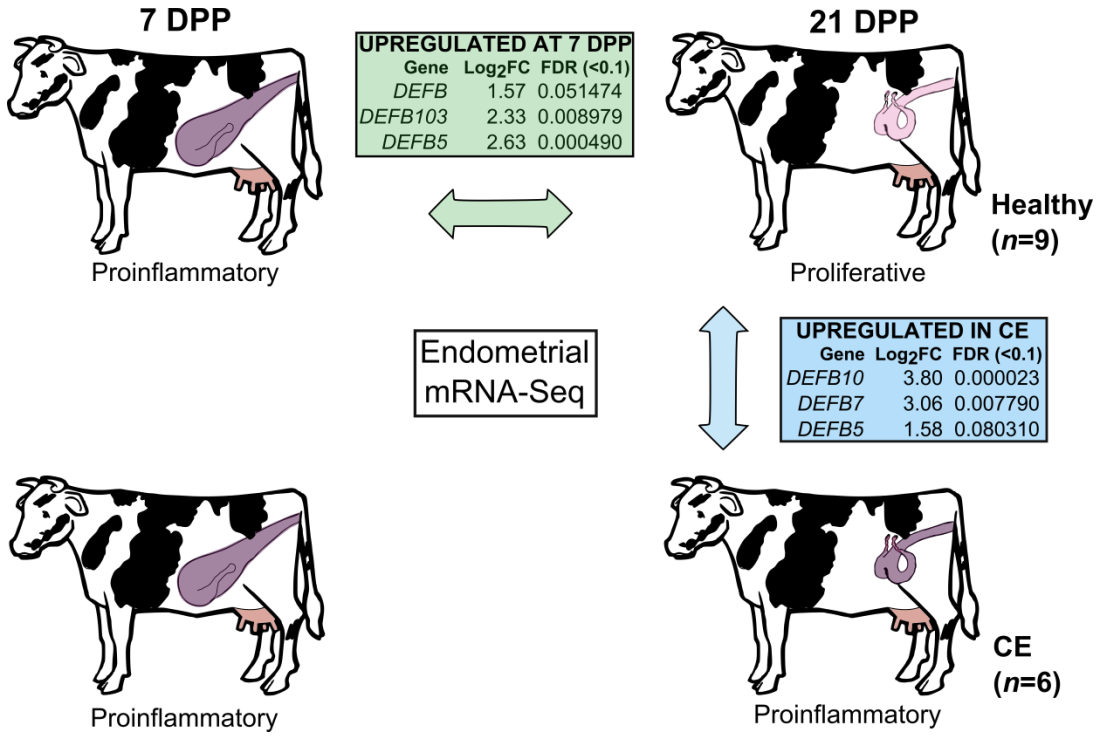


**Figure 4.1 RNA-Seq detects differential regulation of β-defensin genes in endometrial biopsies of post-partum cows (Foley et al., 2015).**
Endometrial biopsies were taken from Holstein-Friesian cows at 7 and 21 DPP. Histopathological analysis classified 9 animals as healthy and 6 as having CE based on infiltration of leukocytes at 21 days. RNA-Seq analysis allowed identification of differentially-expressed genes. KEGG pathway analysis indicated there was an overall upregulation of inflammatory genes at 7 days in both groups. At 21DPP, inflammation persists in cows with CE while healthy animals have switched to tissue repair. Several β-defensin genes were found to be upregulated in healthy animals at 7 versus 21DPP and in animals with endometritis versus healthy animals at 21DPP. Figure based on data from (Foley et al., 2015)

IL-1 and IL-17 signalling has been shown to regulate β-defensin expression in other models. IL-1β drives expression of human *DEFB4A* in primary nasal epithelium (Harder et al., 2000) and in a colonic epithelial cell line (Witthöft et al., 2005), while *DEFB1*, *DEFB4A*, *DEFB103* and *DEFB104* are all upregulated by IL-1β in primary keratinocytes (Harder et al., 2004). Bovine bronchial epithelial cells upregulate *TAP* expression in response to IL-17A (Berghuis et al., 2014). Simanski et al., (2013) report that IL-17A, in combination with IFNγ, but not alone, induced *DEFB4A* and *DEFB103* expression in human keratinocytes, however, IL-17A alone upregulates *DEFB4A* but not *DEFB103* in human primary tracheobronchial epithelial cells (Kao et al., 2004). Both these cytokines activate signalling pathways that can culminate in AP-1 activity (Kasahara et al., 1991; Kim et al., 2013).

IL-22 is a potent inducer of β-defensin expression. *DEFB4A* expression is driven by IL-22 in human alveolar epithelium (Li et al., 2014). IL-22, in combination with IL-

17A, upregulates gastric epithelial cell expression of *DEFB1*, *DEFB103* and *DEFB104* (Dixon et al., 2016). β-defensin expression in murine gastric epithelium is not effected by *IL22* knockout (Dixon et al., 2016), however a separate study found β-defensin expression is abolished in the nasal epithelium of *IL22* knockout mice (Mulcahy et al., 2016). While STAT3 is the classical IL-22 pathway transcription factor (Xie et al., 2000), IL-22 also activates the AP-1 complex (Kim et al., 2014a).

IL-22 is produced locally by a variety of infiltrating cell types, including Th17 cells, Th22 cells, γδ T cells and NK cells (Zenewicz and Flavell, 2011). In bovine, IL-22 has been shown to be expressed by γδ T cells in the peripheral blood of calves (Ma et al., 2010) and is important in successful vaccination of calves against TB (Bhuju et al., 2012). The leukocyte population within the bovine uterus has been examined and contains CD4+ T cells of as yet undefined subtype and smaller numbers of γδ T and CD335+ NK cells (Oliveira et al., 2013). Therefore, a role for IL-22 in regulating bovine β-defensin expression is worthy of investigation.

### 4.1.2 The structure of the endometrium

The bovine endometrium is composed of an upper functional layer and lower basal layer. The functional layer is covered by stratified columnar epithelium. Underlying this is a stromal layer interspersed with blood vessels and uterine glands lined with epithelial cells (Frandson et al., 2003). This layer provides mechanical strength to the tissue, is exposed to the external environment after parturition when the epithelial barrier has been damaged, and is mainly composed of cells of mesenchymal origin (Aghajanova et al., 2010). These cells have been traditionally referred to as endometrial stromal cells in the literature, to differentiate from a pluripotent cell which can be differentiated into a range of other cell types (Dunn et al., 2003). However these cells have the morphology and collagen-producing capabilities originally attributed to cells called fibroblasts (Brewer, 1967; Tanaka et al., 2008). In addition, bovine endometrial stromal cells can be differentiated into osteoclasts and are indistinguishable from bovine bone marrow stromal cells in terms of morphology and cytokine production (Donofrio et al., 2008). The human literature has begun to refer to these cells as endometrial stromal fibroblasts, while the

bovine literature calls them endometrial stromal cells. Phylogenetic analysis of the transcriptome of human endometrial stromal fibroblasts/cells and other mesenchyme-derived cell types indicates endometrial stromal cells are a sister cell type of follicular dendritic cells; with similar gene expression changes driving differentiation of both cell types (Kin et al., 2015).

Research into endometrial stromal cells has focused on their role in reproduction. They mediate the paracrine effects of estrogen upon adjacent epithelial cells (Astrahantseff and Morris, 1994; Cooke et al., 1997) and, in the human, differentiate into decidual cells during pregnancy (reviewed in Zhu et al., 2014). However fibroblast-type cells from different sites in the body have been shown to express a variety of immune genes including those encoding MCP-1, IL8 and RANTES (Brouty-Boyé et al., 2000). Synovial fluid from the temperomandibular joint of patients with inflammatory joint conditions contains IL-17A and synovial fibroblasts respond to IL-17A by producing a range of cytokines (Hattori et al., 2015). Bronchial fibroblasts also respond to IL-17A (Molet et al., 2001). Human peritoneal fibroblasts respond to IL-1β by activating NF-κB and producing IL-8 and MCP-1 (Witowski et al., 2001).

IL-22 is expressed in endometrial stromal cells in women with conditions in which endometrial tissue grows ectopically, either outside the uterus, i.e. endometriosis (Guo et al., 2013), or within the deeper myometrium of the uterus, i.e. adenomyosis (Wang et al., 2014b). In both conditions, IL-22 stimulates proliferation of endometrial stromal cells and upregulates *IL8* expression. Thus, while the endometrial cells lining the uterine lumen are the first to detect and respond to invading pathogens, the stromal cells will be the first to respond to cytokines and infiltrating leukocytes from the bloodstream, and may mediate the response of the epithelial layer to these as they have been shown to do with sex steroids.

β-defensins are also produced by fibroblast-type cells. Rizzo et al., (2008) have shown that gingival fibroblasts express *DEFB4A* and a variety of cytokines in response to infection with *Chlamydia pneumoniae* and speculate that this may be a mechanism driving periodontitis. hBD-4 secretion is increased in fibroblasts from burned skin (Noronha et al., 2014). Fibroblasts from the corneal stroma secrete hBD-1 (Castañeda-Sánchez et al., 2013).

β-defensins promote fibroblast proliferation. hBD-3 induces proliferation of primary human gingival fibroblasts without cytotoxicity (Nishimura et al., 2004), while hBD-2 promotes proliferation of conjunctival fibroblasts (Li et al., 2006).

An *in vitro* culture model of bovine endometrial epithelial and stromal cells has been developed to investigate bovine endometrial immunity. Of the ten bovine *TLR* genes, cultured primary stromal cells express all but *TLR5* and *TLR8,* while epithelial cells express all genes except *TLR8* and *TLR10*. Challenge with various PAMPs leads to prostaglandin secretion, indicating TLRs are expressed at protein level and are functional (Davies et al., 2008).

These cells express *IL1B*, *IL6* and *IL8* in response to LPS in a TLR4- and MyD88-dependent manner (Cronin et al., 2012). A separate study also found LPS upregulates expression of *TNF* and *INOS,* which encodes for the nitric oxide synthase (iNOS) gene (Herath et al., 2006), while binding of bacterial lipopolypeptides to TLR1/2 heterodimers drives *IL8* and *IL6* expression via ERK and NF-κB pathways (Turner et al., 2014). qPCR for a selected panel of β-defensin genes indicated epithelial cells express the chromosome 27 β-defensins *BNBD4*, *DEFB5*, *TAP* and *LAP*, which were upregulated in response to LPS, and the chromosome 13 gene *DEFB123*, while stromal cells expressed just *LAP* and *TAP* (Davies et al., 2008).

Use of an *in vitro* model of β-defensin expression will allow us to interrogate the mechanisms regulating β-defensin gene expression in the bovine endometrium. While bovine endometrial cells express cytokine genes, their responsiveness to cytokines has not been investigated. Stimulation with IL-1β, IL-17A and IL-22, followed by quantification of β-defensin expression will allow us to determine whether the endometrium can respond to some of the cytokines circulating in the transition/post-partum cow, and whether the β-defensin expression observed in post-partum uterine biopsies is being driven by these factors.

## 4.2 Hypothesis and specific aims

*We hypothesise that proinflammatory cytokines regulate expression of post-partum inflammation-associated β-defensin genes in endometrial stromal cells.*

**Specific aims:**

1. Profile β-defensin expression in a panel of cow reproductive tract tissues from both phases of the estrus cycle.
2. Establish a primary endometrial stromal cell model and determine whether syntenic cluster D chromosome 27 β-defensin genes are expressed in these cells.
3. Stimulate endometrial stromal cells with a variety of cytokines and quantify β-defensin expression in response.

## 4.3 Results

### 4.3.1 Several chromosome 27 β-defensin genes are expressed in the female reproductive tract

Expression of bovine syntenic cluster B β-defensin genes has previously been profiled in the endometrium and ovary (Narciandi et al., 2011). However, syntenic cluster D genes, found on bovine chromosome 27, are expressed in both the upper and lower FRT in other species. To quantify expression in the cow reproductive tract, tissue samples were collected from throughout the reproductive tract of a group of healthy Holstein-Friesian cows slaughtered for food production. As hormonal changes throughout the estrus cycle may alter β-defensin expression, four follicular phase and four luteal phase reproductive tracts were selected. Cows in the follicular phase had no developing or mature corpus lutea and had a developing pre-ovulatory follicle on the ovaries. Animals in the luteal phase had a mature corpus luteum. Vaginal samples were taken from the anterior, or upper, vagina. Cervical samples were collected from the endocervix, which is next to the uterine opening. Endometrial samples were collected from between visible caruncles. Oviduct samples were taken from the ampulla, which was located based on intermediate distance from either end of the oviduct. The ovary was sampled by avoiding developing follicles or corpus lutea (Figure 4.2).

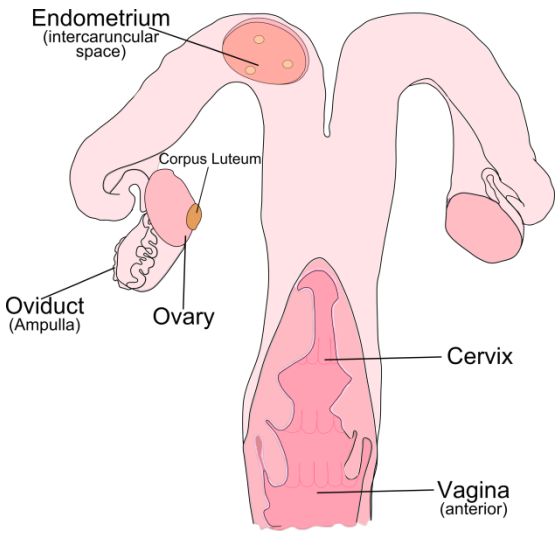


**Figure 4.2 FRT tissue samples collected for β-defensin quantification**
These tissues were collected from each of eight Holstein-Friesian multiparous cows, including four animals in the follicular phase of the estrus cycle and four in the luteal phase, as determined by presence or absence of a corpus luteum. Only non-pregnant animals, free from visible disease, were used in this study.

mRNA-Seq data generated within our lab (Foley et al., 2015) indicate that a number of chromosome 27 genes are expressed in the bovine endometrium (Figure 4.1; Foley et al., 2015). Before designing qPCR primers for these genes, some bioinformatics analysis was necessary. The mRNA-Seq analysis detected expression of the gene named *DEFB103B*/*DEFB300*. However, there are two unique, complete *DEFB103* genes in the most recent bovine genome assembly. *DEFB103A* had been predicted by the NCBI Gnomon gene prediction tool, based on 3 protein records and RefSeq records. *DEFB103B*, sometimes called *DEFB300*, was annotated by alignment of human RefSeq proteins to the bovine genome assembly (Zimin et al., 2009). The predicted bovine DEFB103A protein contains an additional 26 amino acids at the N-terminus, but otherwise is highly similar in peptide sequence to DEFB103B and to other mammalian DEFB103 peptides (Figure 4.3).

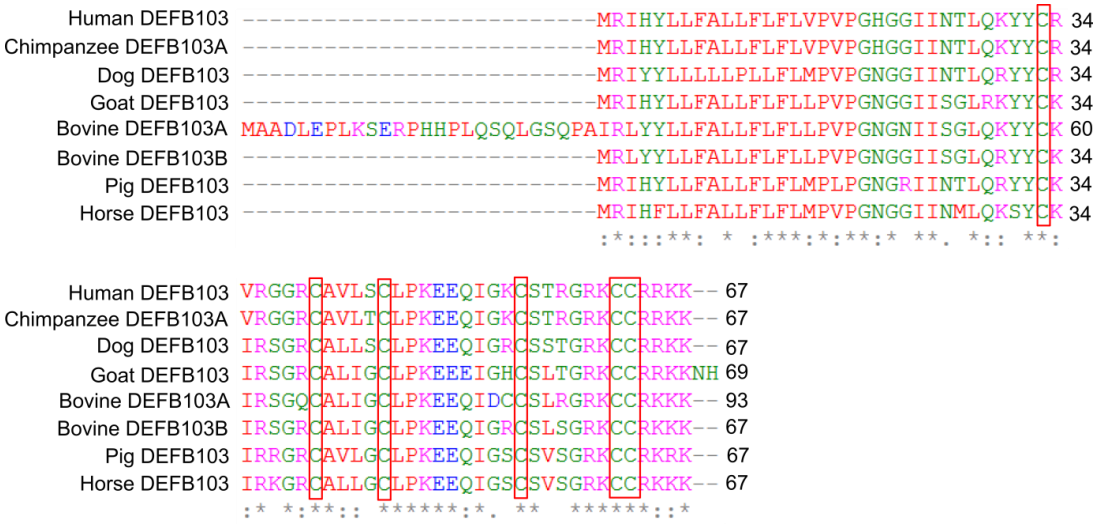


**Figure 4.3 Alignment of DEFB103 precursor peptides**
Peptide sequences were downloaded from GenBank and aligned using Clustal Omega (http://www.ebi.ac.uk/Tools/msa/clustalo/). Amino acids are coloured according to physicochemical groupings; * indicates identical residues at a position in the alignment, : indicates highly biochemically-similar amino acids, . indicates weakly similar amino acids; numbers indicate position in each individual nucleotide sequence. The conserved cysteines characteristic of β-defensins are indicated by the red boxes. All GenBank accession numbers are provided in Appendix Table A.5.

Using Clustal Omega to compute percent identity between the *DEFB103A* (without the 5' extension to the open reading frame) and *DEFB103B* nucleotides indicates they share 94% identity. The qPCR primer set was designed based on *DEFB103B*, however the forward primer also matches *DEFB103A* at 15 out of 17 nucleotides and the reverse primer matches at 19 of 20 nucleotides. Therefore the primer set is capable of amplifying both genes. The amplicon of this primer set will be referred to as *DEFB103* for the remainder of this thesis.

The β-defensin 2 gene has undergone expansion in the bovine genome, leading to several genes of highly-similar sequence (Figure 1.4). Having searched GenBank for bovine β-defensin gene records and having mapped these against the most recent bovine genome assembly, there are 8 genes with complete reading frames across two exons, whose sequences are similar to each other. Accession numbers for these genes are available in Table A.6.

A percent identity matrix for the open reading frames of these genes, computed using the Clustal Omega multiple sequence alignment tool, indicates these genes are between 80.42 and 95.77% identical in nucleotide sequence to each other (Table 4.1).

**Table 4.1 Clustal Omega percent identity matrix based on bovine chromosome 27 β-defensin nucleotide sequences**

| | ***DEFB10*** | ***DEFB4A*** | ***DEFB5*** | ***TAP*** | ***DEFB1/EBD*** | ***LAP*** | ***DEFB3*** | ***DEFB7*** |
|---|---|---|---|---|---|---|---|---|
| ***DEFB10*** | 100 | 80.95 | 82.01 | 80.42 | 84.66 | 85.71 | 85.71 | 87.3 |
| ***DEFB4A*** | 80.95 | 100 | 92.71 | 80.21 | 83.85 | 87.5 | 85.42 | 84.13 |
| ***DEFB5*** | 82.01 | 92.71 | 100 | 80.51 | 85.13 | 87.69 | 84.62 | 85.19 |
| ***TAP*** | 80.42 | 80.21 | 80.51 | 100 | 83.59 | 87.69 | 83.08 | 84.66 |
| ***DEFB1/EBD*** | 84.66 | 83.85 | 85.13 | 83.59 | 100 | 88.72 | 88.21 | 88.36 |
| ***LAP*** | 85.71 | 87.5 | 87.69 | 87.69 | 88.72 | 100 | 87.69 | 89.42 |
| ***DEFB3*** | 85.71 | 85.42 | 84.62 | 83.08 | 88.21 | 87.69 | 100 | 95.77 |
| ***DEFB7*** | 87.3 | 84.13 | 85.19 | 84.66 | 88.36 | 89.42 | 95.77 | 100 |

The alignment of these nucleotide sequences (Figure 4.4) highlights the difficulty in trying to design PCR primers that will amplify any one of these genes individually, i.e., there is no stretch of ≥15 nucleotides within which the majority of nucleotide positions are unique to one gene. Therefore, a qPCR primer set was designed to target all eight

genes. Throughout this thesis, the amplicon of this primer set will be referred to as expanded *DEFB4A*, or e*DEFB4A.*

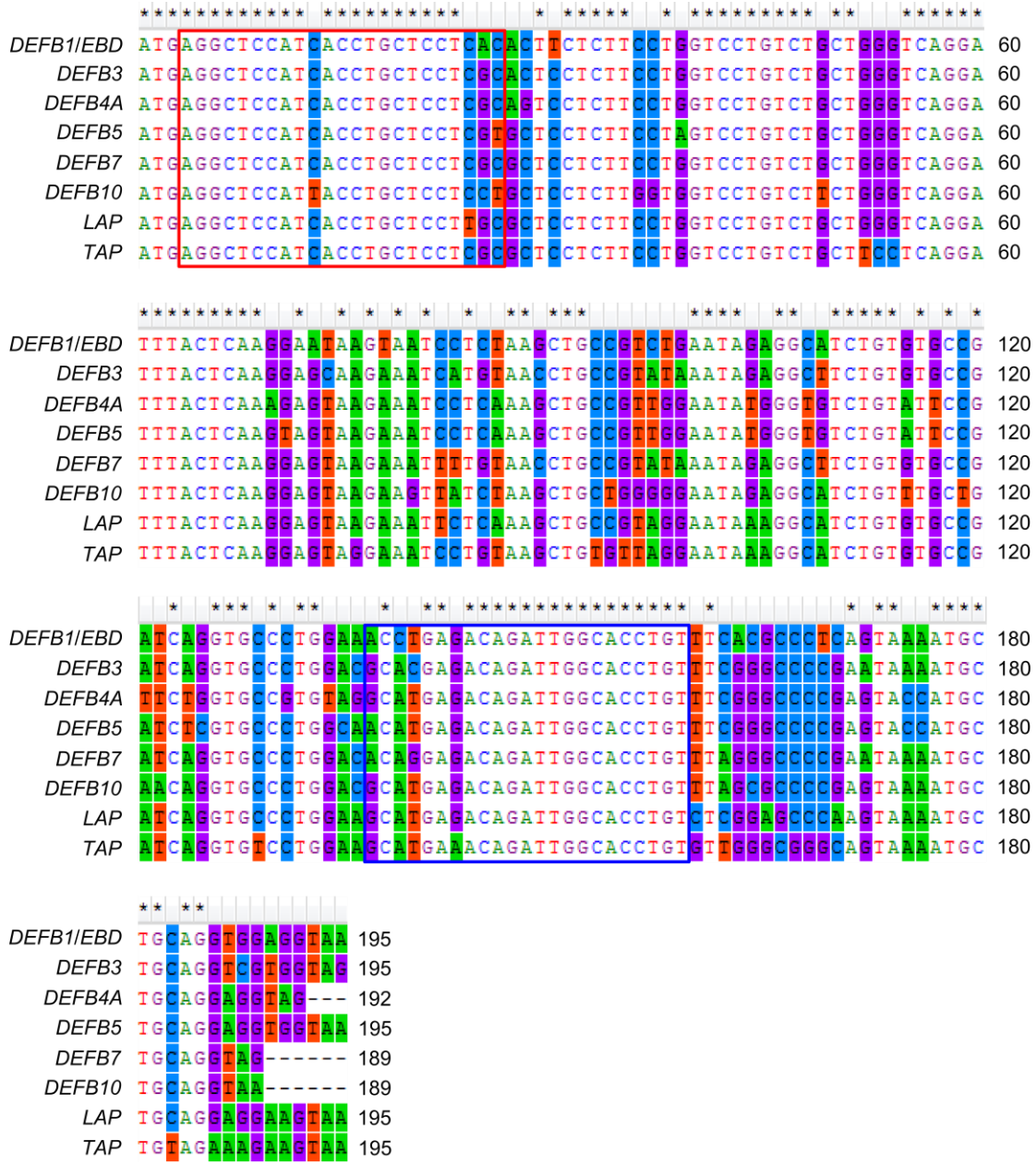


**Figure 4.4 Nucleotide sequence alignment of the open reading frames of highly-similar chromosome 27 β-defensins**

Nucleotide sequences were downloaded from GenBank and aligned using MEGA6.06 (Tamura et al., 2013). * indicates identical nucleotides at a position in the alignment; numbers indicate position in each individual nucleotide sequence. The sequences targeted by the e*DEFB4A* forward and reverse primer (sequences given in Table A.7) are indicated by the red and blue boxes respectively. All GenBank accession numbers are provided in Table A.6.

Application of the *DEFB103* and e*DEFB4A* qPCR primer sets to the panel of FRT tissues collected indicates both are expressed throughout the reproductive tract (Figure 4.5). *DEFB103* is expressed in all five tissues from each of the eight cows. e*DEFB4A* is expressed in all five tissues, however two animals do not express e*DEFB4A* in the oviduct. The expression level of *DEFB103* is generally higher than that of e*DEFB4A*.

Expression of either gene does not significantly differ between regions of the reproductive tract or between the estrogen-dominant follicular phase and progesterone-dominant luteal phase of the estrus cycle.

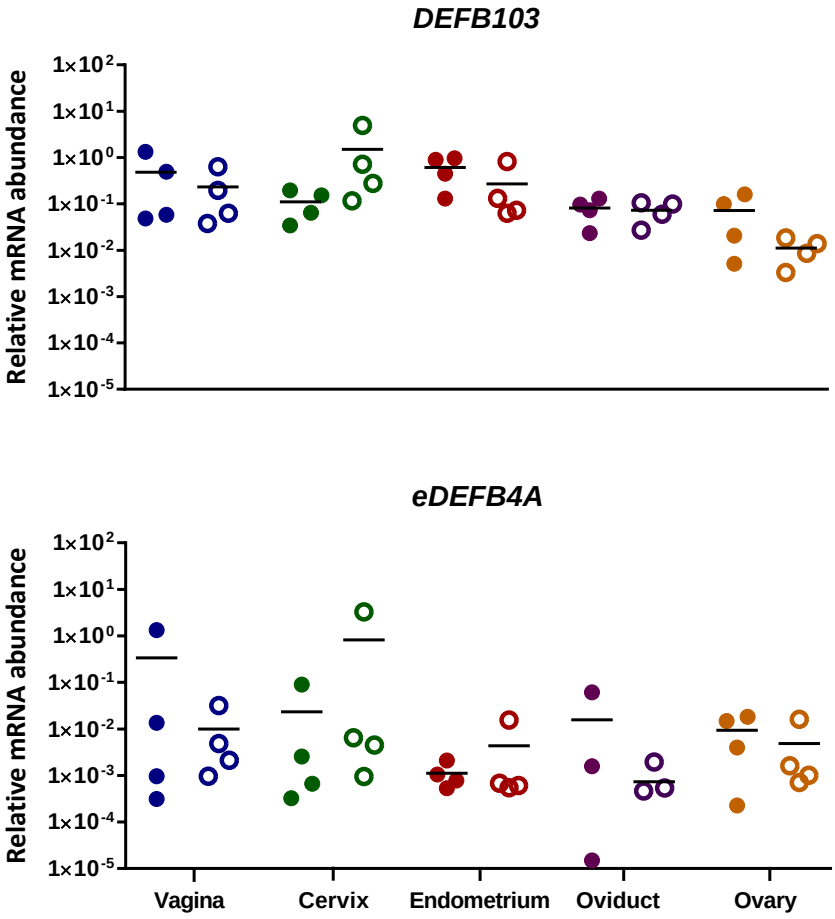


**Figure 4.5 β-defensin gene expression in female reproductive tract tissues.**
Expression of 2 β-defensin gene targets from chromosome 27 was quantified in eight multiparous Holstein-Friesian cows, with four being in follicular phase of the estrus cycle (closed shapes) and four in the luteal phase (open shapes). β-defensin gene expression is plotted as proportional to the geometric mean of a reference gene panel composed of *RPS9*, *MRPS6* and *SF3A1*. Horizontal bars represent mean expression values. A two-way ANOVA indicates there is no significant difference in expression in any of the targets between the two phases of the estrus cycle for any tissue.

### 4.3.2 Validation of the predicted gene *DEFB106* is expressed in the female reproductive tract

Human β-defensin 6 (DEFB106) was discovered in 2002 (Yamaguchi et al., 2002) and was subsequently demonstrated to have antimicrobial properties against *S. aureus* and *C. albicans* as well as LPS-binding activity (Xin et al., 2014). A bovine ortholog of the *DEFB106* gene was previously predicted through BLAST searching and hidden Markov modelling (Cormican, 2009), but expression had not been assessed.

Alignment of the predicted bovine DEFB106 peptide sequence with those from other species in which this gene has been annotated indicates a high degree of conservation (Figure 4.6).


**Figure 4.6 Alignment of DEFB106 peptide sequences**
Amino acid sequences of canine, human and chimpanzee DEFB106 peptides were downloaded from GenBank. The amino acid sequence of bovine DEFB106 was obtained from (Cormican, 2009) and aligned using Clustal Omega (http://www.ebi.ac.uk/Tools/msa/clustalo/). Amino acids are coloured according to physicochemical groupings., red boxes indicate conserved cysteine residues. * indicates identical residues at a position in the alignment, : indicates highly biochemically-similar amino acids, . indicates weakly similar amino acids; numbers indicate position in each individual amino acid sequence. All GenBank accession numbers are provided in Appendix Table A.5.

*DEFB106*-specific qPCR primers were designed and applied to the FRT tissues, with testis and epididymis cDNAs being included for comparison. *DEFB106* was amplified in all samples (Figure 4.7).

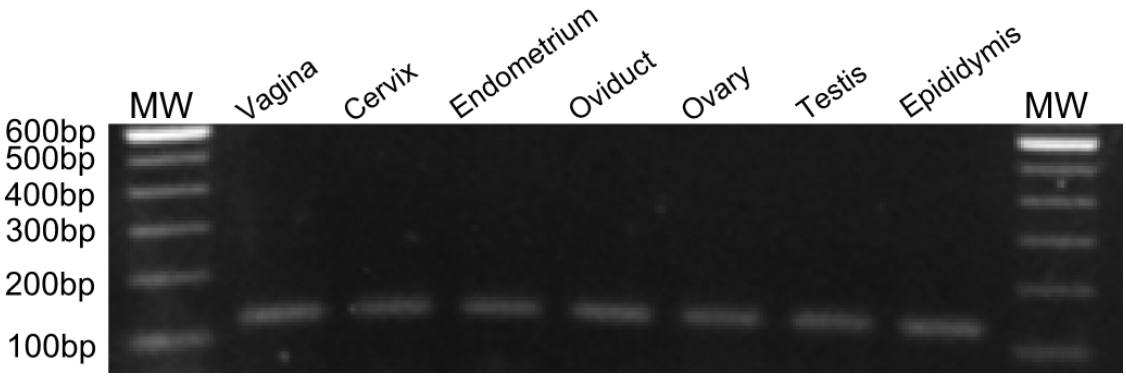


**Figure 4.7 DEFB106 expression in selected bovine tissues.**
*DEFB106*-targeting qPCR primers were applied to cDNA from male and female reproductive tract tissues. Following qPCR amplification, 2% agarose gel electrophoresis allowed confirmation of expected amplicon size. *DEFB106* amplicon size= 125bp. MW= DNA ladder indicating amplicon size on the gel.

Quantification of gene expression in the panel of female tissues indicates it is expressed in all five regions examined in all cows. However, as with the other chromosome 27 β-defensin genes, *DEFB106* is not significantly differentially expressed between tissues or between the follicular and luteal phases of the estrus cycle (Figure 4.7).

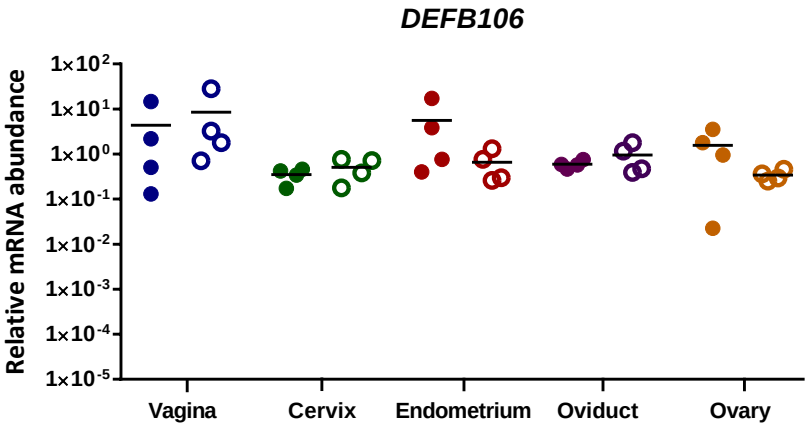


**Figure 4.8 *DEFB106* is expressed throughout the female reproductive tract**
*DEFB106* expression was quantified in eight multiparous Holstein- Friesian cows, with four being in follicular phase of the estrus cycle (closed shapes) and four in the luteal phase (open shapes). Gene expression is plotted as proportional to the geometric mean of a reference gene panel composed of *RPS9*, *MRPS6* and *SF3A1*. Horizontal bars represent mean expression values. A two-way ANOVA indicates there is no significant difference in expression of *DEFB106* between the two phases of the estrus cycle for any tissue.

### 4.3.3 Optimisation of primary endometrial cell cultures

Having demonstrated expression of several β-defensins in the bovine female reproductive tract, the next step was to examine the stimuli driving expression of these genes in this context via an *in vitro* cell culture model. The observation that the lower reproductive tract expressed β-defensins was hugely interesting given this region is the first to detect an influx of foreign pathogens. However, expression of bovine β-defensins has been associated with post-partum inflammation of the endometrium ((Foley et al., 2012, 2015). The economic impact of endometritis means the immune response of the bovine endometrium has long been of interest, with primary culture of bovine endometrial stromal and epithelial cells being first carried out in 1988 (Fortier et al., 1988). While our

lab has previously collaborated with a research group who routinely culture these primary cells (Davies et al., 2008), they had not been isolated in our own lab.

Working from a commonly-used adaptation of the original protocol (Herath et al., 2006), the presence of a stage I corpus luteum/corpus hemmorhagicum on an ovary was used to identify animals at the start of the estrus cycle (Ireland et al., 1980). This approximately standardised sex steroid levels within the endometrium across cows (Stabenfeldt et al., 1969). While published protocols store the entire reproductive tract on ice during transport to the laboratory, where removal of the endometrium is then carried out, harvesting endometrial samples at the abattoir immediately after removal of the tract from the carcass consistently improved cell yields. While this initally led to microbial contamination of cultures, cleaning of the outside of the tract and work surface at the abattoir with 70% ethanol, coupled with irrigation of the endometrial surface with antibiotic-supplemented PBS and storage of the sample in serum-free media subsequently eliminated this issue.

The uterine lumen is lined with epithelial cells which cover a functional layer composed of a stromal matrix with spiral arterioles and epithelium-lined glands (Figure 4.9). The manual endometrial removal technique used collected luminal and glandular epithelium along with a proportion of the stromal layer.

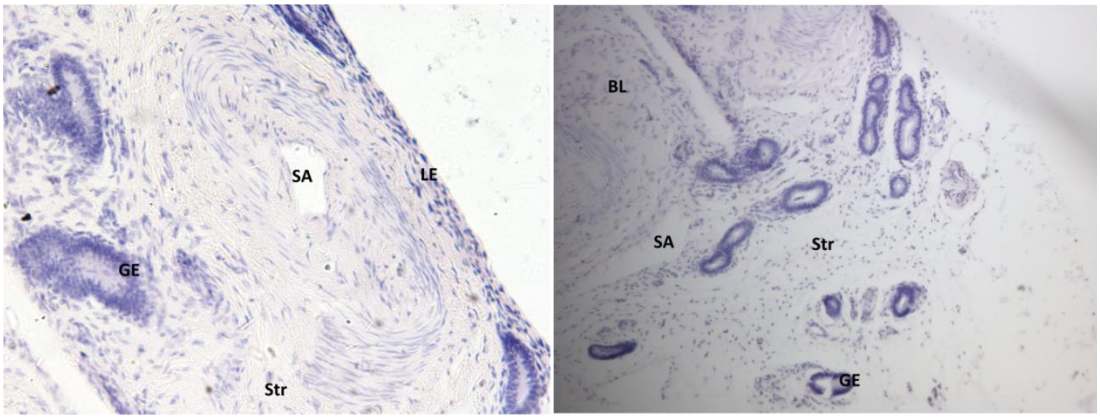


**Figure 4.9 Haematoxylin-stained histology sections of bovine endometrium: Left- 20X before, Right- 10X after curettage of endometrial surface for isolation of cells**
LE=luminal epithelium, SA= spiral arteriole, GE= glandular epithelium, Str=stroma, BL=basal layer. The curettage technique employed removes the luminal epithelium has been removed but does not contact the basal layer; ensuring only endometrial cells are collected.

The data presented in the remainder of this section were generated from stromal cell cultures. Stromal cells make up the majority of the collected tissue and thus a larger number are retrieved from each sample relative to the epithelial cells.

The composition of the isolated cell populations was verified using a number of methods. Visual examination under a light microscope provides information on the cell morphology. Stromal cells are characterised by a mesenchymal-like appearance with branched projections (Figure 4.10), in contrast to the more cuboidal epithelial cells which grow closely together in sheets.

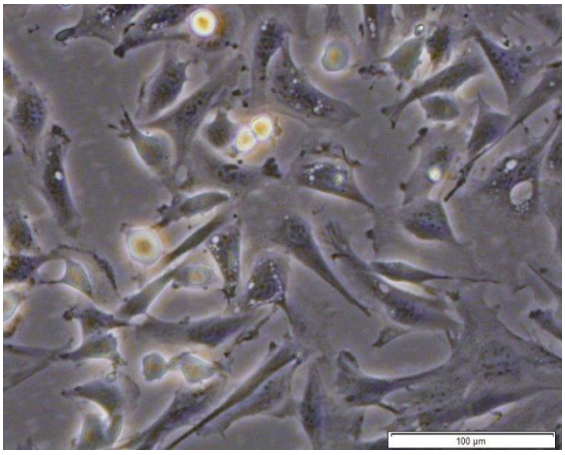


**Figure 4.10 10X magnification of bovine endometrial stromal cells**
Visual examination of the cell cultures under light microscope aids in confirming nature and purity of cell population.

Immunostaining of cytoskeletal proteins, followed by fluorescence microscopy, is used to differentiate epithelial from stromal cells. Stromal cells express vimentin but not cytokeratin (Figure 4.11). Immunostaining was carried out initially to validate differential identification via morphology. On an ongoing basis, culture purity was assessed via visual examination under the light microscope, ensuring the cells were >95% stromal cells.

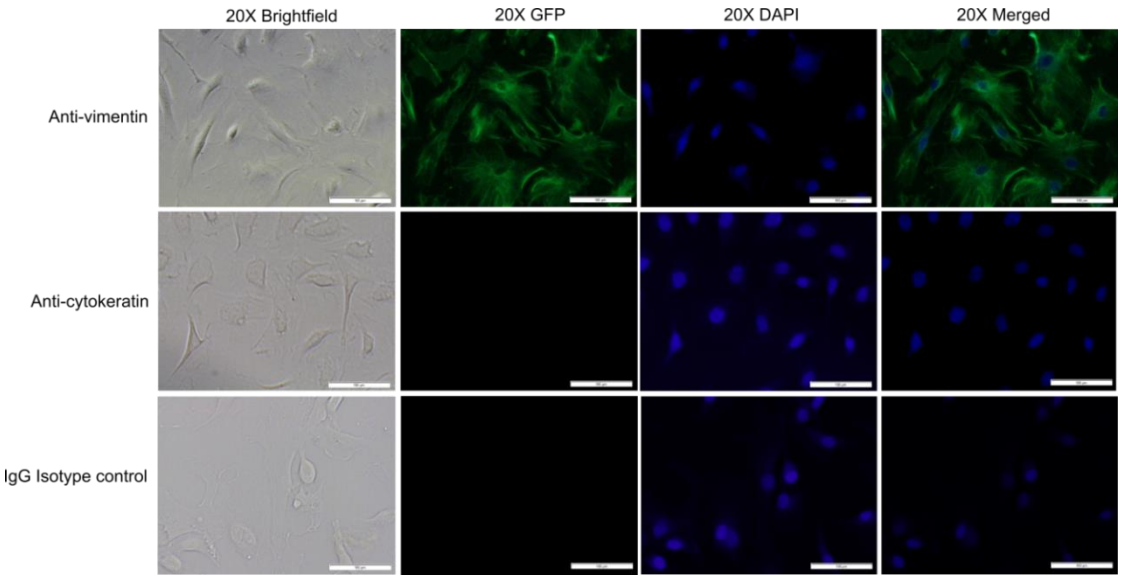


**Figure 4.11 Immunofluorescence staining of bovine endometrial stromal cells with antibodies against cytoskeletal proteins vimentin and cytokeratin**
Formalin-fixed cells were stained with murine antibodies against human vimentin and cytokeratin cytoskeletal proteins, which are characteristic of stromal and epithelial cells respectively, followed by a FITC-conjugated goat anti-mouse polyclonal secondary antibody. DAPI stain was applied to identify nuclei. Scale bar=100μm.

Given that the intention was to use these cultures for the investigation of immune gene expression, it was important to check for leukocyte contamination. This was achieved through PCR, carried out on cDNA prepared from cultured cells, for the pan-leukocyte marker *PTPRC*, which encodes the protein CD45. All of the stromal cell isolations for which gene expression data are presented here were negative for *PTPRC* cDNA (Figure 4.12).

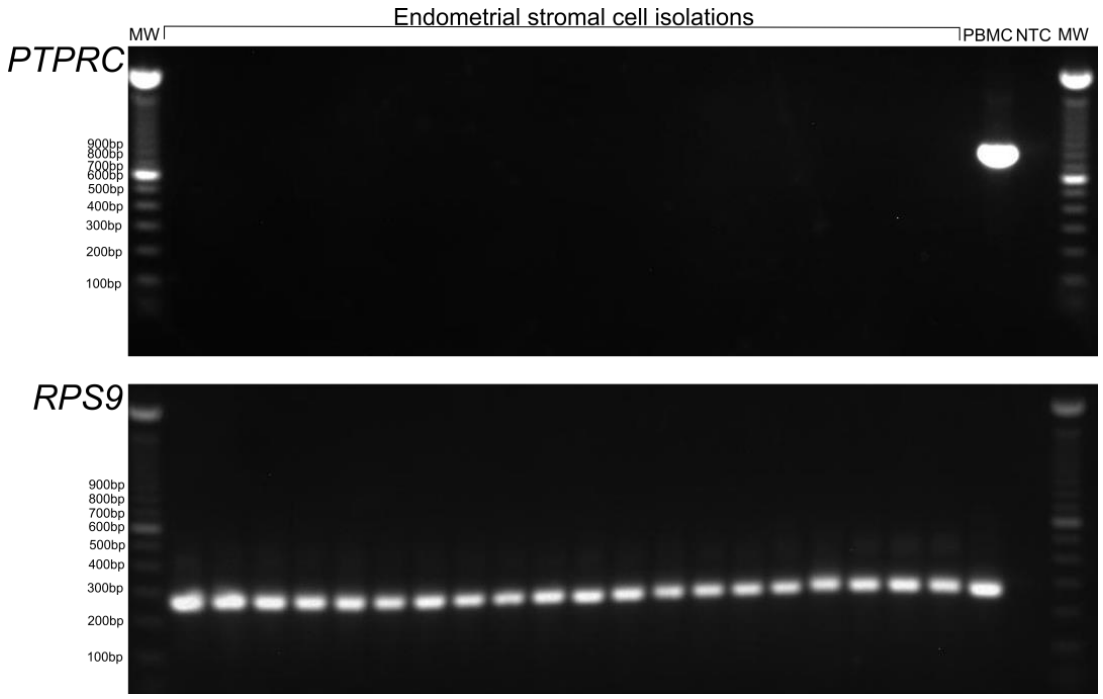


**Figure 4.12 Gel electrophoresis of PTPRC and RPS9 PCR products amplified from cDNA made from endometrial stromal cell cultures used in this thesis**

*PTPRC*-targeting PCR primers were applied to cDNA from each of the stromal cell isolations used in this thesis to detect leukocyte contamination. PBMC cDNA was used as a positive control for *PTPRC* amplification, lane non-template control from which DNA was omitted was included to detect any nucleic acid contamination. Following PCR amplification, 2% agarose gel electrophoresis allowed confirmation of expected amplicon size. *PTPRC* amplicon size= 845bp; *RPS9*= 270bp. MW= DNA ladder indicating amplicon size on the gel.

In order to quantify β-defensin gene expression by qPCR, it was necessary to establish a reference gene panel for expression level normalisation. An initial panel of five constitutively-expressed genes, including *TUBA1*, *RPL13A*, *MRPS6*, *SF3A1* and *RPS9*, were quantified in a pilot study of stromal cells from 4 animals stimulated with 10μg/mL of the dsRNA ligand poly(I:C). $C_q$ values from stimulated cells were normalised against those of unstimulated cells and these values entered into GeNorm software which calculates the stability of expression and assigns an M value which is a representation of this expression stability across animals, treatments and genes. A lower M value indicates a gene is more stable in expression. *MRPS6, SF3A1* and *RPS9* had the lowest M values and were therefore the most stably expressed genes within the initial panel (Figure 4.13).

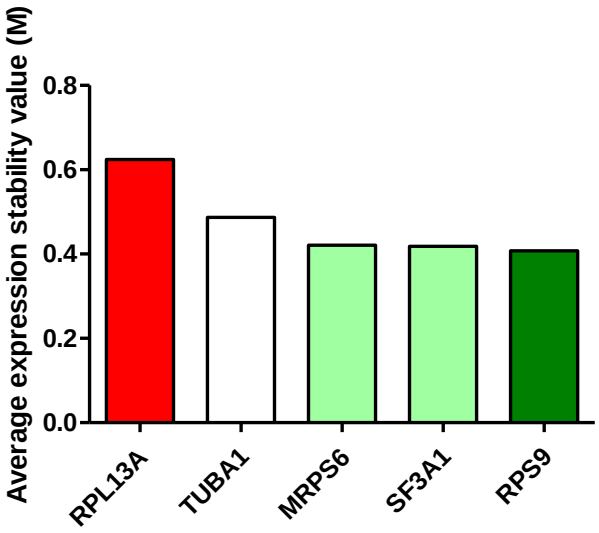


**Figure 4.13 GeNorm analysis of stability of reference gene expression in primary endometrial stromal cells**
qPCR was carried out on cDNA samples from experiments in which primary bovine endometrial stromal cells were stimulated with poly(I:C), using primer sets for five potential reference genes. Relative expression values were analysed with GeNorm software which assigned an average stability value across all the samples. The three most-stably expressed genes, *MRPS6*, *SF3A1* and *RPS9* were chosen.

This final panel of three reference genes has been applied to cDNA from all the stimulations used in this thesis.

Endometrial stromal cells express both *DEFB103* and e*DEFB4A* constitutively, with *DEFB103* being expressed at a higher level than e*DEFB4A* under baseline conditions. *DEFB106* is not expressed in these cells (Figure 4.14).

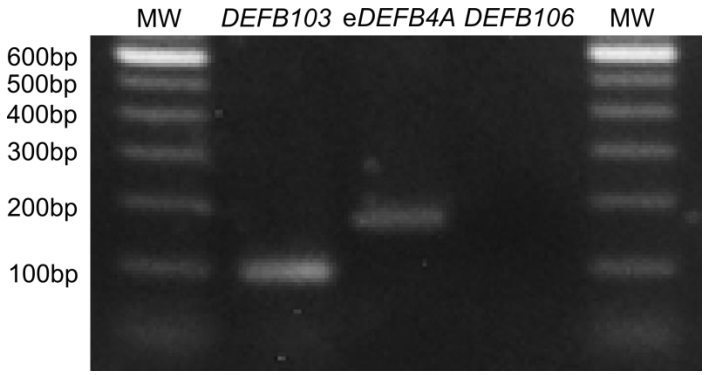


**Figure 4.14 β-defensin expression in bovine endometrial stromal cells**
$1x10^5$ primary bovine endometrial stromal cells were lysed with TRIzol and total RNA extracted. First-strand cDNA was reverse transcribed and qPCR using β-defensin gene primers was carried out. PCR products were run on a 2% agarose gel to confirm expected amplicon size. *DEFB103* amplicon size= 91bp; *eDEFB4A*= 151bp. MW= DNA ladder indicating amplicon size on the gel.

### 4.3.4 β-defensin expression is upregulated by IL-1β stimulation

As important soluble mediators of immunity, cytokines were the first group of possible β-defensin regulators to be examined. Bovine endometrial stromal cells were isolated and stimulated with recombinant bovine IL-1β at 10, 50 or 100ng/mL concentrations for 6, 12, 18 or 24 hours before the cells were harvested using TRIzol and RNA was extracted for reverse transcription and qPCR analysis. The cells used in this experiment were from Friesian cows. The age range was 3-15 years (*n*=6). Statistics were computed using a repeated measures two-way ANOVA with Dunnett's post-hoc multiple comparison test, comparing each stimulation to the unstimulated control within that time point.

*IL8* was chosen as the positive control as IL-1β has been shown to drive IL-8 production (Kasahara et al., 1991) via both NF-κB and AP-1 transcription factors (Jung et al., 2002). *IL8* is significantly differentially upregulated by IL-1β stimulation at 18 and 24 hours (Figure 4.15). 50ng/mL of IL-1β for 24 hours led to a mean 66-fold (±20 SEM) increase in *IL8* expression compared to the untreated control (adjusted p=0.0355).

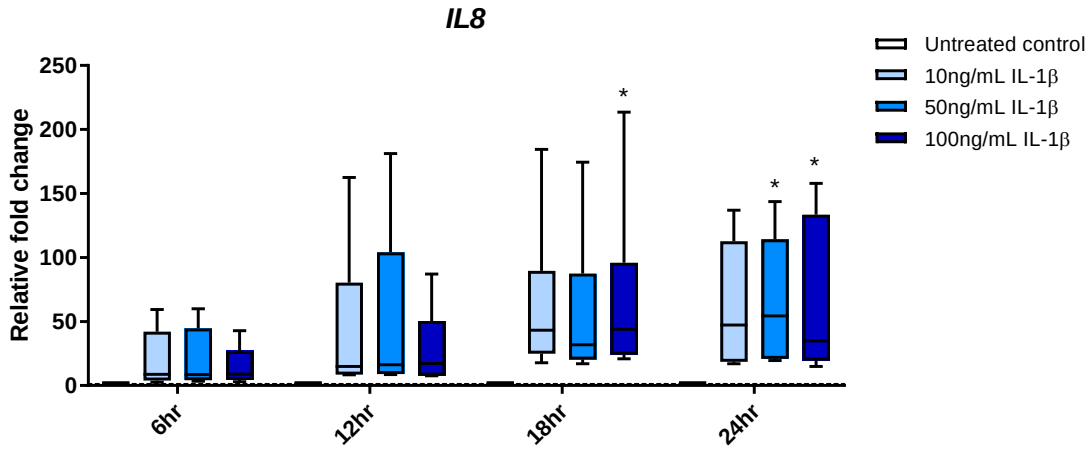


**Figure 4.15 IL-1β upregulates *IL8* expression**
$1x10^5$ /well primary bovine endometrial stromal cells were plated in 6-well plates and allowed to settle overnight. Cells were stimulated with 10ng/mL, 50ng/mL or 100ng/mL recombinant bovine IL-1β and harvested in TRIzol after 6, 12, 18 or 24 hours. Total RNA was extracted and first-strand cDNA reverse transcribed. qPCR was carried out and gene-of-interest $C_q$ values normalised to the reference gene panel using the method described by Hellemans et al. (2007). Boxes indicate median, $25^{th}$ and $75^{th}$ percentile fold change in gene expression relative to the untreated control within the same time point; whiskers indicate minimum and maximum values. The horizontal dotted line indicates the y-value of the untreated control. Statistics were computed using a repeated measures two-way ANOVA followed by Dunnett's post-hoc multiple comparison test. The mean fold change of each stimulation was compared to the untreated control within the same time point, with asterisks indicating statistically-significant differences: *=adjusted $p \leq 0.05$. The cells used in this experiment were isolated from Friesian cows; age range is 3-15 years; *n*=6.

Both *DEFB103* and e*DEFB4A* are upregulated by IL-1β, with e*DEFB4A* showing an earlier response which is also of a greater magnitude (Figure 4.16). 50ng/mL of IL-1β upregulates *DEFB103* 2.63±0.59 fold (adjusted p= 0.0020), while e*DEFB4A* is upregulated 7.05±2.16 fold (adjusted p= 0.0164) after 24 hours of treatment.

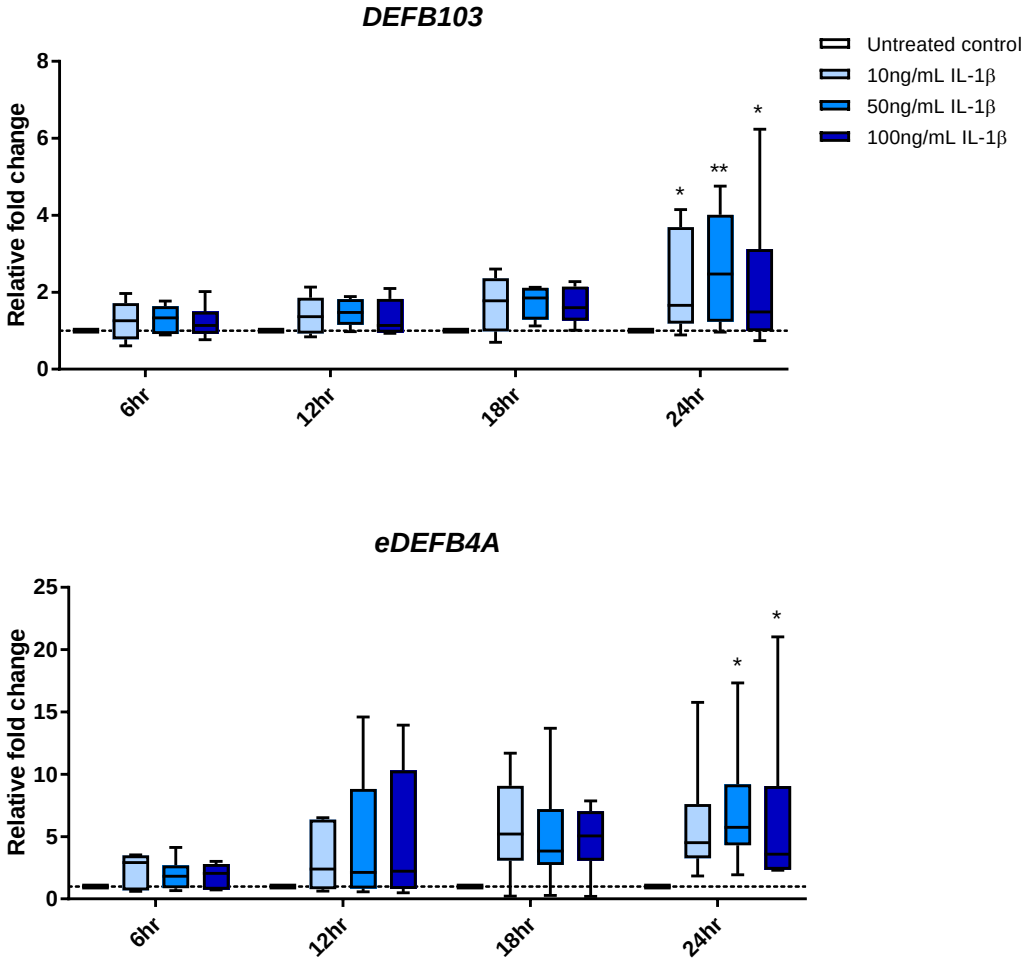


**Figure 4.16 IL-1β upregulates β-defensin expression**
1x10$^5$ /well primary bovine endometrial stromal cells were plated in 6-well plates and allowed to settle overnight. Cells were stimulated with 10ng/mL, 50ng/mL or 100ng/mL recombinant bovine IL-1β and harvested in TRIzol after 6, 12, 18 or 24 hours. Total RNA was extracted and first-strand cDNA reverse transcribed. qPCR was carried out and gene-of-interest $C_q$ values normalised to the reference gene panel using the method described by Hellemans et al. (2007). Boxes indicate median, 25$^{th}$ and 75$^{th}$ percentile fold change in gene expression relative to the untreated control within the same time point; whiskers indicate minimum and maximum values. The horizontal dotted line indicates the y-value of the untreated control. Statistics were computed using a repeated measures two-way ANOVA followed by Dunnett's post-hoc multiple comparison test. The mean fold change of each stimulation was compared to the untreated control within the same time point, with asterisks indicating statistically-significant differences: *=adjusted p≤0.05; **=adjusted p≤0.01. The cells used in this experiment were isolated from Friesian cows; age range is 3-15 years; *n*=6.

### 4.3.5 *DEFB4A* expression is upregulated by IL-17A stimulation

Alignment of the bovine and human IL-17A amino acid sequences using Clustal Omega indicated a high level of similarity between the orthologs (Figure 4.17). The full length precursor proteins, including the N-terminal signal sequence, share 74.51% identity. This increases to 76.30% when just the mature proteins are compared. A recombinant human IL-17A protein, produced by Peprotech, has been used in these experiments.

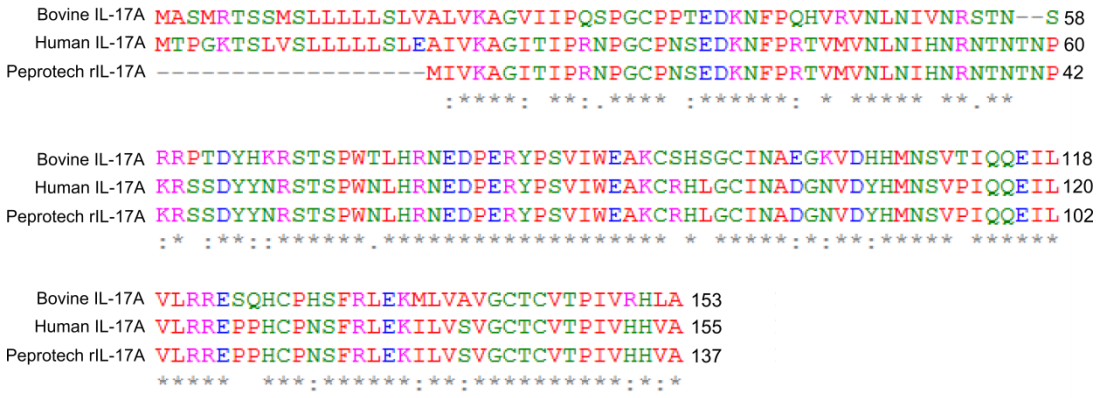


**Figure 4.17 Alignment of bovine and human IL-17A precursor proteins, with the recombinant human IL-17A used in these experiments**
Amino acid sequences for the bovine and human IL-17A precursor proteins were downloaded from GenBank. The accession numbers are given in Table A.5. The amino acid sequence of the commercial recombinant protein used was obtained from the manufacturer (Peprotech, catalogue #200-17). The sequences were aligned using Clustal Omega[2]. Amino acids are coloured according to physicochemical groupings., red boxes indicate conserved cysteine residues. * indicates identical residues at a position in the alignment, : indicates highly biochemically-similar amino acids, . indicates weakly similar amino acids; numbers indicate position in each individual nucleotide sequence.

The cells used in this experiment were from Friesian cows and the age range was 3-15 years (*n*=6). Stromal cells were isolated, plated and stimulated with 100pg/mL, 10ng/mL or 100ng/mL IL-17A for 6, 12, 18 or 24 hours. *IL8* expression was selected as the positive control. IL-17A is capable of driving IL-8 protein production in human foreskin fibroblasts (Yao et al., 1995). IL-17A also upregulates the expression of the

[2] (http://www.ebi.ac.uk/Tools/msa/clustalo/)

genes encoding the c-fos and c-jun proteins which encompass AP-1, leading to increased AP-1 activity (Kim et al., 2013).

*IL8* expression in response to IL-17A stimulation is both time- and dose-dependent. 100pg/mL has no effect, however 10ng/mL has a statistically significant effect from 18 hours, while 100ng/mL has an effect from 12 hours. 100ng/mL IL-17A leads to a 25.37±7.44 fold increase in expression after 24 hours (adjusted p<0.0001) (Figure 4.18).

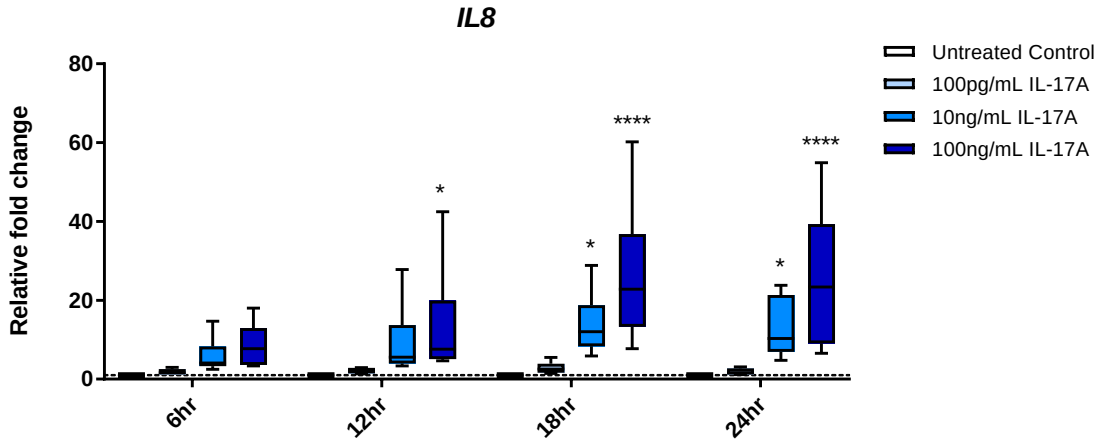


**Figure 4.18 IL-17A upregulates IL8 expression**
$1x10^5$ /well primary bovine endometrial stromal cells were plated in 6-well plates and allowed to settle overnight. Cells were stimulated with 100pg/mL, 10ng/mL or 100ng/mL recombinant human IL-17A and harvested in TRIzol after 6, 12, 18 or 24 hours. Total RNA was extracted and first-strand cDNA reverse transcribed. qPCR was carried out and gene-of-interest $C_q$ values normalised to the reference gene panel using the method described by Hellemans et al. (2007). Boxes indicate median, 25$^{th}$ and 75$^{th}$ percentile fold change in gene expression relative to the untreated control within the same time point; whiskers indicate minimum and maximum values. The horizontal dotted line indicates the y-value of the untreated control. Statistics were computed using a repeated measures two-way ANOVA followed by Dunnett's post-hoc multiple comparison test. The mean fold change of each stimulation was compared to the untreated control within the same time point, with asterisks indicating statistically-significant differences: *=adjusted p≤0.05; ****= adjusted p<0.0001. The cells used in this experiment were isolated from Friesian cows; age range is 3-15 years; *n*=6.

*DEFB103* expression is modestly but significantly upregulated by IL-17A stimulation, with 100ng/mL causing a 1.62±0.30 fold induction at 24 hours (Figure 4.19). Expression of the amplicon representing the *DEFB4A* expansion is upregulated at 18 and 24 hours, with 100ng/mL IL-17A leading to a 6.90±4.78 fold increase after for 24 hours, however this is not statistically significant (adjusted p=0.0768). Thus, the pro-inflammatory cytokine IL-17A is a driver of β-defensin expression in cultured endometrial stromal cells.

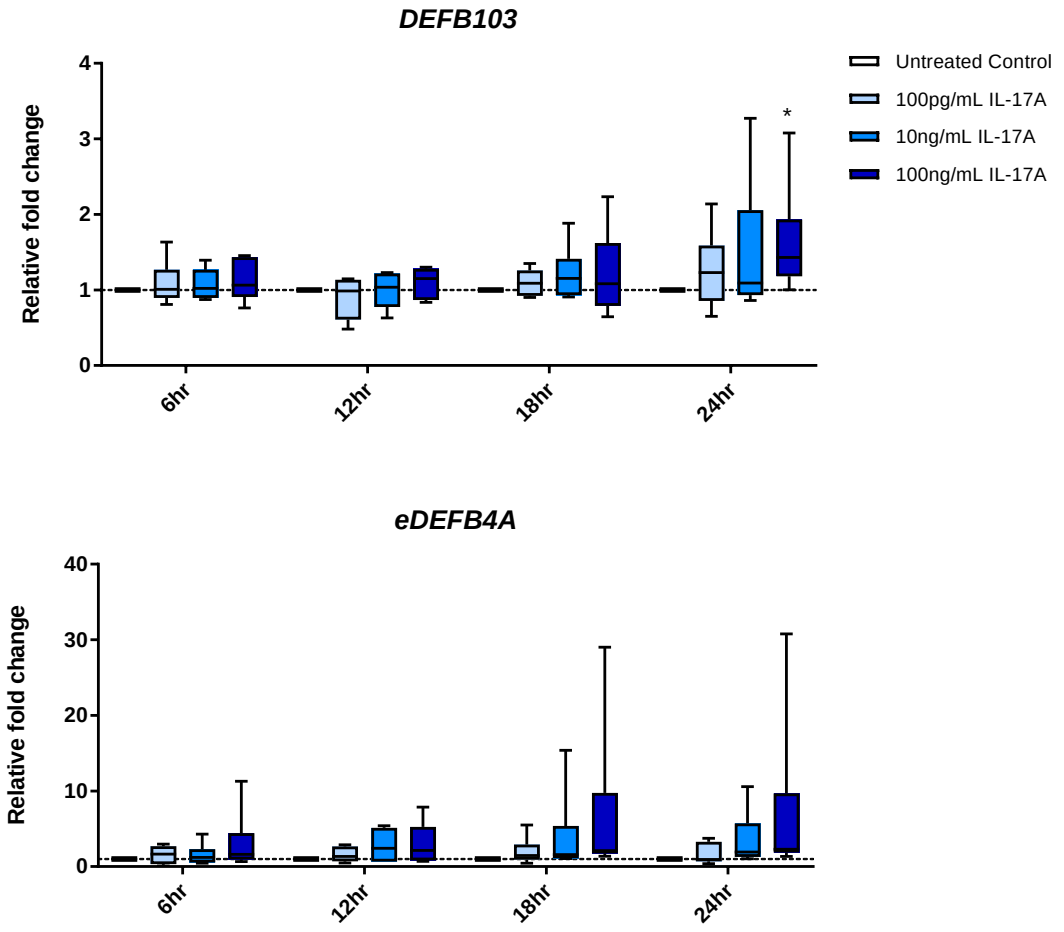


**Figure 4.19 IL-17A upregulates β-defensin gene expression**
$1x10^5$ /well primary bovine endometrial stromal cells were plated in 6-well plates and allowed to settle overnight. Cells were stimulated with 100pg/mL, 10ng/mL or 100ng/mL recombinant human IL-17A and harvested in TRIzol after 6, 12, 18 or 24 hours. Total RNA was extracted and first-strand cDNA reverse transcribed. qPCR was carried out and gene-of-interest $C_q$ values normalised to the reference gene panel using the method described by Hellemans et al. (2007). Boxes indicate median, 25$^{th}$ and 75$^{th}$ percentile fold change in gene expression relative to the untreated control within the same time point; whiskers indicate minimum and maximum values. The horizontal dotted line indicates the y-value of the untreated control. Statistics were computed using a repeated measures two-way ANOVA followed by Dunnett's post-hoc multiple comparison test. The mean fold change of each stimulation was compared to the untreated control within the same time point, with asterisks indicating statistically-significant differences: *=adjusted p≤0.05. The cells used in this experiment were isolated from Friesian cows; age range is 3-15 years; *n*=6.

### 4.3.6 β-defensin expression in response to IL-22

The *IL10RA* and *IL22RA1* genes encoding the IL-22 receptor heterodimer are both upregulated in endometrial biopsies collected at 7 DPP from animals whose inflammation has resolved by 21 days (Foley et al., 2015). However, looking at the raw reads counts from the RNA-Seq data indicates that *IL22RA1* expression is relatively low. While the read counts for *IL10RA* range from 49-847, with a mean of 299 reads in the 30 biopsies used (9 healthy and 6 endometritic animals, with biopsies being collected at two time points), those for *IL22RA1* range from 4-383, with a mean of 78. Therefore, *IL22RA1* expression in endometrial stromal cells was quantified. *IL22RA1* is expressed at mRNA level, however the expression level varies between animals and is mostly low compared to that within the large intestinal sample which has been included as a positive control (Figure 4.20).

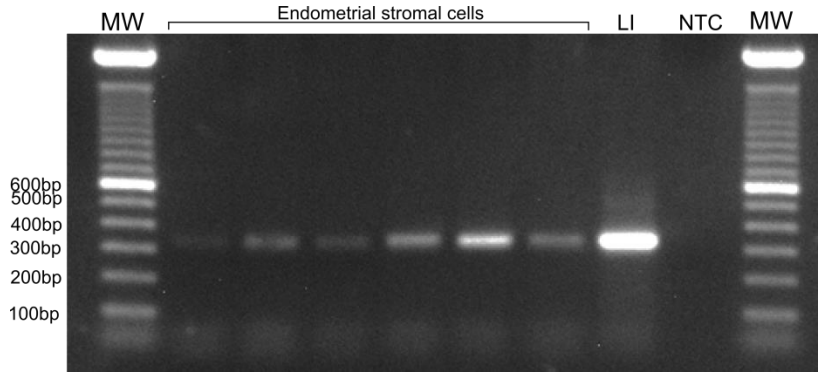


**Figure 4.20 *IL22RA1* is expressed at a low level by endometrial stromal cells**
Total RNA was extracted from primary bovine endometrial stromal cells and first-strand cDNA reverse transcribed. qPCR was carried out using a primer set targeting *IL22RA1*. 2% agarose gel electrophoresis allowed confirmation of expected amplicon size (331bp). Large intestine (LI) cDNA was included as a positive control. NTC= non-template control; MW= DNA ladder indicating amplicon size on the gel.

As there is no recombinant bovine IL-22 commercially available, the amino acid sequences of the human and bovine IL-22 protein precursors were aligned (Figure 4.21). Across the full precursor protein, there is 69% identity in amino acid sequence between the human and bovine IL-22 proteins. Across the mature protein, without the N-terminal signal portion, there is 71% identity between the proteins from both species. Within 147

amino acids, 103 are identical, 30 are highly biochemically similar, 3 are weakly similar and 11 are different.


**Figure 4.21 Alignment of bovine and human IL-22 precursor proteins, with the recombinant human IL-22 used in these experiments**
Amino acid sequences for the bovine and human IL-22 precursor proteins were downloaded from GenBank. The accession numbers are given in Table A.5. The amino acid sequence of the commercial recombinant protein used were obtained from the manufacturer (Peprotech, catalogue #200-22). The sequences were aligned using Clustal Omega (http://www.ebi.ac.uk/Tools/msa/clustalo/). Amino acids are coloured according to physicochemical groupings., red boxes indicate conserved cysteine residues. * indicates identical residues at a position in the alignment, : indicates highly biochemically-similar amino acids, . indicates weakly similar amino acids; numbers indicate position in each individual nucleotide sequence.

Stromal cells were isolated from the endometria of 6 animals including two Charolais, one Charolais cross, one Friesian and two Limousin crosses. The age range was 4-15 years. The cells were stimulated with 10ng/mL, 50ng/mL or 200ng/mL recombinant human IL-22 for 6, 12, 18 or 24 hours before for being harvested and processed for qPCR analysis.

*IL8* expression is increased slightly after 12 hours treatment with 200ng/mL IL-22 (Figure 4.22- mean fold change 1.71±0.7059, adjusted p=0.0307). However the response is not consistent across animals.

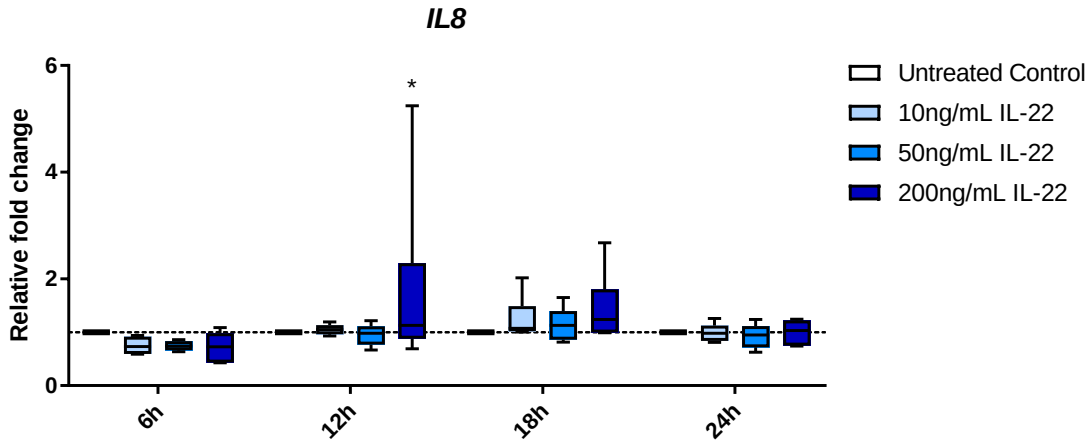


**Figure 4.22 *IL8* expression in response to IL-22 treatment**
$1x10^5$ /well primary bovine endometrial stromal cells were plated in 6-well plates and allowed to settle overnight. Cells were stimulated with 10ng/mL, 50ng/mL or 200ng/mL recombinant human IL-22 and harvested in TRIzol after 6, 12, 18 or 24 hours. Total RNA was extracted and first-strand cDNA reverse transcribed. qPCR was carried out and gene-of-interest $C_q$ values normalised to the reference gene panel using the method described by Hellemans et al. (2007). Boxes indicate median, 25$^{th}$ and 75$^{th}$ percentile fold change in gene expression relative to the untreated control within the same time point; whiskers indicate minimum and maximum values. The horizontal dotted line indicates the y-value of the untreated control. Statistics were computed using a repeated measures two-way ANOVA followed by Dunnett's post-hoc multiple comparison test. The mean fold change of each stimulation was compared to the untreated control within the same time point, with asterisks indicating statistically-significant differences: *=adjusted $p \leq 0.05$. The cells used for this experiment were isolated from two Charolais, one Charolais cross, one Friesian and two Limousin cross cows; age range is 4-15 years; *n*=6.

*DEFB103* is significantly upregulated by 200ng/mL IL-22 after 18 hours (mean fold change 2.77±1.59; adjusted p=0.0332) (Figure 4.23) . However, this is driven by two animals from the sample of 6 which have responded; the remaining four have not.

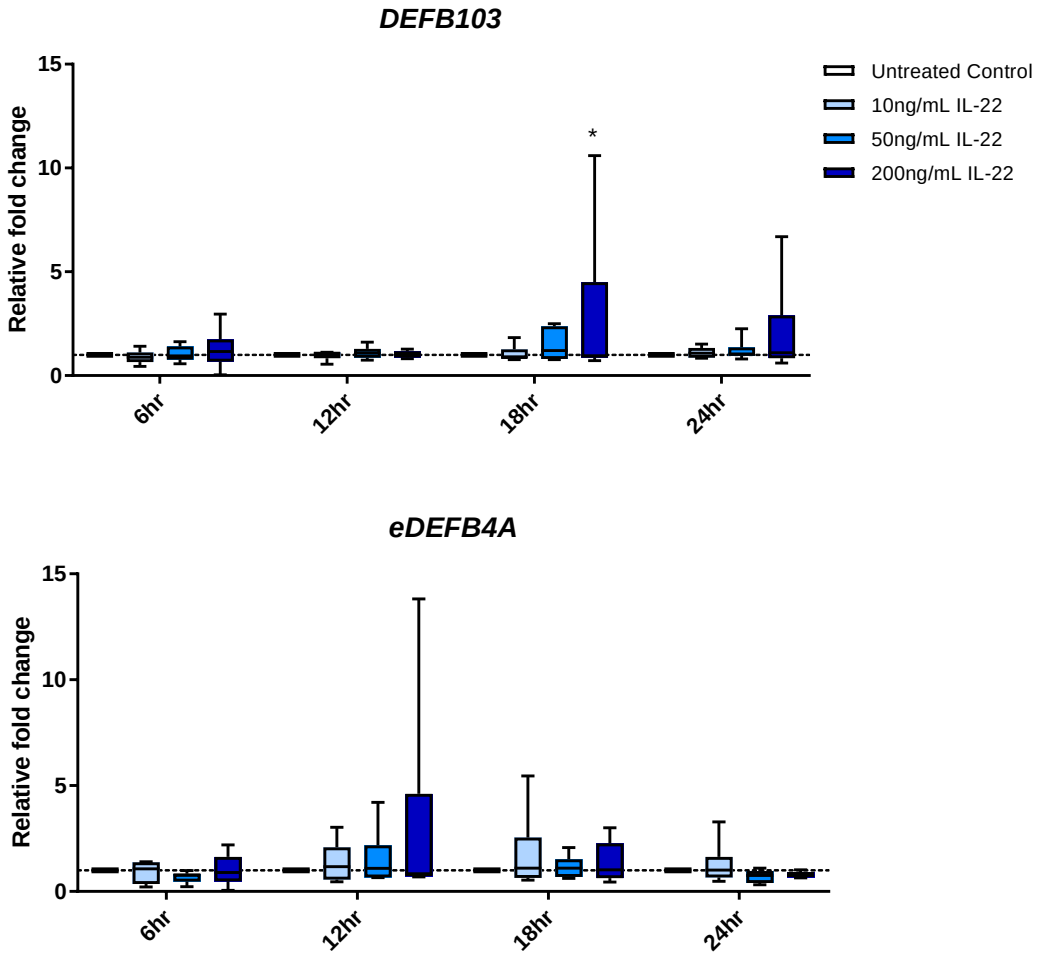


**Figure 4.23 β-defensin expression in response to IL-22 treatment**
$1x10^5$ /well primary bovine endometrial stromal cells were plated in 6-well plates and allowed to settle overnight. Cells were stimulated with 10ng/mL, 50ng/mL or 200ng/mL recombinant human IL-22 and harvested in TRIzol after 6, 12, 18 or 24 hours. Total RNA was extracted and first-strand cDNA reverse transcribed. qPCR was carried out and gene-of-interest $C_q$ values normalised to the reference gene panel using the method described by Hellemans et al. (2007). Boxes indicate median, $25^{th}$ and $75^{th}$ percentile fold change in gene expression relative to the untreated control within the same time point; whiskers indicate minimum and maximum values. The horizontal dotted line indicates the y-value of the untreated control. Statistics were computed using a repeated measures two-way ANOVA followed by Dunnett's post-hoc multiple comparison test. The mean fold change of each stimulation was compared to the untreated control within the same time point, with asterisks indicating statistically-significant differences: *=adjusted p≤0.05. The cells used for this experiment were isolated from two Charolais, one Charolais cross, one Friesian and two Limousin cross cows; age range is 4-15 years; *n*=6.

There is no obvious relationship between gene induction and *IL22R1* expression. The two biological replicates which have responded are not those with the highest receptor expression (first and second from left in Figure 4.20). These cells were isolated from one Charolais and one Charolais cross cow; both were 9 years old. There were cells from another Charolais animal included in this experiment and these animals are in the middle of the age range of 4-15 years for this experiment. Therefore age and breed are unlikely to account for this variation in response.

## 4.4 Discussion

Here we show that the β-defensin genes *DEFB103*, *DEFB106* and at least one gene within the ruminant expansion of *DEFB4A* are expressed throughout the cow reproductive tract. Despite representing up to 8 genes, or copies of a gene, the *eDEFB4A* amplicon is expressed at a lower level than *DEFB103* or *DEFB106*. This is in agreement with the known expression pattern for the human orthologs of these genes; with *DEFB103* and *DEFB106* being expressed constitutively within tissues (Harder et al., 2001; Yamaguchi et al., 2002), while *DEFB4A* is expressed at a lower level but can be highly induced (O'Neil et al., 1999).

This is the first time *DEFB106* has been shown to be expressed in the bovine. In addition, *DEFB106* expression has only previously been shown in the epididymis, bone marrow and skin (Xin et al., 2014; Yamaguchi et al., 2002). Therefore, demonstration of expression within the FRT is both novel and interesting, given the antibacterial and antifungal properties having been attributed to *DEFB106* (Xin et al., 2014).

In light of our growing understanding of the prevalence and impact of lower reproductive tract inflammation, as separate from uterine inflammation in the cow, it is appropriate that we begin to elucidate the host defence mechanisms at these sites. In contrast to the human and murine vaginal microbiome, in which a dominant and defensin-resistant *Lactobacillus* community secrete lactic acid and bacteriocins to kill invading pathogens (reviewed in Smith and Ravel, 2017; Yarbrough et al., 2014), the ruminant vaginal microbiome is of low abundance and diversity, high inter-individual variability and contributes to a neutral pH (Otero et al., 2000; Swartz et al., 2014). Enteric bacteria from the GI tract are common and *E. coli* are isolated in increasing numbers from the vagina of metritic post-partum cows versus healthy ones (Wang et al., 2013b). Therefore, protection of the bovine reproductive tract from ascending infection is likely more dependent on host defence mechanisms than in other species. With β-defensins implicated in protection of the vagina and cervix against bacteria (Fan et al., 2008; Racicot et al., 2013) and viruses (Ghosh et al., 2010), expression of β-defensins and other immunomodulatory and antimicrobial genes may be of increased importance in the bovine lower reproductive tract.

None of the β-defensin genes examined here are differentially expressed between the estrogen-dominant follicular and progesterone-dominant luteal phases of the cycle. A more detailed study including several stages of each phase would provide a more complete picture of β-defensin gene expression throughout the cycle. Additionally, sex steroids may modulate the β-defensin response to pathogens or other immunomodulatory factors. *DEFB4A* expression in human vaginal epithelium is not modified by estrogen or progesterone alone, however both modulate the LPS-driven response (Han et al., 2010).

Optimisation of a primary culture model has hugely extended our ability to investigate the immune function of the bovine FRT and has allowed us to examine the regulation of β-defensins in more detail. The pro-inflammatory cytokine IL-1β increases expression of both *DEFB103* and *eDEFB4A* in endometrial stromal cells. Though there is a high level of inter-animal variation, *IL8* expression is induced from 6 hours, with *eDEFB4A* being induced from 12 hours. In contrast, *DEFB103* is not induced until 24 hours, and the fold changes are smaller. Human endometrial epithelial cells significantly upregulate *DEFB103* expression ~3 fold in response to IL-1β (King et al., 2003), however the mechanisms driving this have not been investigated. In contrast, a number of studies have investigated IL-1β induction in human primary keratinocytes. The fold changes observed in these keratinocyte studies are larger than those observed here, however differentiation of the cultured keratinocytes via $Ca^{2+}$ is essential for β-defensin induction, with inhibition of induction via trans-retinoic acid blocking induction via the range of pro-inflammatory stimuli used (Harder et al., 2004). IL-1β is a potent and direct inducer of *DEFB4A* in keratinocytes (Sørensen et al., 2005), while the effect on *DEFB103* is mainly via the EGF receptor as opposed to the IL-1 receptor. IL-1β upregulates TGF-α gene expression which then activates the EGF receptor, however it transactivates EGFR more directly through activation of matrix metalloproteinases at the cell surface, which cleave TGF-α and other EGFR ligands from the cell surface (Sanchez-Guerrero et al., 2012; Sørensen et al., 2005). The relatively late upregulation of *DEFB103* suggest a number of these mechanisms could be involved. EGFR signalling can also culminate in AP-1 activation (Cichocki et al., 2012), so IL-1β-mediated induction of *DEFB103* may be partly direct even if EGFR is involved.

A similar trend is seen following IL-17A stimulation. While the induction of e*DEFB4A* is not statistically significant due to a high level of inter-animal variation, the

level of induction is higher and begins earlier than for *DEFB103*. This is in agreement with the pattern observed for the human and murine orthologs of these genes (Archer et al., 2016; Kolbinger et al., 2017). However, the signalling pathways driving IL-17A stimulation of β-defensins are not well understood. Blocking the IL-17A receptor, but not the IL-1 or IL-6 receptors, blocks the IL-17A-mediated induction of *DEFB4A* in keratinocytes (Kao et al., 2004). In these cells, OCT-1 is constitutively bound to the *DEFB4A* promoter and IL-17A induction involves p38 activation and IκBζ binding to the p50 subunit of NF-κB (Johansen et al., 2016). IL-17A regulation of *DEFB103* expression in the reproductive tract has not been previously demonstrated, nor is the signalling mechanism understood in any model. IL-17A regulates *CXCL8* and *CXCL10* expression in colonic epithelium via EGFR signalling (Lee et al., 2008), therefore EGFR signalling in this stromal cell model in response both stimuli used warrants further investigation.

The IL-22 stimulation data shown here do not convincingly indicate that the stromal cells are truly responsive to the recombinant human IL-22 used. While the effect on *IL8* and *DEFB103* stimulation is statistically significant, this is driven by a positive response of only ~2 of the 6 biological replicates. Responsiveness does not depend on extent of *IL22R1* expression, or animal age or breed. The percent identity between bovine and human IL-22 proteins may not be high enough for bovine cells to be able to respond to human IL-22. Detection of STAT3 phosphorylation via western blot would determine whether intracellular signalling was occurring in response to stimulation.

Alternatively, IL-22 may genuinely not be a potent inducer of β-defensins or *IL8* in these cells. Knock-down of *IL22* but not *IL17A* eliminates β-defensin expression in murine nasal epithelium (Mulcahy et al., 2016), however, the reverse occurs in murine gastric epithelium (Dixon et al., 2016). While *IL8* is induced by IL-22 in endometrial stromal cells from women with endometriosis and adenomyosis, the fact this does not occur in healthy patients indicates there is an additional factor present in diseased patients which facilitates IL-22 mediated induction. Upregulation of *IL8* expression in human gastric epithelium requires IL-17A in combination with IL-22 (Dixon et al., 2016). In keratinocytes, IL-22 can also work synergistically with IL-1β to induce β-defensins (Wolk et al., 2006).

Other combinations of cytokines are able to work synergistically to mediate β-defensin expression. IL-17A and TNFα in combination induce β-defensin expression in human keratinocytes (Chiricozzi et al., 2014). In human endometrial epithelium, IL-1β-mediated induction of *DEFB103* is increased by TNFα (King et al., 2003). IL-1β and IL-17A have been studied here as expression of the signalling pathway components for both cytokines are increased in the post-partum endometrium (Foley et al., 2015). However, *TNF* expression is also increased in the early post-partum period, therefore it may modulate β-defensin expression either alone or in combination with IL-1β or IL-17A.

Together, these data indicate that bovine endometrial stromal cells respond to pro-inflammatory cytokines which are expressed by cells within the endometrium and whose expression may also be increased systemically in the post-partum animal. Induction of β-defensin expression by these cytokines confirms the association between β-defensins and an overall inflammatory state in the post-partum endometrium (Foley et al., 2015). In addition, the data presented here broadly support the hypothesised importance of AP-1 signalling in regulation of *DEFB103* expression, as both IL-1β and IL-17A signalling pathways are known to culminate in AP-1 activation. Further elucidation of the regulatory mechanisms driving this induction, coupled with an improved understanding of the role of these pleiotropic molecules in this context, will help us understand how to harness the immune system towards more effective post-partum healing and earlier resumption of homeostasis.

# Chapter 5 1α,25-dihydroxyvitamin D3 modulates viral mimic-mediated β-defensin expression

## 5.1 Introduction

### 5.1.1 Antiviral properties of β-defensins

While β-defensins gained their name due to their observed antibacterial properties, an emerging body of literature points to a variety of direct and indirect anti-viral functions, including host cell receptor binding, modulating receptor expression and altering intracellular signalling (Wilson et al., 2013). hBD-2 destabilises the respiratory syncytial virus (RSV) envelope and inhibits viral entry into host cells (Kota et al., 2008). It can also block HIV reverse transcription (Sun et al., 2005). Human and porcine BD3 peptides inhibit replication of porcine reproductive and respiratory syndrome virus (Sang et al., 2009).

Human β-defensins 2 and 3 bind to the same heparin sulfate proteoglycans on the host cell surface as HIV gp120 peptides. While the β-defensins do not inactivate HIV while on the cell surface, they are endocytosed along with the viral particles and synergistically inactivate the virus once inside the endosome (Herrera et al., 2016). This study used polarised tonsil epithelial cells, which express *DEFB4A* and *DEFB103* only in adults. This may underlie the observation that rates of mother-to-child transmission of HIV through oral epithelia are much higher than between adults.

In addition, β-defensins indirectly impact viral infection by modulating the host immune response. mBD-1 knockout mice die sooner than wildtypes following influenza infection (Ryan et al., 2011). While viral burdens were the same between the two groups, knockouts suffered increased leukocyte infiltration and vascular oedema, suggesting mBD-1 has immunomodulatory properties rather than direct antiviral properties in this model. Preincubation of influenza A virus with hBD-2 slightly reduces viral infectivity, but injection of hBD-2 into mice before infection more significantly decreases viral burden. IFNγ production increases and numbers of alveolar macrophages and neutrophils in the infected lung decrease (LeMessurier et al., 2016). hBD-3 enhances bone marrow-

derived macrophage uptake of the dsRNA mimic poly(I:C), to the same extent as the commercial transfection reagent Lipofectamine, with both increasing IFN-β production compared to poly(I:C) alone. However, while Lipofectamine increases poly(I:C) uptake into endosomes, hBD-3 delivers the nucleic acid to the cytoplasm, inhibiting TLR3 signalling and enhancing activity of the cytoplasmic sensor melanoma differentiation-associated gene 5 (MDA5) (Semple et al., 2015). Thus, β-defensins are important components of the anti-viral response, due to a range of both direct and indirect mechanisms.

As might be expected given the above, viruses and nucleic acids can regulate β-defensin expression. Influenza A infection increases *DEFB4A* expression in the murine lung (LeMessurier et al., 2016). Infection of pDCs and monocytes with HSV-1 or Sendai virus increases hBD-1 production, however, influenza infection decreases hBD-1. Plasmacytoid dendritic cells (pDCs) and monocytes increase hBD-1 production in response to HSV-1 infection, but gingival epithelial cells decrease it (Ryan et al., 2011). Respiratory bovine herpesvirus (BoHV)-1 infection increases bovine *DEFB103* expression in buccal epithelium, but not tongue epithelium, of calves (Mirabzadeh-Ardakani et al., 2016). These examples indicate regulatory mechanisms are cell specific. None of these infection studies have determined whether β-defensin induction is directly driven by the virus.

Both viral proteins and host cytokines have been implicated as mediators of virus-driven β-defensin expression. In malignant cells from human papilloma virus 16-associated oropharyngeal cancers, *DEFB103* overexpression is driven by binding of the HPV-16 protein E6 to a p53 binding site in the *DEFB103* promoter (DasGupta et al., 2016). In acutely HIV-infected monocytes, *DEFB1* expression is increased via induction of IFN-α (Corleis et al., 2017). However, *DEFB103*, but not *DEFB1*, is induced by IFN-α in lung epithelium (Basu et al., 2010).

Nucleic acids themselves regulate β-defensin expression in a number of *in vitro* models. *DEFB4A* is upregulated by poly(I:C) in human oviduct epithelial cells and immortalised colonic epithelial cells, with the response in the latter cell type being NF-κB dependent (Ghosh et al., 2008; Omagari et al., 2011). In uterine epithelial cells, poly(I:C) added to culture medium upregulates *DEFB1* and *DEFB4A* in a TLR3-

independent manner, though the fold changes are an order of magnitude smaller than those observed for known interferon-stimulated genes (ISGs) (Schaefer et al., 2005). Therefore, a combination of the genetic material and capsule material of the virus, the proteins encoded by the virus and the cytokines produced by the host cells contribute to regulation of β-defensin expression, with the studies discussed here indicating the response is virus- and cell type-specific.

A number of viruses infect the cow reproductive tract and are economically important in modern farming. The dsRNA-generating bovine viral diarrhoea virus (BVDV) reduces conception rate and induces abortion and failure of calves to thrive (Houe, 1999). Fortunately, a national eradication programme, instigated in 2013, has reduced the number of persistently-infected animals born in Ireland in 2016 to less than 25% of that born in 2013 (Animal Health Ireland, 2017).

Several members of the Herpesviridae family also infect the reproductive tract. This family is characterised by a double-stranded DNA genome and various morphological characteristics, including an icosahedral capsid (Pellett and Roiz, 2013). The biological cycle of herpesviruses has three stages: initiation of infection, lytic replication and latency. During the latent phase, the viral genome temporarily assumes a closed circular state, with only a subset of viral genes being expressed. While no infectious particles are shed from host cells at this time, the lytic phase can later restart; though the factors driving this for a given virus are poorly understood.

BoHV-1 causes a severe and prevalent respiratory disease, named infectious bovine rhinotracheitis. However, it also causes infectious pustular vulvovaginitis (McKercher, 1973). BoHV-4 infects a wide range of tissues, and can establish latency in lymph nodes and bone marrow (Egyed and Bartha, 1998), with dexamethasone treatment awakening the virus from latency. It can infect both epithelial and stromal cells of the endometrium (Donofrio et al., 2007), though whether it can establish latency in these cells is unknown. There is a high incidence of infection with both viruses in Irish herds. Within 1589 sera from 318 herds, 31% and 44% tested positive for BoHV-1 and BoHV-4 antibodies respectively (O'Neill et al., 2016). In addition, 17% of herds had 100% BoHV-4 positivity.

While several studies have investigated a potential link between BoHV-4 and uterine disease, the contribution and exact pathology of the virus remain unclear (Chastant-Maillard, 2015). Among 400 cows from 10 Austrian dairy farms, 5.8% of animals had detectable BoHV-4 in uterine cytology samples. These animals had a higher mean percentage polymorphonuclear cells (PMN) and there was a higher incidence of endometritis, though BoHV-4 infection was not significantly associated with endometritis risk (Klamminger et al., 2017).

The association between BoHV-4 and perturbed fertility is clearer. In the Austrian study discussed above, BoHV-4 significantly decreased the risk of pregnancy within 200 days post-partum (DPP). Among 273 Turkish Holstein-Friesian cows, 69% of those who had repeatedly failed to conceive were BoHV-4 seropositive, compared to 44% of reproductively healthy cows (Gür and Doğan, 2010). Thus, BoHV-4 does have a negative impact on FRT function.

A common supposition is that any association between BoHV-4 infection and pathology is due to a co-occurrence with bacterial infection (Chastant-Maillard, 2015). Indeed, the cytokine response associated with bacterial infection facilitates the BoHV-4 biological cycle. TNFα directly increases BoHV-4 replication in immortalised endometrial stromal cells via NF-κB response elements in the viral immediate early (IE)2 gene promoter (Jacca et al., 2013). In addition, prostaglandin E2 promotes BoHV-4 replication in macrophages (Donofrio et al., 2005), meaning increased prostaglandin E2 production in the infected post-partum uterus may encourage reactivation of the virus (Sheldon et al., 2009b). Transcriptomic analysis of BoHV-4-infected endometrial stromal cells indicates a remarkable lack of immune gene induction (Tebaldi et al., 2016), with the exception of *IL8*, which is activated by direct binding of IE2 to the *IL8* promoter (Donofrio et al., 2010). This means BoHV-4 itself may increase PMN influx into the uterus. Matrix metalloproteinase (MMP)1 is the most highly induced gene in infected cells, possibly impairing tissue healing post-partum (Tebaldi et al., 2016). Thus, a latent BoHV-4 infection may be reactivated in the post-partum inflammatory environment, with endometrial stromal cells acting as a facultative reservoir of infection, allowing BoHV-4 to delay the return of uterine homeostasis and negatively impact fertility.

Endometrial stromal cells can be infected *in vitro* with a number of other viruses, including Zika virus (Pagani et al., 2017) and cytomegalovirus (Kowalik et al., 1994). These cells actively enhance HIV infection: infection of $CD4^+$ T cells increases in the presence of cultured endometrial stromal cells, despite the stromal cells themselves not being productively infected (Neidleman et al., 2017). Physical separation of the two populations abrogates this effect. Stromal cells are more than ten times more effective at *trans*-infecting $CD4^+$ T cells than DCs and also render $CD4^+$ T cells more permissive to HIV infection, though the mechanism behind this has not been identified. In contrast, endometrial epithelial cells actively inhibit HIV infection. The most differentially-expressed genes between epithelial and stromal cells are secretory leukocyte protease inhibitor (*SLPI*) and *DEFB4A*. *DEFB1* is also more highly expressed by epithelial cells. In addition, fibroblasts from the cervix, urethra, intestine and foreskin all enhance HIV infection of T cells. Thus, this body of work indicates that endometrial stromal cells are an important but understudied cell type in the context of viral infection. Modulation of β-defensin expression within these cells may improve host antiviral responses.

### 5.1.2 Innate sensing of nucleic acids

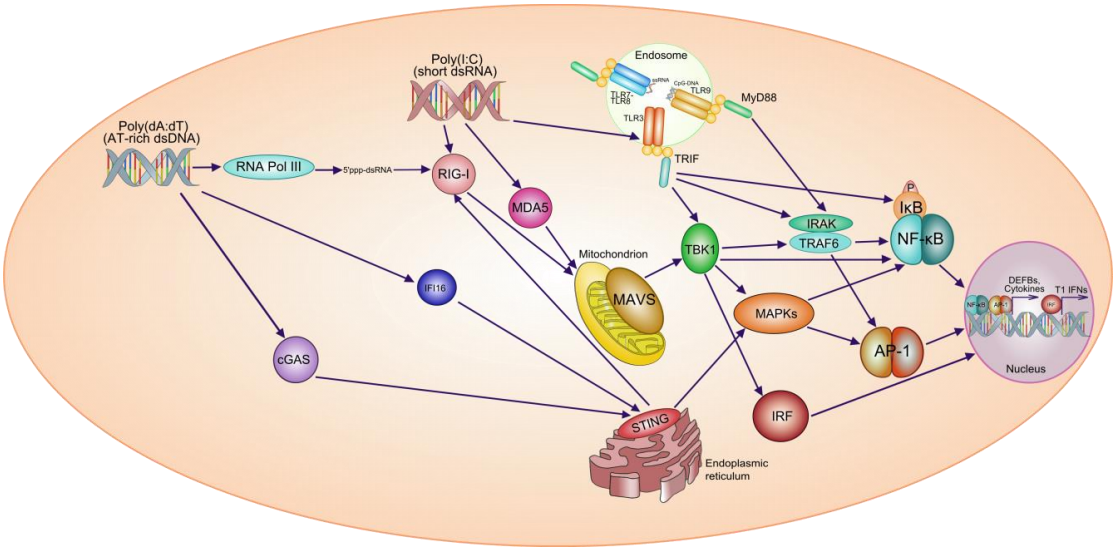


**Figure 5.1 Nucleic acid sensors and signalling pathways**
Nucleic acids can be sensed via a range of PRRs, including TLRs, RLRs and PYHIN proteins. MAPK and NF-κB pathway activation culminates in AP-1 and NF-κB transcription factor translocation respectively. These transcription factors induce expression of a wide range of cytokine and antiviral effector genes, including HDPs. Type I interferon production is induced by IRF family transcription factors. Based on Abe and Barber, (2014); Ma and Damania, (2016); Thompson and Locarnini, (2007).

Nucleic acid sensing pathways involve a complex network of sensors, signalling pathways and transcription factors (Chan and Gack, 2016; Ma and Damania, 2016;). TLR3 was the first identified receptor for dsRNA, being essential for Poly(I:C)-mediated activation of macrophages and activating NF-κB and mitogen-activated protein kinase (MAPK) signalling (Alexopoulou et al., 2001). There is a small amount of TLR3 on the surface of some cell types, with the majority being found within endosomes, where TLR3 signalling is initiated. The endosome also hosts the nucleic acid-binding TLRs TLR7, TLR8 and TLR9 (O'Neill et al., 2013). Lundberg et al., (2007) found the exact TLR3 signalling pathways used vary between cell types. Human synovial fibroblasts and endothelial cells and murine DCs activate NF-κB in response to poly(I:C), while human DCs and macrophages do not. Similarly, the human myeloid cells do not activate MAPK pathway signalling, while several MAPK pathways are activated in synovial fibroblasts.

Several dsRNA helicases of the RIG-like receptor (RLR) family sense dsRNA generated by viral replication in the cytoplasm (Thompson and Locarnini, 2007). Retinoic

acid inducible gene I (RIG-I) is essential for IFN-β production in response to Newcastle virus (Yoneyama et al., 2004). MDA5 also drives IFN-β production in response to dsRNA stimulation, with IRF3 activity driving IFN-β gene expression in response to both sensors (Yoneyama et al., 2005).

The relative importance of TLR3, retinoic acid-inducible gene I (RIG-I) and MDA5 is cell type, gene and virus specific. *In vitro* experiments using poly(I:C) can add the nucleic acid to the culture medium, where it is endocytosed and delivered to TLR3. Alternatively, it can be transfected using a cationic lipid, which enhances delivery to the cytoplasm. Poly(I:C)-mediated induction of the IFN-β gene *IFNB1* in human monocyte-derived macrophages is potentiated by transfection and IFN-β protein is only detected when poly(I:C) is transfected. In these cells, IFN-β production is independent of NF-κB or IRF3 signalling (Reimer et al., 2008). Murine fibroblasts and conventional DCs sense RNA viruses with RIG-I, while pDCs use TLR3 (Kato et al., 2005). Intravenous injection of poly(I:C) into mice with various nucleic acid-sensing genes knocked out indicates that MDA5 mediates poly(I:C)-driven production of IFN-α and IFN-β, while TLR3 drives IL-12 production and signalling from both sensors drives IL-6 production. In this study, both bone marrow-derived DCs and embryonic fibroblasts sensed poly(I:C) primarily via MDA5, while *in vitro* transcribed dsRNA was sensed by RIG-I. RIG-I was essential for responding to influenza virus, while MDA5 was indispensable in picornavirus sensing (Kato et al., 2006).

DNA sensing pathways are more poorly characterised (Ma and Damania, 2016). The dsDNA mimic poly(dA:dT) can be transcribed by RNA polymerase III to a 5'-triphosphate RNA intermediate which is then sensed by RIG-I (Ablasser et al., 2009). Endoplasmic reticulum-associated stimulator of interferon genes (STING) is necessary for negative-stranded virus sensing and can associate with RIG-I (Ishikawa and Barber, 2008). STING also associates with the DNA-sensing PYHIN family protein interferon-inducible (IFI)16 (Unterholzner et al., 2010). Named based on their characteristic pyrin and HIN domains, PYHINs are DNA sensors which vary in number between species. While the human and mouse genomes have four and seven PYHIN family genes respectively, IFI16 is the only predicted intact PYHIN gene within the bovine genome (Cridland et al., 2012). STING is also activated by cyclic guanosine monophosphate-adenosine monophosphate synthase (cGAS), which signals via production of the second

messenger cGAMP (Sun et al., 2013). Each sensor signals through a diverse range of pathways, reviewed well by Ma & Damania, (2016) and Thompson & Locarnini (2007) and summarised in Figure 5.1.

Viral sensing in the bovine has been best studied in the context of BVDV infection. The genes encoding RIG-I and MDA5 are upregulated in foetuses whose dams have been infected with BVDV during gestation (Smirnova et al., 2012) and in naturally-infected steers (Shoemaker et al., 2009). Inclusion of a RIG-I agonist-encoding plasmid in a DNA-based vaccine against bovine viral diarrhoea virus generates an increased antibody response over plasmids encoding BVDV antigen alone (R. El-Attar et al., 2015). Within the endometrium, expression of the MDA5-encoding gene *IFIH1* is increased in post-partum cows in negative energy balance (Wathes et al., 2009). MDA5-, RIG-I- and IFI16-encoding genes are all upregulated in the endometrium of cows in early pregnancy (Klein et al., 2006). This is likely driven by IFN-τ, which is secreted by the ruminant peri-implantation conceptus to modulate uterine gene expression in preparation for implantation. Ovine endometrial stromal cells upregulate *IFIH1* in response to IFN-τ (Song et al., 2007).

Although the dsDNA herpesviruses contribute to a wide range of pathologies, DNA-sensing mechanisms are understudied in bovine. In bovine kidney cells, IFI16 protein production and cytoplasmic localisation can be induced by BoHV-1 infection (Wang et al., 2014a). The expression pattern and function of the wider DNA sensing machinery is unknown in cattle. Within bovine endometrial stromal cells, the TLRs are the only PRRs to have been profiled in response to infection (Davies et al., 2008).

### 5.1.3 Immunomodulatory properties of vitamin D

25-hydroxyvitamin $D_2$, (25D), acquired via cutaneous synthesis or dietary intake, is hydroxylated by cytochrome P450 (CYP)27B1 to generate metabolically-active 1α,25-dihydroxyvitamin $D_3$ (1,25D). Originally thought to be confined to the kidney, CYP27B1 is now known to be widely expressed. 1,25D induces expression of the enzyme CYP24A1 which catabolises it. Thus, the level of active vitamin D is tightly regulated. 1,25D binds

to vitamin D receptor (VDR), which then translocates to the nucleus and binds vitamin D response elements (VDREs) within target genes (White, 2012).

The classical function of 1,25D is regulation of calcium metabolism. However, in the human it has wide-ranging immunomodulatory functions, which are mostly anti-inflammatory. A systematic review of seven papers studying the effect of 1,25D on cell lines and sixteen on PBMCs found 1,25D blocks the response to the relevant proinflammatory stimulus in the majority of cases (Calton et al., 2015), though this may be due to a bias towards using PBMCs as a model. Activated VDR destabilises the interaction between AP-1 and nuclear factor of activated T cells (NFAT) which precedes binding to the *IL2* gene promoter (Alroy et al., 1995). As AP-1/NFAT cooperation regulates a wide range of cytokines including IL-4, IL-5, IL-13, IFN-γ and granulocyte macrophage colony-stimulating factor (GM-CSF) (Rao et al., 1997), this may explain the anti-inflammatory effect of vitamin D on PBMCs.

The demonstrable anti-inflammatory properties of 1,25D within the human are in many cases accomplished through modulating activity of the NF-κB inhibitor IκBα. IκBα constitutively binds to the p50 and p65 subunits of NF-κB, preventing their translocation to the nucleus until it is phosphorylated and degraded. Supplementation of pregnant mice with 25D attenuates the LPS-driven increase in serum TNFα, IL-1β and IL-6. Within placental trophoblast cells, VDR itself binds the p65 subunit of NF-κB, inhibiting nuclear translocation and preventing fetal intrauterine growth restriction in response to LPS (Chen et al., 2015). In human tracheobronchial epithelial cells, 1,25D upregulates IκBα expression, which inhibits NF-κB signalling and reverses respiratory syncytial virus (RSV)-driven *CXCL10*, *IFNB1* and *ISG15* induction without an increase in viral replication (Hansdottir et al., 2010). Calcipotriol is a vitamin D analogue used to treat psoriasis. In human keratinocytes, calcipotriol blocks IL-17A-mediated induction of *DEFB4A* and *DEFB103* via inhibition of IκBα phosphorylation (Peric et al., 2009).

1,25D can promote inflammation by inducing genes with VDREs in regulatory gene regions, such as the human cathelicidin gene *CAMP* (Wang et al., 2004). The human *DEFB4A* gene contains a VDRE and is induced up to 8-fold by 1,25D in a variety of human leukocytes and epithelial cells (Wang et al., 2004). The gene encoding the intracellular PRR NOD2 is directly upregulated via binding of both proximal and distal

VDREs, with NOD2 activation itself potentiating 1,25D regulation of *DEFB4A* (Wang et al., 2010). Similarly, *DEFB4A* is modestly induced by 1,25D in human bronchial epithelial cells, but this is boosted by *Aspergillus fumigatus* exposure (Li et al., 2015). In this model, 1,25D attenuates *A. fumigatus*-driven IL-6, IL-8 and TNF-α production. Thus, 1,25D treatment can strike an appropriate balance between effective antimicrobial responses and limited systemic inflammation.

In contrast, 1,25D induces *CAMP*, but not *DEFB4A* or *DEFB103* in human sebocytes (Lee et al., 2012). In human gingival cells, hBD-3 is upregulated 3-fold by 1,25D (De Filippis et al., 2017). In human DCs, 100nM 1,25D upregulates hBD-3 along with IL-1β and NOD2 (Olliver et al., 2013). Therefore, the effect of 1,25D on β-defensin expression depends on the presence or absence of other stimuli and the intracellular signalling pathways driving expression in a given cell type.

Emerging evidence suggests a pre-existing inflammatory state itself impacts the nature and extent of 1,25D activity. Prior exposure to TNFα and IL-1β attenuated 1,25D-mediated expression of LL-37 by primary bronchial epithelial cells and inhibited killing of *Hemophilus influenzae*, due to downregulation of the vitamin D activating enzyme CYP27B1 and upregulation of the catabolising enzyme CYP24A1 (Schrumpf et al., 2017).

Viruses can also impact vitamin D metabolism and signalling. Human cytomegalovirus downregulates *VDR* expression in foreskin fibroblasts, meaning viral replication is not inhibited by various vitamin D analogues (Rieder et al., 2017). The same study found neither influenza virus nor adenovirus decreased *VDR* expression in bronchial epithelium, but did not report whether vitamin D affected replication of these viruses. This contrasts with another recent study which has found rhinovirus and RSV both decrease expression of *VDR* and *CYP27B1* in human bronchial epithelial cells. In this study, 1,25D increases expression of ISGs and cathelicidin, while decreasing viral replication (Telcian et al., 2017). The proteins expressed by each virus probably contribute to this effect, however, differences in intracellular sensing and signalling may also be important. 1,25D differentially impacts TLR signalling depending on which TLRs are involved. 1,25D inhibits proinflammatory cytokine production in human monocytes in response to the TLR4 ligand LPS but not to the TLR7/8 ligand CL075 or to RSV

infection. Stimulation of TLR7/8, but not TLR4, downregulates *VDR* expression while signalling from TLR4 but not TLR7/8 induced IκBα (Fitch et al., 2016). Thus, increased vitamin D supplementation, or inclusion of an additional immunomodulatory agent, may be necessary to improve the host response to some viruses, particularly if there is a background of ongoing inflammation.

Caution must be applied when interpreting this human literature as many of the discussed effects of 1,25D are primate specific. Within a single study, *NOD2*, *DEFB4A* and *CAMP* were induced by 1,25D in human but not murine macrophages (Dimitrov and White, 2016). The human, chimp, gorilla and rhesus monkey orthologs of these genes contain VDREs, but the rodent orthologs do not. 1,25D regulation of the *CAMP* gene is primate specific due to a VDRE-containing transposable element in the promoter which was acquired after the split between prosimians and the clade leading to apes and monkeys (Gombart et al., 2009). Accordingly, 1,25D does not upregulate expression of bovine cathelicidins in monocytes (Nelson et al., 2010a).

However, vitamin D does boost expression of some bovine β-defensins. Injection of 25D into the infected mammary gland reduces bacterial counts and mastitis severity (Lippolis et al., 2011). Both mammary epithelial cells and circulating myeloid cells, which infiltrate the mammary gland in response to infection, respond to 1,25D. 1,25D intensifies the LPS-driven upregulation of *IL1B*, chemokine (c-c motif) ligand (*CCL*)*5* and *NOS2* in bovine peripheral blood monocytes (Nelson et al., 2010a). Little change in β-defensin expression was observed in these cells after 18 hours with 100ng/mL LPS, but inclusion of 1,25D upregulated several genes within the *DEFB4A* expansion. Similarly, *DEFB4A* expansion genes are upregulated by 1,25D in primary bovine mammary epithelial cells (Téllez-Pérez et al., 2012). Blocking protein translation eliminates the effect of 1,25D on β-defensin transcription, suggesting 1,25D is acting indirectly to boost β-defensin expression (Merriman et al., 2015). Thus, vitamin D is a promising mastitis therapeutic. However, it has not been investigated in the context of uterine disease or viral infection. Additionally, the role of vitamin D in regulation of bovine β-defensins outside the *DEFB4A* expansion is unknown.

Vitamin D in the context of post-partum uterine inflammation is of particular interest as the low sunlight and indoor housing practises prevalent in Ireland when cows

give birth in early spring means animals may well be vitamin D deficient at this time. Hymøller et al. (2009) found 25D plasma levels in animals reared in Sweden without supplementation drop from 20-50ng/mL in the summer to 2ng/mL in the winter, indicating vitamin stores accrued during summer grazing are not maintained during indoor housing over winter. Vitamin D regulation of β-defensin expression would suggest dietary supplementation may be an effective way to boost levels of these peptides. In addition, one study has found circulating 1,25D drops 3 DPP following a transient increase associated with the onset of lactation (Goff et al., 2002).

If vitamin D can promote effective local antiviral immunity through differential regulation of β-defensin expression in endometrial stromal cells, then supplementation or local delivery may overcome the immunosuppressive effects of BoHV-4. Given that BoHV-4 potentially promotes PMN influx and delays tissue healing, such a mechanism would likely reduce the incidence of prolonged and pathological post-partum uterine inflammation.

## 5.2 Hypothesis and specific aims

*We hypothesise that hormonally-active vitamin D can alter nucleic acid-driven β-defensin expression in endometrial stromal cells.*

**Specific aims:**

1. Profile β-defensin expression in endometrial stromal cells in response to the viral mimics poly(I:C) and poly(dA:dT).
2. Quantify expression of viral-sensing genes in endometrial stromal cells in response to these stimuli.
3. Investigate 1,25D as a potential regulator of β-defensin expression in stromal cells.
4. Apply 1,25D in combination with viral mimics to investigate whether it modulates the antiviral response.

## 5.3 Results

### 5.3.1 β-defensin genes are differentially regulated by the dsRNA mimic poly(I:C)

Poly(I:C) is a synthetic nucleic acid molecule whose structure is similar to that of viral dsRNA. It acts as an agonist for TLR3 (Alexopoulou et al., 2001), which is expressed by bovine endometrial stromal cells (Davies et al., 2008). Endometrial stromal cells from six animals were stimulated with 10μg/mL low molecular weight poly(I:C) for 6, 12, 18 and 24 hours. All animals were Friesians and the age range was 3-15 years. As there was only one concentration used here, statistics were computed using a one-way, repeated measures, non-parametric ANOVA.

*IFNB1* has been shown to be regulated by poly(I:C) via TLR3 (Alexopoulou et al., 2001), therefore it was used as a positive control. Unexpectedly, endometrial stromal cells downregulate *IFNB1* expression (Figure 5.2). While the trend is not statistically significant, downregulation of *IFNB1* begins at 6 hours and increases until 18 hours (mean fold change =-0.62±0.77).

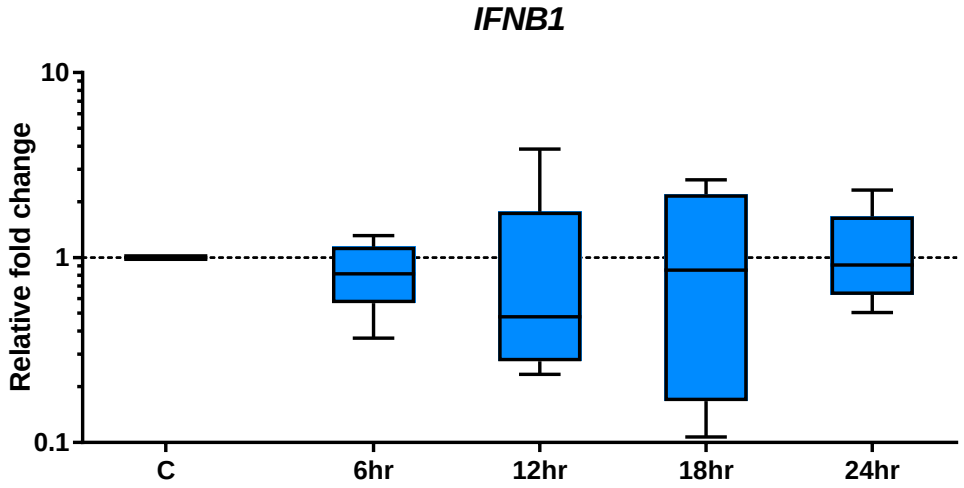


**Figure 5.2 *IFNB1* is not significantly differentially regulated by 10µg/mL Poly(I:C)**
$1x10^5$ /well primary bovine endometrial stromal cells were plated in 6-well plates and allowed to settle overnight. Cells were stimulated with 10µg/mL poly(I:C) and harvested in TRIzol after 6, 12, 18 or 24 hours. Total RNA was extracted and first-strand cDNA reverse transcribed. qPCR was carried out and gene-of-interest $C_q$ values normalised to the reference gene panel using the method described by Hellemans et al. (2007). Boxes indicate median, $25^{th}$ and $75^{th}$ percentile fold change in gene expression relative to the untreated control within the same time point; whiskers indicate minimum and maximum values. All values were normalised to the untreated control within the same time point, however only one control value is shown here for clarity. The horizontal dotted line indicates the y-value of the untreated control. Statistics were computed using Friedman's ANOVA followed by Dunn's post-hoc multiple comparison test, comparing the mean of each column to that of the untreated control. The cells isolated for this experiment were from Friesian cows; age range is 3-15 years; *n*=6.

Quantification of *DEFB103* expression in these cells indicates it is increasingly upregulated across the time course, with a 3.45±0.87 fold change at 24 hours (adjusted p=0.0041) (Figure 5.3). In contrast, e*DEFB4A* is downregulated by this same stimulus, with a mean 0.40±0.26 fold change relative to the unstimulated control value of 1 at 24 hours (adjusted p=0.0139).

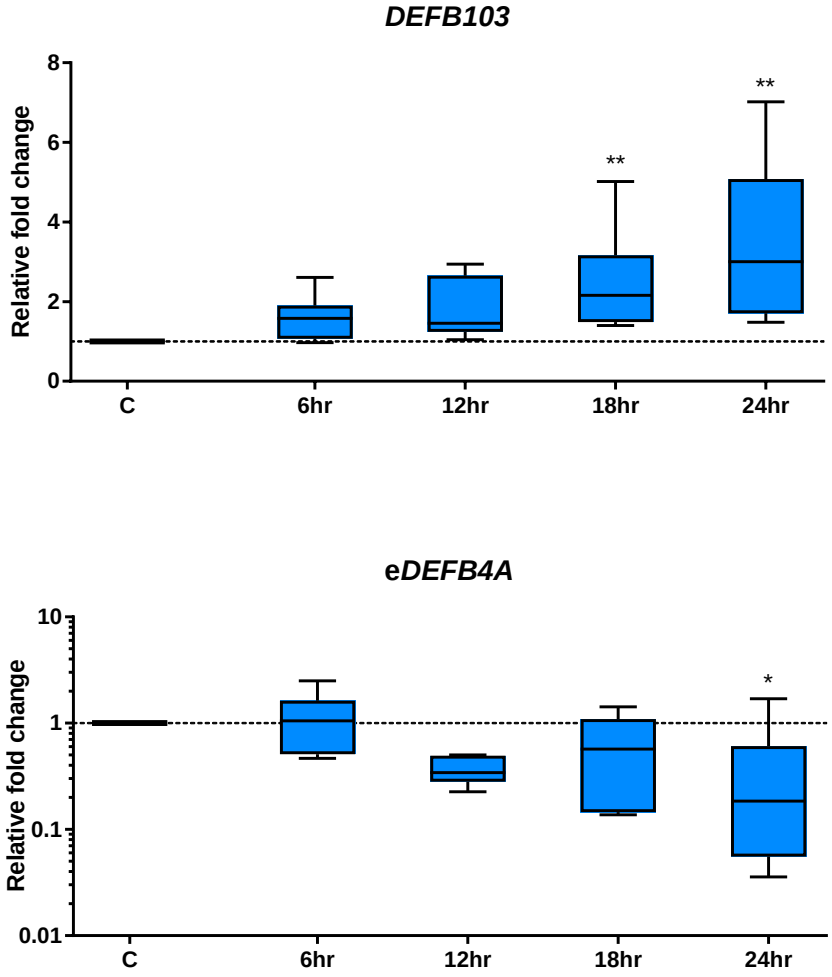


**Figure 5.3 Poly(I:C) differentially regulates *DEFB103* and e*DEFB4A* expression**
$1x10^5$ /well primary bovine endometrial stromal cells were plated in 6-well plates and allowed to settle overnight. Cells were stimulated with 10µg/mL poly(I:C) and harvested in TRIzol after 6, 12, 18 or 24 hours. Total RNA was extracted and first-strand cDNA reverse transcribed. qPCR was carried out and gene-of-interest $C_q$ values normalised to the reference gene panel using the method described by Hellemans et al. (2007). Boxes indicate median, $25^{th}$ and $75^{th}$ percentile fold change in gene expression relative to the untreated control within the same time point; whiskers indicate minimum and maximum values. All values were normalised to the untreated control within the same time point, however only one control value is shown here for clarity. The horizontal dotted line indicates the y-value of the untreated control. Statistics were computed using Friedman's ANOVA followed by Dunn's post-hoc multiple comparison test, comparing the mean of each column to that of the untreated control. Asterisks indicate statistically-significant differences relative to the untreated control: *=adjusted p≤0.05; **=adjusted p≤ 0.01. The cells isolated for this experiment were from Friesian cows; age range is 3-15 years; *n*=6.

### 5.3.2 Primary bovine endometrial stromal cells express several viral-sensing genes

Having demonstrated that stromal cells respond to poly(I:C) via differential β-defensin gene expression, we were interested in determining what capability these cells might have to respond to other types of viral mimics. TLR gene expression in these cells has been profiled (Davies et al., 2008), however, the expression of other viral-sensing genes has not. qPCR assays for genes encoding RIG-I (*DDX58*), MDA5 (*IFIH1*), cGAS (*MB21D1*) and STING (*TMEM173*) were designed and optimised. Several sets of qPCR primers, each targeting different regions of the IFI16 gene were also designed. However, when PCR products generated using these were sent for sequencing, all contained multiple products. Endometrial stromal cells express all four of these genes at the mRNA level (Figure 5.4). *TLR3* has been included for comparison.

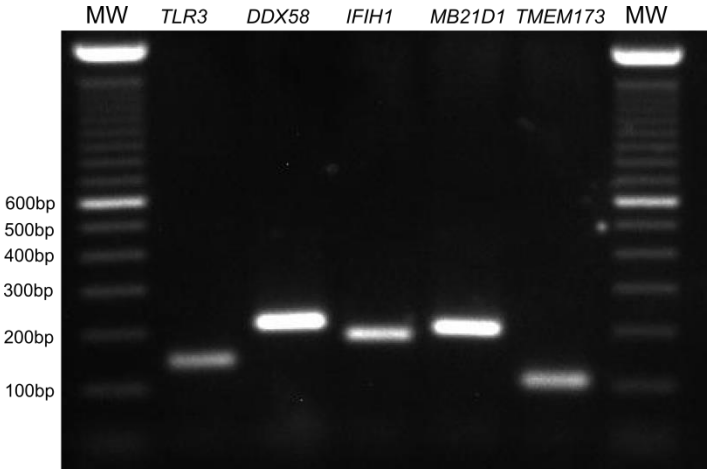


**Figure 5.4 Bovine endometrial stromal cells express several viral-sensing genes**
Total RNA was extracted from primary bovine endometrial stromal cells and first-strand cDNA reverse transcribed. qPCR was carried out using primer sets targeting *TLR3*, *IFIH1*, *DDX58*, *MB21D1* and *TMEM173*. 2% agarose gel electrophoresis allowed confirmation of expected amplicon size. *TLR3* set amplicon size= 143bp; *DDX58*= 219bp; *IFIH1*= 191bp; MB21D1= 207bp; TMEM173= 102bp. MW= DNA ladder indicating amplicon size on the gel.

### 5.3.3 Viral-sensing genes are differentially regulated by poly(I:C)

Expression of these genes in the poly(I:C)-stimulated samples was quantified. *TLR3*, *MB21D1*, *DDX58* and *IFIH1* are all upregulated by poly(I:C) (Figure 5.5), however the magnitude varies hugely between genes, with *TLR3* being upregulated 4.02±1.59 fold at 6 hours (adjusted p=0.0021) while *IFIH1* is upregulated 1502±1066 fold (adjusted p=0.0002) at the same time point.

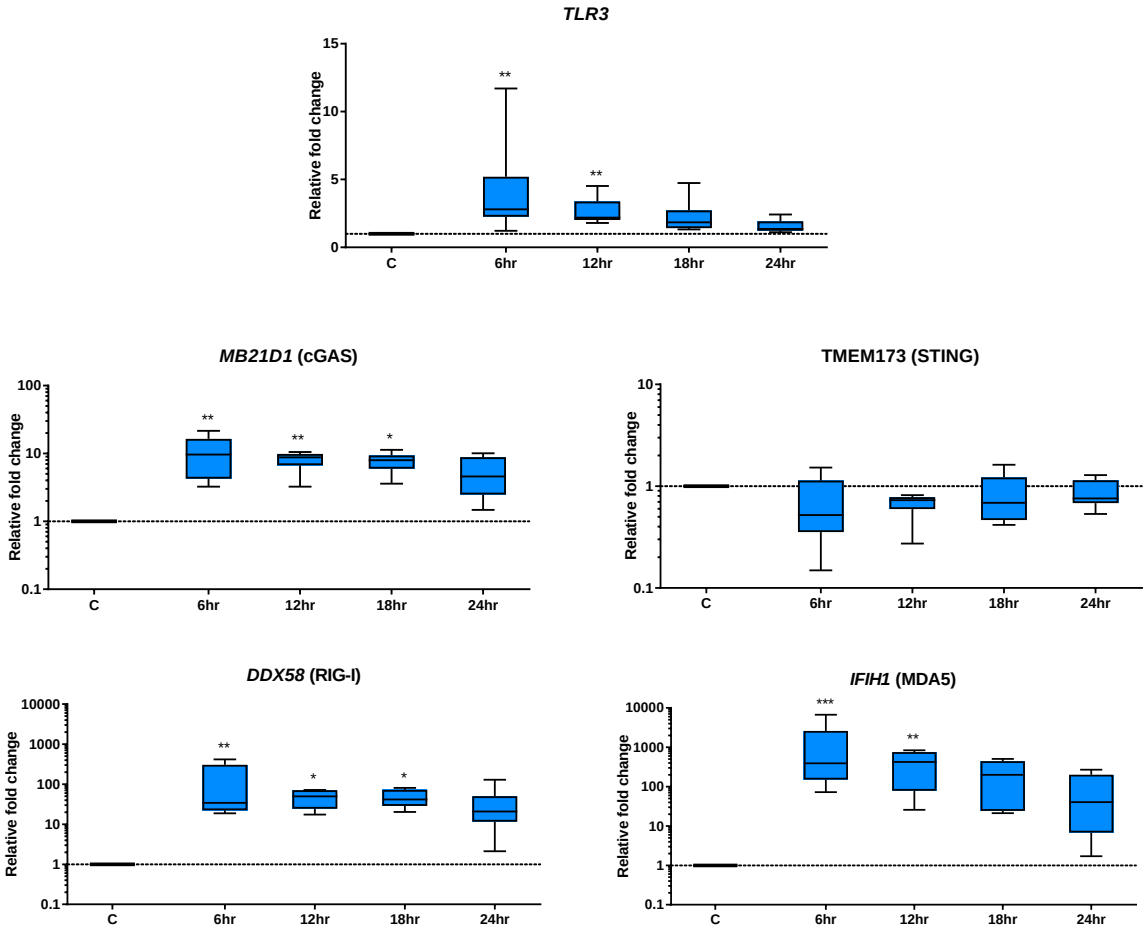


**Figure 5.5 Poly(I:C) differentially regulates viral-sensing genes**
$1x10^5$ /well primary bovine endometrial stromal cells were plated in 6-well plates and allowed to settle overnight. Cells were stimulated with 10µg/mL poly(I:C) and harvested in TRIzol after 6, 12, 18 or 24 hours. Total RNA was extracted and first-strand cDNA reverse transcribed. qPCR was carried out and gene-of-interest $C_q$ values normalised to the reference gene panel using the method described by Hellemans et al. (2007). Boxes indicate median, $25^{th}$ and $75^{th}$ percentile fold change in gene expression relative to the untreated control within the same time point; whiskers indicate minimum and maximum values. All values were normalised to the untreated control within the same time point, however only one control value is shown here for clarity. The horizontal dotted line indicates the y-value of the untreated control. Statistics were computed using Friedman's ANOVA followed by Dunn's post-hoc multiple comparison test, comparing the mean of each column to that of the untreated control. Asterisks indicate statistically-significant differences relative to the untreated control: *= adjusted $p<0.05$; **= adjusted $p<0.01$; ***=adjusted $p<0.001$. The cells isolated for this experiment were from Friesian cows; age range is 3-15 years; *n*=6.

### 5.3.4 *DEFB103* is upregulated by the dsDNA mimic poly(dA:dT)

Having demonstrated differential β-defensin expression in response to poly(I:C) and expression of the DNA-sensing pathway components cGAS and STING, the dsDNA mimic poly(dA:dT) was next used to stimulate endometrial stromal cells. Cells were isolated from two Charolais, one Charolais cross, one Friesian and two Limousin cows with an age range of 4-15 years. The cells were transfected with 50ng/mL, 100ng/mL or 500ng/mL Poly(I:C) for 6, 12, 18 or 24 hours. A treatment consisting of the transfection reagent Lipofectamine 2000 alone was also included (mock transfection).

dsDNA is capable of driving *IFNB1* expression in a TLR-independent manner (Ishii et al., 2006). *IFNB1* is upregulated by 500ng/mL poly(dA:dT) 1862±1038 fold at 24 hours (adjusted p=0.0011; Figure 5.6).

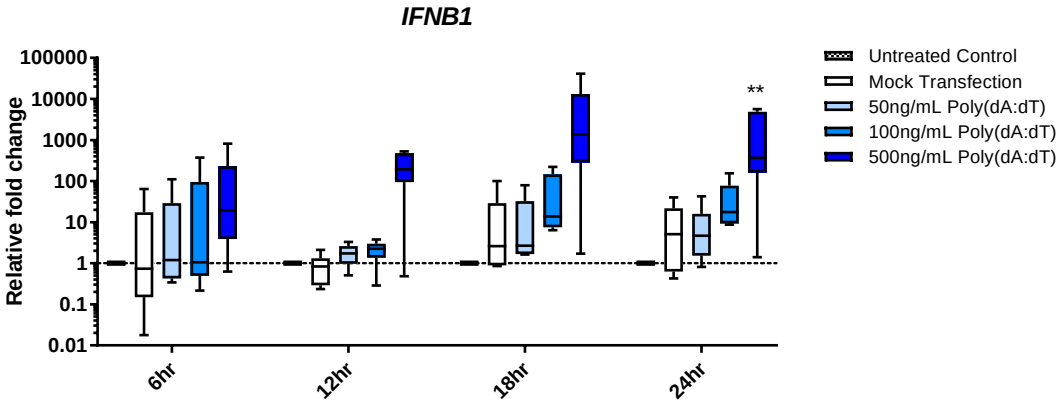


**Figure 5.6 Poly(dA:dT) significantly upregulates *IFNB1* expression**
$1x10^5$ /well primary bovine endometrial stromal cells were plated in 6-well plates and allowed to settle overnight. Cells were transfected with 50ng/mL, 100ng/mL or 500ng/mL poly(dA:dT) and harvested in TRIzol after 6, 12, 18 or 24 hours. A mock transfection consisting of Lipofectamine 2000 only was also included. Total RNA was extracted and first-strand cDNA reverse transcribed. qPCR was carried out and gene-of-interest $C_q$ values normalised to the reference gene panel using the method described by Hellemans et al. (2007). Boxes indicate median, 25$^{th}$ and 75$^{th}$ percentile fold change in gene expression relative to the untreated control; whiskers indicate minimum and maximum values. The horizontal dotted line indicates the y-value of the unstimulated control. All values were normalised to the untreated control within the same time point. Statistics were computed using a repeated measures two-way ANOVA followed by Dunnett's post-hoc multiple comparison test, comparing the mean fold change of each stimulation to the untreated control within the same time point. Asterisks indicate statistically-significant differences relative to the untreated control: **=adjusted p≤0.05. The cells used for this experiment were isolated from two Charolais, one Charolais cross, one Friesian and two Limousin cross cows; age range is 4-15 years; *n*=6.

*DEFB103* is also upregulated by 500ng/mL poly(dA:dT) at 18 and 24 hours, with a 5.30±1.65 fold change evident at 24 hours (adjusted p=0.0001) (Figure 5.7). e*DEFB4A* displays an opposing trend, though this is not statistically significant and the mock transfection also appears to be effecting gene expression to a similar extent at 18 and 24 hours.

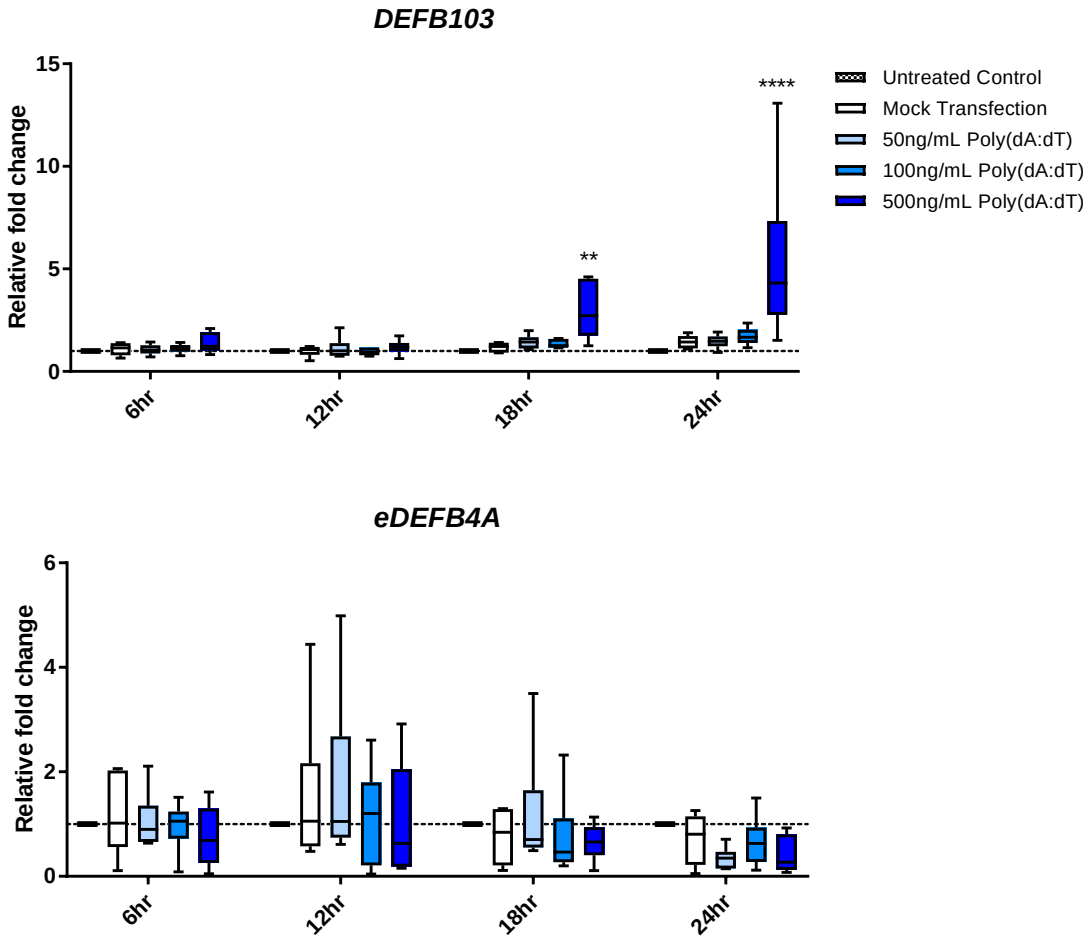


**Figure 5.7 Poly(dA:dT) significantly upregulates *DEFB103* expression**
$1x10^5$/well primary bovine endometrial stromal cells were plated in 6-well plates and allowed to settle overnight. Cells were transfected with 50ng/mL, 100ng/mL or 500ng/mL poly(dA:dT) and harvested in TRIzol after 6, 12, 18 or 24 hours. A mock transfection consisting of Lipofectamine 2000 only was also included. Total RNA was extracted and first-strand cDNA reverse transcribed. qPCR was carried out and gene-of-interest $C_q$ values normalised to the reference gene panel using the method described by Hellemans et al. (2007). Boxes indicate median, 25$^{th}$ and 75$^{th}$ percentile fold change in gene expression relative to the untreated control; whiskers indicate minimum and maximum values. The horizontal dotted line indicates the y-value of the unstimulated control. All values were normalised to the untreated control within the same time point. Statistics were computed using a repeated measures two-way ANOVA followed by Dunnett's post-hoc multiple comparison test, comparing the mean fold change of each stimulation to the untreated control within the same time point. Asterisks indicate statistically-significant differences relative to the untreated control: **=adjusted p≤0.05; ****=adjusted p<0.0001. The cells used for this experiment were isolated from two Charolais, one Charolais cross, one Friesian and two Limousin cross cows; age range is 4-15 years; *n*=6.

### 5.3.5 Viral-sensing genes are differentially regulated by poly(dA:dT)

Quantification of our panel of viral-sensing genes in cDNA samples from this experiment indicates the expression of several genes is increased in response to dsDNA stimulation (Figure 5.8). In contrast to poly(I:C) stimulation, poly(dA:dT) drives a gradual increase in expression across the time course that peaks at 24 hours. Again, the magnitude of this differential expression varies between genes, with *TLR3* being increased 3.11±0.77 fold (adjusted p=0.0001) after 24 hours of 100ng/mL poly(dA:dT) and *IFIH1* being increased 1209±381 fold after 24 hours of stimulation with 500ng/mL poly(dA:dT) (adjusted p=0.0006). *TMEM173* is not differentially regulated by poly(dA:dT).

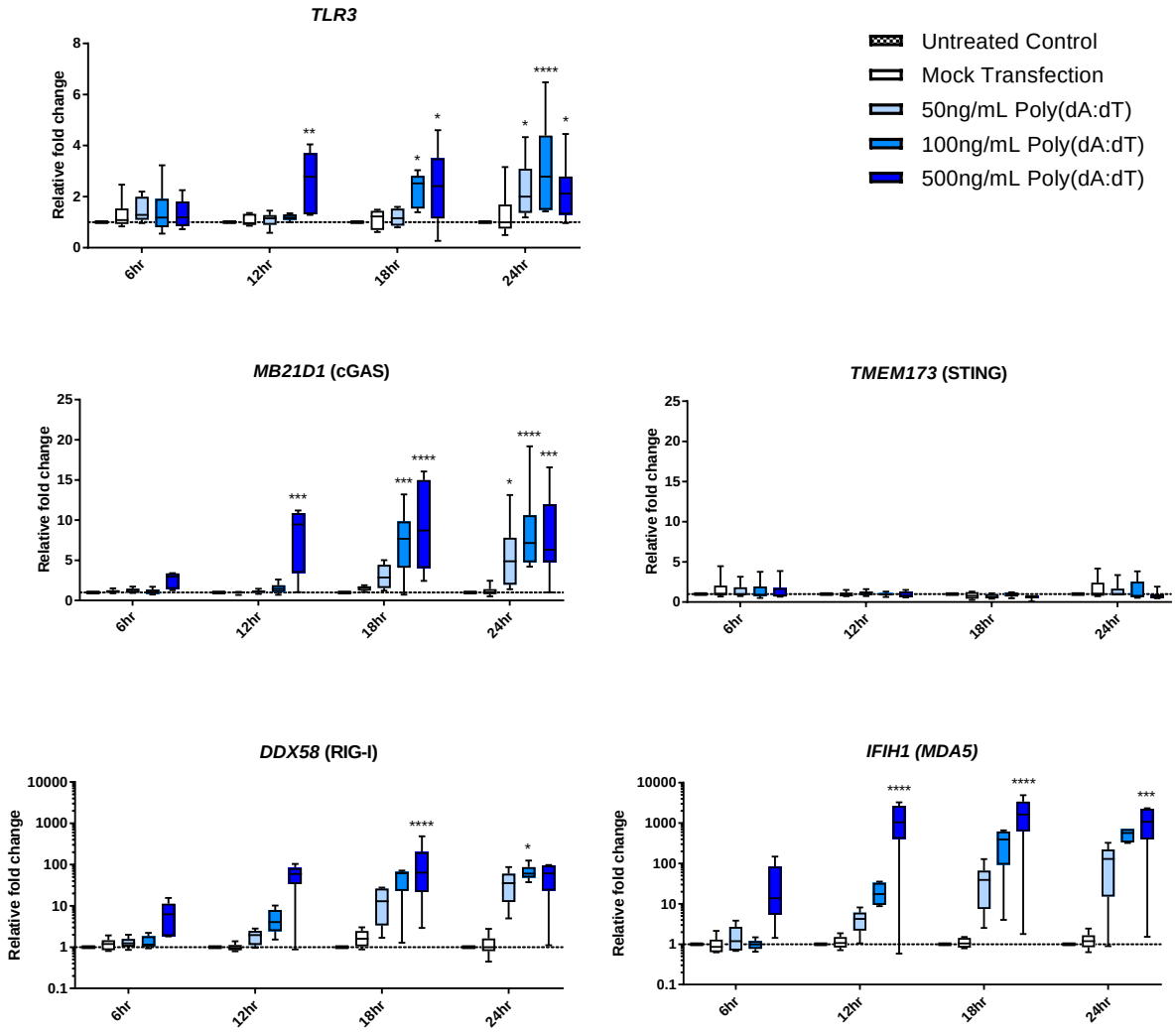


**Figure 5.8 Viral-sensing genes are upregulated by poly(dA:dT) stimulation**
$1x10^5$/well primary bovine endometrial stromal cells were plated in 6-well plates and allowed to settle overnight. Cells were transfected with 50ng/mL, 100ng/mL or 500ng/mL poly(dA:dT) and harvested in TRIzol after 6, 12, 18 or 24 hours. A mock transfection consisting of Lipofectamine 2000 only was also included. Total RNA was extracted and first-strand cDNA reverse transcribed. qPCR was carried out and gene-of-interest $C_q$ values normalised to the reference gene panel using the method described by Hellemans et al. (2007). Boxes indicate median, 25$^{th}$ and 75$^{th}$ percentile fold change in gene expression relative to the untreated control; whiskers indicate minimum and maximum values. The horizontal dotted line indicates the y-value of the unstimulated control. All values were normalised to the untreated control within the same time point. Statistics were computed using a repeated measures two-way ANOVA followed by Dunnett's post-hoc multiple comparison test, comparing the mean fold change of each stimulation to the untreated control within the same time point. Asterisks indicate statistically-significant differences relative to the untreated control: *=adjusted p≤0.05; **=adjusted p≤0.01; ***=adjusted p≤0.001; ****=adjusted p≤0.0001. The cells used for this experiment were isolated from two Charolais, one Charolais cross, one Friesian and two Limousin cross cows; age range is 4-15 years; *n*=6.

### 5.3.6 Expression of the expanded *DEFB4A* amplicon is upregulated by 1α,25-dihydroxyvitamin D3

To assess the impact of active vitamin D, 1,25-dihydroxyvitamin D3 (1,25D), stromal cells were isolated from 6 cows, with breeds including three Friesian, one Limousin and two Limousin cross cows; age range is 3-15 years. The cells were treated with 10nM or 100nM 1,25D for 6, 12, 18 or 24 hours. As ethanol had been used as the solvent, a vehicle control was included which consisted of the same volume of ethanol used in the 100nM treatment, resulting in a final ethanol concentration of 0.2%.

1,25D induces the expression of the enzyme which catabolises it- CYP24A1 (Lohnes and Jones, 1987). Quantification of *CYP24A1* in 1,25D-stimulated and unstimulated samples indicates that *CYP24A1* is not always expressed in unstimulated cells. Therefore the *CYP24A1* expression data presented in Figure 5.9 are shown as a proportion of the geometric mean of the reference gene panel since calculation of fold change relative to unstimulated control was impossible in some cases.

*CYP24A1* is induced by 100nM 1,25D at 18 and 24 hours (24 hour *CYP24A1* mean ratio to geometric mean of reference gene panel 0.13±0.12 in 100nM 1,25D versus 4.14±1.98 in unstimulated cells; adjusted p=0.0017).

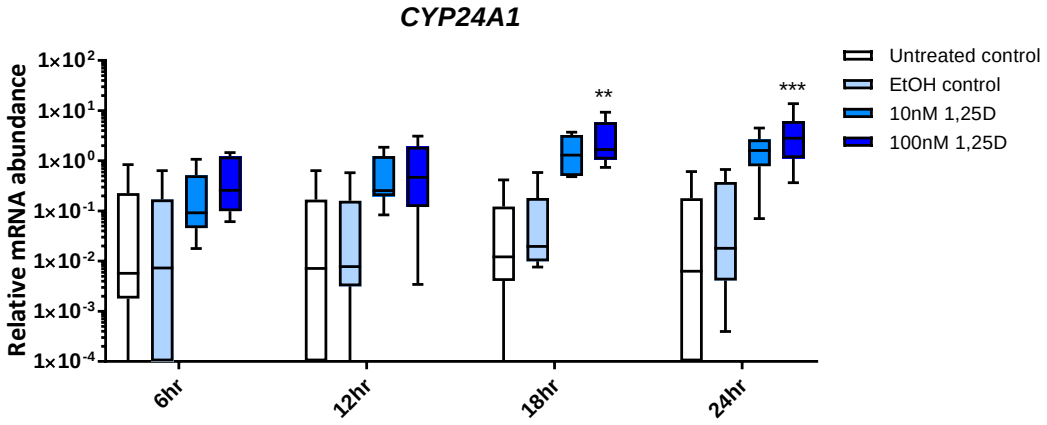


**Figure 5.9 1,25D upregulates *CYP24A1* expression**

$1x10^5$/well primary bovine endometrial stromal cells were plated in 6-well plates and allowed to settle overnight. Cells were treated with ethanol (vehicle control), 10nM or 100nM 1,25D and harvested in TRIzol after 6, 12, 18 or 24 hours. Total RNA was extracted, first-strand cDNA reverse transcribed, and *CYP24A1* transcription quantified via qPCR. Gene expression is plotted as proportional to the geometric mean of the reference gene panel. Boxes indicate median, 25$^{th}$ and 75$^{th}$ percentile fold change in gene expression relative to the untreated control; whiskers indicate minimum and maximum values. Statistics were computed using a repeated measures, two-way ANOVA with Dunnett's post-hoc comparison of each stimulated value to the unstimulated control value within the same time point. Asterisks indicate statistically-significant differences relative to the unstimulated control: **= adjusted $p \leq 0.01$. The cells used in this experiment were isolated from three Friesian, one Limousin and two Limousin cross cows; age range is 3-15 years; *n*=6.

*eDEFB4A* expression is increased by both concentrations of 1,25D (Figure 5.10 e*DEFB4A* expression is significantly upregulated by 1,25D. After 24 hours, 100nM 1,25D resulted in a mean 25.51±11.48 fold e*DEFB4A* induction (adjusted p=0.0005). *DEFB103* is not induced by 1,25D.

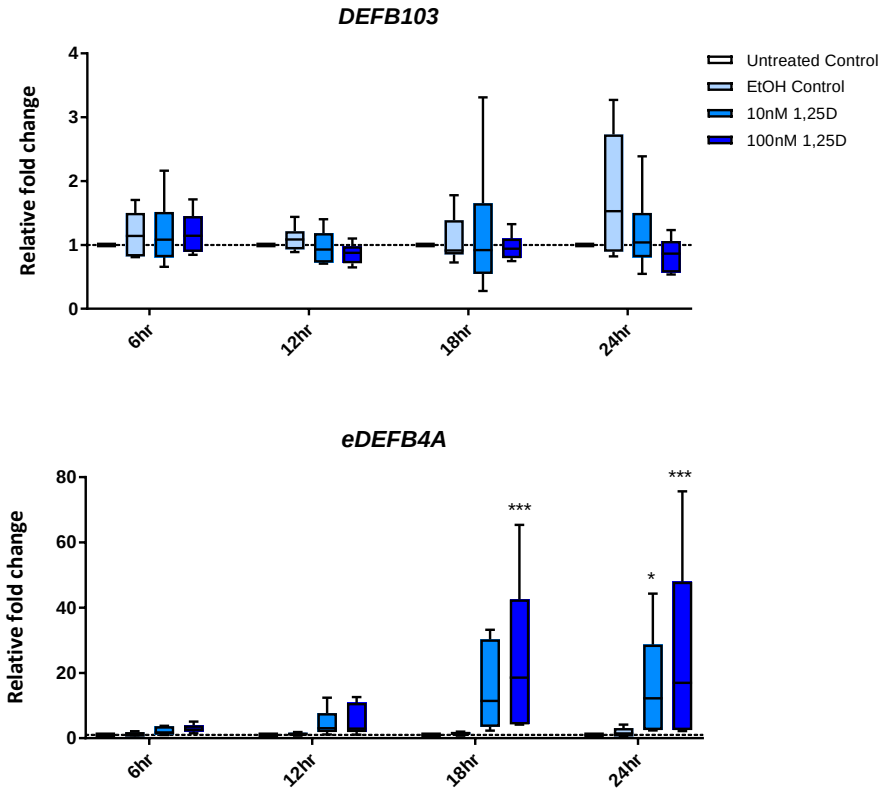


**Figure 5.10 e*DEFB4A* expression is significantly upregulated by 1,25D**
$1x10^5$/well primary bovine endometrial stromal cells were plated in 6-well plates and allowed to settle overnight. Cells were treated with ethanol (vehicle control), 10nM or 100nM 1,25D and harvested in TRIzol after 6, 12, 18 or 24 hours. Total RNA was extracted and first-strand cDNA reverse transcribed. qPCR was carried out and gene-of-interest $C_q$ values normalised to the reference gene panel using the method described by Hellemans et al. (2007). Boxes indicate median, 25$^{th}$ and 75$^{th}$ percentile fold change in gene expression relative to the untreated control; whiskers indicate minimum and maximum values. The horizontal dotted line indicates the y-value of the unstimulated control. All values were normalised to the untreated control within the same time point. Statistics were computed using a repeated measures two-way ANOVA followed by Dunnett's post-hoc multiple comparison test, comparing the mean fold change of each stimulation to the untreated control within the same time point. Asterisks indicate statistically-significant differences relative to the unstimulated control: *= adjusted p<0.05; ***= adjusted p< 0.001. The cells isolated for this experiment were from three Friesian, one Limousin and two Limousin cross cows; age range is 3-15 years; *n*=6.

### 5.3.7 1,25D modulates the β-defensin response to viral ligands

To examine whether the demonstrable ability of 1,25D to regulate β-defensin expression can modulate the response to nucleic acid stimulation, endometrial stromal cells from 6 animals were pre-treated with 100nM 1,25D or vehicle control for 12 hours, before the media was changed to include 10μg/mL untransfected poly(I:C) or 500ng/mL transfected poly(dA:dT), both with and without 1,25D or vehicle control. After 24 hours, the cells were harvested and β-defensin expression quantified. The cells were from three Friesian, one Limousin and two Limousin cross cows and the age range was 3-15 years.

*DEFB103* is slightly downregulated by 1,25D and upregulated by poly(I:C) (Figure 5.11). Unexpectedly, the two in combination increase *DEFB103* expression more than poly(I:C) alone (poly(I:C) mean fold change 1.77±0.34 versus 2.30±0.53). e*DEFB4A* expression is increased by 1,25D (mean fold change 53.54±16.24) and slightly decreased by poly(I:C) (mean fold change 1.96±1.585 relative to the unstimulated control value of 1). Addition of 1,25D to poly (I:C) reverses this trend and leads to a mean expression fold change of 31.24±12.76.

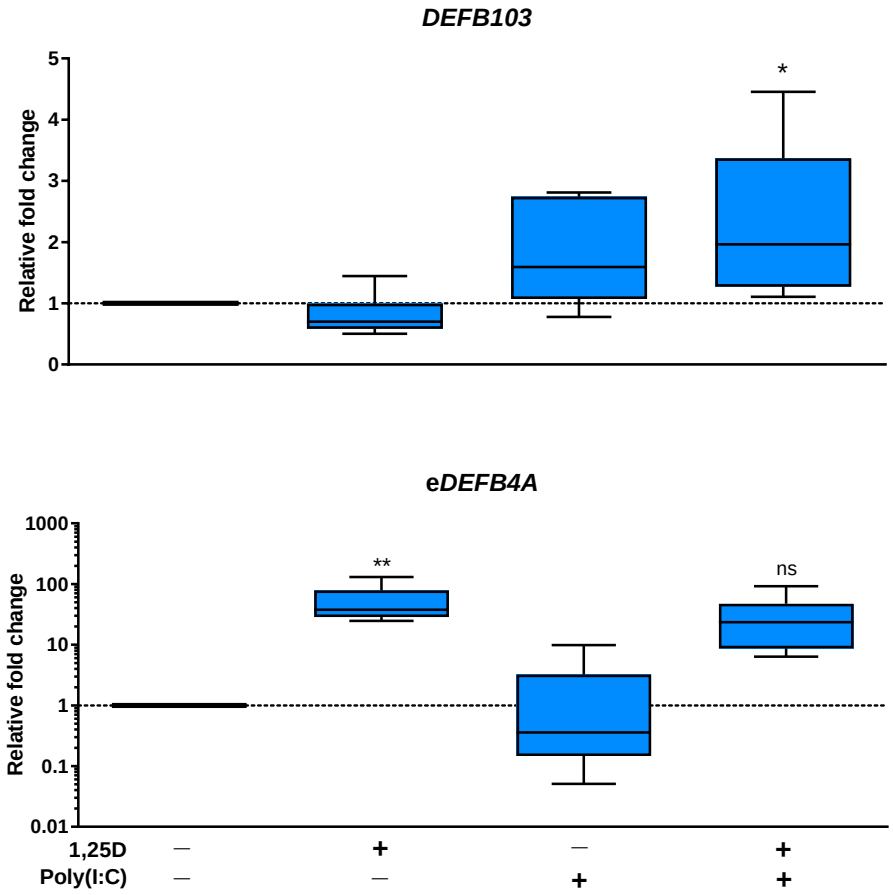


**Figure 5.11 1,25D reverses the poly(I:C)-mediated downregulation of e*DEFB4A***
$1x10^5$/well primary bovine endometrial stromal cells were plated in 6-well plates and allowed to settle overnight. Cells were treated with 100nM 1,25D or an equivalent volume of ethanol for 12 hours before adding fresh 1,25D, 10µg/mL untransfected poly(I:C), 500ng/mL poly(dA:dT) or a combination of 1,25D and viral ligand for 24 hours. Cells were harvested in TRIzol, total RNA was extracted and first-strand cDNA reverse transcribed. qPCR was carried out and gene-of-interest $C_q$ values normalised to the reference gene panel using the method described by Hellemans et al. (2007). Boxes indicate median, 25$^{th}$ and 75$^{th}$ percentile fold change in gene expression relative to the untreated control; whiskers indicate minimum and maximum values. The horizontal dotted line indicates the y-value of the unstimulated control. All values were normalised to the untreated control within the same time point, however only one control value is shown here for clarity. Statistics were computed using Friedman's ANOVA followed by Dunn's post-hoc multiple comparison test, comparing the mean of each column to that of the untreated control. Asterisks indicate statistically-significant differences relative to the control: *= adjusted $p \leq 0.05$, **= adjusted $p \leq 0.01$; ns= no significant difference. The cells isolated for this experiment were from three Friesian, one Limousin and two Limousin cross cows; age range is 3-15 years; *n*=6.

Poly(dA:dT) alone increases *DEFB103* expression 3.36±0.44 fold (adjusted p=0.0110). Inclusion of 1,25D reduces this to 2.15±0.29 fold (adjusted p=0.3526). Poly(dA:dT) has the opposite effect on e*DEFB4A*: poly(dA:dT) alone induces a mean 0.99±0.27 fold change which is increased to 23.54±16.24 when 1,25D is included (Figure 5.12).

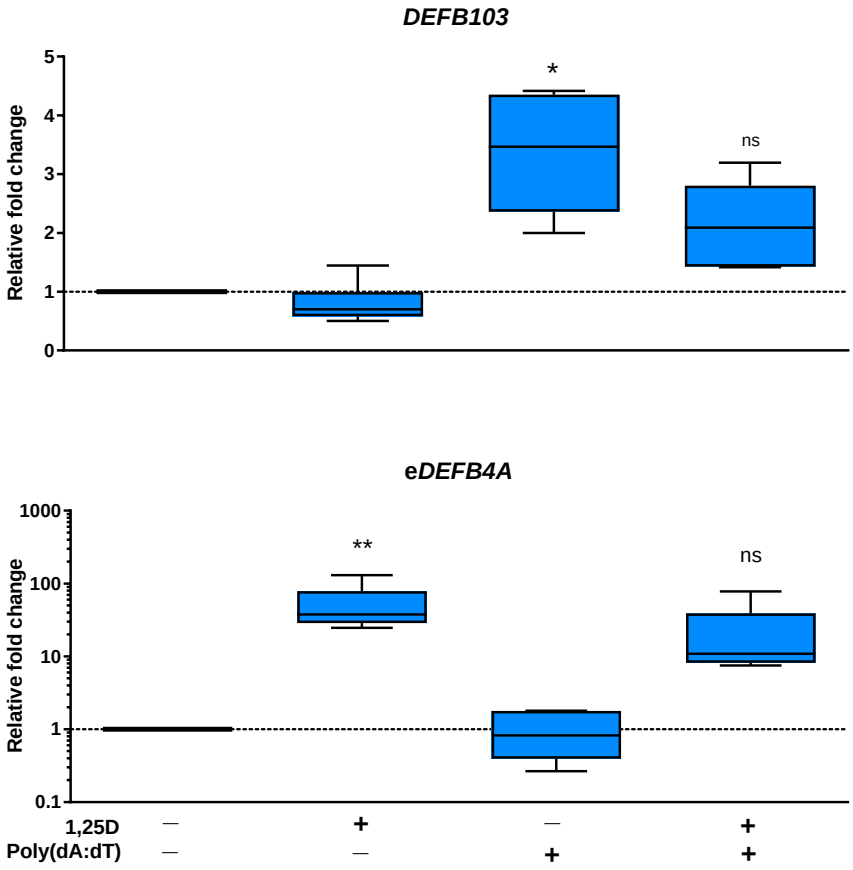


**Figure 5.12 1,25D reduces the poly(dA:dT)-mediated upregulation of *DEFB103***
1x10$^5$/well primary bovine endometrial stromal cells were plated in 6-well plates and allowed to settle overnight. Cells were treated with 100nM 1,25D or an equivalent volume of ethanol for 12 hours before adding fresh 1,25D, 10µg/mL untransfected poly(I:C), 500ng/mL poly(dA:dT) or a combination of 1,25D and viral ligand for 24 hours. Cells were harvested in TRIzol, total RNA was extracted and first-strand cDNA reverse transcribed. qPCR was carried out and gene-of-interest $C_q$ values normalised to the reference gene panel using the method described by Hellemans et al. (2007). Boxes indicate median, 25$^{th}$ and 75$^{th}$ percentile fold change in gene expression relative to the untreated control; whiskers indicate minimum and maximum values. The horizontal dotted line indicates the y-value of the unstimulated control. All values were normalised to the untreated control within the same time point, however only one control value is shown here for clarity. Statistics were computed using Friedman's ANOVA followed by Dunn's post-hoc multiple comparison test, comparing the mean of each column to that of the untreated control. Asterisks indicate statistically-significant differences relative to the control: *= adjusted p<0.05, **= adjusted p<0.01; ns= no significant difference. The cells isolated for this experiment were from three Friesian, one Limousin and two Limousin cross cows; age range is 3-15 years; *n*=6.

### 5.3.8 Delivery of poly(I:C) via transfection boosts poly(I:C)-mediated *DEFB103* expression

Bovine β-defensins have been shown here to be regulated by both dsRNA and dsDNA, with this being modulated by 1,25D. However, dsDNA viruses also generate significant quantities of dsRNA within infected cells (Weber et al., 2006). In addition, poly(dA:dT) is reverse transcribed by RNA polymerase III to a dsRNA intermediate which is subsequently detected via RIG-I (Ablasser et al., 2009). Therefore, the dsRNA-mediated regulation of β-defensins was examined in more detail. Poly(I:C) is sensed differently depending on how it is delivered to the cell. Addition of poly(I:C) to the medium, as already performed, drives cytokine production in a TLR3-mediated manner (Alexopoulou et al., 2001; Gitlin et al., 2006). In contrast, delivery via transfection to promote cellular uptake leads to a cytosolic receptor-mediated response in which TLR3 is non-essential (Gitlin et al., 2006). Having shown that intracellular nucleic acid sensors are expressed in endometrial stromal cells, the cells were next stimulated with varying quantities of both transfected and untransfected poly(I:C). The transfection reagent Lipofectamine 2000 was also applied alone (mock transfection). The cells used here were all isolated from Friesian cows and the age range was 3-9 years ($n$=3).

*IFNB1* expression in response to poly(I:C) is highly dependent on delivery method. While gene expression in response to untransfected poly(I:C) is downregulated or in some cases mildly upregulated, transfection clearly upregulates expression, though a large degree of inter-animal variation is evident (Figure 5.13).

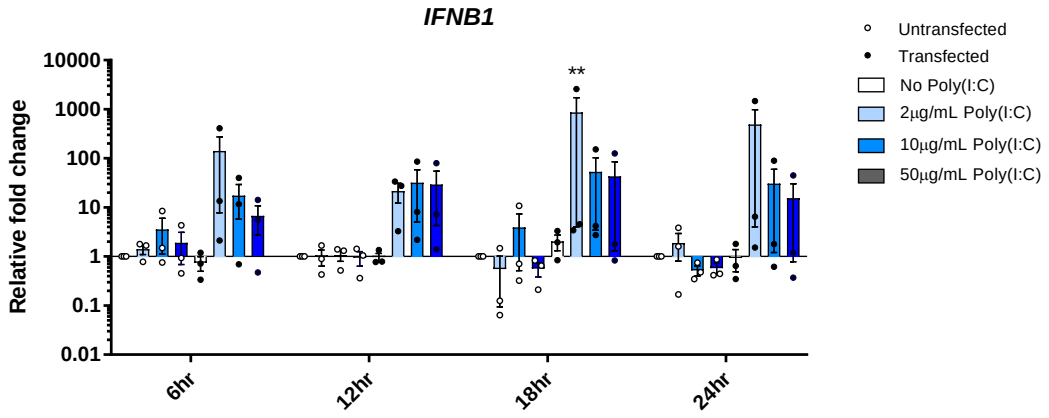


**Figure 5.13 Transfection of poly(I:C) potentiates *IFNB1* induction**
$1x10^5$/well primary bovine endometrial stromal cells were plated in 6-well plates and allowed to settle overnight. Cells were treated with 2μg/mL, 10μg/mL or 50μg/mL poly(I:C), both with and without transfection using Lipofectamine 2000, and harvested in TRIzol after 6, 12, 18 or 24 hours. A mock transfection consisting of Lipofectamine 2000 only was also included. Total RNA was extracted and first-strand cDNA reverse transcribed. qPCR was carried out and gene-of-interest $C_q$ values normalised to the reference gene panel using the method described by Hellemans et al. (2007). Columns and error bars indicate mean fold change and SEM respectively. Points above the y=1 horizontal line indicated upregulation relative to the unstimulated control; those below downregulation. Statistics were computed using a repeated measures two-way ANOVA with Dunnett's post-hoc comparison of each stimulated value to the unstimulated control value within the same time point. Asterisks indicate statistically-significant differences relative to the control: **= adjusted $p<0.01$. The cells isolated for this experiment were from three Friesian cows; age range is 3-9 years; *n*=3.

Upregulation of *DEFB103* in response to poly(I:C) is enhanced via transfection. At 24 hours, 2μg/mL of poly(I:C) generates a mean fold change of 11.39±4.58 when transfected, versus 1.34±0.53 when delivered without transfection (Figure 5.14). The effect on e*DEFB4A* is less clear. At 6 hours, all treatments generate a slight upregulation (<2 fold change). However, by 24 hours, all treatments lead to a downregulation in gene expression.

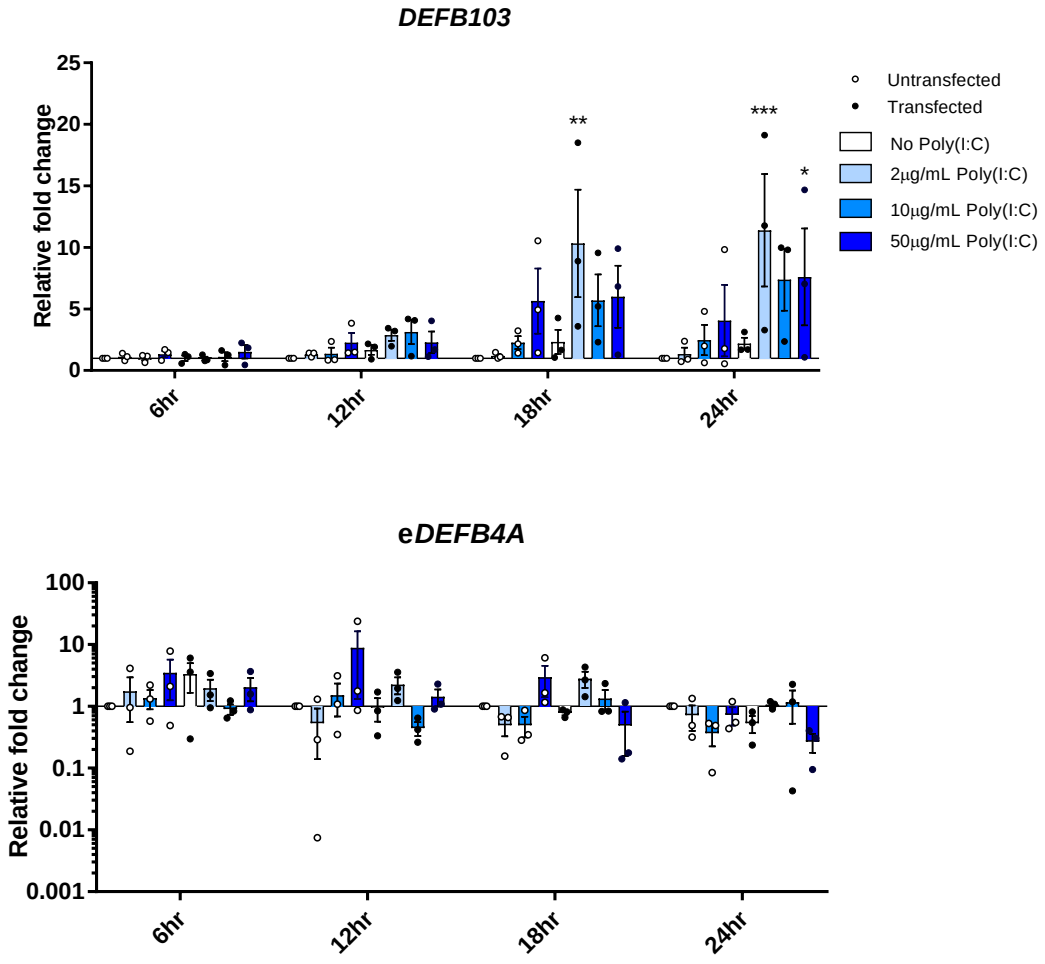


**Figure 5.14 Transfection of poly(I:C) potentiates *DEFB103* induction**
1x10$^5$/well primary bovine endometrial stromal cells were plated in 6-well plates and allowed to settle overnight. Cells were treated with 2μg/mL, 10μg/mL or 50μg/mL poly(I:C), both with and without transfection using Lipofectamine 2000, and harvested in TRIzol after 6, 12, 18 or 24 hours. A mock transfection consisting of Lipofectamine 2000 only was also included. Total RNA was extracted and first-strand cDNA reverse transcribed. qPCR was carried out and gene-of-interest $C_q$ values normalised to the reference gene panel using the method described by Hellemans et al. (2007). Columns and error bars indicate mean fold change and SEM respectively. Points above the y=1 horizontal line indicated upregulation relative to the unstimulated control; those below downregulation. Statistics were computed using a repeated measures two-way ANOVA with Dunnett's post-hoc comparison of each stimulated value to the unstimulated control value within the same time point. Asterisks indicate statistically-significant differences relative to the control: **= adjusted p<0.01; ***=adjusted p<0.001. The cells isolated for this experiment were from three Friesian cows; age range is 3-9 years; *n*=3.

Quantification of nucleic acid-sensing gene expression indicates *TLR3* and *MB21D1* are induced by poly(I:C), though this is unaffected by delivery method (Figure 5.15). *TMEM173* is induced in a single animal at 12 hours, but is otherwise downregulated. At 24 hours, transfection has a more pronounced effect (2μg/mL untransfected mean fold change 0.95±0.19 versus 0.31±0.07 transfected). *DDX58* and *IFIH1* are more strongly upregulated via transfection. At 12 hours, 2μg/mL poly(I:C) drives a 117.30±98.57 fold change in *DDX58* expression when untransfected, compared to a 153.80±92.87 fold change when transfected. *IFIH1* is upregulated 735.40±492.90 fold when poly(I:C) is delivered naked, while a 6315±3505 fold induction is observed when the transfection method of delivery is used.

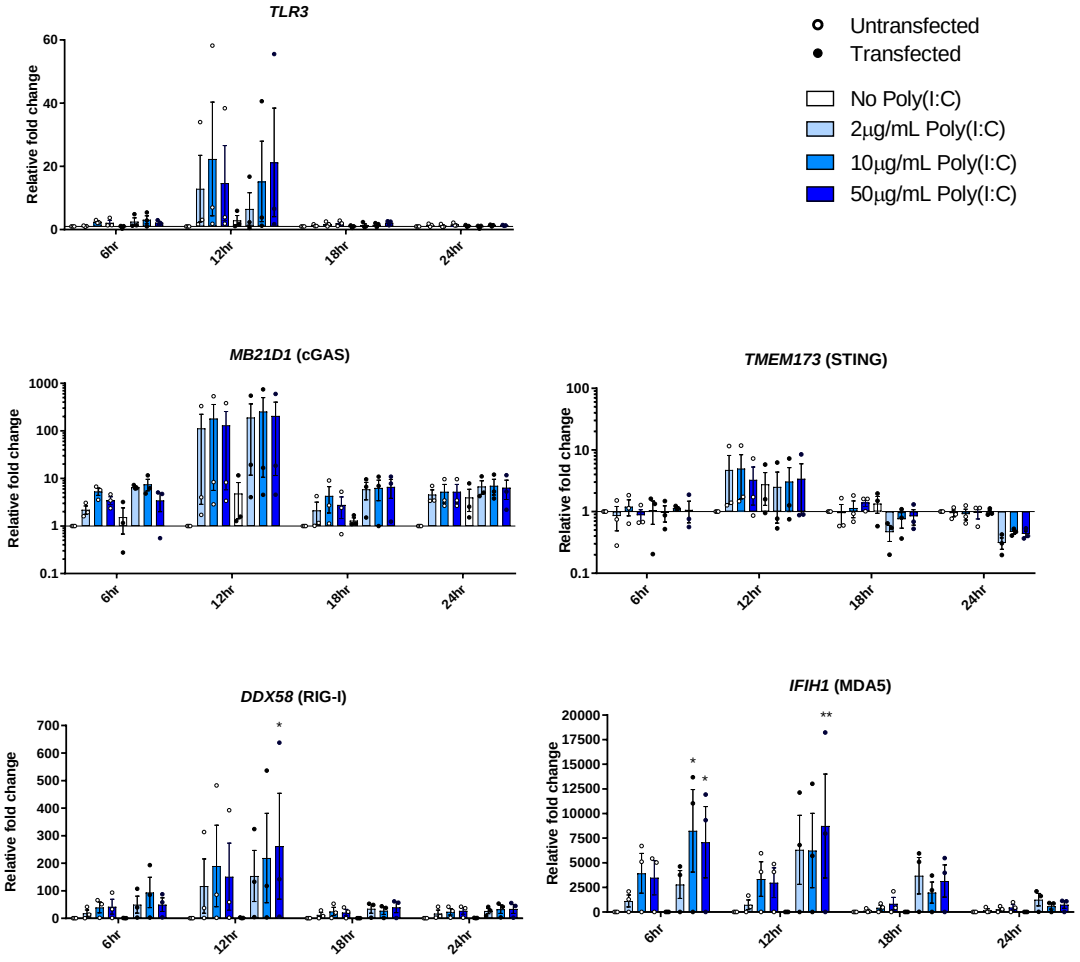


**Figure 5.15 Transfection of poly(I:C) potentiates induction of the dsRNA receptor-encoding gene IFIH1**

$1x10^5$/well primary bovine endometrial stromal cells were plated in 6-well plates and allowed to settle overnight. Cells were treated with 2μg/mL, 10μg/mL or 50μg/mL poly(I:C), both with and without transfection using Lipofectamine 2000, and harvested in TRIzol after 6, 12, 18 or 24 hours. A mock transfection consisting of Lipofectamine 2000 only was also included. Total RNA was extracted and first-strand cDNA reverse transcribed. qPCR was carried out and gene-of-interest $C_q$ values normalised to the reference gene panel using the method described by Hellemans et al. (2007). Columns and error bars indicate mean fold change and SEM respectively. Points above the y=1 horizontal line indicated upregulation relative to the unstimulated control; those below downregulation. Statistics were computed using a repeated measures two-way ANOVA with Dunnett's post-hoc comparison of each stimulated value to the unstimulated control value within the same time point. Asterisks indicate statistically-significant differences relative to the control: **= adjusted $p<0.01$. The cells isolated for this experiment were from three Friesian cows; age range is 3-9 years; *n*=3.

The results of this experiment are summarised in Table 5.1. *DEFB103*, *DDX58* and *IFIH1* are all upregulated by poly(I:C) stimulation, and increasingly so when the poly(I:C) is delivered by transfection. e*DEFB4A* and *TMEM173* are downregulated, while poly(I:C) has opposing effects on *IFNB1* depending on how it is delivered.

**Table 5.1 Summary of results of poly(I:C) stimulation**

| **Gene** | ***DEFB103*** | ***DDX58*** | ***IFIH1*** | ***eDEFB4A*** | ***IFNB1*** | ***TMEM173*** | ***TLR3*** | ***MB21D1*** |
|---|---|---|---|---|---|---|---|---|
| **Up/Down-regulated** | Up | Up | Up | Up/Down | Up/Down | Down | Up | Up |
| **Affected by delivery method** | Yes | Yes | Yes | No | Yes | Yes | No | No |

## 5.4 Discussion

Here we show that endometrial stromal cells express cytosolic sensors for both RNA and DNA viruses and respond to both RNA and DNA stimulation by upregulating β-defensin expression. Addition of poly(I:C) to the culture medium targets it to endosomal TLR3 (Alexopoulou et al., 2001). *IFNB1* is not upregulated under these conditions, and is actually slightly downregulated in expression, with the trend being most pronounced at 18 hours. The same quantity of untransfected poly(I:C) used here upregulates *IFNB1* 150-fold in oviductal epithelial cells (Ghosh et al., 2008), however monocyte-derived macrophages require transfection of poly(I:C) to drive IFN-β production (Reimer et al., 2008). Thus, the mechanisms that drive *IFNB1* expression differ between cells types, with TLR3 activity being likely insufficient in these cells.

The cells have responded to poly(I:C) stimulation with early and significant differential regulation of several nucleic acid-sensing genes. The genes encoding MDA5 (Kang et al., 2003), RIG-I (Wang et al., 2008), cGAS (Ma et al., 2015a) and STING (Ma et al., 2015b) are all regulated by type I interferon. The type I interferons most important in the antiviral response are IFN-α, which has multiple subtypes, and IFN-β; originally named leukocyte and fibroblast interferon respectively (Pestka et al., 2004). Type I interferons bind the type I interferon receptor, composed of interferon-α/β receptor (IFNAR)1 and IFNAR2 subunits (Hervas-Stubbs et al., 2011). Therefore, IFNAR knockdown has been used to demonstrate the necessity for type I interferon in driving expression of these genes in leukocytes.

Thus, the finding that these viral sensing genes are upregulated in the absence of upregulation of interferon is somewhat surprising. The IFN-β gene rather than the IFN-α gene was quantified here because several studies have shown that IFN-α production is secondary to IFN-β. Mice with an additional *IFNB1* gene increase IFN-α production also (Asano et al., 1990). Murine fibroblasts in which *IFNB1* has been knocked down produce neither IFN-α nor IFN-β (Erlandsson et al., 1998). However, exogenous IFN-β restores IFN-α production, while leukocytes from the same knockout mice do not require IFN-β to produce IFN-α. IFN-β production is regulated at the post-transcriptional level, with "super-induction" resulting from mRNA stabilisation after cell stimulation (Khabar and

Young, 2007). If this mechanism were occurring here, it should be detectable by qPCR. Quantification of protein level via ELISA would determine whether interferon protein production is increased. Blocking IFNAR signalling would indicate whether type I interferon is driving the differential expression of the viral-sensing genes observed here.

The inability to design a primer set targeting only the *IFI16* gene may be due to the similarity of other PYHIN family genes, pseudogenised or otherwise. The imminent release of a new draft of the bovine genome (expected 2017) will help clarify the structural variation that may exist in the bovine PYHIN gene family.

Though few studies have profiled β-defensin expression in response to poly(I:C), those results differ from the pattern observed here. 1-10μg/mL poly(I:C) added to the culture medium without transfection upregulates *DEFB4A* in epithelial cells of the human oviduct (Ghosh et al., 2008), endometrium (Schaefer et al., 2005) and colon (Morampudi et al., 2011; Omagari et al., 2011). In contrast, the amplicon representing the ruminant *DEFB4A* gene expansion is significantly downregulated, though the fold change is modest. Until an antibody is available to quantify protein levels, it is difficult to speculate whether this change in transcription would have implications for the antiviral response of the cell.

Only one study has quantified *DEFB103* expression in response to poly(I:C); finding no change in expression in human colonic epithelium (Morampudi et al., 2011). Repetition of this experiment in bovine endometrial epithelial cells would help determine whether these differences are species- or cell type-driven.

The contribution of TLR3 to β-defensin regulation in this experiment could be verified by using chloroquine to block endosomal acidification and therefore activation of TLRs which function in endosomes (Lundberg et al., 2007). TLR3 is known to activate the AP-1 complex, with this being the dominant pathway inducing cytokine expression in *Chlamydia pneumoniae*-infected endothelial cells and monocytes (Wang et al., 2013a). Japanese encephalitis virus infection of murine microglia also activates AP-1 as well as NF-κB, through both TLR3 and RIG-I signalling. Therefore, the upregulation of *DEFB103* by poly(I:C) under conditions that favour TLR3 activation is consistent with our prediction of AP-1 as being the main transcription factor regulating *DEFB103* expression. Various components of the MAPK, IRF and NF-κB signalling pathways can

be inhibited with commercially available reagents. AP-1 can also be directly inhibited with the retinoid SR11302 (Fanjul et al., 1994).

Endometrial stromal cells are capable of sensing poly(dA:dT). This dsDNA mimic is sensed by cGAS and IFI16, which both activate STING, while RIG-I senses the 5'-triphosphate RNA intermediate transcribed from poly(dA:dT) by RNA Pol III, with each pathway inducing type I interferon (Ablasser et al., 2009; Ma et al., 2015a; Thompson et al., 2014). Poly(dA:dT) induction of these viral-sensing genes peaks at 24 hours, as does *IFNB1* expression. This suggests that IFN-β is inducing these genes. However, *TMEM173* is not induced by poly(dA:dT), despite type I interferon being the key driver of expression in murine macrophages (Ma et al., 2015b).

The upregulation of *DEFB103* may be direct or indirect. Poly(dA:dT) stimulation of human melanocytes activates MAPK JNK and NF-κB p65 to induce IL-6, IL-8 and TNF-α, while MAPK p38 also takes part in IL-6 and IL-8 induction (Wang et al., 2015). In addition, this study indicates RIG-I is the main poly(dA:dT) sensor in this cell type. STING signalling in response to poly(dA:dT) also activates MAPK pathway components JNK and p38 in a TBK1-independent manner (Abe and Barber, 2014), with feline STING known to activate AP-1 (Zhang et al., 2016). However, IFI16 can also signal independently of STING to activate NF-κB through downregulation of IκBα expression (Caposio et al., 2007). Therefore, there is ample evidence to indicate that poly(dA:dT) could induce *DEFB103* via AP-1.

Alternatively, this *DEFB103* induction may be indirect via IFN-β. In human lung epithelium, IFN-α upregulates *DEFB103* expression, though the authors did not investigate if this was direct or indirect (Basu et al., 2010). While the JAK-STAT pathway is the classical mode of IFNAR signalling, this receptor is known to activate a wider suite of intracellular signalling components (Hervas-Stubbs et al., 2011). The MAPK p38 pathway, and to a lesser extent the MEK-ERK and JNK pathways are also involved in some cases. García et al., (2001) predicted a STAT1 site in the *DEFB103* promoter, but did not investigate whether it was functional. Our *in silico* analysis did not identify STAT or GAS sites as being enriched in the promoters of *DEFB103* orthologs. Thus, stimulation of stromal cells with IFN-β would confirm whether it can directly regulate *DEFB103* independently of nucleic acids/viruses or an intermediate cytokine.

This body of work extends our understanding of the immune function of bovine endometrial stromal cells, with previous studies focusing on bacterial stimulation. As dsDNA alone can induce β-defensin and DNA sensor expression, the lack of immune gene induction within stromal cells following BoHV-4 infection (Tebaldi et al., 2016) suggests this virus can evade the immune system. With a multitude of antiviral properties ascribed to β-defensins, understanding how to boost expression could provoke viral clearance and attenuate BoHV-4-driven inflammation.

Provision of vitamin D may be one such mechanism. e*DEFB4A* is upregulated here by 1,25D, though with a high degree of inter-animal variation. This is in agreement with the human literature, which indicates *DEFB4A* is upregulated by 1,25D in the majority of cell types examined. *DEFB103* is not upregulated here and is in fact slightly downregulated. It is more difficult to compare this result to the human literature, as only three studies have quantified *DEFB103* expression after 1,25D stimulation, with each paper looking at a different cell type and only two out of the three reporting upregulation.

Direct vitamin D induction of the antimicrobial peptide cathelicidin is primate specific (Gombart, 2009). With 1,25 induction of bovine e*DEFB4A* known to be secondary in monocytes (Merriman et al., 2015) and with VDR binding sites not enriched in *DEFB103* promoter orthologs, it is possible that direct vitamin D regulation of β-defensins is also species-specific. Cyclohexamide-blocking of mRNA translation would be needed to identify whether the e*DEFB4A* induction observed here is primary or secondary.

It is difficult to speculate on what intermediate factor might be driving e*DEFB4A* here, given that the human literature mostly reports downregulation of cytokine expression. Profiling of the particular cytokine response following 1,25 stimulation of these cells will be necessary to identify a potential intermediate, if indeed β-defensins are secondarily regulated.

As vitamin D is capable of ameliorating both infection and inflammation in the mammary gland (Lippolis et al., 2011), this first preliminary demonstration of vitamin D as a potential immunomodulator in the uterus is interesting. With systemic inflammation within the post-partum cow potentially exacerbating local uterine inflammation, the concept of simultaneously boosting antimicrobial responses while dampening cytokine

expression is enticing. 25D, but not 1,25D, improves mastitis symptoms when injected into the mammary gland (Merriman et al., 2017). Therefore, assessing the ability of endometrial cells to produce *CYP27B1* and convert 25D to active 1,25D will be necessary to identify whether local 25D delivery into the uterus is a viable therapeutic option.

Having demonstrated that vitamin D and nucleic acids have opposing effects on β-defensin expression, application of both factors in combination indicates 1,25D can modulate the effects of poly(I:C) and poly(dA:dT) on β-defensin expression. Quantification of *DEFB103* mRNA in an additional 6 animals reveals the same modest trend towards downregulation. EGFR, which can directly induce *DEFB103* in human keratinocytes (Sørensen et al., 2005), can be downregulated by 1,25D. This has been demonstrated in breast cancer (McGaffin et al., 2004) and ovarian cancer (Shen et al., 2011) cell lines, with the latter study identifying an active intronic VDRE in the *EGFR* gene. Therefore, this is a potential mechanism by which 1,25D can downregulate *DEFB103*.

TLR3 signalling upregulates the EGFR ligands TGF-α and amphiregulin (Zhu et al., 2009), with activated EGFR binding TLR3 and recruiting the protein tyrosine kinase Src, so that both can then tyrosine phosphorylate the adaptor protein TRIF (Yamashita et al., 2012). Attenuation of TLR3 activity through downregulation of *EGFR* may explain the ability of 1,25D to reverse the poly(I:C)-mediated effect on e*DEFB4A* expression.

The effect of 1,25D on DNA sensor expression or activity is unknown. Elucidation of the signalling pathways or intermediate cytokines driving β-defensin expression will be necessary in order to identify the best way to use vitamin D to modulate the endometrial immune response. Indeed, understanding the function of β-defensins themselves and whether they are contributing to or alleviating post-partum pathology within the endometrium will be essential.

Comparison of gene induction patterns after stimulation with transfected and untransfected poly(I:C) indicates transfection potentiates induction of some, but not all of the genes studied. *IFIH1* expression peaks at 12 hours, with *IFNB1* and *DEFB103* being upregulated from 18 hours on. Both *DEFB103* and *IFNB1* are maximally stimulated by 2μg/mL transfected poly(I:C) for 18 hours. *IFNB1* is more highly induced in some cell types when poly(I:C) is transfected (Reimer et al., 2008), as the cytoplasmic

sensors RIG-I and MDA5 regulate *IFNB1* expression (Yoneyama et al., 2005). Both receptors are themselves IFN-β inducible (Kang et al., 2003; Wang et al., 2008), though here there is only a slight increase in RIG-I gene expression when poly(I:C) is transfected and *IFNB1* is upregulated. The pattern observed here suggests *DEFB103* may similarly be regulated by RIG-I/MDA5 signalling, or may be driven by type 1 interferon itself.

A number of mechanisms may explain the pattern of *DEFB103* induction seen here. Transfection-mediated delivery of poly(I:C) to the cytoplasm preferentially targets RIG-I and MDA5. Kato et al., (2006) have shown that different sensors induce different cytokines in response to poly(I:C), with MDA5 driving IFN-α production, while TLR3 signalling regulates IL-12. Thus, signalling from cytoplasmic dsRNA sensors may be a more potent inducer of *DEFB103* expression than TLR3 signalling. As *IFIH1* is similarly upregulated, MDA5 is likely the more important cytoplasmic sensor here, indeed Kato et al., (2006) have reported that MDA5 is more important than RIG-I in sensing poly(I:C). A preference for cytoplasmic signalling might be stromal cell-specific, with murine fibroblasts using RIG-I rather than TLR3 to sense RNA viruses, though murine pDCs use TLR3 (Kato et al., 2005). This may be due to the fact that TLR3 will sense dsRNA taken up into endosomes from outside the cell, while in infected cells, viral replication means dsRNA will be found in the cytoplasm. Both RIG-I and MDA5 bind to the adaptor mitochondrion-associated antiviral signalling protein (MAVS) (Figure 5.1). MAVS activates a variety of tumour necrosis factor receptor-associated factor (TRAF) family members, which in turn determine whether IRF, NF-κB or AP-1 pathways are activated (Xie, 2013). MAVS can also activate MAPK signalling in response to viral infection independently of either RIG-I or MDA5 (Huang et al., 2014). Therefore, RLR-mediated signalling may induce *DEFB103* expression via the JDP2/AP-1 site as we have predicted.

Inhibition of STAT and MAPK pathway components would identify which pathways are involved. Given that *DEFB103* can be induced by poly(I:C) without transfection, albeit to a lesser extent, it is likely that several pathways contribute to nucleic acid-induced *DEFB103* induction.

The expression pattern observed for *TMEM173* and e*DEFB4A* is less clear. At 12 hours, TMEM173 expression is lightly upregulated, though this trend is driven by the response of one animal. By 24 hours, both *TMEM173* and e*DEFB4A* are downregulated

by transfected poly(I:C). STING is not involved in poly(I:C)-mediated signalling (Ishikawa and Barber, 2008). This would suggest that any link between *TMEM173* and e*DEFB4A* is due to them being regulated by the same induced cytokine. However, IFN-α generated by both poly(I:C) and poly(dA:dT) induces *TMEM173* in murine bone marrow-derived macrophages (Ma et al., 2015b), so the expression pattern observed here is unexpected. *DEFB4A* expression in response to type I interferon has not been shown. These results indicate that it is not responsive. Expression of the cGAS-encoding gene *MB21D1* is also not increased by transfection and *IFNB1* induction, suggesting an alternative mechanism is inducing cGAS in these cells.

Identification of the mechanisms driving viral induction of β-defensins has lagged behind testing of their antiviral functions, with neither having been investigated in the bovine. These results open up a variety of avenues for further investigation so that we may better understand how to harness β-defensins towards improved antiviral immunity. The responsiveness of endometrial stromal cells to vitamin D offers the possibility of a new approach in treating post-partum uterine inflammation.

# Chapter 6 General Discussion

Rapid evolution of microbial resistance to commercial antibiotics is one of the most significant health issues facing man in the 21st century (World Health Organisation, 2015). Immune-competent individuals defend themselves against multiple pathogens each day without pharmaceutical intervention. This is partly due to the exquisitely complex system of tightly-regulated host defence peptides (HDPs) within our own bodies. As multifunctional immune effector molecules, these HDPs have significant potential to improve human and animal health. However, despite decades of research, there is a discrepancy between the claimed potential of HDP-based agents as stated in patents and their performance in the comparatively smaller body of clinical trials carried out to date (Kosikowska and Lesner, 2016; Mahlapuu et al., 2016). A major challenge remains the poor understanding of how these molecules function physiologically. Even less is known about how their expression is regulated. With both under- and over-production of β-defensins linked to common human diseases, understanding how expression of these molecules is regulated endogenously may represent the next frontier in HDP research (Zhang and Gallo, 2016). As regulation is very context specific, using a model that is as close as possible to the condition in question, in terms of species, cell type and stimulus, is crucial.

Current understanding of β-defensin regulation is limited to a small fraction of the total gene repertoire, namely the genes in one of four syntenic clusters, in selected cell types and mostly in human. The literature on regulation of genes in another syntenic cluster implicated in fertility is particularly scant, despite evidence linking these genes to fertility of the male macaque (Tollner et al., 2012), human (Dubé et al., 2008), mouse (Dorin, 2015), rat (Zhou et al., 2004) and bull (Fernandez-Fuertes et al., 2016).

Hence, we began this study with a hypothesis-generating exercise, using a powerful comparative genomics approach to identify conserved non-coding elements in β-defensin gene regions with potential regulatory function (Chapter 3, p54). Several logical potential regulatory mechanisms have been identified via this approach, particularly in relation to β-defensins 129, 128, and 126. All three genes appear to be androgen-regulated in the bovine, as they are expressed only in the sexually-mature male

(Narciandi et al., 2011). However, our bioinformatics results suggest androgen regulation of gene expression is exerted differently for each gene, with different transcription factors (TFs) co-operating with androgen receptor, or being themselves regulated by androgen. This is likely because each gene functions differently within the male reproductive tract.

However, at this point the only gene within this cluster whose exact role in reproduction has been investigated is *DEFB126*. Our group has shown it binds to the bull sperm surface and promotes sperm motility (Fernandez-Fuertes et al., 2016). *DEFB126* expression is downregulated in the epididymis of sub-fertile men with impaired sperm production (Dubé et al., 2008), suggesting that if we are to improve fertility in economically-important agricultural species or overcome human infertility, we need to understand how this gene is regulated. We hypothesise that transcriptional regulation of *DEFB126* involves the proximal promoter and a distal element downstream which may function as an enhancer. Similar mechanisms operate within the Th2 interleukin gene region (Loots et al., 2000) and possibly in the human β-defensin syntenic cluster D region, as a *DEFB1* promoter SNP also regulates *DEFB103* expression (Nurjadi et al., 2013). We hypothesise that activating enhancer-binding protein 2 (AP-2)α, a known androgen receptor (AR) co-factor in the epididymis (Pihlajamaa et al., 2014), mediates contact between the distal element, which contains AR binding sites, and the *DEFB126* proximal promoter (Figure 3.26, p111).

Validation of any of these predictions could begin with chromatin-immunoprecipitation (ChIP) on male reproductive tract tissues from sexually mature and immature bulls to determine whether the implicated TFs bind the putative binding sites. This technique involves formaldehyde cross-linking of a biological sample to preserve DNA-protein complexes. Fragmentation of DNA and antibody pull-down of TF-bound fragments is followed by reversal of protein crosslinks and qPCR to quantitate the amount of the targeted DNA region which was bound by the TF in the sample. In addition, modified versions of this type of assay include a step to ligate fragments of DNA bound to a single TF molecule despite them being at distant locations in the intact genome, allowing PCR quantification of their physical interaction when bound by that TF (Dekker et al., 2013). However, TF binding of a DNA region does not automatically mean this contact initiates transcription. Comparison of high-throughput TF-binding data with the results of TF gene knockdowns indicates only a fraction of genes bound by a TF are

genuinely regulated by it (Cusanovich et al., 2014). Hence, while the conservation of binding site sequence among distant mammals is more likely to indicate true function, detection of TF-DNA binding alone will not validate the predictions made here.

Ideally, an *in vitro* model would be used to dissect the regulatory mechanisms in more detail. Unfortunately, immortalisation of epididymal epithelial cells has had mixed results (Sipilä et al., 2004). A review of attempts to immortalise epididymal cells in various species indicates most have lost expression of genes crucial for normal epididymal function, while cells immortalised via SV40 T antigen exhibit massively decreased AR expression (Sipilä et al., 2004). This is likely due to a transcription factor called b-myc, which is epididymis-specific in expression and antagonises the transcriptional activation and transformative properties of the proto-oncogene c-myc (Resar et al., 1993). Indeed, immortalisation of epididymal epithelial cells causes upregulation of c-myc and downregulation of b-myc (Sipilä et al., 2004). Thus, a primary culture model of epididymal epithelial cells would be needed. To our knowledge, this is not routinely carried out in the bovine, but has been done in boar (Bassols et al., 2005). Reporter assays could be used to determine whether the exact sequence of a predicted TFBS was crucial for transcriptional activation, while the predicted enhancer could be cloned into a reporter plasmid downstream of the luciferase gene to model the scenario hypothesised here.

As primary culture of bovine cells was not carried out in our lab prior to this study, we opted instead to turn to a validated cell culture model based on the cow reproductive tract, namely the endometrium. Previous transcriptomic analysis implied *DEFB103* was associated with a pro-inflammatory gene signature in the pathologically-inflamed post-partum endometrium (Foley et al., 2015). The relatively simple orthology of this gene between mammals facilitated our comparative genomics approach. The enrichment of activator protein 1 (AP-1) binding sites agrees with the experimental literature, thus this gene acts as a proof of concept for our *in silico* analysis. Diverse stimuli drive AP-1 regulation of *DEFB103* in different cell types, including epidermal growth factor receptor in keratinocytes (Sørensen et al., 2005) and bacteria in pulmonary epithelium (Scharf et al., 2010). Here, we have selected stimuli that are relevant to bovine uterine inflammation.

The small sample sizes used here for our *in vitro* work do not demonstrate a clear breed-specific difference in β-defensin response, especially as all six animals were Holstein-Friesians in several instances. In any case, sourcing pedigree animals of different breeds raised on the same farm would be necessary to rule out management or environmental factors. An elegant study used this approach to demonstrate that macrophages from Holstein-Friesians are less efficient at bacterial killing and produce more IL-1β than those from Brown Swiss cows, due to greater production of reactive oxygen/nitrogen species in the latter (Gibson et al., 2016). Since Brown Swiss cattle are anecdotally less susceptible to infection than Holstein-Friesians, understanding the factors driving this will improve our ability to manage the health of different breeds. The described study did not examine β-defensin expression, however β-defensin genes are some of the most highly copy number variable both between *Bos taurus* breeds and between *Bos taurus* and the hardier *Bos indicus* species preferred in the Southern hemisphere (Liu et al., 2010, Bickhart et al., 2012). Therefore, comparison of the effects of the stimuli used here on cells from different breeds will improve our understanding of breed-specific immune responses in the context of an economically-important inflammatory condition, i.e., endometritis.

The study of endometritis has focused on the host response to invading bacteria, with bacterial ligands being used to stimulate *in vitro* models and elucidate the activated signalling pathways (e.g. Cronin et al., 2012). However, the issue of systemic inflammation in the post-partum cow, driven by both metabolic and infectious/inflammatory causes is gaining increased attention (Bradford et al., 2015). In addition, the importance of stromal cells in driving a switch between acute but resolving and chronic inflammation is now appreciated within human disease models such as rheumatoid arthritis (Barone et al., 2013). Being proximal to endometrial blood vessels, endometrial stromal cells experience infiltrating cytokines and leukocytes as well as the range of microbes contaminating the damaged post-partum uterus. Therefore, the finding that these cells can respond to proinflammatory cytokines by producing immune-modulating β-defensins positions this cell type as being an important mediator between externally- and internally-derived inflammatory signals (Chapter 4, p116). Despite being the most highly studied human β-defensin, the expression of *DEFB103* has been rarely

examined in bovine (Mirabzadeh-Ardakani et al., 2016) and the demonstration of induction via IL-1β and IL-17A is novel in this cell type and species.

An important next step will be to develop a bovine β-defensin 3 ELISA so that protein levels in response to these stimuli can be quantified. Particularly as the mRNA fold changes are small, this would give a better idea of whether such changes in expression level are likely to be biologically meaningful.

β-defensin upregulation by these cytokines of course begs the question as to whether the β-defensins are pro- or anti-inflammatory in the endometrium. The published literature on the antimicrobial, wound-healing and bacterial protease-inhibiting properties of β-defensins (Harder et al., 2001; Niyonsaba et al., 2006; Wang et al., 2017) paint a beguiling picture of these peptides as a multifunctional remedy in the wounded and contaminated past-partum uterus. Indeed, while the β-defensin expression pattern in the post-partum endometrium occurs as part of an overall proinflammatory transcriptomic signature, that does not automatically mean they themselves have pro-inflammatory function. One possibility is that relative upregulation of β-defensins at 7 days post-partum (DPP) in animals with restored homeostasis at 21 DPP is due to anti-inflammatory or wound healing functions of the β-defensins. However, if this were the case, one might expect that at 7 DPP, β-defensins would be relatively upregulated in healthy animals compared to those which are still inflamed by 21 DPP. Our previous work indicates this is not the case (Foley et al., 2015). Therefore, transcriptomic analyses appear to indicate that β-defensins are contributing to inflammation in the uterus.

This scenario raises a number of possibilities as to what the β-defensins may be doing. Given that endometritis is diagnosed based on polymorphonuclear cell (PMN) infiltration, chemoattraction is an obvious suggestion since their chemokine-like secondary structure means human and murine β-defensins are chemotactic for monocytes, macrophages, neutrophils, dendritic cells (DCs) and T cells (Niyonsaba et al., 2004; Röhrl et al., 2010a; Yang et al., 1999). The fact that percentage PMN does not always correlate with bacterial contamination of the endometrium (Ricci et al., 2015; Walker et al., 2015) suggests this may be occurring in some instances.

The effect of the β-defensins on cytokine secretion from both leukocytes and endometrial cells is harder to predict, as these peptides have been reported to have both

pro- and anti-inflammatory effects, particularly in the context of bacterial/LPS exposure (e.g. Barabas et al., 2013; Semple et al., 2010). Comparison of a range of β-defensin concentrations in a single model indicates higher concentrations are more likely to be proinflammatory (Harvey et al., 2013). If endometrial expression of β-defensins is driven by cytokines released into peripheral blood in response to a variety of post-partum inflammatory conditions (Shuster et al., 1993; Usman et al., 2017; Zhang et al., 2015), then systemic inflammation may push β-defensin concentrations into the pro-inflammatory range, thus potentiating local endometrial inflammation. Of course, measurement of β-defensin peptide levels in the post-partum uterus would be necessary to determine if this is the case, as indeed would a variety of functional assays to determine the effects of β-defensins on cytokine expression in endometrial cells. Of course, such proinflammatory functions do not preclude the simultaneous occurrence of more positive effector functions such as those described earlier. In reality, controlling the extent and duration of β-defensin expression may direct their function in the desired manner.

The few studies on β-defensins and nucleic acid-mediated inflammation indicate β-defensins are proinflammatory within that context. Human β-defensins can be upregulated by nucleic acids such as poly(I:C) (Ghosh et al., 2008; Omagari et al., 2011; Schaefer et al., 2005) and in turn form complexes with these that promote leukocyte uptake and interferon production (Lande et al., 2015; McGlasson et al., 2017). The suggestion that such β-defensin-self DNA complexes underlie the association between β-defensins and psoriasis, an inflammatory skin condition driven by cytokines including IL-1β and IL-17A (Lande et al., 2015), is potentially interesting in relation to endometritis. The tissue damage from parturition would surely result in the release of self-DNA. Therefore, if β-defensin levels in the endometrium were already high, such a mechanism would likely perpetuate inflammation.

Demonstration of nucleic acid regulation of β-defensin expression is completely novel in bovine (Chapter 5, p157). While *DEFB103* is upregulated in bovine buccal epithelium (though not tongue epithelium) in response to bovine herpesvirus (BoHV-)1 infection, that study did not show whether viral proteins, nucleic acids, or intermediary cytokines regulate this effect (Mirabzadeh-Ardakani et al., 2016). As herpesviruses are dsDNA and produce dsRNA during replication (Weber et al., 2006), the fact that *DEFB103* is upregulated in endometrial stromal cells by synthetic analogs of both

suggests BoHV-4 infection of stromal cells should stimulate expression of this gene. In fact, BoHV-4 infection of these cells has remarkably little effect and *IL8* is the only immune gene induced (Tebaldi et al., 2016). This indicates that the virus has evolved mechanisms to evade immune detection and clearance within the cells. To this end, demonstrating the expression and differential regulation of cytoplasmic viral sensors, which is novel for this cell type, adds to our understanding of the host machinery which may be manipulated by the virus. Within the cell preparations used here, only one tested positive for BoHV-4, making it impossible to determine whether existing viral infection affects induction of these sensors. Such an investigation would be an important step in elucidating the immune evasion properties of the virus.

Since BoHV-4 is associated with reduced fertility (Klamminger et al., 2017), boosting the antiviral response would be desirable. With a variety of antiviral roles attributed to β-defensins (Wilson et al., 2013), application of exogenous β-defensin itself or of an immunostimulatory factor to boost β-defensin expression within appropriate limits may be beneficial against BoHV-4.

Vitamin D may be one such factor. The demonstration that hormonally-active vitamin D (1α,25-dihydroxyvitamin D/1,25D) can stimulate innate immune gene expression in bovine endometrial stromal cells is completely novel and opens up the possibility of a new therapeutic for uterine disease. 1,25D modulates the immune response in a number of conditions affecting the bovine. It boosts reactive nitrogen species production in monocytes and decreases IL-17A and IFNγ production from T cells of BCG-vaccinated calves (Nelson et al., 2011). This indicates 1,25D can boost local immunity while dampening T cell-induced inflammation. In the mammary gland, injection of a 25D concentration three orders of magnitude larger than that found in the peripheral blood can clear experimental bacterial infection and lower somatic cell counts without impacting serum concentrations (Lippolis et al., 2011). Epithelial cells lining the mammary gland express the 1α-hydroxylase enzyme which converts 25D to 1,25D (Nelson et al., 2010b) and upregulate β-defensin expression in response to 1,25D *in vitro* (Merriman et al., 2015).

Local delivery of vitamin D is of interest as this nutrient is unevenly stored throughout the body, with skeletal muscle and adipose tissue being the main sites of

vitamin D storage in human (Mawer et al., 1972). Thus, intramammary injection improves mastitis even in cows with serum vitamin D concentrations considered sufficient (Lippolis et al., 2011). Human endometrial cells express the 1α-hydroxylase gene and therefore can likely activate vitamin D (Viganò et al., 2006). Demonstration of the same property in bovine cells would be necessary for vitamin D to be a viable treatment option for endometritis.

As the exact mechanisms whereby 1,25D regulates immunity differ between primates and other species (Dimitrov and White, 2016; Gombart, 2009), it is difficult to predict how 1,25D is regulating β-defensins in this model. A cytokine array may identify mediators of β-defensin induction. qPCR and western blot techniques would detect induction or phosphorylation of intracellular signalling components such as IκBα.

Ultimately, the opposing effect of vitamin D on *DEFB103* and e*DEFB4A* brings into sharp focus the need to understand what each peptide is doing in the bovine endometrium. The human data indicate that the functions of hBD-2 and hBD-3 are not redundant. The two peptides display differing salt sensitivities (Harder et al., 1997), and hBD-2 is most active against Gram-negative bacteria, while hBD-3 can also kill Gram-positive bacteria (Schröder and Harder, 2006). This means that within a given context, induction of one β-defensin over another may be more useful. Hence, in-depth understanding of the regulation of each β-defensin in the bovine endometrium is worthwhile and the work presented here contributes towards this goal.

In conclusion, these data identify putative regulatory mechanisms of male fertility-related β-defensins which pertain to the bovine but also to other mammals. Demonstration of β-defensin induction in the endometrium in response to proinflammatory cytokines, viral ligands and vitamin D is novel in this important agricultural species and presents several potential avenues towards exploitation of β-defensins for improved uterine health.

# References


Abe, T., and Barber, G.N. (2014). Cytosolic-DNA-Mediated, STING-Dependent Proinflammatory Gene Induction Necessitates Canonical NF-κB Activation through TBK1. J. Virol. *88*, 5328–5341.

Aberg, K.M., Radek, K.A., Choi, E.-H., Kim, D.-K., Demerjian, M., Hupe, M., Kerbleski, J., Gallo, R.L., Ganz, T., Mauro, T., et al. (2007). Psychological stress downregulates epidermal antimicrobial peptide expression and increases severity of cutaneous infections in mice. J. Clin. Invest. *117*, 3339–3349.

Ablasser, A., Bauernfeind, F., Hartmann, G., Latz, E., Fitzgerald, K.A., and Hornung, V. (2009). RIG-I-dependent sensing of poly(dA:dT) through the induction of an RNA polymerase III–transcribed RNA intermediate. Nat. Immunol. *10*, 1065–1072.

Adams, B., Dörfler, P., Aguzzi, A., Kozmik, Z., Urbánek, P., Maurer-Fogy, I., and Busslinger, M. (1992). Pax-5 encodes the transcription factor BSAP and is expressed in B lymphocytes, the developing CNS, and adult testis. Genes Dev. *6*, 1589–1607.

Adelson, D.L., Qu, Z.P., Raison, J.M., and Lim, S.L. (2014). Bovine Genomics. In The Genetics of Cattle, (Oxfordshire: CABI), pp. 130–152.

Aghajanova, L., Horcajadas, J.A., Esteban, F.J., and Giudice, L.C. (2010). The Bone Marrow-Derived Human Mesenchymal Stem Cell: Potential Progenitor of the Endometrial Stromal Fibroblast. Biol. Reprod. *82*, 1076–1087.

Aguilar-Jiménez, W., Zapata, W., Caruz, A., and Rugeles, M.T. (2013). High Transcript Levels of Vitamin D Receptor Are Correlated with Higher mRNA Expression of Human Beta Defensins and IL-10 in Mucosa of HIV-1-Exposed Seronegative Individuals. PLoS ONE *8*, e82717.

Akbar, H., Cardoso, F.C., Meier, S., Burke, C., McDougall, S., Mitchell, M., Walker, C., Rodriguez-Zas, S.L., Everts, R.E., Lewin, H.A., et al. (2014). Postpartal Subclinical Endometritis Alters Transcriptome Profiles in Liver and Adipose Tissue of Dairy Cows. Bioinforma. Biol. Insights *8*, 45–63.

Alexopoulou, L., Holt, A.C., Medzhitov, R., and Flavell, R.A. (2001). Recognition of double-stranded RNA and activation of NF-κB by Toll-like receptor 3. Nature *413*, 732–738.

Alroy, I., Towers, T.L., and Freedman, L.P. (1995). Transcriptional repression of the interleukin-2 gene by vitamin D3: direct inhibition of NFATp/AP-1 complex formation by a nuclear hormone receptor. Mol. Cell. Biol. *15*, 5789–5799.

Andersson, L., Archibald, A.L., Bottema, C.D., Brauning, R., Burgess, S.C., Burt, D.W., Casas, E., Cheng, H.H., Clarke, L., Couldrey, C., et al. (2015). Coordinated international action to accelerate genome-to-phenome with FAANG, the Functional Annotation of Animal Genomes project. Genome Biol. *16*, 57.

Angrizano, T., Pero, R., Paoletti, I., Keller, S., Lembo, L., Baroni, A., Chiariotti, L., Lembo, F., and Donnarumma, G. (2013). Epigenetic Regulation of IL-8 and Beta-Defensin Genes in Human Keratinocytes in Response to Malassezia furfur. J. Investig. Dermatol. *133*, 2101–2104.

Animal Health Ireland (2017). BVD Eradication - Programme KEY Points for 2017.

Archer, N.K., Adappa, N.D., Palmer, J.N., Cohen, N.A., Harro, J.M., Lee, S.K., Miller, L.S., and Shirtliff, M.E. (2016). Interleukin-17A (IL-17A) and IL-17F Are Critical for Antimicrobial Peptide Production and Clearance of Staphylococcus aureus Nasal Colonization. Infect. Immun. *84*, 3575–3583.

Aronheim, A., Zandi, E., Hennemann, H., Elledge, S.J., and Karin, M. (1997). Isolation of an AP-1 repressor by a novel method for detecting protein-protein interactions. Mol. Cell. Biol. *17*, 3094–3102.

Asano, M., Hayashi, M., Yoshida, E., Kawade, Y., and Iwakura, Y. (1990). Induction of interferon-alpha by interferon-beta, but not of interferon-beta by interferon-alpha, in the mouse. Virology *176*, 30–38.

Astrahantseff, K.N., and Morris, J.E. (1994). Estradiol-17β stimulates proliferation of uterine epithelial cells cultured with stromal cells but not cultured separately. Vitro Cell. Dev. Biol. - Anim. *30*, 769–776.

Aungier, S.P.M., Roche, J.F., Diskin, M.G., and Crowe, M.A. (2014). Risk factors that affect reproductive target achievement in fertile dairy cows. J. Dairy Sci. *97*, 3472–3487.

Badis, G., Berger, M.F., Philippakis, A.A., Talukder, S., Gehrke, A.R., Jaeger, S.A., Chan, E.T., Metzler, G., Vedenko, A., Chen, X., et al. (2009). Diversity and Complexity in DNA Recognition by Transcription Factors. Science *324*, 1720–1723.

Baliwag, J., Barnes, D.H., and Johnston, A. (2015). Cytokines in psoriasis. Cytokine *73*, 342–350.

Bamberger, A.M., Bamberger, C.M., Gellersen, B., and Schulte, H.M. (1996). Modulation of AP-1 activity by the human progesterone receptor in endometrial adenocarcinoma cells. Proc. Natl. Acad. Sci. U. S. A. *93*, 6169–6174.

Barabas, N., Röhrl, J., Holler, E., and Hehlgans, T. (2013). Beta-defensins activate macrophages and synergize in pro-inflammatory cytokine expression induced by TLR ligands. Immunobiology *218*, 1005–1011.

Barone, F., Nayar, S., and Buckley, C.D. (2013). The role of non-hematopoietic stromal cells in the persistence of inflammation. Front. Immunol. *3*.

Bassols, J., Kádár, E., Briz, M., Pinart, E., Sancho, S., Garcia-Gil, N., Badia, E., Pruneda, A., Bussalleu, E., Yeste, M., et al. (2005). Evaluation of boar sperm maturation after co-incubation with caput, corpus and cauda epididymal cultures: Evaluation of boar sperm maturation in vitro. Theriogenology *64*, 1995–2009.

Basu, M., Kota Srikanth, Amiya Banerjee, and Santunu Bose (2010). Role of human beta defensin 3 during type I interferon mediated antiviral response against vesicular stomatitis virus. Int. J. Interferon Cytokine Mediat. Res. *2*, 23–32.

Bedran, T.B.L., Mayer, M.P.A., Spolidorio, D.P., and Grenier, D. (2014). Synergistic Anti-Inflammatory Activity of the Antimicrobial Peptides Human Beta-Defensin-3 (hBD-3) and Cathelicidin (LL-37) in a Three-Dimensional Co-Culture Model of Gingival Epithelial Cells and Fibroblasts. PLoS ONE *9*, e106766.

Bell, A.W. (1995). Regulation of organic nutrient metabolism during transition from late pregnancy to early lactation. J. Anim. Sci. *73*, 2804–2819.

Belleannée, C., Labas, V., Teixeira-Gomes, A.-P., Gatti, J.L., Dacheux, J.-L., and Dacheux, F. (2011). Identification of luminal and secreted proteins in bull epididymis. J. Proteomics *74*, 59–78.

Berghuis, L., Abdelaziz, K., Bierworth, J., Wyer, L., Jacob, G., Karrow, N.A., Sharif, S., Clark, M., and Caswell, J.L. (2014). Comparison of innate immune agonists for induction of tracheal antimicrobial peptide gene expression in tracheal epithelial cells of cattle. Vet. Res. *45*, 105.

Berry, D.P., Evans, R.D., and Mc Parland, S. (2011). Evaluation of bull fertility in dairy and beef cattle using cow field data. Theriogenology *75*, 172–181.

Berry, D.P., Wall, E., and Pryce, J.E. (2014). Genetics and genomics of reproductive performance in dairy and beef cattle. Animal *8*, 105–121.

Berry, D.P., Friggens, N.C., Lucy, M., and Roche, J.R. (2016). Milk Production and Fertility in Cattle. Annu. Rev. Anim. Biosci. *4*, 269–290.

Bhuju, S., Aranday-Cortes, E., Villarreal-Ramos, B., Xing, Z., Singh, M., and Vordermeier, H.M. (2012). Global Gene Transcriptome Analysis in Vaccinated Cattle Revealed a Dominant Role of IL-22 for Protection against Bovine Tuberculosis. PLOS Pathog. *8*, e1003077.

Bickhart, D.M., Hou, Y., Schroeder, S.G., Alkan, C., Cardone, M.F., Matukumalli, L.K., Song, J., Schnabel, R.D., Ventura, M., Taylor, J.F., et al. (2012). Copy number variation of individual cattle genomes using next-generation sequencing. Genome Res. *22*, 778–790.

Biragyn, A., Ruffini, P.A., Leifer, C.A., Klyushnenkova, E., Shakhov, A., Chertov, O., Shirakawa, A.K., Farber, J.M., Segal, D.M., Oppenheim, J.J., et al. (2002). Toll-Like Receptor 4-Dependent Activation of Dendritic Cells by beta -Defensin 2. Science *298*, 1025–1029.

Biswas, B., and Yenugu, S. (2011). Antimicrobial Responses in the Male Reproductive Tract of Lipopolysaccharide Challenged Rats. Am. J. Reprod. Immunol. *65*, 557–568.

Biswas, B., and Yenugu, S. (2013). Lipopolysaccharide induces epididymal and testicular antimicrobial gene expression in vitro: insights into the epigenetic regulation of sperm-associated antigen 11e gene. Immunogenetics *65*, 239–253.

Biswas, B., and Yenugu, S. (2014). Transcriptional regulation of the rat sperm-associated antigen 11e (Spag 11e) gene during endotoxin challenge. Mol. Genet. Genomics *289*, 837–845.

Blatti, C., Kazemian, M., Wolfe, S., Brodsky, M., and Sinha, S. (2015). Integrating motif, DNA accessibility and gene expression data to build regulatory maps in an organism. Nucleic Acids Res. gkv195.

Boldenow, E., Jones, S., Lieberman, R.W., Chames, M.C., Aronoff, D.M., Xi, C., and Loch-Caruso, R. (2013). Antimicrobial peptide response to Group B Streptococcus in human extraplacental membranes in culture. Placenta *34*, 480–485.

Bradford, B.J., Yuan, K., Farney, J.K., Mamedova, L.K., and Carpenter, A.J. (2015). Invited review: Inflammation during the transition to lactation: New adventures with an old flame. J. Dairy Sci. *98*, 6631–6650.

Brahmachary, M., Schönbach, C., Yang, L., Huang, E., Tan, S.L., Chowdhary, R., Krishnan, S.P.T., Lin, C.-Y., Hume, D.A., Kai, C., et al. (2006). Computational promoter analysis of mouse, rat and human antimicrobial peptide-coding genes. BMC Bioinformatics *7*, S8.

Brewer, D.B. (1967). The fibroblast. Proc. R. Soc. Med. *60*, 778–781.

Brogden, K.A. (2005). Antimicrobial peptides: pore formers or metabolic inhibitors in bacteria? Nat. Rev. Microbiol. *3*, 238–250.

Brouty-Boyé, D., Pottin-Clémenceau, C., Doucet, C., Jasmin, C., and Azzarone, B. (2000). Chemokines and CD40 expression in human fibroblasts. Eur. J. Immunol. *30*, 914–919.

Bruhn, O., Paul, S., Tetens, J., and Thaller, G. (2009). The repertoire of equine intestinal alpha-defensins. Bmc Genomics *10*, 631.

Buhimschi, I.A., Jabr, M., Buhimschi, C.S., Petkova, A.P., Weiner, C.P., and Saed, G.M. (2004). The novel antimicrobial peptide β3-defensin is produced by the amnion: A possible role of the fetal membranes in innate immunity of the amniotic cavity. Am. J. Obstet. Gynecol. *191*, 1678–1687.

Calton, E.K., Keane, K.N., Newsholme, P., and Soares, M.J. (2015). The Impact of Vitamin D Levels on Inflammatory Status: A Systematic Review of Immune Cell Studies. PLOS ONE *10*, e0141770.

Caposio, P., Gugliesi, F., Zannetti, C., Sponza, S., Mondini, M., Medico, E., Hiscott, J., Young, H.A., Gribaudo, G., Gariglio, M., et al. (2007). A novel role of the interferon-inducible protein IFI16 as inducer of proinflammatory molecules in endothelial cells. J. Biol. Chem. *282*, 33515–33529.

Castañeda-Delgado, J., Hernández-Pando, R., Serrano, C.J., Aguilar-León, D., León-Contreras, J., Rivas-Santiago, C., Méndez, R., González-Curiel, I., Enciso-Moreno, A., and Rivas-Santiago, B. (2010). Kinetics and cellular sources of cathelicidin during the course of experimental latent tuberculous infection and progressive pulmonary tuberculosis. Clin. Exp. Immunol. *161*, 542–550.

Castañeda-Sánchez, J.I., García-Pérez, B.E., Muñoz-Duarte, A.R., Baltierra-Uribe, S.L., Mejia-López, H., López-López, C., Lucio, V.M.B.-D., Robles-Contreras, A., and Luna-Herrera, J. (2013). Defensin Production by Human Limbo-Corneal Fibroblasts Infected with Mycobacteria. Pathogens *2*, 13–32.

Chan, Y.K., and Gack, M.U. (2016). Viral evasion of intracellular DNA and RNA sensing. Nat. Rev. Microbiol. *14*, 360–373.

Chang, L., and Karin, M. (2001). Mammalian MAP kinase signalling cascades. Nature *410*, 37–40.

Chapwanya, A., Meade, K.G., Foley, C., Narciandi, F., Evans, A.C.O., Doherty, M.L., Callanan, J.J., and O'Farrelly, C. (2012). The postpartum endometrial inflammatory response: a normal physiological event with potential implications for bovine fertility. Reprod. Fertil. Dev. *24*, 1028–1039.

Chapwanya, A., Meade, K.G., Doherty, M.L., Callanan, J.J., and O'Farrelly, C. (2013). Endometrial epithelial cells are potent producers of tracheal antimicrobial peptide and serum amyloid A3 gene expression in response to E. coli stimulation. Vet. Immunol. Immunopathol. *151*, 157–162.

Chastant-Maillard, S. (2015). Impact of Bovine Herpesvirus 4 (BoHV-4) on Reproduction. Transbound. Emerg. Dis. *62*, 245–251.

Chen, Q., Mosovsky, K.L., and Ross, A.C. (2013). Retinoic acid and α-galactosylceramide regulate the expression of costimulatory receptors and transcription factors responsible for B cell activation and differentiation. Immunobiology *218*, 1477–1487.

Chen, Y.-H., Yu, Z., Fu, L., Wang, H., Chen, X., Zhang, C., Lv, Z.-M., and Xu, D.-X. (2015). Vitamin D3 inhibits lipopolysaccharide-induced placental inflammation through reinforcing interaction between vitamin D receptor and nuclear factor kappa B p65 subunit. Sci. Rep. *5*.

Cheong, S.H., Nydam, D.V., Galvão, K.N., Crosier, B.M., and Gilbert, R.O. (2011). Cow-level and herd-level risk factors for subclinical endometritis in lactating Holstein cows. J. Dairy Sci. *94*, 762–770.

Chiricozzi, A., Nograles, K.E., Johnson-Huang, L.M., Fuentes-Duculan, J., Cardinale, I., Bonifacio, K.M., Gulati, N., Mitsui, H., Guttman-Yassky, E., Suárez-Fariñas, M., et al. (2014). IL-17 Induces an Expanded Range of Downstream Genes in Reconstituted Human Epidermis Model. PLoS ONE *9*.

Cichocki, M., Szamałek, M., Dałek, M., and Baer-Dubowska, W. (2012). Correlation between EGFR Y1068 tyrosine phosphorylation and AP-1 activation by tumor promoter 12-O-tetradecanoylphorbol-13-acetate in mouse skin. Environ. Toxicol. Pharmacol. *33*, 92–97.

Com, E., Bourgeon, F., Evrard, B., Ganz, T., Colleu, D., Jégou, B., and Pineau, C. (2003). Expression of Antimicrobial Defensins in the Male Reproductive Tract of Rats, Mice, and Humans. Biol. Reprod. *68*, 95–104.

Consortium, T.E.P. (2012). An integrated encyclopedia of DNA elements in the human genome. Nature *489*, 57–74.

Cooke, P.S., Buchanan, D.L., Young, P., Setiawan, T., Brody, J., Korach, K.S., Taylor, J., Lubahn, D.B., and Cunha, G.R. (1997). Stromal estrogen receptors mediate mitogenic effects of estradiol on uterine epithelium. Proc. Natl. Acad. Sci. *94*, 6535–6540.

Corleis, B., Lisanti, A.C., Körner, C., Schiff, A.E., Rosenberg, E.S., Allen, T.M., Altfeld, M., and Kwon, D.S. (2017). Early type I Interferon response induces upregulation of human β-defensin 1 during acute HIV-1 infection. PLOS ONE *12*, e0173161.

Cormican, P. (2009). A comparative genomics analysis of the vertebrate immune system: genes, pathways and evolution. Trinity College Dublin.

Cormican, P., Meade, K.G., Cahalane, S., Narciandi, F., Chapwanya, A., Lloyd, A.T., and O'Farrelly, C. (2008). Evolution, expression and effectiveness in a cluster of novel bovine β-defensins. Immunogenetics *60*, 147–156.

Costa, S.L., Boekelheide, K., Vanderhyden, B.C., Seth, R., and McBurney, M.W. (1997). Male Infertility Caused by Epididymal Dysfunction in Transgenic Mice Expressing a Dominant Negative Mutation of Retinoic Acid Receptor α. Biol. Reprod. *56*, 985–990.

Cridland, J.A., Curley, E.Z., Wykes, M.N., Schroder, K., Sweet, M.J., Roberts, T.L., Ragan, M.A., Kassahn, K.S., and Stacey, K.J. (2012). The mammalian PYHIN gene family: Phylogeny, evolution and expression. BMC Evol. Biol. *12*, 140.

Cronin, J.G., Turner, M.L., Goetze, L., Bryant, C.E., and Sheldon, I.M. (2012). Toll-Like Receptor 4 and MYD88-Dependent Signaling Mechanisms of the Innate Immune System Are Essential for the

Response to Lipopolysaccharide by Epithelial and Stromal Cells of the Bovine Endometrium. Biol. Reprod. *86*, 51.

Cusanovich, D.A., Pavlovic, B., Pritchard, J.K., and Gilad, Y. (2014). The Functional Consequences of Variation in Transcription Factor Binding. PLoS Genet *10*, e1004226.

DasGupta, T., Nweze, E.I., Yue, H., Wang, L., Jin, J., Ghosh, S.K., Kawsar, H.I., Zender, C., Androphy, E.J., Weinberg, A., et al. (2016). Human papillomavirus oncogenic E6 protein regulates human β-defensin 3 (hBD3) expression via the tumor suppressor protein p53. Oncotarget.

Davies, D., Meade, K.G., Herath, S., Eckersall, P.D., Gonzalez, D., White, J.O., Conlan, R.S., O'Farrelly, C., and Sheldon, I.M. (2008). Toll-like receptor and antimicrobial peptide expression in the bovine endometrium. Reprod. Biol. Endocrinol. *6*, 53.

De Caleya, R.F., Gonzalez-Pascual, B., Garcia-Olmedo, F., and Carbonero, P. (1972). Susceptibility of Phytopathogenic Bacteria to Wheat Purothionins In Vitro. Appl. Microbiol. *23*, 998–1000.

De Filippis, A., Fiorentino, M., Guida, L., Annunziata, M., Nastri, L., and Rizzo, A. (2017). Vitamin D reduces the inflammatory response by Porphyromonas gingivalis infection by modulating human β-defensin-3 in human gingival epithelium and periodontal ligament cells. Int. Immunopharmacol. *47*, 106–117.

Deguillaume, L., Geffré, A., Desquilbet, L., Dizien, A., Thoumire, S., Vornière, C., Constant, F., Fournier, R., and Chastant-Maillard, S. (2012). Effect of endocervical inflammation on days to conception in dairy cows. J. Dairy Sci. *95*, 1776–1783.

Dekker, J., Marti-Renom, M.A., and Mirny, L.A. (2013). Exploring the three-dimensional organization of genomes: interpreting chromatin interaction data. Nat. Rev. Genet. *14*, 390–403.

Diamond, G., Zasloff, M., Eck, H., Brasseur, M., Maloy, W.L., and Bevins, C.L. (1991). Tracheal antimicrobial peptide, a cysteine-rich peptide from mammalian tracheal mucosa: peptide isolation and cloning of a cDNA. Proc. Natl. Acad. Sci. *88*, 3952–3956.

Diamond, G., Kaiser, V., Rhodes, J., Russell, J.P., and Bevins, C.L. (2000). Transcriptional Regulation of β-Defensin Gene Expression in Tracheal Epithelial Cells. Infect. Immun. *68*, 113–119.

Diao, R., Fok, K.L., Chen, H., Yu, M.K., Duan, Y., Chung, C.M., Li, Z., Wu, H., Li, Z., Zhang, H., et al. (2014). Deficient human β-defensin 1 underlies male infertility associated with poor sperm motility and genital tract infection. Sci. Transl. Med. *6*, 249ra108-249ra108.

van Dijk, A., Veldhuizen, E.J.A., and Haagsman, H.P. (2008). Avian defensins. Vet. Immunol. Immunopathol. *124*, 1–18.

Dimitrov, V., and White, J.H. (2016). Species-specific regulation of innate immunity by vitamin D signaling. J. Steroid Biochem. Mol. Biol. *164*, 246–253.

Dixon, B.R.E.A., Radin, J.N., Piazuelo, M.B., Contreras, D.C., and Algood, H.M.S. (2016). IL-17a and IL-22 Induce Expression of Antimicrobials in Gastrointestinal Epithelial Cells and May Contribute to Epithelial Cell Defense against Helicobacter pylori. PLoS ONE *11*.

Donofrio, G., Cavirani, S., Santen, V. van, and Flammini, C.F. (2005). Potential Secondary Pathogenic Role for Bovine Herpesvirus 4. J. Clin. Microbiol. *43*, 3421–3426.

Donofrio, G., Herath, S., Sartori, C., Cavirani, S., Flammini, C.F., and Sheldon, I.M. (2007). Bovine herpesvirus 4 is tropic for bovine endometrial cells and modulates endocrine function. Reproduction *134*, 183–197.

Donofrio, G., Franceschi, V., Capocefalo, A., Cavirani, S., and Sheldon, I.M. (2008). Bovine endometrial stromal cells display osteogenic properties. Reprod. Biol. Endocrinol. RBE *6*, 65.

Donofrio, G., Capocefalo, A., Franceschi, V., Price, S., Cavirani, S., and Sheldon, I.M. (2010). The Chemokine IL8 Is Up-Regulated in Bovine Endometrial Stromal Cells by the BoHV-4 IE2 Gene Product, ORF50/Rta: A Step Ahead Toward a Mechanism for BoHV-4 Induced Endometritis. Biol. Reprod. *83*, 919–928.

Dorin, J. (2015). Novel phenotype of mouse spermatozoa following deletion of epididymal expression of β-defensins. Asian J. Androl. *0*, 0.

Doss, M., White, M.R., Tecle, T., Gantz, D., Crouch, E.C., Jung, G., Ruchala, P., Waring, A.J., Lehrer, R.I., and Hartshorn, K.L. (2009). Interactions of α-, β-, and θ-Defensins with Influenza A Virus and Surfactant Protein D. J. Immunol. *182*, 7878–7887.

Drackley, J.K. (1999). Biology of Dairy Cows During the Transition Period: the Final Frontier? J. Dairy Sci. *82*, 2259–2273.

Duan, S., Shi, C., Chen, G., Zheng, J.-F., Wu, B., Diao, H., Ji, L., Gu, Y., Xin, A., Wu, Y., et al. (2015). Another functional frame-shift polymorphism of DEFB126 (rs11467497) associated with male infertility. J. Cell. Mol. Med. *19*, 1077–1084.

Dubé, E., Hermo, L., Chan, P.T.K., and Cyr, D.G. (2008). Alterations in gene expression in the caput epididymides of nonobstructive azoospermic men. Biol. Reprod. *78*, 342–351.

Dubuc, J., Duffield, T.F., Leslie, K.E., Walton, J.S., and LeBlanc, S.J. (2010). Definitions and diagnosis of postpartum endometritis in dairy cows. J. Dairy Sci. *93*, 5225–5233.

Dubuc, J., Duffield, T.F., Leslie, K.E., Walton, J.S., and LeBlanc, S.J. (2011). Effects of postpartum uterine diseases on milk production and culling in dairy cows. J. Dairy Sci. *94*, 1339–1346.

Duits, L.A., Rademaker, M., Ravensbergen, B., van Sterkenburg, M.A.J.A., van Strijen, E., Hiemstra, P.S., and Nibbering, P.H. (2001). Inhibition of hBD-3, but Not hBD-1 and hBD-2, mRNA Expression by Corticosteroids. Biochem. Biophys. Res. Commun. *280*, 522–525.

Dunn, C.L., Kelly, R.W., and Critchley, H.O. (2003). Decidualization of the human endometrial stromal cell: an enigmatic transformation. Reprod. Biomed. Online *7*, 151–161.

Eferl, R., and Wagner, E.F. (2003). AP-1: a double-edged sword in tumorigenesis. Nat. Rev. Cancer *3*, 859–868.

Egyed, L., and Bartha, A. (1998). Pcr studies on the potential sites for latency of BHV-4 in calves. Vet. Res. Commun. *22*, 209–216.

Eriksson, M., Taskinen, M., and Leppä, S. (2007). Mitogen activated protein kinase-dependent activation of c-Jun and c-Fos is required for neuronal differentiation but not for growth and stress response in PC12 cells. J. Cell. Physiol. *210*, 538–548.

Erlandsson, L., Blumenthal, R., Eloranta, M.-L., Engel, H., Alm, G., Weiss, S., and Leanderson, T. (1998). Interferon-β is required for interferon-α production in mouse fibroblasts. Curr. Biol. *8*, 223–226.

Evans, E.W., Beach, G.G., Wunderlich, J., and Harmon, B.G. (1994). Isolation of antimicrobial peptides from avian heterophils. J. Leukoc. Biol. *56*, 661–665.

Fahey, J.V., Wright, J.A., Shen, L., Smith, J.M., Ghosh, M., Rossoll, R.M., and Wira, C.R. (2008). Estradiol selectively regulates innate immune function by polarized human uterine epithelial cells in culture. Mucosal Immunol. *1*, 317–325.

Fan, S.R., Liu, X.P., and Liao, Q.P. (2008). Human defensins and cytokines in vaginal lavage fluid of women with bacterial vaginosis. Int. J. Gynecol. Obstet. *103*, 50–54.

Fanjul, A., Dawson, M.I., Hobbs, P.D., Jong, L., Cameron, J.F., Harlev, E., Graupner, G., Lu, X.-P., and Pfahl, M. (1994). A new class of retinoids with selective inhibition of AP-1 inhibits proliferation. Nature *372*, 107–111.

Fernandez-Fuertes, B., Narciandi, F., O'Farrelly, C., Kelly, A.K., Fair, S., Meade, K.G., and Lonergan, P. (2016). Cauda Epididymis-Specific Beta-Defensin 126 Promotes Sperm Motility but Not Fertilizing Ability in Cattle. Biol. Reprod. *95*, 122.

Ferris, L.K., Mburu, Y.K., Mathers, A.R., Fluharty, E.R., Larregina, A.T., Ferris, R.L., and Falo Jr, L.D. (2013). Human Beta-Defensin 3 Induces Maturation of Human Langerhans Cell–Like Dendritic

Cells: An Antimicrobial Peptide that Functions as an Endogenous Adjuvant. J. Invest. Dermatol. *133*, 460–468.

Fitch, N., Becker, A.B., and HayGlass, K.T. (2016). Vitamin D [1,25(OH)2D3] Differentially Regulates Human Innate Cytokine Responses to Bacterial versus Viral Pattern Recognition Receptor Stimuli. J. Immunol. *196*, 2965–2972.

Fjell, C.D., Jenssen, H., Fries, P., Aich, P., Griebel, P., Hilpert, K., Hancock, R.E.W., and Cherkasov, A. (2008). Identification of novel host defense peptides and the absence of α-defensins in the bovine genome. Proteins Struct. Funct. Bioinforma. *73*, 420–430.

Flores Saiffe Farías, A., Jaime Herrera López, E., Moreno Vázquez, C.J., Li, W., and Prado Montes de Oca, E. (2015). Predicting functional regulatory SNPs in the human antimicrobial peptide genes DEFB1 and CAMP in tuberculosis and HIV/AIDS. Comput. Biol. Chem. *59*, *Part A*, 117–125.

Foley, C., Chapwanya, A., Creevey, C.J., Narciandi, F., Morris, D., Kenny, E.M., Cormican, P., Callanan, J.J., O'Farrelly, C., and Meade, K.G. (2012). Global endometrial transcriptomic profiling: transient immune activation precedes tissue proliferation and repair in healthy beef cows. BMC Genomics *13*, 489–501.

Foley, C., Chapwanya, A., Callanan, J.J., Whiston, R., Miranda-CasoLuengo, R., Lu, J., Meijer, W.G., Lynn, D.J., Farrelly, C.O., and Meade, K.G. (2015). Integrated analysis of the local and systemic changes preceding the development of post-partum cytological endometritis. BMC Genomics *16*, 811.

Fortier, M.A., Guilbault, L.A., and Grasso, F. (1988). Specific properties of epithelial and stromal cells from the endometrium of cows. J. Reprod. Fertil. *83*, 239–248.

Fourichon, C., Seegers, H., and Malher, X. (2000). Effect of disease on reproduction in the dairy cow: a meta-analysis. Theriogenology *53*, 1729–1759.

Frandson, R.D., Wilke, W.L., and Fails, A.D. (2003). Anatomy and Physiology of Farm Animals (Wiley-Blackhall).

Frew, L., and Stock, S.J. (2011). Antimicrobial peptides and pregnancy. Reproduction *141*, 725–735.

Funderburg, N., Lederman, M.M., Feng, Z., Drage, M.G., Jadlowsky, J., Harding, C.V., Weinberg, A., and Sieg, S.F. (2007). Human beta-defensin-3 activates professional antigen-presenting cells via Toll-like receptors 1 and 2. Proc. Natl. Acad. Sci. U. S. A. *104*, 18631–18635.

García, J.-R., Jaumann, F., Schulz, S., Krause, A., Rodríguez-Jiménez, J., Forssmann, U., Adermann, K., Klüver, E., Vogelmeier, C., Becker, D., et al. (2001a). Identification of a novel, multifunctional β-defensin (human β-defensin 3) with specific antimicrobial activity. Cell Tissue Res. *306*, 257–264.

García, J.-R.C., Krause, A., Schulz, S., Rodríguez-Jiménez, F.-J., Klüver, E., Adermann, K., Forssmann, U., Frimpong-Boateng, A., Bals, R., and Forssmann, W.-G. (2001b). Human β-defensin 4: a novel inducible peptide with a specific salt-sensitive spectrum of antimicrobial activity. FASEB J. *15*, 1819–1821.

Ghosh, M., Schaefer, T.M., Fahey, J.V., Wright, J.A., and Wira, C.R. (2008). Antiviral Responses of Human Fallopian Tube Epithelial Cells to Toll-like Receptor 3 Agonist Poly(I:C). Fertil. Steril. *89*, 1497–1506.

Ghosh, M., Fahey, J.V., Shen, Z., Lahey, T., Cu-Uvin, S., Wu, Z., Mayer, K., Wright, P.F., Kappes, J.C., Ochsenbauer, C., et al. (2010). Anti-HIV Activity in Cervical-Vaginal Secretions from HIV-Positive and -Negative Women Correlate with Innate Antimicrobial Levels and IgG Antibodies. PLoS ONE *5*, e11366.

Gibson, A.J., Woodman, S., Pennelegion, C., Patterson, R., Stuart, E., Hosker, N., Siviter, P., Douglas, C., Whitehouse, J., Wilkinson, W., et al. (2016). Differential macrophage function in Brown Swiss and Holstein Friesian cattle. Vet. Immunol. Immunopathol. *181*, 15–23.

Gilbert, R.O. (2016). Management of Reproductive Disease in Dairy Cows. Vet. Clin. Food Anim. Pract. *32*, 387–410.

Gitlin, L., Barchet, W., Gilfillan, S., Cella, M., Beutler, B., Flavell, R.A., Diamond, M.S., and Colonna, M. (2006). Essential role of mda-5 in type I IFN responses to polyriboinosinic:polyribocytidylic acid and encephalomyocarditis picornavirus. Proc. Natl. Acad. Sci. U. S. A. *103*, 8459–8464.

Goff, J.P., Kimura, K., and Horst, R.L. (2002). Effect of Mastectomy on Milk Fever, Energy, and Vitamins A, E, and β-Carotene Status at Parturition1. J. Dairy Sci. *85*, 1427–1436.

Gombart, A.F. (2009). The vitamin D–antimicrobial peptide pathway and its role in protection against infection. Future Microbiol. *4*, 1151.

Gombart, A.F., Saito, T., and Koeffler, H.P. (2009). Exaptation of an ancient Alu short interspersed element provides a highly conserved vitamin D-mediated innate immune response in humans and primates. BMC Genomics *10*, 321.

Groth, M., Szafranski, K., Taudien, S., Huse, K., Mueller, O., Rosenstiel, P., Nygren, A.O.H., Schreiber, S., Birkenmeier, G., and Platzer, M. (2008). High-resolution mapping of the 8p23.1 beta-defensin cluster reveals strictly concordant copy number variation of all genes. Hum. Mutat. *29*, 1247–1254.

Guo, Y., Chen, Y., Liu, L.-B., Chang, K.-K., Li, H., Li, M.-Q., and Shao, J. (2013). IL-22 in the endometriotic milieu promotes the proliferation of endometrial stromal cells via stimulating the secretion of CCL2 and IL-8. Int. J. Clin. Exp. Pathol. *6*, 2011–2020.

Gür, S., and Doğan, N. (2010). The possible role of bovine herpesvirus type-4 infection in cow infertility. Anim. Sci. J. *81*, 304–308.

Haarmann, H., Steiner, T., Schreiber, F., Heinrich, A., Zweigner, J., N'Guessan, P.D., and Slevogt, H. (2015). The role and regulation of Moraxella catarrhalis-induced human beta-defensin 3 expression in human pulmonary epithelial cells. Biochem. Biophys. Res. Commun. *467*, 46–52.

Han, J.H., Kim, M.S., Lee, M.Y., Kim, T.H., Lee, M.-K., Kim, H.R., and Myung, S.C. (2010). Modulation of human β-defensin-2 expression by 17β-estradiol and progesterone in vaginal epithelial cells. Cytokine *49*, 209–214.

Hancock, R.E.W., and Sahl, H.-G. (2006). Antimicrobial and host-defense peptides as new anti-infective therapeutic strategies. Nat. Biotechnol. *24*, 1551–1557.

Hancock, R.E.W., Haney, E.F., and Gill, E.E. (2016). The immunology of host defence peptides: beyond antimicrobial activity. Nat. Rev. Immunol. *16*, 321–334.

Hansdottir, S., Monick, M.M., Lovan, N., Powers, L., Gerke, A., and Hunninghake, G.W. (2010). Vitamin D Decreases Respiratory Syncytial Virus Induction of NF-κB–Linked Chemokines and Cytokines in Airway Epithelium While Maintaining the Antiviral State. J. Immunol. *184*, 965–974.

Harder, J., Bartels, J., Christophers, E., and Schröder, J.-M. (1997). A peptide antibiotic from human skin. Nature *387*, 861–861.

Harder, J., Meyer-Hoffert, U., Teran, L.M., Schwichtenberg, L., Bartels, J., Maune, S., and Schröder, J.M. (2000). Mucoid Pseudomonas aeruginosa, TNF-alpha, and IL-1beta, but not IL-6, induce human beta-defensin-2 in respiratory epithelia. Am. J. Respir. Cell Mol. Biol. *22*, 714–721.

Harder, J., Bartels, J., Christophers, E., and Schröder, J.-M. (2001). Isolation and Characterization of Human β-Defensin-3, a Novel Human Inducible Peptide Antibiotic. J. Biol. Chem. *276*, 5707–5713.

Harder, J., Meyer-Hoffert, U., Wehkamp, K., Schwichtenberg, L., and Schröder, J.-M. (2004). Differential Gene Induction of Human β-Defensins (hBD-1, -2, -3, and -4) in Keratinocytes Is Inhibited by Retinoic Acid. J. Invest. Dermatol. *123*, 522–529.

Hardison, R.C., and Taylor, J. (2012). Genomic approaches towards finding cis-regulatory modules in animals. Nat. Rev. Genet. *13*, 469–483.

Hardwick, R.J., Machado, L.R., Zuccherato, L.W., Antolinos, S., Xue, Y., Shawa, N., Gilman, R.H., Cabrera, L., Berg, D.E., Tyler-Smith, C., et al. (2011). A worldwide analysis of beta-defensin copy number variation suggests recent selection of a high-expressing DEFB103 gene copy in East Asia. Hum. Mutat. *32*, 743–750.

Harvey, L.E., Kohlgraf, K.G., Mehalick, L.A., Raina, M., Recker, E.N., Radhakrishnan, S., Prasad, S.A., Vidva, R., Progulske-Fox, A., Cavanaugh, J.E., et al. (2013). Defensin DEFB103 bidirectionally regulates chemokine and cytokine responses to a pro-inflammatory stimulus. Sci. Rep. *3*.

Hattori, T., Ogura, N., Akutsu, M., Kawashima, M., Watanabe, S., Ito, K., and Kondoh, T. (2015). Gene Expression Profiling of IL-17A-Treated Synovial Fibroblasts from the Human Temporomandibular Joint. Mediators Inflamm. *2015*, e436067.

Hazrati, E., Galen, B., Lu, W., Wang, W., Ouyang, Y., Keller, M.J., Lehrer, R.I., and Herold, B.C. (2006). Human alpha- and beta-defensins block multiple steps in herpes simplex virus infection. J. Immunol. Baltim. Md 1950 *177*, 8658–8666.

Hein, M., Valore, E.V., Helmig, R.B., Uldbjerg, N., and Ganz, T. (2002). Antimicrobial factors in the cervical mucus plug. Am. J. Obstet. Gynecol. *187*, 137–144.

Hellemans, J., Mortier, G., Paepe, A.D., Speleman, F., and Vandesompele, J. (2007). qBase relative quantification framework and software for management and automated analysis of real-time quantitative PCR data. Genome Biol. *8*, R19.

Henseler, T., and Christophers, E. (1995). Disease concomitance in psoriasis. J. Am. Acad. Dermatol. *32*, 982–986.

Herath, S., Fischer, D.P., Werling, D., Williams, E.J., Lilly, S.T., Dobson, H., Bryant, C.E., and Sheldon, I.M. (2006). Expression and Function of Toll-Like Receptor 4 in the Endometrial Cells of the Uterus. Endocrinology *147*, 562–570.

Herrera, R., Morris, M., Rosbe, K., Feng, Z., Weinberg, A., and Tugizov, S. (2016). Human beta-defensins 2 and -3 cointernalize with human immunodeficiency virus via heparan sulfate proteoglycans and reduce infectivity of intracellular virions in tonsil epithelial cells. Virology *487*, 172–187.

Hervas-Stubbs, S., Perez-Gracia, J.L., Rouzaut, A., Sanmamed, M.F., Bon, A.L., and Melero, I. (2011). Direct Effects of Type I Interferons on Cells of the Immune System. Clin. Cancer Res. *17*, 2619–2627.

Hickey, D.K., Fahey, J.V., and Wira, C.R. (2013). Mouse estrous cycle regulation of vaginal versus uterine cytokines, chemokines, α-/β-defensins and TLRs. Innate Immun. *19*, 121–131.

Hindorff, L.A., Sethupathy, P., Junkins, H.A., Ramos, E.M., Mehta, J.P., Collins, F.S., and Manolio, T.A. (2009). Potential etiologic and functional implications of genome-wide association loci for human diseases and traits. Proc. Natl. Acad. Sci. *106*, 9362–9367.

Hirsch, T., Spielmann, M., Zuhaili, B., Fossum, M., Metzig, M., Koehler, T., Steinau, H.-U., Yao, F., Onderdonk, A.B., Steinstraesser, L., et al. (2009). Human beta-defensin-3 promotes wound healing in infected diabetic wounds. J. Gene Med. *11*, 220–228.

Hogarth, C.A., and Griswold, M.D. (2010). The key role of vitamin A in spermatogenesis. J. Clin. Invest. *120*, 956–962.

Holcmann, M., and Sibilia, M. (2015). Mechanisms underlying skin disorders induced by EGFR inhibitors. Mol. Cell. Oncol. *2*.

Hollox, E.J., Huffmeier, U., Zeeuwen, P.L.J.M., Palla, R., Lascorz, J., Rodijk-Olthuis, D., van de Kerkhof, P.C.M., Traupe, H., de Jongh, G., den Heijer, M., et al. (2008). Psoriasis is associated with increased beta-defensin genomic copy number. Nat. Genet. *40*, 23–25.

Houe, H. (1999). Epidemiological features and economical importance of bovine virus diarrhoea virus (BVDV) infections. Vet. Microbiol. *64*, 89–107.

Hu, S., Yao, G., Guan, X., Ni, Z., Ma, W., Wilson, E.M., French, F.S., Liu, Q., and Zhang, Y. (2010). Research Resource: Genome-Wide Mapping of in Vivo Androgen Receptor Binding Sites in Mouse Epididymis. Mol. Endocrinol. *24*, 2392.

Hu, S.-G., Zou, M., Yao, G.-X., Ma, W.-B., Zhu, Q.-L., Li, X.-Q., Chen, Z.-J., and Sun, Y. (2014). Androgenic regulation of beta-defensins in the mouse epididymis. Reprod. Biol. Endocrinol. *12*, 76.

Huang, Y., Liu, H., Li, S., Tang, Y., Wei, B., Yu, H., and Wang, C. (2014). MAVS-MKK7-JNK2 Defines a Novel Apoptotic Signaling Pathway during Viral Infection. PLOS Pathog. *10*, e1004020.

Hultmark, D., Steiner, H., Rasmuson, T., and Boman, H.G. (1980). Insect Immunity. Purification and Properties of Three Inducible Bactericidal Proteins from Hemolymph of Immunized Pupae of Hyalophora cecropia. Eur. J. Biochem. *106*, 7–16.

Hural, J.A., Kwan, M., Henkel, G., Hock, M.B., and Brown, M.A. (2000). An Intron Transcriptional Enhancer Element Regulates IL-4 Gene Locus Accessibility in Mast Cells. J. Immunol. *165*, 3239–3249.

Hymøller, L., Jensen, S.K., Lindqvist, H., Johansson, B., Nielsen, M.O., and Nadeau, E. (2009). Supplementing dairy steers and organically managed dairy cows with synthetic vitamin D3 is unnecessary at pasture during exposure to summer sunlight. J. Dairy Res. *76*, 372–378.

ICBF (2016). ICBF 2016 Calving Statistics.

Ireland, J.J., Murphee, R.L., and Coulson, P.B. (1980). Accuracy of Predicting Stages of Bovine Estrous Cycle by Gross Appearance of the Corpus Luteum1. J. Dairy Sci. *63*, 155–160.

Ishikawa, H., and Barber, G.N. (2008). STING is an endoplasmic reticulum adaptor that facilitates innate immune signalling. Nature *455*, 674–678.

Ishikawa, T., Kanda, N., Hau, C.S., Tada, Y., and Watanabe, S. (2009). Histamine induces human beta-defensin-3 production in human keratinocytes. J. Dermatol. Sci. *56*, 121–127.

Jacca, S., Franceschi, V., Colagiorgi, A., Sheldon, M., and Donofrio, G. (2013). Bovine Endometrial Stromal Cells Support Tumor Necrosis Factor Alpha-Induced Bovine Herpesvirus Type 4 Enhanced Replication. Biol. Reprod. *88*, 135.

Jarczak, J., Kościuczuk, E.M., Lisowski, P., Strzałkowska, N., Jóźwik, A., Horbańczuk, J., Krzyżewski, J., Zwierzchowski, L., and Bagnicka, E. (2013). Defensins: Natural component of human innate immunity. Hum. Immunol. *74*, 1069–1079.

Jin, G., Kawsar, H.I., Hirsch, S.A., Zeng, C., Jia, X., Feng, Z., Ghosh, S.K., Zheng, Q.Y., Zhou, A., McIntyre, T.M., et al. (2010). An Antimicrobial Peptide Regulates Tumor-Associated Macrophage Trafficking via the Chemokine Receptor CCR2, a Model for Tumorigenesis. PLoS ONE *5*, e10993.

Johansen, C., Bertelsen, T., Ljungberg, C., Mose, M., and Iversen, L. (2016). Characterization of TNF-α– and IL-17A–Mediated Synergistic Induction of DEFB4 Gene Expression in Human Keratinocytes through IκBζ. J. Invest. Dermatol. *136*, 1608–1616.

Jolma, A., Yin, Y., Nitta, K.R., Dave, K., Popov, A., Taipale, M., Enge, M., Kivioja, T., Morgunova, E., and Taipale, J. (2015). DNA-dependent formation of transcription factor pairs alters their binding specificity. Nature *527*, 384–388.

Joly, S., Maze, C., McCray, P.B., and Guthmiller, J.M. (2004). Human β-Defensins 2 and 3 Demonstrate Strain-Selective Activity against Oral Microorganisms. J. Clin. Microbiol. *42*, 1024–1029.

Joly, S., Organ, C.C., Johnson, G.K., McCray Jr., P.B., and Guthmiller, J.M. (2005). Correlation between β-defensin expression and induction profiles in gingival keratinocytes. Mol. Immunol. *42*, 1073–1084.

de Jongh, G.J., Zeeuwen, P.L.J.M., Kucharekova, M., Pfundt, R., van der Valk, P.G., Blokx, W., Dogan, A., Hiemstra, P.S., van de Kerkhof, P.C., and Schalkwijk, J. (2005). High Expression Levels of Keratinocyte Antimicrobial Proteins in Psoriasis Compared with Atopic Dermatitis. J. Invest. Dermatol. *125*, 1163–1173.

Juven-Gershon, T., and Kadonaga, J.T. (2010). Regulation of gene expression via the core promoter and the basal transcriptional machinery. Dev. Biol. *339*, 225–229.

Kaikkonen, M.U., Lam, M.T.Y., and Glass, C.K. (2011). Non-coding RNAs as regulators of gene expression and epigenetics. Cardiovasc. Res. *90*, 430–440.

Kallsen, K., Andresen, E., and Heine, H. (2012). Histone Deacetylase (HDAC) 1 Controls the Expression of Beta Defensin 1 in Human Lung Epithelial Cells. PLOS ONE *7*, e50000.

Kalus, A.A., Fredericks, L.P., Hacker, B.M., Dommisch, H., Presland, R.B., Kimball, J.R., and Dale, B.A. (2009). Association of a genetic polymorphism (-44 C/G SNP) in the human DEFB1 gene with expression and inducibility of multiple β-defensins in gingival keratinocytes. BMC Oral Health *9*, 1.

Kanda, N., Ishikawa, T., and Watanabe, S. (2010). Prostaglandin D2 induces the production of human beta-defensin-3 in human keratinocytes. Biochem. Pharmacol. *79*, 982–989.

Kanda, N., Kamata, M., Tada, Y., Ishikawa, T., Sato, S., and Watanabe, S. (2011). Human β-defensin-2 enhances IFN-γ and IL-10 production and suppresses IL-17 production in T cells. J. Leukoc. Biol. *89*, 935–944.

Kandaswamy, K., Liew, T.H., Wang, C.Y., Huston-Warren, E., Meyer-Hoffert, U., Hultenby, K., Schröder, J.M., Caparon, M.G., Normark, S., Henriques-Normark, B., et al. (2013). Focal targeting by human β-defensin 2 disrupts localized virulence factor assembly sites in Enterococcus faecalis. Proc. Natl. Acad. Sci. 201319066.

Kang, D., Gopalkrishnan, R.V., Lin, L., Randolph, A., Valerie, K., Pestka, S., and Fisher, P.B. (2003). Expression analysis and genomic characterization of human melanoma differentiation associated gene-5, mda-5: a novel type I interferon-responsive apoptosis-inducing gene. Oncogene *23*, 1789–1800.

Kao, C.-Y., Chen, Y., Thai, P., Wachi, S., Huang, F., Kim, C., Harper, R.W., and Wu, R. (2004). IL-17 Markedly Up-Regulates β-Defensin-2 Expression in Human Airway Epithelium via JAK and NF-κB Signaling Pathways. J. Immunol. *173*, 3482–3491.

Kao, C.-Y., Kim, C., Huang, F., and Wu, R. (2008). Requirements for Two Proximal NF-κB Binding Sites and IκB-ζ in IL-17A-induced Human β-Defensin 2 Expression by Conducting Airway Epithelium. J. Biol. Chem. *283*, 15309–15318.

Karhausen, J., Furuta, G.T., Tomaszewski, J.E., Johnson, R.S., Colgan, S.P., and Haase, V.H. (2004). Epithelial hypoxia-inducible factor-1 is protective in murine experimental colitis. J. Clin. Invest. *114*, 1098–1106.

Kasahara, T., Mukaida, N., Yamashita, K., Yagisawa, H., Akahoshi, T., and Matsushima, K. (1991). IL-1 and TNF-alpha induction of IL-8 and monocyte chemotactic and activating factor (MCAF) mRNA expression in a human astrocytoma cell line. Immunology *74*, 60–67.

Kasimanickam, R.K., Kasimanickam, V.R., Olsen, J.R., Jeffress, E.J., Moore, D.A., and Kastelic, J.P. (2013). Associations among serum pro- and anti-inflammatory cytokines, metabolic mediators,

body condition, and uterine disease in postpartum dairy cows. Reprod. Biol. Endocrinol. RBE *11*, 103.

Kastelic, J., and Thundathil, J. (2008). Breeding Soundness Evaluation and Semen Analysis for Predicting Bull Fertility. Reprod. Domest. Anim. *43*, 368–373.

Kato, H., Sato, S., Yoneyama, M., Yamamoto, M., Uematsu, S., Matsui, K., Tsujimura, T., Takeda, K., Fujita, T., Takeuchi, O., et al. (2005). Cell Type-Specific Involvement of RIG-I in Antiviral Response. Immunity *23*, 19–28.

Kato, H., Takeuchi, O., Sato, S., Yoneyama, M., Yamamoto, M., Matsui, K., Uematsu, S., Jung, A., Kawai, T., Ishii, K.J., et al. (2006). Differential roles of MDA5 and RIG-I helicases in the recognition of RNA viruses. Nature *441*, 101–105.

Kawsar, H.I., Weinberg, A., Hirsch, S.A., Venizelos, A., Howell, S., Jiang, B., and Jin, G. (2009). Overexpression of human β-defensin-3 in oral dysplasia: Potential role in macrophage trafficking. Oral Oncol. *45*, 696–702.

Kellis, M., Wold, B., Snyder, M.P., Bernstein, B.E., Kundaje, A., Marinov, G.K., Ward, L.D., Birney, E., Crawford, G.E., Dekker, J., et al. (2014). Defining functional DNA elements in the human genome. Proc. Natl. Acad. Sci. *111*, 6131–6138.

Kelly, C.J., Glover, L.E., Campbell, E.L., Kominsky, D.J., Ehrentraut, S.F., Bowers, B.E., Bayless, A.J., Saeedi, B.J., and Colgan, S.P. (2013). Fundamental role for HIF-1α in constitutive expression of human β defensin-1. Mucosal Immunol.

Khabar, K.S.A., and Young, H.A. (2007). Post-transcriptional control of the interferon system. Biochimie *89*, 761–769.

Kim, G., Khanal, P., Lim, S.-C., Yun, H.J., Ahn, S.-G., Ki, S.H., and Choi, H.S. (2013). Interleukin-17 induces AP-1 activity and cellular transformation via upregulation of tumor progression locus 2 activity. Carcinogenesis *34*, 341–350.

Kim, K., Kim, G., Kim, J.-Y., Yun, H.J., Lim, S.-C., and Choi, H.S. (2014a). Interleukin-22 promotes epithelial cell transformation and breast tumorigenesis via MAP3K8 activation. Carcinogenesis *35*, 1352–1361.

Kim, K.-H., Lee, J., Han, J.H., and Myung, S.C. (2014b). Beta-Defensin 124 Is Required for Efficient Innate Immune Responses in Prostate Epithelial RWPE-1 Cells. Korean J. Urol. *55*, 417–425.

Kin, K., Nnamani, M.C., Lynch, V.J., Michaelides, E., and Wagner, G.P. (2015). Cell-type phylogenetics and the origin of endometrial stromal cells. Cell Rep. *10*, 1398–1409.

King, A.E., Fleming, D.C., Critchley, H.O.D., and Kelly, R.W. (2002). Regulation of natural antibiotic expression by inflammatory mediators and mimics of infection in human endometrial epithelial cells. Mol. Hum. Reprod. *8*, 341–349.

King, A.E., Fleming, D.C., Critchley, H.O.., and Kelly, R.W. (2003). Differential expression of the natural antimicrobials, beta-defensins 3 and 4, in human endometrium. J. Reprod. Immunol. *59*, 1–16.

King, A.E., Paltoo, A., Kelly, R.W., Sallenave, J.-M., Bocking, A.D., and Challis, J.R.G. (2007). Expression of Natural Antimicrobials by Human Placenta and Fetal Membranes. Placenta *28*, 161–169.

Klamminger, S., Prunner, I., Giuliodori, M., and Drillich, M. (2017). Uterine infection with bovine herpesvirus type 4 in dairy cows. Reprod. Domest. Anim. *52*, 115–121.

Klein, C., Bauersachs, S., Ulbrich, S.E., Einspanier, R., Meyer, H.H.D., Schmidt, S.E.M., Reichenbach, H.-D., Vermehren, M., Sinowatz, F., Blum, H., et al. (2006). Monozygotic Twin Model Reveals Novel Embryo-Induced Transcriptome Changes of Bovine Endometrium in the Preattachment Period. Biol. Reprod. *74*, 253–264.

Knudsen, L.R.V., Karstrup, C.C., Pedersen, H.G., Angen, Ø., Agerholm, J.S., Rasmussen, E.L., Jensen, T.K., and Klitgaard, K. (2016). An investigation of the microbiota in uterine flush samples and endometrial biopsies from dairy cows during the first 7 weeks postpartum. Theriogenology *86*, 642–650.

Kolbinger, F., Loesche, C., Valentin, M.-A., Jiang, X., Cheng, Y., Jarvis, P., Thomas Peters, Calonder, C., Bruin, G., Polus, F., et al. (2017). β-defensin-2 is a responsive biomarker of IL-17A-driven skin pathology in psoriasis. J. Allergy Clin. Immunol. *139*, 923–932.

Kosikowska, P., and Lesner, A. (2016). Antimicrobial peptides (AMPs) as drug candidates: a patent review (2003–2015). Expert Opin. Ther. Pat. *26*, 689–702.

Kota, S., Sabbah, A., Chang, T.H., Harnack, R., Xiang, Y., Meng, X., and Bose, S. (2008). Role of Human β-Defensin-2 during Tumor Necrosis Factor-α/NF-κB-mediated Innate Antiviral Response against Human Respiratory Syncytial Virus. J. Biol. Chem. *283*, 22417–22429.

Kowalik, T.F., Yurochko, A.D., Rinehart, C.A., Lee, C.-Y.G., and Huang, E.-S. (1994). Productive Infection of Human Endometrial Stromal Cells by Human Cytomegalovirus. Virology *202*, 247–257.

Krisanaprakornkit, S., Kimball, J.R., and Dale, B.A. (2002). Regulation of Human β-Defensin-2 in Gingival Epithelial Cells: The Involvement of Mitogen-Activated Protein Kinase Pathways, But Not the NF-κB Transcription Factor Family. J. Immunol. *168*, 316–324.

Kwon, A.T., Arenillas, D.J., Worsley Hunt, R., and Wasserman, W.W. (2012). oPOSSUM-3: advanced analysis of regulatory motif over-representation across genes or ChIP-Seq datasets. G3 Bethesda Md *2*, 987–1002.

Lande, R., Gregorio, J., Facchinetti, V., Chatterjee, B., Wang, Y.-H., Homey, B., Cao, W., Wang, Y.-H., Su, B., Nestle, F.O., et al. (2007). Plasmacytoid dendritic cells sense self-DNA coupled with antimicrobial peptide. Nature *449*, 564–569.

Lande, R., Chamilos, G., Ganguly, D., Demaria, O., Frasca, L., Durr, S., Conrad, C., Schröder, J., and Gilliet, M. (2015). Cationic antimicrobial peptides in psoriatic skin cooperate to break innate tolerance to self-DNA. Eur. J. Immunol. *45*, 203–213.

LeBlanc, S. (2012). Interactions of Metabolism, Inflammation, and Reproductive Tract Health in the Postpartum Period in Dairy Cattle. Reprod. Domest. Anim. *47*, 18–30.

LeBlanc, S.J., Duffield, T.F., Leslie, K.E., Bateman, K.G., Keefe, G.P., Walton, J.S., and Johnson, W.H. (2002). Defining and Diagnosing Postpartum Clinical Endometritis and its Impact on Reproductive Performance in Dairy Cows. J. Dairy Sci. *85*, 2223–2236.

Lee, J., Han, J.H., Jang, A., Kim, J.W., Hong, S.A., and Myung, S.C. (2016). DNA Methylation-Mediated Downregulation of DEFB1 in Prostate Cancer Cells. PLOS ONE *11*, e0166664.

Lee, J.W., Wang, P., Kattah, M.G., Youssef, S., Steinman, L., DeFea, K., and Straus, D.S. (2008). Differential Regulation of Chemokines by IL-17 in Colonic Epithelial Cells. J. Immunol. *181*, 6536–6545.

Lee, W.J., Cha, H.W., Sohn, M.Y., Lee, S.-J., and Kim, D.W. (2012). Vitamin D increases expression of cathelicidin in cultured sebocytes. Arch. Dermatol. Res. *304*, 627–632.

Lehrer, R.I., and Ganz, T. (1999). Antimicrobial peptides in mammalian and insect host defence. Curr. Opin. Immunol. *11*, 23–27.

Lehrer, R.I., and Lu, W. (2012). α-Defensins in human innate immunity. Immunol. Rev. *245*, 84–112.

LeMessurier, K.S., Lin, Y., McCullers, J.A., and Samarasinghe, A.E. (2016). Antimicrobial peptides alter early immune response to influenza A virus infection in C57BL/6 mice. Antiviral Res.

Leung, J.Y., McKenzie, F.E., Uglialoro, A.M., Flores-Villanueva, P.O., Sorkin, B.C., Yunis, E.J., Hartl, D.L., and Goldfeld, A.E. (2000). Identification of phylogenetic footprints in primate tumor necrosis factor-α promoters. Proc. Natl. Acad. Sci. *97*, 6614–6618.

Lewis, G.S. (2003). Steroidal regulation of uterine resistance to bacterial infection in livestock. Reprod. Biol. Endocrinol. *1*, 117.

Li, A., Gan, Y., Wang, R., Liu, Y., Ma, T., Huang, M., and Cui, X. (2014). IL-22 Up-Regulates β-Defensin-2 Expression in Human Alveolar Epithelium via STAT3 but Not NF-κB Signaling Pathway. Inflammation.

Li, J., Raghunath, M., Tan, D., Lareu, R.R., Chen, Z., and Beuerman, R.W. (2006). Defensins HNP1 and HBD2 Stimulation of Wound-Associated Responses in Human Conjunctival Fibroblasts. Invest. Ophthalmol. Vis. Sci. *47*, 3811–3819.

Li, P., Wu, T., Su, X., and Shi, Y. (2015). Activation of Vitamin D Regulates Response of Human Bronchial Epithelial Cells to Aspergillus fumigatus in an Autocrine Fashion. Mediators Inflamm. *2015*, e208491.

Lichtenberger, B.M., Gerber, P.A., Holcmann, M., Buhren, B.A., Amberg, N., Smolle, V., Schrumpf, H., Boelke, E., Ansari, P., Mackenzie, C., et al. (2013). Epidermal EGFR Controls Cutaneous Host Defense and Prevents Inflammation. Sci. Transl. Med. *5*, 199ra111-199ra111.

Lioi, A.B., Ferrari, B.M., Dubyak, G.R., Weinberg, A., and Sieg, S.F. (2015). Human β Defensin-3 Increases CD86 Expression on Monocytes by Activating the ATP-Gated Channel P2X7. J. Immunol. 1401319.

Lippolis, J.D., Reinhardt, T.A., Sacco, R.A., Nonnecke, B.J., and Nelson, C.D. (2011). Treatment of an Intramammary Bacterial Infection with 25-Hydroxyvitamin D3. PLoS ONE *6*, e25479.

Liu, G.E., Hou, Y., Zhu, B., Cardone, M.F., Jiang, L., Cellamare, A., Mitra, A., Alexander, L.J., Coutinho, L.L., Dell'Aquila, M.E., et al. (2010). Analysis of copy number variations among diverse cattle breeds. Genome Res. *20*, 693–703.

Liu, H., Yu, H., Gu, Y., Xin, A., Zhang, Y., Diao, H., and Lin, D. (2013). Human beta-defensin DEFB126 is capable of inhibiting LPS-mediated inflammation. Appl. Microbiol. Biotechnol. *97*, 3395–3408.

Liu, L., Zhao, C., Heng, H.H.Q., and Ganz, T. (1997). The Human β-Defensin-1 and α-Defensins Are Encoded by Adjacent Genes: Two Peptide Families with Differing Disulfide Topology Share a Common Ancestry. Genomics *43*, 316–320.

Lohnes, D., and Jones, G. (1987). Side chain metabolism of vitamin D3 in osteosarcoma cell line UMR-106. Characterization of products. J. Biol. Chem. *262*, 14394–14401.

Loots, G.G., Locksley, R.M., Blankespoor, C.M., Wang, Z.E., Miller, W., Rubin, E.M., and Frazer, K.A. (2000). Identification of a Coordinate Regulator of Interleukins 4, 13, and 5 by Cross-Species Sequence Comparisons. Science *288*, 136–140.

Lu, Z., Kim, K.-A., Suico, M.A., Shuto, T., Li, J.-D., and Kai, H. (2004). MEF up-regulates human β-defensin 2 expression in epithelial cells. FEBS Lett. *561*, 117–121.

Lundberg, A.M., Drexler, S.K., Monaco, C., Williams, L.M., Sacre, S.M., Feldmann, M., and Foxwell, B.M. (2007). Key differences in TLR3/poly I:C signaling and cytokine induction by human primary cells: a phenomenon absent from murine cell systems. Blood *110*, 3245–3252.

Lynn, D.J., and Bradley, D.G. (2007). Discovery of α-defensins in basal mammals. Dev. Comp. Immunol. *31*, 963–967.

Lyu, J., Bian, T., Chen, B., Cui, D., Li, L., Gong, L., and Yan, F. (2017). β-defensin 3 modulates macrophage activation and orientation during acute inflammatory response to Porphyromonas gingivalis lipopolysaccharide. Cytokine *92*, 48–54.

Ma, Z., and Damania, B. (2016). The cGAS-STING Defense Pathway and Its Counteraction by Viruses. Cell Host Microbe *19*, 150–158.

Ma, F., Li, B., Liu, S., Iyer, S.S., Yu, Y., Wu, A., and Cheng, G. (2015a). Positive feedback regulation of type I IFN production by the IFN-inducible DNA sensor cGAS. J. Immunol. Baltim. Md 1950 *194*, 1545–1554.

Ma, F., Li, B., Yu, Y., Iyer, S.S., Sun, M., and Cheng, G. (2015b). Positive feedback regulation of type I interferon by the interferon-stimulated gene STING. EMBO Rep. *16*, 202–212.

Ma, S.-D., Lancto, C.A., Enomoto, S., Abrahamsen, M.S., and Rutherford, M.S. (2010). Expression and regulation of IL-22 by bovine peripheral blood gamma/delta T cells. Gene *451*, 6–14.

Mahlapuu, M., Håkansson, J., Ringstad, L., and Björn, C. (2016). Antimicrobial Peptides: An Emerging Category of Therapeutic Agents. Front. Cell. Infect. Microbiol. *6*.

Mansour, S.C., Pena, O.M., and Hancock, R.E.W. (2014). Host defense peptides: front-line immunomodulators. Trends Immunol. *35*, 443–450.

Marsman, J., and Horsfield, J.A. (2012). Long distance relationships: Enhancer–promoter communication and dynamic gene transcription. Biochim. Biophys. Acta BBA - Gene Regul. Mech. *1819*, 1217–1227.

Martin, D., Pantoja, C., Miñán, A.F., Valdes-Quezada, C., Moltó, E., Matesanz, F., Bogdanović, O., Calle-Mustienes, E. de la, Domínguez, O., Taher, L., et al. (2011). Genome-wide CTCF distribution in vertebrates defines equivalent sites that aid the identification of disease-associated genes. Nat. Struct. Mol. Biol. *18*, 708–714.

Martineau, A.R., Wilkinson, K.A., Newton, S.M., Floto, R.A., Norman, A.W., Skolimowska, K., Davidson, R.N., Sørensen, O.E., Kampmann, B., Griffiths, C.J., et al. (2007). IFN-γ- and TNF-Independent Vitamin D-Inducible Human Suppression of Mycobacteria: The Role of Cathelicidin LL-37. J. Immunol. *178*, 7190–7198.

Mathelier, A., Zhao, X., Zhang, A.W., Parcy, F., Worsley-Hunt, R., Arenillas, D.J., Buchman, S., Chen, C., Chou, A., Ienasescu, H., et al. (2013). JASPAR 2014: an extensively expanded and updated open-access database of transcription factor binding profiles. Nucleic Acids Res. gkt997.

Mawer, E.B., Backhouse, J., Holman, C.A., Lumb, G.A., and Stanbury, S.W. (1972). The Distribution and Storage of Vitamin D and its Metabolites in Human Tissues. Clin. Sci. *43*, 413–431.

McGaffin, K.R., Acktinson, L.E., and Chrysogelos, S.A. (2004). Growth and EGFR Regulation in Breast Cancer Cells by Vitamin D and Retinoid Compounds. Breast Cancer Res. Treat. *86*, 55–73.

McGlasson, S.L., Semple, F., MacPherson, H., Gray, M., Davidson, D.J., and Dorin, J.R. (2017). Human β-defensin 3 increases the TLR9-dependent response to bacterial DNA. Eur. J. Immunol. n/a-n/a.

McKercher, D. (1973). Viruses of other vertebrates. In The Herpesviruses, (Academic Press), pp. 427–494.

Meade, K.G., Cormican, P., Narciandi, F., Lloyd, A.T., and O'Farrelly, C. (2013). The Bovine β-defensin Gene Family; Opportunities to Improve Animal Health? Physiol. Genomics *46*, 17–28.

Merriman, K.E., Kweh, M.F., Powell, J.L., Lippolis, J.D., and Nelson, C.D. (2015). Multiple β-defensin genes are upregulated by the vitamin D pathway in cattle. J. Steroid Biochem. Mol. Biol. *154*, 120–129.

Merriman, K.E., Poindexter, M.B., Kweh, M.F., Santos, J.E.P., and Nelson, C.D. (2017). Intramammary 1,25-dihydroxyvitamin D3 treatment increases expression of host-defense genes in mammary immune cells of lactating dairy cattle. J. Steroid Biochem. Mol. Biol.

Mignone, F., Gissi, C., Liuni, S., and Pesole, G. (2002). Untranslated regions of mRNAs. Genome Biol. *3*, reviews0004.1-reviews0004.10.

Mirabzadeh-Ardakani, A., Griebel, P., and Schmutz, S.M. (2014). Identification of a new non-coding exon and haplotype variability in the cattle DEFB103 gene. Gene *551*, 183–188.

Mirabzadeh-Ardakani, A., Solie, J., Gonzalez-Cano, P., Schmutz, S.M., and Griebel, P.J. (2016). Tissue- and age-dependent expression of the bovine DEFB103 gene and protein. Cell Tissue Res. *363*, 479–490.

Mitchell, P.J., and Tjian, R. (1989). Transcriptional regulation in mammalian cells by sequence-specific DNA binding proteins. Science *245*, 371–378.

Molet, S., Hamid, Q., Davoineb, F., Nutku, E., Tahaa, R., Pagé, N., Olivenstein, R., Elias, J., and Chakir, J. (2001). IL-17 is increased in asthmatic airways and induces human bronchial fibroblasts to produce cytokines. J. Allergy Clin. Immunol. *108*, 430–438.

Mor, G., Cardenas, I., Abrahams, V., and Guller, S. (2011). Inflammation and pregnancy: the role of the immune system at the implantation site. Ann. N. Y. Acad. Sci. *1221*, 80–87.

Morampudi, V., Braun, M.Y., and D'Souza, S. (2011). Modulation of Early β-Defensin-2 Production as a Mechanism Developed by Type I Toxoplasma gondii To Evade Human Intestinal Immunity. Infect. Immun. *79*, 2043–2050.

More, S.J., McKenzie, K., O'Flaherty, J., Doherty, M.L., Cromie, A.R., and Magan, M.J. (2010). Setting priorities for non-regulatory animal health in Ireland: Results from an expert Policy Delphi study and a farmer priority identification survey. Prev. Vet. Med. *95*, 198–207.

Morizane, S., and Gallo, R.L. (2012). Antimicrobial peptides in the pathogenesis of psoriasis. J. Dermatol. *39*, 225–230.

Muhammad, J.S., Zaidi, S.F., Zhou, Y., Sakurai, H., and Sugiyama, T. (2016). Novel epidermal growth factor receptor pathway mediates release of human β-defensin 3 from Helicobacter pylori-infected gastric epithelial cells. Pathog. Dis. *74*, ftv128.

Mulcahy, M.E., Leech, J.M., Renauld, J.-C., Mills, K.H., and McLoughlin, R.M. (2016). Interleukin-22 regulates antimicrobial peptide expression and keratinocyte differentiation to control Staphylococcus aureus colonization of the nasal mucosa. Mucosal Immunol.

Nagaoka, I., Niyonsaba, F., Tsutsumi-Ishii, Y., Tamura, H., and Hirata, M. (2008). Evaluation of the effect of human β-defensins on neutrophil apoptosis. Int. Immunol. *20*, 543–553.

Narciandi, F. (2013). Structural and functional characterisation of a novel bovine beta-defensin gene cluster. Trinity College Dublin.

Narciandi, F., Lloyd, A.T., Chapwanya, A., Farrelly, C.O., and Meade, K.G. (2011). Reproductive tissue-specific expression profiling and genetic variation across a 19 gene bovine β-defensin cluster. Immunogenetics *63*, 641–651.

Neidleman, J.A., Chen, J.C., Kohgadai, N., Müller, J.A., Laustsen, A., Thavachelvam, K., Jang, K.S., Stürzel, C.M., Jones, J.J., Ochsenbauer, C., et al. (2017). Mucosal stromal fibroblasts markedly enhance HIV infection of CD4+ T cells. PLOS Pathog. *13*, e1006163.

Nelson, C.D., Reinhardt, T.A., Thacker, T.C., Beitz, D.C., and Lippolis, J.D. (2010a). Modulation of the bovine innate immune response by production of 1α,25-dihydroxyvitamin D3 in bovine monocytes. J. Dairy Sci. *93*, 1041–1049.

Nelson, C.D., Reinhardt, T.A., Beitz, D.C., and Lippolis, J.D. (2010b). In Vivo Activation of the Intracrine Vitamin D Pathway in Innate Immune Cells and Mammary Tissue during a Bacterial Infection. PLoS ONE *5*, e15469.

Nelson, C.D., Nonnecke, B.J., Reinhardt, T.A., Waters, W.R., Beitz, D.C., and Lippolis, J.D. (2011). Regulation of Mycobacterium-Specific Mononuclear Cell Responses by 25-Hydroxyvitamin D3. PLoS ONE *6*, e21674.

Newcomer, M.E., and Ong, D.E. (1990). Purification and crystallization of a retinoic acid-binding protein from rat epididymis. Identity with the major androgen-dependent epididymal proteins. J. Biol. Chem. *265*, 12876–12879.

Nickel, D., Busch, M., Mayer, D., Hagemann, B., Knoll, V., and Stenger, S. (2012). Hypoxia triggers the expression of human β defensin 2 and antimicrobial activity against Mycobacterium tuberculosis in human macrophages. J. Immunol. Baltim. Md 1950 *188*, 4001–4007.

Nishimura, M., Abiko, Y., Kurashige, Y., Takeshima, M., Yamazaki, M., Kusano, K., Saitoh, M., Nakashima, K., Inoue, T., and Kaku, T. (2004). Effect of defensin peptides on eukaryotic cells: primary epithelial cells, fibroblasts and squamous cell carcinoma cell lines. J. Dermatol. Sci. *36*, 87–95.

Niyonsaba, F., Someya, A., Hirata, M., Ogawa, H., and Nagaoka, I. (2001). Evaluation of the effects of peptide antibiotics human β-defensins-1/-2 and LL-37 on histamine release and prostaglandin D2 production from mast cells. Eur. J. Immunol. *31*, 1066–1075.

Niyonsaba, F., Ogawa, H., and Nagaoka, I. (2004). Human beta-defensin-2 functions as a chemotactic agent for tumour necrosis factor-alpha-treated human neutrophils. Immunology *111*, 273–281.

Niyonsaba, F., Ushio, H., Nakano, N., Ng, W., Sayama, K., Hashimoto, K., Nagaoka, I., Okumura, K., and Ogawa, H. (2006). Antimicrobial Peptides Human β-Defensins Stimulate Epidermal Keratinocyte Migration, Proliferation and Production of Proinflammatory Cytokines and Chemokines. J. Invest. Dermatol. *127*, 594–604.

Nonnecke, B.J., Kimura, K., Goff, J.P., and Kehrli, M.E. (2003). Effects of the Mammary Gland on Functional Capacities of Blood Mononuclear Leukocyte Populations from Periparturient Cows1. J. Dairy Sci. *86*, 2359–2368.

Noronha, S.A.A.C. de, Noronha, S.M.R. de, Lanziani, L.E., Ipolito, M.Z., Ferreira, L.M., and Gragnani, A. (2014). Human beta defensin-4 and keratinocyte growth factor gene expression in cultured keratinocyte and fibroblasts of burned patients. Acta Cir. Bras. *29 Suppl 3*, 39–43.

Nurjadi, D., Herrmann, E., Hinderberger, I., and Zanger, P. (2013). Impaired β-Defensin Expression in Human Skin Links DEFB1 Promoter Polymorphisms With Persistent Staphylococcus aureus Nasal Carriage. J. Infect. Dis. *207*, 666–674.

Oliveira, L.J., Mansourri-Attia, N., Fahey, A.G., Browne, J., Forde, N., Roche, J.F., Lonergan, P., and Fair, T. (2013). Characterization of the Th Profile of the Bovine Endometrium during the Oestrous Cycle and Early Pregnancy. PLoS ONE *8*, e75571.

Olliver, M., Spelmink, L., Hiew, J., Meyer-Hoffert, U., Henriques-Normark, B., and Bergman, P. (2013). Immunomodulatory Effects of Vitamin D on Innate and Adaptive Immune Responses to Streptococcus pneumoniae. J. Infect. Dis. *208*, 1474–1481.

Omagari, D., Takenouchi-Ohkubo, N., Endo, S., Ishigami, T., Sawada, A., Moro, I., Asano, M., and Komiyama, K. (2011). Nuclear factor kappa B plays a pivotal role in polyinosinic-polycytidylic acid-induced expression of human β-defensin 2 in intestinal epithelial cells. Clin. Exp. Immunol. *165*, 85–93.

O'Neil, D.A., Porter, E.M., Elewaut, D., Anderson, G.M., Eckmann, L., Ganz, T., and Kagnoff, M.F. (1999). Expression and regulation of the human beta-defensins hBD-1 and hBD-2 in intestinal epithelium. J. Immunol. Baltim. Md 1950 *163*, 6718–6724.

O'Neill, L.A.J., Golenbock, D., and Bowie, A.G. (2013). The history of Toll-like receptors- redefining innate immunity. Nat. Rev. Immunol. *13*, 453–460.

O'Neill, R., Gallagher, C., Tratalos, J., and Graham, D. (2016). Patterns of exposure to bovine herpesvirus-1 and -4 in Irish cattle. In Proceedings of the 29th World Buiatrics Congress, Dublin, Ireland, 3-8 July 2016, (Dublin, Ireland), p.

Ong, D.E., Newcomer, M.E., Lareyre, J.-J., and Orgebin-Crist, M.-C. (2000). Epididymal retinoic acid-binding protein. Biochim. Biophys. Acta BBA - Protein Struct. Mol. Enzymol. *1482*, 209–217.

Ong, P.Y., Ohtake, T., Brandt, C., Strickland, I., Boguniewicz, M., Ganz, T., Gallo, R.L., and Leung, D.Y.M. (2002). Endogenous Antimicrobial Peptides and Skin Infections in Atopic Dermatitis. N. Engl. J. Med. *347*, 1151–1160.

Otero, C., Saavedra, L., Silva de Ruiz, C., Wilde, O., Holgado, A. r., and Nader-Macías, M. e. (2000). Vaginal bacterial microflora modifications during the growth of healthy cows. Lett. Appl. Microbiol. *31*, 251–254.

Otte, J.-M., Werner, I., Brand, S., Chromik, A.M., Schmitz, F., Kleine, M., and Schmidt, W.E. (2008). Human beta defensin 2 promotes intestinal wound healing in vitro. J. Cell. Biochem. *104*, 2286–2297.

Ovcharenko, I., Stubbs, L., and Loots, G.G. (2004). Interpreting mammalian evolution using Fugu genome comparisons. Genomics *84*, 890–895.

Ovcharenko, I., Loots, G.G., Giardine, B.M., Hou, M., Ma, J., Hardison, R.C., Stubbs, L., and Miller, W. (2005). Mulan: Multiple-sequence local alignment and visualization for studying function and evolution. Genome Res. *15*, 184–194.

Ozturk, A., Famili, P., and Vieira, A.R. (2010). The Antimicrobial Peptide DEFB1 Is Associated with Caries. J. Dent. Res. *89*, 631–636.

Pagani, I., Ghezzi, S., Ulisse, A., Rubio, A., Turrini, F., Garavaglia, E., Candiani, M., Castilletti, C., Ippolito, G., Poli, G., et al. (2017). Human Endometrial Stromal Cells Are Highly Permissive To Productive Infection by Zika Virus. Sci. Rep. *7*, 44286.

Parkinson, T.J. (2004). Evaluation of fertility and infertility in natural service bulls. Vet. J. *168*, 215–229.

Pascottini, O.B., Hostens, M., Dini, P., Van Eetvelde, M., Vercauteren, P., and Opsomer, G. (2016). Prevalence of cytological endometritis and effect on pregnancy outcomes at the time of insemination in nulliparous dairy heifers. J. Dairy Sci. *99*, 9051–9056.

Patel, M.V., Fahey, J.V., Rossoll, R.M., and Wira, C.R. (2013). Innate Immunity in the Vagina (Part I): Estradiol Inhibits HBD2 and Elafin Secretion by Human Vaginal Epithelial Cells. Am. J. Reprod. Immunol. *69*, 463–474.

Patil, A.A. (2005). Cross-species analysis of the mammalian beta-defensin gene family: presence of syntenic gene clusters and preferential expression in the male reproductive tract. Physiol. Genomics *23*, 5–17.

Pellett, P.E., and Roiz (2013). Herpesviridae. In Fields Virology, (New York: Wolters Kluwer), pp. 1802–1822.

Peng Jia, H., Schutte, B.C., Schudy, A., Linzmeier, R., Guthmiller, J.M., Johnson, G.K., Tack, B.F., Mitros, J.P., Rosenthal, A., Ganz, T., et al. (2001). Discovery of new human β-defensins using a genomics-based approach. Gene *263*, 211–218.

Peric, M., Koglin, S., Dombrowski, Y., Groß, K., Bradac, E., Büchau, A., Steinmeyer, A., Zügel, U., Ruzicka, T., and Schauber, J. (2009). Vitamin D Analogs Differentially Control Antimicrobial Peptide/“Alarmin”Expression in Psoriasis. PLoS ONE *4*, e6340.

Pestka, S., Krause, C.D., and Walter, M.R. (2004). Interferons, interferon-like cytokines, and their receptors. Immunol. Rev. *202*, 8–32.

Peyrin-Biroulet, L., Beisner, J., Wang, G., Nuding, S., Oommen, S.T., Kelly, D., Parmentier-Decrucq, E., Dessein, R., Merour, E., Chavatte, P., et al. (2010). Peroxisome proliferator-activated receptor gamma activation is required for maintenance of innate antimicrobial immunity in the colon. Proc. Natl. Acad. Sci. *107*, 8772–8777.

Pihlajamaa, P., Sahu, B., Lyly, L., Aittomäki, V., Hautaniemi, S., and Jänne, O.A. (2014). Tissue-specific pioneer factors associate with androgen receptor cistromes and transcription programs. EMBO J. *33*, 312–326.

Pingel, L.C., Kohlgraf, K.G., Hansen, C.J., Eastman, C.G., Dietrich, D.E., Burnell, K.K., Srikantha, R.N., Xiao, X., Bélanger, M., Progulske-Fox, A., et al. (2008). Human β-defensin 3 binds to hemagglutinin B (rHagB), a non-fimbrial adhesin from Porphyromonas gingivalis, and attenuates a pro-inflammatory cytokine response. Immunol. Cell Biol. *86*, 643–649.

Polesello, V., Zupin, L., Di Lenarda, R., Biasotto, M., Ottaviani, G., Gobbo, M., Cecco, L., Alberi, G., Pozzato, G., Crovella, S., et al. (2015). Impact of DEFB1 gene regulatory polymorphisms on hBD-1 salivary concentration. Arch. Oral Biol. *60*, 1054–1058.

Portales-Casamar, E., Thongjuea, S., Kwon, A.T., Arenillas, D., Zhao, X., Valen, E., Yusuf, D., Lenhard, B., Wasserman, W.W., and Sandelin, A. (2010). JASPAR 2010: the greatly expanded open-access database of transcription factor binding profiles. Nucleic Acids Res. *38*, D105–D110.

Prencipe, M., O'Neill, A., O'Hurley, G., Nguyen, L.K., Fabre, A., Bjartell, A., Gallagher, W.M., Morrissey, C., Kay, E.W., and Watson, R.W. (2015). Relationship between serum response factor and androgen receptor in prostate cancer. The Prostate *75*, 1704–1717.

Prietl, B., Treiber, G., Pieber, T.R., and Amrein, K. (2013). Vitamin D and Immune Function. Nutrients *5*, 2502.

Qu, Y., Fadden, A.N., Traber, M.G., and Bobe, G. (2014). Potential risk indicators of retained placenta and other diseases in multiparous cows. J. Dairy Sci. *97*, 4151–4165.

Quiñones-Mateu, M.E., Lederman, M.M., Feng, Z., Chakraborty, B., Weber, J., Rangel, H.R., Marotta, M.L., Mirza, M., Jiang, B., Kiser, P., et al. (2003). Human epithelial beta-defensins 2 and 3 inhibit HIV-1 replication. AIDS Lond. Engl. *17*, F39-48.

R. El-Attar, L.M., Thomas, C., Luke, J., A. Williams, J., and Brownlie, J. (2015). Enhanced neutralising antibody response to bovine viral diarrhoea virus (BVDV) induced by DNA vaccination in calves. Vaccine *33*, 4004–4012.

Racicot, K., Cardenas, I., Wünsche, V., Aldo, P., Guller, S., Means, R.E., Romero, R., and Mor, G. (2013). Viral Infection of the Pregnant Cervix Predisposes to Ascending Bacterial Infection. J. Immunol. *191*, 934–941.

Radhakrishnan, Y., Fares, M.A., French, F.S., and Hall, S.H. (2007). Comparative genomic analysis of a mammalian β-defensin gene cluster. Physiol. Genomics *30*, 213–222.

Rao, A., Luo, C., and Hogan, P.G. (1997). Transcription factors of the NFAT family: regulation and function. Annu. Rev. Immunol. *15*, 707–747.

Raverdeau, M., Gely-Pernot, A., Féret, B., Dennefeld, C., Benoit, G., Davidson, I., Chambon, P., Mark, M., and Ghyselinck, N.B. (2012). Retinoic acid induces Sertoli cell paracrine signals for spermatogonia differentiation but cell autonomously drives spermatocyte meiosis. Proc. Natl. Acad. Sci. *109*, 16582–16587.

Reimer, T., Brcic, M., Schweizer, M., and Jungi, T.W. (2008). poly(I:C) and LPS induce distinct IRF3 and NF-κB signaling during type-I IFN and TNF responses in human macrophages. J. Leukoc. Biol. *83*, 1249–1257.

Resar, L.M., Dolde, C., Barrett, J.F., and Dang, C.V. (1993). B-myc inhibits neoplastic transformation and transcriptional activation by c-myc. Mol. Cell. Biol. *13*, 1130–1136.

Ribeiro, E.S., Gomes, G., Greco, L.F., Cerri, R.L.A., Vieira-Neto, A., Monteiro Jr., P.L.J., Lima, F.S., Bisinotto, R.S., Thatcher, W.W., and Santos, J.E.P. (2016). Carryover effect of postpartum inflammatory diseases on developmental biology and fertility in lactating dairy cows. J. Dairy Sci. *99*, 2201–2220.

Ricci, A., Gallo, S., Molinaro, F., Dondo, A., Zoppi, S., and Vincenti, L. (2015). Evaluation of Subclinical Endometritis and Consequences on Fertility in Piedmontese Beef Cows. Reprod. Domest. Anim. *50*, 142–148.

Rieder, F.J.J., Gröschel, C., Kastner, M.-T., Kosulin, K., Laengle, J., Zadnikar, R., Marculescu, R., Schneider, M., Lion, T., Bergmann, M., et al. (2017). Human cytomegalovirus infection downregulates vitamin-D receptor in mammalian cells. J. Steroid Biochem. Mol. Biol. *165, Part B*, 356–362.

Rizzo, A., Paolillo, R., Buommino, E., Lanza, A.G., Guida, L., Annunziata, M., and Carratelli, C.R. (2008). Modulation of cytokine and beta-defensin 2 expressions in human gingival fibroblasts infected with Chlamydia pneumoniae. Int. Immunopharmacol. *8*, 1239–1247.

Rodríguez-Jiménez, F.-J., Krause, A., Schulz, S., Forssmann, W.-G., Conejo-Garcia, J.-R., Schreeb, R., and Motzkus, D. (2003). Distribution of new human β-defensin genes clustered on chromosome 20 in functionally different segments of epididymis. Genomics *81*, 175–183.

Röhrl, J., Yang, D., Oppenheim, J.J., and Hehlgans, T. (2010a). Human β-Defensin 2 and 3 and Their Mouse Orthologs Induce Chemotaxis through Interaction with CCR2. J. Immunol. *184*, 6688–6694.

Röhrl, J., Yang, D., Oppenheim, J.J., and Hehlgans, T. (2010b). Specific Binding and Chemotactic Activity of mBD4 and Its Functional Orthologue hBD2 to CCR6-expressing Cells. J. Biol. Chem. *285*, 7028–7034.

Roupé, K.M., Nybo, M., Sjöbring, U., Alberius, P., Schmidtchen, A., and Sørensen, O.E. (2010). Injury Is a Major Inducer of Epidermal Innate Immune Responses during Wound Healing. J. Invest. Dermatol. *130*, 1167–1177.

Ryan, L.K., Rhodes, J., Bhat, M., and Diamond, G. (1998). Expression of β-Defensin Genes in Bovine Alveolar Macrophages. Infect. Immun. *66*, 878–881.

Ryan, L.K., Dai, J., Yin, Z., Megjugorac, N., Uhlhorn, V., Yim, S., Schwartz, K.D., Abrahams, J.M., Diamond, G., and Fitzgerald-Bocarsly, P. (2011). Modulation of human β-defensin-1 (hBD-1) in plasmacytoid dendritic cells (PDC), monocytes, and epithelial cells by influenza virus, Herpes simplex virus, and Sendai virus and its possible role in innate immunity. J. Leukoc. Biol. *90*, 343–356.

Sakaguchi, S., Hombauer, M., Hassan, H., Tanaka, H., Yasmin, N., Naoe, Y., Bilic, I., Moser, M.A., Hainberger, D., Mayer, H., et al. (2015). A novel Cd8-cis-regulatory element preferentially directs expression in CD44hiCD62L+ CD8+ T cells and in CD8αα+ dendritic cells. J. Leukoc. Biol. *97*, 635–644.

Sanchez-Guerrero, E., Chen, E., Kockx, M., An, S.-W., Chong, B.H., and Khachigian, L.M. (2012). IL-1beta Signals through the EGF Receptor and Activates Egr-1 through MMP-ADAM. PLOS ONE *7*, e39811.

Sang, Y., Ruchala, P., Lehrer, R.I., Ross, C.R., Rowland, R.R.R., and Blecha, F. (2009). Antimicrobial host defense peptides in an arteriviral infection: differential peptide expression and virus inactivation. Viral Immunol. *22*, 235–242.

Sass, V., Schneider, T., Wilmes, M., Körner, C., Tossi, A., Novikova, N., Shamova, O., and Sahl, H.-G. (2010). Human β-Defensin 3 Inhibits Cell Wall Biosynthesis in Staphylococci. Infect. Immun. *78*, 2793–2800.

Schaefer, T.M., Fahey, J.V., Wright, J.A., and Wira, C.R. (2005). Innate Immunity in the Human Female Reproductive Tract: Antiviral Response of Uterine Epithelial Cells to the TLR3 Agonist Poly(I:C). J. Immunol. *174*, 992–1002.

Scharf, S., Vardarova, K., Lang, F., Schmeck, B., Opitz, B., Flieger, A., Heuner, K., Hippenstiel, S., Suttorp, N., and N'Guessan, P.D. (2010). Legionella pneumophila induces human beta Defensin-3 in pulmonary cells. Respir. Res. *11*, 93.

Schauber, J., Dorschner, R.A., Yamasaki, K., Brouha, B., and Gallo, R.L. (2006). Control of the innate epithelial antimicrobial response is cell-type specific and dependent on relevant microenvironmental stimuli. Immunology *118*, 509–519.

Schibli, D.J., Hunter, H.N., Aseyev, V., Starner, T.D., Wiencek, J.M., McCray, P.B., Tack, B.F., and Vogel, H.J. (2002). The Solution Structures of the Human β-Defensins Lead to a Better Understanding of the Potent Bactericidal Activity of HBD3 against Staphylococcus aureus. J. Biol. Chem. *277*, 8279–8289.

Schonwetter, B.S., Stolzenberg, E.D., and Zasloff, M.A. (1995). Epithelial antibiotics induced at sites of inflammation. Science *267*, 1645–1648.

Schröder, J.M., and Harder, J. (2006). Antimicrobial skin peptides and proteins. Cell. Mol. Life Sci. CMLS *63*, 469–486.

Schroeder, B.O., Wu, Z., Nuding, S., Groscurth, S., Marcinowski, M., Beisner, J., Buchner, J., Schaller, M., Stange, E.F., and Wehkamp, J. (2011). Reduction of disulphide bonds unmasks potent antimicrobial activity of human β-defensin 1. Nature *469*, 419–423.

Schrumpf, J.A., Amatngalim, G.D., Veldkamp, J.B., Verhoosel, R.M., Ninaber, D.K., Ordonez, S.R., van der Does, A.M., Haagsman, H.P., and Hiemstra, P.S. (2017). Pro-inflammatory Cytokines Impair Vitamin D-induced Host Defense in Cultured Airway Epithelial Cells. Am. J. Respir. Cell Mol. Biol.

Scott, M.G., Vreugdenhil, A.C.E., Buurman, W.A., Hancock, R.E.W., and Gold, M.R. (2000). Cutting Edge: Cationic Antimicrobial Peptides Block the Binding of Lipopolysaccharide (LPS) to LPS Binding Protein. J. Immunol. *164*, 549–553.

Selsted, M.E., and Ouellette, A.J. (2005). Mammalian defensins in the antimicrobial immune response. Nat. Immunol. *6*, 551–557.

Selsted, M.E., Szklarek, D., and Lehrer, R.I. (1984). Purification and antibacterial activity of antimicrobial peptides of rabbit granulocytes. Infect. Immun. *45*, 150–154.

Selsted, M.E., Harwig, S.S., Ganz, T., Schilling, J.W., and Lehrer, R.I. (1985). Primary structures of three human neutrophil defensins. J. Clin. Invest. *76*, 1436–1439.

Selsted, M.E., Tang, Y.-Q., Morris, W.L., McGuire, P.A., Novotny, M.J., Smith, W., Henschen, A.H., and Cullor, J.S. (1993). Purification, primary structures, and antibacterial activities of beta-defensins, a new family of antimicrobial peptides from bovine neutrophils. J. Biol. Chem. *268*, 6641–6648.

Semlali, A., Amri, A.A., Azzi, A., Shahrani, O.A., Arafah, M., Kohailan, M., Aljebreen, A.M., Alharbi, O., Almadi, M.A., Azzam, N.A., et al. (2015). Expression and New Exon Mutations of the Human Beta Defensins and Their Association on Colon Cancer Development. PLOS ONE *10*, e0126868.

Semple, F., Webb, S., Li, H.-N., Patel, H.B., Perretti, M., Jackson, I.J., Gray, M., Davidson, D.J., and Dorin, J.R. (2010). Human β-defensin 3 has immunosuppressive activity in vitro and in vivo. Eur. J. Immunol. *40*, 1073–1078.

Semple, F., MacPherson, H., Webb, S., Cox, S.L., Mallin, L.J., Tyrrell, C., Grimes, G.R., Semple, C.A., Nix, M.A., Millhauser, G.L., et al. (2011). Human β-defensin 3 affects the activity of pro-inflammatory pathways associated with MyD88 and TRIF. Eur. J. Immunol. *41*, 3291–3300.

Semple, F., MacPherson, H., Webb, S., Kilanowski, F., Lettice, L., McGlasson, S.L., Wheeler, A.P., Chen, V., Millhauser, G.L., Melrose, L., et al. (2015). Human β-D-3 Exacerbates MDA5 but Suppresses TLR3 Responses to the Viral Molecular Pattern Mimic Polyinosinic:Polycytidylic Acid. PLOS Genet *11*, e1005673.

Shalloo, L., Cromie, A., and McHugh, N. (2014). Effect of fertility on the economics of pasture-based dairy systems. Animal *8*, 222–231.

Sheldon, I., Price, S., Cronin, J., Gilbert, R., and Gadsby, J. (2009a). Mechanisms of Infertility Associated with Clinical and Subclinical Endometritis in High Producing Dairy Cattle. Reprod. Domest. Anim. *44*, 1–9.

Sheldon, I.M., Lewis, G.S., LeBlanc, S., and Gilbert, R.O. (2006). Defining postpartum uterine disease in cattle. Theriogenology *65*, 1516–1530.

Sheldon, I.M., Cronin, J., Goetze, L., Donofrio, G., and Schuberth, H.-J. (2009b). Defining Postpartum Uterine Disease and the Mechanisms of Infection and Immunity in the Female Reproductive Tract in Cattle. Biol. Reprod. *81*, 1025–1032.

Shen, Z., Zhang, X., Tang, J., Kasiappan, R., Jinwal, U., Li, P., Hann, S., Nicosia, S.V., Wu, J., Zhang, X., et al. (2011). The coupling of epidermal growth factor receptor down regulation by 1alpha,25-dihydroxyvitamin D3 to the hormone-induced cell cycle arrest at the G1-S checkpoint in ovarian cancer cells. Mol. Cell. Endocrinol. *338*, 58–67.

Shoemaker, M.L., Smirnova, N.P., Bielefeldt-Ohmann, H., Austin, K.J., van Olphen, A., Clapper, J.A., and Hansen, T.R. (2009). Differential expression of the type I interferon pathway during persistent and transient bovine viral diarrhea virus infection. J. Interferon Cytokine Res. Off. J. Int. Soc. Interferon Cytokine Res. *29*, 23–35.

Shuster, D.E., Kehrli, M.E., and Stevens, M.G. (1993). Cytokine production during endotoxin-induced mastitis in lactating dairy cows. Am. J. Vet. Res. *54*, 80–85.

Shuyi, Y., Feng, W., Jing, T., Hongzhang, H., Haiyan, W., Pingping, M., Liwu, Z., Zwahlen, R.A., and Hongyu, Y. (2011). Human beta-defensin-3 (hBD-3) upregulated by LPS via epidermal growth

factor receptor (EGFR) signaling pathways to enhance lymphatic invasion of oral squamous cell carcinoma. Oral Surg. Oral Med. Oral Pathol. Oral Radiol. Endodontology *112*, 616–625.

Simanski, M., Rademacher, F., Schröder, L., Schumacher, H.M., Gläser, R., and Harder, J. (2013). IL-17A and IFN-γ Synergistically Induce RNase 7 Expression via STAT3 in Primary Keratinocytes. PLOS ONE *8*, e59531.

Singh, P.K., Jia, H.P., Wiles, K., Hesselberth, J., Liu, L., Conway, B.-A.D., Greenberg, E.P., Valore, E.V., Welsh, M.J., Ganz, T., et al. (1998). Production of beta-defensins by human airway epithelia. Proc. Natl. Acad. Sci. U. S. A. *95*, 14961–14966.

Sipilä, P., Shariatmadari, R., Huhtaniemi, I.T., and Poutanen, M. (2004). Immortalization of Epididymal Epithelium in Transgenic Mice Expressing Simian Virus 40 T Antigen: Characterization of Cell Lines and Regulation of the Polyoma Enhancer Activator 3. Endocrinology *145*, 437–446.

Smirnova, N.P., Webb, B.T., Bielefeldt-Ohmann, H., Van Campen, H., Antoniazzi, A.Q., Morarie, S.E., and Hansen, T.R. (2012). Development of fetal and placental innate immune responses during establishment of persistent infection with bovine viral diarrhea virus. Virus Res. *167*, 329–336.

Smith, S.B., and Ravel, J. (2017). The vaginal microbiota, host defence and reproductive physiology. J. Physiol. *595*, 451–463.

Song, G., Bazer, F.W., and Spencer, T.E. (2007). Pregnancy and interferon tau regulate RSAD2 and IFIH1 expression in the ovine uterus. Reprod. Camb. Engl. *133*, 285–295.

Sordillo, L.M., Contreras, G.A., and Aitken, S.L. (2009). Metabolic factors affecting the inflammatory response of periparturient dairy cows. Anim. Health Res. Rev. *10*, 53–63.

Sørensen, O.E., Thapa, D.R., Rosenthal, A., Liu, L., Roberts, A.A., and Ganz, T. (2005). Differential regulation of beta-defensin expression in human skin by microbial stimuli. J. Immunol. Baltim. Md 1950 *174*, 4870–4879.

Stabenfeldt, G.H., Ewing, L.L., and McDonald, L.E. (1969). Peripheral plasma progesterone levels during the bovine oestrous cycle. J. Reprod. Fertil. *19*, 433–442.

Steinstraesser, L., Kraneburg, U., Jacobsen, F., and Al-Benna, S. (2011). Host defense peptides and their antimicrobial-immunomodulatory duality. Immunobiology *216*, 322–333.

Steubesand, N., Kiehne, K., Brunke, G., Pahl, R., Reiss, K., Herzig, K.-H., Schubert, S., Schreiber, S., Fölsch, U.R., Rosenstiel, P., et al. (2009). The expression of the β-defensins hBD-2 and hBD-3 is differentially regulated by NF-κB and MAPK/AP-1 pathways in an in vitro model of Candida esophagitis. BMC Immunol. *10*, 36.

Sun, L., Finnegan, C.M., Kish-Catalone, T., Blumenthal, R., Garzino-Demo, P., Maggiore, G.M.L.T., Berrone, S., Kleinman, C., Wu, Z., Abdelwahab, S., et al. (2005). Human β-Defensins Suppress Human Immunodeficiency Virus Infection: Potential Role in Mucosal Protection. J. Virol. *79*, 14318–14329.

Sun, L., Wu, J., Du, F., Chen, X., and Chen, Z.J. (2013). Cyclic GMP-AMP Synthase Is a Cytosolic DNA Sensor That Activates the Type I Interferon Pathway. Science *339*, 786–791.

Swartz, J.D., Lachman, M., Westveer, K., O'Neill, T., Geary, T., Kott, R.W., Berardinelli, J.G., Hatfield, P.G., Thomson, J.M., Roberts, A., et al. (2014). Characterization of the Vaginal Microbiota of Ewes and Cows Reveals a Unique Microbiota with Low Levels of Lactobacilli and Near-Neutral pH. Front. Vet. Sci. *1*.

Tagle, D.A., Koop, B.F., Goodman, M., Slightom, J.L., Hess, D.L., and Jones, R.T. (1988). Embryonic ε and γ globin genes of a prosimian primate (Galago crassicaudatus): Nucleotide and amino acid sequences, developmental regulation and phylogenetic footprints. J. Mol. Biol. *203*, 439–455.

Taher, L., Narlikar, L., and Ovcharenko, I. (2012). CLARE: Cracking the LAnguage of Regulatory Elements. Bioinformatics *28*, 581–583.

Tamura, K., Stecher, G., Peterson, D., Filipski, A., and Kumar, S. (2013). MEGA6: Molecular Evolutionary Genetics Analysis version 6.0. Mol. Biol. Evol. *30*, 2725–2729.

Tanaka, T., Wang, C., and Umesaki, N. (2008). Autocrine/paracrine regulation of human endometrial stromal remodeling by laminin and type IV collagen. Int. J. Mol. Med. *22*, 581–587.

Tang, Y.-Q., Yuan, J., Ösapay, G., Ösapay, K., Tran, D., Miller, C.J., Ouellette, A.J., and Selsted, M.E. (1999). A Cyclic Antimicrobial Peptide Produced in Primate Leukocytes by the Ligation of Two Truncated α-Defensins. Science *286*, 498–502.

Tarver, A.P., Clark, D.P., Diamond, G., Russell, J.P., Erdjument-Bromage, H., Tempst, P., Cohen, K.S., Jones, D.E., Sweeney, R.W., Wines, M., et al. (1998). Enteric β-Defensin: Molecular Cloning and Characterization of a Gene with Inducible Intestinal Epithelial Cell Expression Associated with Cryptosporidium parvumInfection. Infect. Immun. *66*, 1045–1056.

Tebaldi, G., Jacca, S., Montanini, B., Capra, E., Rosamilia, A., Sala, A., Stella, A., Castiglioni, B., Ottonello, S., and Donofrio, G. (2016). Virus-Mediated Metalloproteinase 1 Induction Revealed by Transcriptome Profiling of Bovine Herpesvirus 4-Infected Bovine Endometrial Stromal Cells. Biol. Reprod. *95*.

Telcian, A.G., Zdrenghea, M.T., Edwards, M.R., Stanca, V.-L., Mallia, P., Johnston, S.L., and Stanciu, L.A. (2017). Vitamin D increases the antiviral activity of bronchial epithelial cells in vitro. Antiviral Res. *137*, 93–101.

Téllez-Pérez, A.D., Alva-Murillo, N., Ochoa-Zarzosa, A., and López-Meza, J.E. (2012). Cholecalciferol (vitamin D) differentially regulates antimicrobial peptide expression in bovine mammary epithelial cells: Implications during Staphylococcus aureus internalization. Vet. Microbiol. *160*, 91–98.

Thompson, A.J.V., and Locarnini, S.A. (2007). Toll-like receptors, RIG-I-like RNA helicases and the antiviral innate immune response. Immunol. Cell Biol. *85*, 435–445.

Thompson, M.R., Sharma, S., Atianand, M., Jensen, S.B., Carpenter, S., Knipe, D.M., Fitzgerald, K.A., and Kurt-Jones, E.A. (2014). Interferon γ-inducible Protein (IFI) 16 Transcriptionally Regulates Type I Interferons and Other Interferon-stimulated Genes and Controls the Interferon Response to both DNA and RNA Viruses. J. Biol. Chem. *289*, 23568–23581.

Tollner, T.L., Yudin, A.I., Treece, C.A., Overstreet, J.W., and Cherr, G.N. (2004). Macaque sperm release ESP13.2 and PSP94 during capacitation: The absence of ESP13.2 is linked to sperm-zona recognition and binding. Mol. Reprod. Dev. *69*, 325–337.

Tollner, T.L., Yudin, A.I., Treece, C.A., Overstreet, J.W., and Cherr, G.N. (2008a). Macaque sperm coating protein DEFB126 facilitates sperm penetration of cervical mucus†. Hum. Reprod. *23*, 2523–2534.

Tollner, T.L., Yudin, A.I., Tarantal, A.F., Treece, C.A., Overstreet, J.W., and Cherr, G.N. (2008b). Beta-Defensin 126 on the Surface of Macaque Sperm Mediates Attachment of Sperm to Oviductal Epithelia. Biol. Reprod. *78*, 400–412.

Tollner, T.L., Venners, S.A., Hollox, E.J., Yudin, A.I., Liu, X., Tang, G., Xing, H., Kays, R.J., Lau, T., Overstreet, J.W., et al. (2011). A Common Mutation in the Defensin DEFB126 Causes Impaired Sperm Function and Subfertility. Sci. Transl. Med. *3*, 92ra65-92ra65.

Tollner, T.L., Bevins, C.L., and Cherr, G.N. (2012). Multifunctional glycoprotein DEFB126—a curious story of defensin-clad spermatozoa. Nat. Rev. Urol.

Tomasinsig, L., Skerlavaj, B., Scarsini, M., Guida, F., Piccinini, R., Tossi, A., and Zanetti, M. (2012). Comparative activity and mechanism of action of three types of bovine antimicrobial peptides against pathogenic Prototheca spp. J. Pept. Sci. Off. Publ. Eur. Pept. Soc. *18*, 105–113.

Tsutsumi-Ishii, Y., and Nagaoka, I. (2002). NF-κB-mediated transcriptional regulation of human β-defensin-2 gene following lipopolysaccharide stimulation. J. Leukoc. Biol. *71*, 154–162.

Turner, M.L., Cronin, J.G., Healey, G.D., and Sheldon, I.M. (2014). Epithelial and Stromal Cells of Bovine Endometrium Have Roles in Innate Immunity and Initiate Inflammatory Responses to Bacterial Lipopeptides In Vitro via Toll-Like Receptors TLR2, TLR1, and TLR6. Endocrinology *155*, 1453–1465.

Unterholzner, L., Keating, S.E., Baran, M., Horan, K.A., Jensen, S.B., Sharma, S., Sirois, C.M., Jin, T., Latz, E., Xiao, T.S., et al. (2010). IFI16 is an innate immune sensor for intracellular DNA. Nat. Immunol. *11*, 997–1004.

Ureta-Vidal, A., Ettwiller, L., and Birney, E. (2003). Comparative genomics: genome-wide analysis in metazoan eukaryotes. Nat. Rev. Genet. *4*, 251–262.

Usman, T., Wang, Y., Liu, C., He, Y., Wang, X., Dong, Y., Wu, H., Liu, A., and Yu, Y. (2017). Novel SNPs in IL-17F and IL-17A genes associated with somatic cell count in Chinese Holstein and Inner-Mongolia Sanhe cattle. J. Anim. Sci. Biotechnol. *8*.

Varoga, D., Pufe, T., Harder, J., Schröder, J.-M., Mentlein, R., Meyer-Hoffert, U., Goldring, M.B., Tillmann, B., Hassenpflug, J., and Paulsen, F. (2005). Human β-defensin 3 mediates tissue remodeling processes in articular cartilage by increasing levels of metalloproteinases and reducing levels of their endogenous inhibitors. Arthritis Rheum. *52*, 1736–1745.

Veldhuizen, E.J.A., Rijnders, M., Claassen, E.A., van Dijk, A., and Haagsman, H.P. (2008). Porcine beta-defensin 2 displays broad antimicrobial activity against pathogenic intestinal bacteria. Mol. Immunol. *45*, 386–394.

Vernet, N., Dennefeld, C., Guillou, F., Chambon, P., Ghyselinck, N.B., and Mark, M. (2006). Prepubertal testis development relies on retinoic acid but not rexinoid receptors in Sertoli cells. EMBO J. *25*, 5816–5825.

Viganò, P., Lattuada, D., Mangioni, S., Ermellino, L., Vignali, M., Caporizzo, E., Panina-Bordignon, P., Besozzi, M., and Di Blasio, A.M. (2006). Cycling and early pregnant endometrium as a site of regulated expression of the vitamin D system. J. Mol. Endocrinol. *36*, 415–424.

Vlahopoulos, S., Zimmer, W.E., Jenster, G., Belaguli, N.S., Balk, S.P., Brinkmann, A.O., Lanz, R.B., Zoumpourlis, V.C., and Schwartz, R.J. (2005). Recruitment of the Androgen Receptor via Serum Response Factor Facilitates Expression of a Myogenic Gene. J. Biol. Chem. *280*, 7786–7792.

Vora, P., Youdim, A., Thomas, L.S., Fukata, M., Tesfay, S.Y., Lukasek, K., Michelsen, K.S., Wada, A., Hirayama, T., Arditi, M., et al. (2004). β-Defensin-2 Expression Is Regulated by TLR Signaling in Intestinal Epithelial Cells. J. Immunol. *173*, 5398–5405.

Wadman, I.A., Osada, H., Grütz, G.G., Agulnick, A.D., Westphal, H., Forster, A., and Rabbitts, T.H. (1997). The LIM-only protein Lmo2 is a bridging molecule assembling an erythroid, DNA-binding complex which includes the TAL1, E47, GATA-1 and Ldb1/NLI proteins. EMBO J. *16*, 3145–3157.

Walker, C.G., Meier, S., Hussein, H., McDougall, S., Burke, C.R., Roche, J.R., and Mitchell, M.D. (2015). Modulation of the immune system during postpartum uterine inflammation. Physiol. Genomics *47*, 89–101.

Wang, A., Al-Kuhlani, M., Johnston, S.C., Ojcius, D.M., Chou, J., and Dean, D. (2013a). Transcription factor complex AP-1 mediates inflammation initiated by Chlamydia pneumoniae infection. Cell. Microbiol. *15*, 779–794.

Wang, B., McHugh, B.J., Qureshi, A., Campopiano, D.J., Clarke, D.J., Fitzgerald, J.R., Dorin, J.R., Weller, R., and Davidson, D.J. (2017). IL-1β–Induced Protection of Keratinocytes against Staphylococcus aureus-Secreted Proteases Is Mediated by Human β-Defensin 2. J. Invest. Dermatol.

Wang, J., Wu, S., Jin, X., Li, M., Chen, S., Teeling, J.L., Perry, V.H., and Gu, J. (2008). Retinoic Acid-Inducible Gene-I Mediates Late Phase Induction of TNF-α by Lipopolysaccharide. J. Immunol. *180*, 8011–8019.

Wang, J., Alexander, J., Wiebe, M., and Jones, C. (2014a). Bovine herpesvirus 1 productive infection stimulates inflammasome formation and caspase 1 activity. Virus Res. *185*, 72–76.

Wang, Q., Wang, L., Shao, J., Wang, Y., Jin, L.-P., Li, D.-J., and Li, M.-Q. (2014b). L-22 enhances the invasiveness of endometrial stromal cells of adenomyosis in an autocrine manner. Int. J. Clin. Exp. Pathol. *7*, 5762–5771.

Wang, S., Liu, D., Ning, W., and Xu, A. (2015). Cytosolic dsDNA triggers apoptosis and pro-inflammatory cytokine production in normal human melanocytes. Exp. Dermatol. *24*, 298–300.

Wang, T.-T., Nestel, F.P., Bourdeau, V., Nagai, Y., Wang, Q., Liao, J., Tavera-Mendoza, L., Lin, R., Hanrahan, J.H., Mader, S., et al. (2004). Cutting Edge: 1,25-Dihydroxyvitamin D3 Is a Direct Inducer of Antimicrobial Peptide Gene Expression. J. Immunol. *173*, 2909–2912.

Wang, T.-T., Dabbas, B., Laperriere, D., Bitton, A.J., Soualhine, H., Tavera-Mendoza, L.E., Dionne, S., Servant, M.J., Bitton, A., Seidman, E.G., et al. (2010). Direct and Indirect Induction by 1,25-Dihydroxyvitamin D-3 of the NOD2/CARD15-Defensin beta 2 Innate Immune Pathway Defective in Crohn Disease. J. Biol. Chem. *285*, 2237–2241.

Wang, Y., Ametaj, B.N., Ambrose, D.J., and Gänzle, M.G. (2013b). Characterisation of the bacterial microbiota of the vagina of dairy cows and isolation of pediocin-producing Pediococcus acidilactici. BMC Microbiol. *13*, 19.

Wathes, D.C., Cheng, Z., Chowdhury, W., Fenwick, M.A., Fitzpatrick, R., Morris, D.G., Patton, J., and Murphy, J.J. (2009). Negative energy balance alters global gene expression and immune responses in the uterus of postpartum dairy cows. Physiol. Genomics *39*, 1–13.

Webb, P., Nguyen, P., Valentine, C., Lopez, G.N., Kwok, G.R., McInerney, E., Katzenellenbogen, B.S., Enmark, E., Gustafsson, J.A., Nilsson, S., et al. (1999). The estrogen receptor enhances AP-1 activity by two distinct mechanisms with different requirements for receptor transactivation functions. Mol. Endocrinol. Baltim. Md *13*, 1672–1685.

Weber, F., Wagner, V., Rasmussen, S.B., Hartmann, R., and Paludan, S.R. (2006). Double-Stranded RNA Is Produced by Positive-Strand RNA Viruses and DNA Viruses but Not in Detectable Amounts by Negative-Strand RNA Viruses. J. Virol. *80*, 5059–5064.

Wehkamp, K., Schwichtenberg, L., Schröder, J.-M.M., and Harder, J. (2006). Pseudomonas Aeruginosa- and IL-1β-Mediated Induction of Human β-Defensin-2 in Keratinocytes Is Controlled by NF-κB and AP-1. J. Invest. Dermatol. *126*, 121–127.

Weinhold, B. (2006). Epigenetics: The Science of Change. Environ. Health Perspect. *114*, A160–A167.

Wen, S., Cao, G., Bao, T., Cheng, L., Li, H., Du, C., Tu, Y., Li, Q., Jian, R., Zhao, P., et al. (2012). Modulation of ovine SBD-1 expression by 17beta-estradiol in ovine oviduct epithelial cells. BMC Vet. Res. *8*, 143.

White, J.H. (2012). Vitamin D metabolism and signaling in the immune system. Rev. Endocr. Metab. Disord. *13*, 21–29.

Whitfield, T.W., Wang, J., Collins, P.J., Partridge, E.C., Aldred, S.F., Trinklein, N.D., Myers, R.M., and Weng, Z. (2012). Functional analysis of transcription factor binding sites in human promoters. Genome Biol. *13*, R50.

Williams, E.J., Fischer, D.P., Noakes, D.E., England, G.C.W., Rycroft, A., Dobson, H., and Sheldon, I.M. (2007). The relationship between uterine pathogen growth density and ovarian function in the postpartum dairy cow. Theriogenology *68*, 549–559.

Wilson, C.L., Ouellette, A.J., Satchell, D.P., Ayabe, T., López-Boado, Y.S., Stratman, J.L., Hultgren, S.J., Matrisian, L.M., and Parks, W.C. (1999). Regulation of Intestinal α-Defensin Activation by the Metalloproteinase Matrilysin in Innate Host Defense. Science *286*, 113–117.

Wilson, S.S., Wiens, M.E., and Smith, J.G. (2013). Antiviral Mechanisms of Human Defensins. J. Mol. Biol. *425*, 4965–4980.

Witowski, J., Thiel, A., Dechend, R., Dunkel, K., Fouquet, N., Bender, T.O., Langrehr, J.M., Gahl, G.M., Frei, U., and Jörres, A. (2001). Synthesis of C-X-C and C-C Chemokines by Human Peritoneal Fibroblasts: Induction by Macrophage-Derived Cytokines. Am. J. Pathol. *158*, 1441–1450.

Witthöft, T., Pilz, C.S., Fellermann, K., Nitschke, M., Stange, E.F., and Ludwig, D. (2005). Enhanced human beta-defensin-2 (hBD-2) expression by corticosteroids is independent of NF-kappaB in colonic epithelial cells (CaCo2). Dig. Dis. Sci. *50*, 1252–1259.

Wolk, K., Kunz, S., Witte, E., Friedrich, M., Asadullah, K., and Sabat, R. (2004). IL-22 Increases the Innate Immunity of Tissues. Immunity *21*, 241–254.

Wolk, K., Witte, E., Wallace, E., Döcke, W.-D., Kunz, S., Asadullah, K., Volk, H.-D., Sterry, W., and Sabat, R. (2006). IL-22 regulates the expression of genes responsible for antimicrobial defense, cellular differentiation, and mobility in keratinocytes: a potential role in psoriasis. Eur. J. Immunol. *36*, 1309–1323.

Woo, J.-I., Oh, S., Webster, P., Lee, Y.J., Lim, D.J., and Moon, S.K. (2014). NOD2/RICK-Dependent β-Defensin 2 Regulation Is Protective for Nontypeable Haemophilus influenzae-Induced Middle Ear Infection. PLoS ONE *9*, e90933.

World Health Organisation (2015). Global Action Plan on Antimicrobial Resistance.

Wu, Z., Hoover, D.M., Yang, D., Boulègue, C., Santamaria, F., Oppenheim, J.J., Lubkowski, J., and Lu, W. (2003). Engineering disulfide bridges to dissect antimicrobial and chemotactic activities of human β-defensin 3. Proc. Natl. Acad. Sci. U. S. A. *100*, 8880.

Xie, P. (2013). TRAF molecules in cell signaling and in human diseases. J. Mol. Signal. *8*.

Xie, M.-H., Aggarwal, S., Ho, W.-H., Foster, J., Zhang, Z., Stinson, J., Wood, W.I., Goddard, A.D., and Gurney, A.L. (2000). Interleukin (IL)-22, a Novel Human Cytokine That Signals through the Interferon Receptor-related Proteins CRF2–4 and IL-22R. J. Biol. Chem. *275*, 31335–31339.

Xin, A., Zhao, Y., Yu, H., Shi, H., Liu, H., Diao, H., and Zhang, Y. (2014). Soluble fusion expression, characterization and localization of human β-defensin 6. Mol. Med. Rep. *9*, 149–155.

Yamaguchi, J., Tanaka, T., Eto, N., and Nangaku, M. (2015). Inflammation and hypoxia linked to renal injury by CCAAT/enhancer-binding protein δ. Kidney Int. *88*, 262–275.

Yamaguchi, Y., Nagase, T., Makita, R., Fukuhara, S., Tomita, T., Tominaga, T., Kurihara, H., and Ouchi, Y. (2002). Identification of multiple novel epididymis-specific β-defensin isoforms in humans and mice. J. Immunol. *169*, 2516–2523.

Yamashita, M., Chattopadhyay, S., Fensterl, V., Saikia, P., Wetzel, J.L., and Sen, G.C. (2012). EGFR is Essential for TLR3 Signaling. Sci. Signal. *5*, ra50.

Yang, D., Chertov, O., Bykovskaia, S.N., Chen, Q., Buffo, M.J., Shogan, J., Anderson, M., Schröder, J.M., Wang, J.M., Howard, O.M.Z., et al. (1999). β-Defensins: Linking Innate and Adaptive Immunity Through Dendritic and T Cell CCR6. Science *286*, 525–528.

Yao, Z., Painter, S.L., Fanslow, W.C., Ulrich, D., Macduff, B.M., Spriggs, M.K., and Armitage, R.J. (1995). Human IL-17: a novel cytokine derived from T cells. J. Immunol. *155*, 5483–5486.

Yarbrough, V.L., Winkle, S., and Herbst-Kralovetz, M.M. (2014). Antimicrobial peptides in the female reproductive tract: a critical component of the mucosal immune barrier with physiological and clinical implications. Hum. Reprod. Update dmu065.

Yenugu, S., Hamil, K.G., Radhakrishnan, Y., French, F.S., and Hall, S.H. (2004). The Androgen-Regulated Epididymal Sperm-Binding Protein, Human β-Defensin 118 (DEFB118) (Formerly ESC42), Is an Antimicrobial β-Defensin. Endocrinology *145*, 3165–3173.

Yin, L., and Chung, W.O. (2011). Epigenetic regulation of human β-defensin 2 and CC chemokine ligand 20 expression in gingival epithelial cells in response to oral bacteria. Mucosal Immunol. *4*, 409–419.

Yin, L., Chino, T., Horst, O.V., Hacker, B.M., Clark, E.A., Dale, B.A., and Chung, W.O. (2010). Differential and coordinated expression of defensins and cytokines by gingival epithelial cells and dendritic cells in response to oral bacteria. BMC Immunol. *11*, 37.

Yoneyama, M., Kikuchi, M., Natsukawa, T., Shinobu, N., Imaizumi, T., Miyagishi, M., Taira, K., Akira, S., and Fujita, T. (2004). The RNA helicase RIG-I has an essential function in double-stranded RNA-induced innate antiviral responses. Nat. Immunol. *5*, 730–737.

Yoneyama, M., Kikuchi, M., Matsumoto, K., Imaizumi, T., Miyagishi, M., Taira, K., Foy, E., Loo, Y.-M., Gale, M., Akira, S., et al. (2005). Shared and Unique Functions of the DExD/H-Box Helicases RIG-I, MDA5, and LGP2 in Antiviral Innate Immunity. J. Immunol. *175*, 2851–2858.

Yoshii, A., Kitahara, S., Ueta, H., Matsuno, K., and Ezaki, T. (2014). Role of Uterine Contraction in Regeneration of the Murine Postpartum Endometrium. Biol. Reprod. *91*, 32.

Yu, H., Dong, J., Gu, Y., Liu, H., Xin, A., Shi, H., Sun, F., Zhang, Y., Lin, D., and Diao, H. (2013). The Novel Human β-Defensin 114 Regulates Lipopolysaccharide (LPS)-mediated Inflammation and Protects Sperm from Motility Loss. J. Biol. Chem. *288*, 12270–12282.

Yudin, A.I., Tollner, T.L., Li, M.-W., Treece, C.A., Overstreet, J.W., and Cherr, G.N. (2003). ESP13.2, a Member of the β-Defensin Family, Is a Macaque Sperm Surface-Coating Protein Involved in the Capacitation Process. Biol. Reprod. *69*, 1118–1128.

Yudin, A.I., Generao, S.E., Tollner, T.L., Treece, C.A., Overstreet, J.W., and Cherr, G.N. (2005). Beta-Defensin 126 on the Cell Surface Protects Sperm from Immunorecognition and Binding of Anti-Sperm Antibodies. Biol. Reprod. *73*, 1243–1252.

Zasloff, M. (2002). Antimicrobial peptides of multicellular organisms. Nature *415*, 389–395.

Zenewicz, L.A., and Flavell, R.A. (2011). Recent advances in IL-22 biology. Int. Immunol. *23*, 159–163.

Zhang, L., and Gallo, R.L. (2016). Antimicrobial peptides. Curr. Biol. *26*, R14–R19.

Zhang, W., and Liu, H.T. (2002). MAPK signal pathways in the regulation of cell proliferation in mammalian cells. Cell Res. *12*, 9–18.

Zhang, G., Hailemariam, D., Dervishi, E., Deng, Q., Goldansaz, S.A., Dunn, S.M., and Ametaj, B.N. (2015). Alterations of Innate Immunity Reactants in Transition Dairy Cows before Clinical Signs of Lameness. Animals *5*, 717–747.

Zhang, X., Wu, H., Liu, C., Sun, X., Zu, S., Tian, J., Qu, L., and Li, S. (2016). The function of feline stimulator of interferon gene (STING) is evolutionarily conserved. Vet. Immunol. Immunopathol. *169*, 54–62.

Zhao, Y., Diao, H., Ni, Z., Hu, S., Yu, H., and Zhang, Y. (2011). The epididymis-specific antimicrobial peptide β-defensin 15 is required for sperm motility and male fertility in the rat (Rattus norvegicus). Cell. Mol. Life Sci. *68*, 697–708.

Zheng, Y., Li, X., and Hu, H. (2014). Comprehensive discovery of DNA motifs in 349 human cells and tissues reveals new features of motifs. Nucleic Acids Res. gku1261.

Zhou, C.X., Zhang, Y.-L., Xiao, L., Zheng, M., Leung, K.M., Chan, M.Y., Lo, P.S., Tsang, L.L., Wong, H.Y., Ho, L.S., et al. (2004). An epididymis-specific β-defensin is important for the initiation of sperm maturation. Nat. Cell Biol. *6*, 458–464.

Zhou, Y.S., Webb, S., Lettice, L., Tardif, S., Kilanowski, F., Tyrrell, C., MacPherson, H., Semple, F., Tennant, P., Baker, T., et al. (2013). Partial Deletion of Chromosome 8 Beta-Defensin Cluster Confers Sperm Dysfunction and Infertility in Male Mice. PLoS Genet. *9*.

Zhu, H., Hou, C.-C., Luo, L.-F., Hu, Y.-J., and Yang, W.-X. (2014). Endometrial stromal cells and decidualized stromal cells: Origins, transformation and functions. Gene *551*, 1–14.

Zhu, L., Lee, P., Lee, W., Zhao, Y., Yu, D., and Chen, Y. (2009). Rhinovirus-Induced Major Airway Mucin Production Involves a Novel TLR3-EGFR–Dependent Pathway. Am. J. Respir. Cell Mol. Biol. *40*, 610–619.

Zimin, A.V., Delcher, A.L., Florea, L., Kelley, D.R., Schatz, M.C., Puiu, D., Hanrahan, F., Pertea, G., Van Tassell, C.P., and Sonstegard, T.S. (2009). A whole-genome assembly of the domestic cow, Bos taurus. Genome Biol *10*, R42.

Zimin, A.V., Kelley, D.R., Roberts, M., Marçais, G., Salzberg, S.L., and Yorke, J.A. (2012). Mis-Assembled "Segmental Duplications" in Two Versions of the Bos taurus Genome. PLOS ONE *7*, e42680.

Zou, J., Mercier, C., Koussounadis, A., and Secombes, C. (2007). Discovery of multiple beta-defensin like homologues in teleost fish. Mol. Immunol. *44*, 638–647.

Zwain, I.H., Grima, J., and Cheng, C.Y. (1992). Rat epididymal retinoic acid-binding protein: development of a radioimmunoassay, its tissue distribution, and its changes in selected androgen-dependent organs after orchiectomy. Endocrinology *131*, 1511–1526.

# Appendices

**Table A.1 Species and genome assemblies used to create β-defensin ortholog list**

| Common name | Scientific name | Genome release |
|---|---|---|
| African elephant | *Loxodonta africana* | Loxafr3 |
| Alpaca | *Vicugna pacos* | vicPac1 |
| Armadillo | *Dasypus novemcinctus* | Dasnov3.0 |
| Bovine | *Bos taurus* | bosTau8 |
| Cat | *Felis cattus* | Felis_catus_6.2 |
| Dog | *Canis lupus familiaris* | CanFam3.1 |
| Dolphin | *Tursiops truncatus* | turTru1 |
| Gibbon | *Nomascus leucogenys* | Nleu1.0 |
| Horse | *Equus caballus* | EquCab2 |
| Human | *Homo sapiens* | GRCm38.p3 |
| Large flying fox | *Pteropus vampyrus* | pteVam1 |
| Little brown bat | *Myotis lucifugus* | MyoLuc2 |
| Mouse | *Mus musculus* | GRCm38.p4 |
| Pig | *Sus scrofa* | Sscrofa10.2 |
| Rabbit | *Oryctolagus caniculus* | OryCan2.0 |
| Rat | *Rattus norvegicus* | Rnor_6.0 |
| Rhesus macaque | *Macaca mulatta* | MMUL_1 |

**Table A.2 ENSEMBL IDs for the β-defensin gene orthologs downloaded**

| Gene Name | ENSEMBL ID |
|---|---|
| ***DEFB103*** | |
| Armadillo | ENSDNOG00000032237 |
| Dog | ENSCAFG00000032247 |
| Dolphin | ENSTTRG00000002707 |
| Elephant | ENSLAFG00000010274 |
| Gibbon | ENSNLEG00000001838 |
| Horse | ENSECAG00000007143 |
| Human | ENSG00000177243 |
| Macaque | ENSMMUG00000007466 |
| Microbat | ENSMLUG00000005572 |
| Pig | ENSSSCG00000020934 |
| Rabbit | ENSOCUG00000026146 |
| Mouse (*Defb14*) | ENSMUSG00000046354 |
| Rat (*Defb14*) | ENSRNOG00000032304 |

***DEFB106***

| | |
|---|---|
| Armadillo | ENSDNOG00000019069 |
| Gibbon | ENSNLEG00000000404 |
| Human | ENSG00000186579 |
| Macaque | ENSMMUG00000007474 |
| Megabat | ENSPVAG00000012936 |
| Microbat | ENSMLUG00000030566 |

***DEFB115***

| | |
|---|---|
| Alpaca | ENSVPAG00000007006 |
| Gibbon | ENSNLEG00000009563 |
| Human | ENSG00000215547 |
| Megabat | ENSPVAG00000002309 |
| Pig | ENSSSCG00000007216 |
| Mouse (*Defb28*) | ENSMUSG00000074679 |
| Rat (*Defb28*) | ENSRNOG00000036900 |

***DEFB116***

| | |
|---|---|
| Alpaca | ENSVPAG00000000791 |
| Dog | ENSCAFG00000025079 |
| Elephant | ENSLAFG00000032181 |
| Gibbon | ENSNLEG00000009565 |
| Human | ENSG00000215545 |
| Macaque | ENSMMUG00000031231 |
| Megabat | ENSPVAG00000008344 |
| Microbat | ENSMLUG00000029317 |
| Pig | ENSSSCG00000007215 |
| Mouse (*Defb29*) | ENSMUSG00000044249 |
| Rat (*Defb29*) | ENSRNOG00000023195 |

***DEFB118***

| | |
|---|---|
| Armadillo | ENSDNOG00000000764 |
| Gibbon | ENSNLEG00000009566 |
| Human | ENSG00000131068 |
| Macaque | ENSMMUG00000008798 |
| Megabat | ENSPVAG00000008251 |
| Mouse (*Defb21*) | ENSMUSG00000056544 |
| Rat (*Defb21*) | ENSRNOG00000023154 |
| Rabbit | ENSOCUG00000017296 |

***DEFB119***

| | |
|---|---|
| Armadillo | ENSDNOG00000043181 |
| Dog | ENSCAFG00000006989 |
| Gibbon | ENSNLEG00000009568 |
| Human | ENSG00000180483 |

| | |
|---|---|
| Macaque | ENSMMUG00000008796 |
| Megabat | ENSPVAG00000008252 |
| Pig | ENSSSCG00000007221 |
| ***DEFB121*** | |
| Alpaca | ENSVPAG00000004067 |
| Armadillo | ENSDNOG00000011801 |
| Dog | ENSCAFG00000025021 |
| Gibbon | ENSNLEG00000009569 |
| Human | ENSG00000204548 |
| Macaque | ENSMMUG00000017530 |
| Microbat | ENSMLUG00000011577 |
| Pig | ENSSSCG00000028629 |
| ***DEFB122*** | |
| Alpaca | ENSVPAG00000004068 |
| Cat | ENSFCAG00000014654 |
| Dog | ENSCAFG00000006990 |
| Elephant | ENSLAFG00000027923 |
| Horse | ENSECAG00000015750 |
| Human | ENSG00000204547 |
| Macaque | ENSMMUG00000017531 |
| Megabat | ENSPVAG00000008253 |
| Microbat | ENSMLUG00000005509 |
| Pig | ENSSSCG00000007219 |
| Rabbit | ENSOCUG00000001431 |
| Rat (*Defb27*) | ENSRNOG00000036896 |
| Mouse (*Defb45*) | ENSMUSG00000062124 |
| ***DEFB123*** | |
| Alpaca | ENSVPAG00000004069 |
| Armadillo | ENSDNOG00000001353 |
| Cat | ENSFCAG00000014655 |
| Dog | ENSCAFG00000030438 |
| Dolphin | ENSTTRG00000005795 |
| Elephant | ENSLAFG00000000115 |
| Gibbon | ENSNLEG00000009574 |
| Horse | ENSECAG00000015886 |
| Human | ENSG00000180424 |
| Macaque | ENSMMUG00000005115 |
| Megabat | ENSPVAG00000008254 |
| Microbat | ENSMLUG00000026134 |
| Pig | ENSSSCG00000007226 |
| Rabbit | ENSOCUG00000026775 |

| | |
|---|---|
| Mouse (*Defb36*) | ENSMUSG00000044863 |
| Rat (*Defb36*) | ENSRNOG00000007558 |
| ***DEFB124*** | |
| Alpaca | ENSVPAG00000006088 |
| Armadillo | ENSDNOG00000032850 |
| Cat | ENSFCAG00000014658 |
| Dog | ENSCAFG00000024871 |
| Dolphin | ENSTTRG00000005806 |
| Elephant | ENSLAFG00000000117 |
| Gibbon | ENSNLEG00000009576 |
| Horse | ENSECAG00000017028 |
| Human | ENSG00000180383 |
| Macaque | ENSMMUG00000005116 |
| Megabat | ENSPVAG00000008255 |
| Microbat | ENSMLUG00000029687 |
| Pig | ENSSSCG00000030733 |
| Rabbit | ENSOCUG00000009984 |
| Mouse (*Defb25*) | ENSMUSG00000074678 |
| Rat (*Defb25*) | ENSRNOG00000036895 |
| ***DEFB125*** | |
| Alpaca | ENSVPAG00000000439 |
| Dog | ENSCAFG00000025097 |
| Dolphin | ENSTTRG00000000944 |
| Elephant | ENSLAFG00000014297 |
| Gibbon | ENSNLEG00000018267 |
| Horse | ENSECAG00000012067 |
| Human | ENSG00000178591 |
| Macaque | ENSMMUG00000012756 |
| Megabat | ENSPVAG00000002308 |
| Microbat | ENSMLUG00000028986 |
| Pig | ENSSSCG00000007217 |
| Rabbit | ENSOCUG00000010206 |
| Mouse (*Defb26*) | ENSMUSG00000074680 |
| Rat (*Defb26*) | ENSRNOG00000053114 |
| ***DEFB126*** | |
| Alpaca | ENSVPAG00000000440 |
| Dog | ENSCAFG00000025122 |
| Elephant | ENSLAFG00000017421 |
| Gibbon | ENSNLEG00000009561 |
| Horse | ENSECAG00000011927 |
| Human | ENSG00000125788 |

| | |
|---|---|
| Macaque | ENSMMUG00000012757 |
| Microbat | ENSMLUG00000014906 |
| Mouse (*Defb22*) | ENSMUSG00000027468 |
| Rat (*Defb22*) | ENSRNOG00000007525 |
| ***DEFB127*** | |
| Alpaca | ENSVPAG00000000444 |
| Armadillo | ENSDNOG00000035342 |
| Dog | ENSCAFG00000006987 |
| Dolphin | ENSTTRG00000000942 |
| Gibbon | ENSNLEG00000009555 |
| Human | ENSG00000088782 |
| Macaque | ENSMMUG00000012758 |
| Megabat | ENSPVAG00000015966 |
| Microbat | ENSMLUG00000014909 |
| Rabbit | ENSOCUG00000002723 |
| ***DEFB128*** | |
| Alpaca | ENSVPAG00000000447 |
| Armadillo | ENSDNOG00000025888 |
| Dog | ENSCAFG00000006984 |
| Dolphin | ENSTTRG00000000941 |
| Elephant | ENSLAFG00000017621 |
| Gibbon | ENSNLEG00000009554 |
| Horse | ENSECAG00000011913 |
| Human | ENSG00000185982 |
| Macaque | ENSMMUG00000012759 |
| Megabat | ENSPVAG00000015964 |
| Microbat | ENSMLUG00000003259 |
| Pig | ENSSSCG00000007214 |
| Rabbit | ENSOCUG00000017788 |
| Mouse (*Defb20*) | ENSMUSG00000049560 |
| Rat (*Defb20*) | ENSRNOG00000023384 |
| ***DEFB129*** | |
| Alpaca | ENSVPAG00000000448 |
| Armadillo | ENSDNOG00000011103 |
| Dog | ENSCAFG00000006980 |
| Dolphin | ENSTTRG00000000725 |
| Elephant | ENSLAFG00000017430 |
| Gibbon | ENSNLEG00000009553 |
| Horse | ENSECAG00000009931 |
| Human | ENSG00000125903 |
| Macaque | ENSMMUG00000017283 |

| | |
|---|---|
| Megabat | ENSPVAG00000007213 |
| Microbat | ENSMLUG00000014911 |
| Pig | ENSSSCG00000007218 |
| Rabbit | ENSOCUG00000010202 |
| Mouse (*Defb23*) | ENSMUSG00000074681 |
| Rat (*Defb23*) | ENSRNOG00000023477 |
| ***DEFB132*** | |
| Alpaca | ENSVPAG00000000449 |
| Human | ENSG00000186458 |
| Gibbon | ENSNLEG00000009551 |
| Macaque | ENSMMUG00000017285 |
| Megabat | ENSPVAG00000010530 |
| Microbat | ENSMLUG00000003579 |

**Table A.3 Genomic co-ordinates for the bovine β-defensin 5kb promoters downloaded**

| Gene | Chromosome | Co-ordinates (UMD3.1.1/bosTau8) | Orientation |
|---|---|---|---|
| *DEFB132* | 13 | 61298937-61303936 | Reverse |
| *DEFB129* | 13 | 61316739-61321738 | Reverse |
| *DEFB128* | 13 | 61322495-61327494 | Forward |
| *DEFB127* | 13 | 61338920-61343919 | Reverse |
| *DEFB126* | 13 | 61353550-61358549 | Reverse |
| *DEFB125* | 13 | 61377488-61382487 | Reverse |
| *DEFB115* | 13 | 61411164-61416163 | Forward |
| *DEFB116* | 13 | 61468036-61473035 | Reverse |
| *DEFB118* | 13 | 61507921-61512920 | Forward |
| *DEFB119* | 13 | 61533380-61538379 | Reverse |
| *DEFB121* | 13 | 61551770-61556769 | Reverse |
| *DEFB122* | 13 | 61577404-61582403 | Reverse |
| *DEFB123* | 13 | 61579483-61584482 | Forward |
| *DEFB124* | 13 | 61615457-61620456 | Reverse |
| *DEFB103* | 27 | 4899618-4904617 | Reverse |
| *DEFB106* | 27 | 4954346-4956823 | Reverse |

**Table A.4 Chromosomal co-ordinates for sequences downloaded for MULAN alignment**

| Species | Chromosome | *DEFB132-128* | *DEFB127-125* | *DEFB115-116* | *DEFB117-121* | *DEFB122-124* |
|---|---|---|---|---|---|---|
| Cow | 13 | 61292225-61331424 | 61331425-61415163 | 61415164-61495924 | 61495925-61556646 | 61556647-61620456 |
| Dog | 24 | 20586719-20669770 | 20669771-20762474 | 20762475-20862392 | 20862393-20933784 | 20933785-20994706 |
| Little brown bat | GL429827 | 171769-1777748 | 1777749-1879680 | 1879681-1907783 | 1907784-1982306 | 1982307-2028115 |
| Human | 20 | 174024-264306 | 82724-174023 | 29841877-29941876 | 29941877-30003672 | 30003673-30063811 |
| Rabbit | 4 | 7897921-7925147 | 7844480-7897920 | 7811694-7844479 | 7756210-7811693 | 7706352-7756209 |

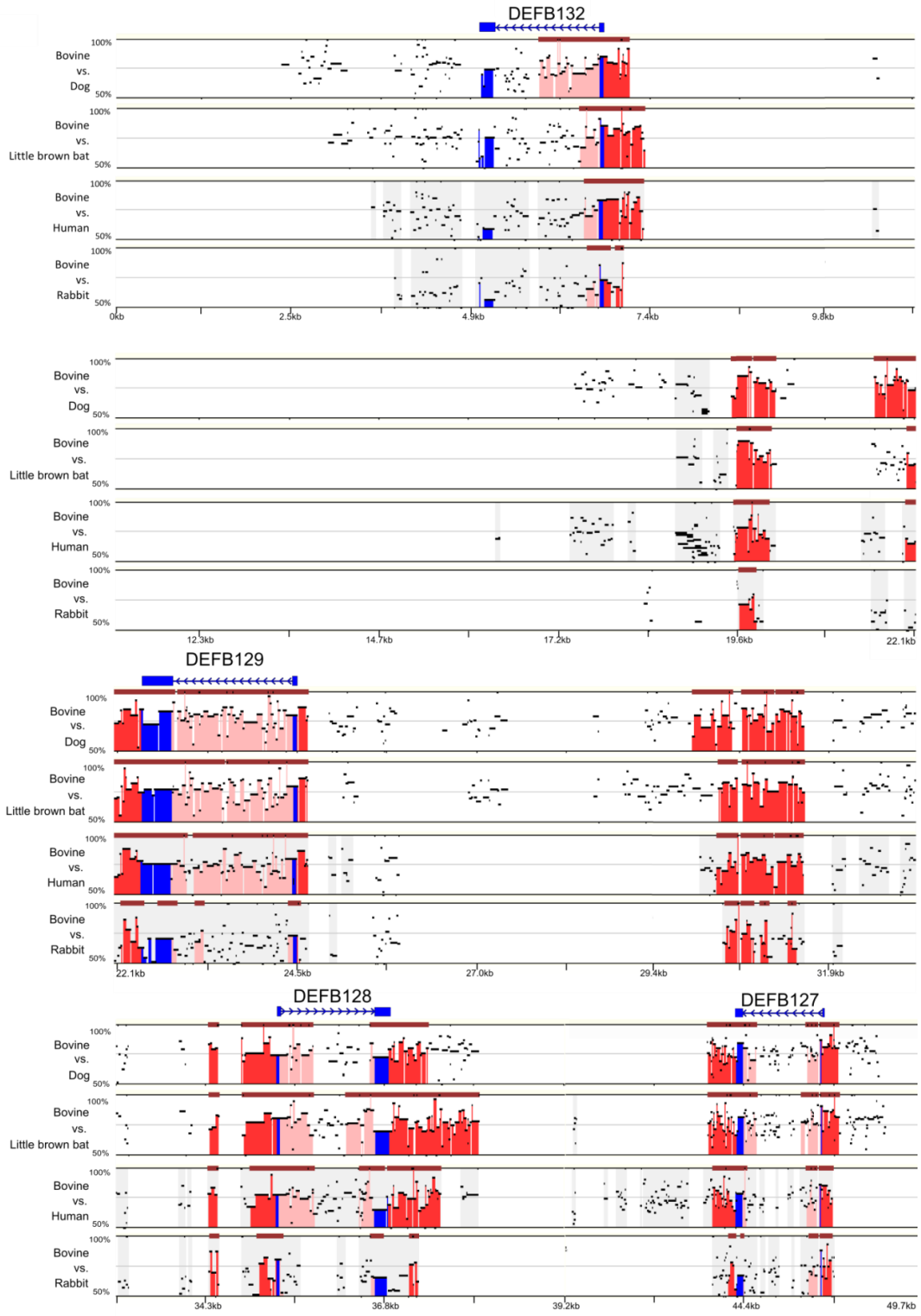


**Figure A.1 Stacked pairwise alignment of β-defensin syntenic cluster B, genes DEFB132 to DEFB125 between bovine and each of dog, little brown bat, human and rabbit.**
Genomic sequences were downloaded from the UCSC browser and aligned using a threaded blockset algorithm within the online MULAN software tool. The ECRs shown are regions of at least 100bp with a minimum of 70% conservation among the 5 species. Following Ovcharenko et al. (2004), an increased threshold of 350bp with >77% similarity was taken to be indicative of a core enhancer. Core enhancers have been shown to be highly conserved among vertebrates and are more likely to be functional. Intergenic regions with this level of conservation among 4 species are indicated with a green box.

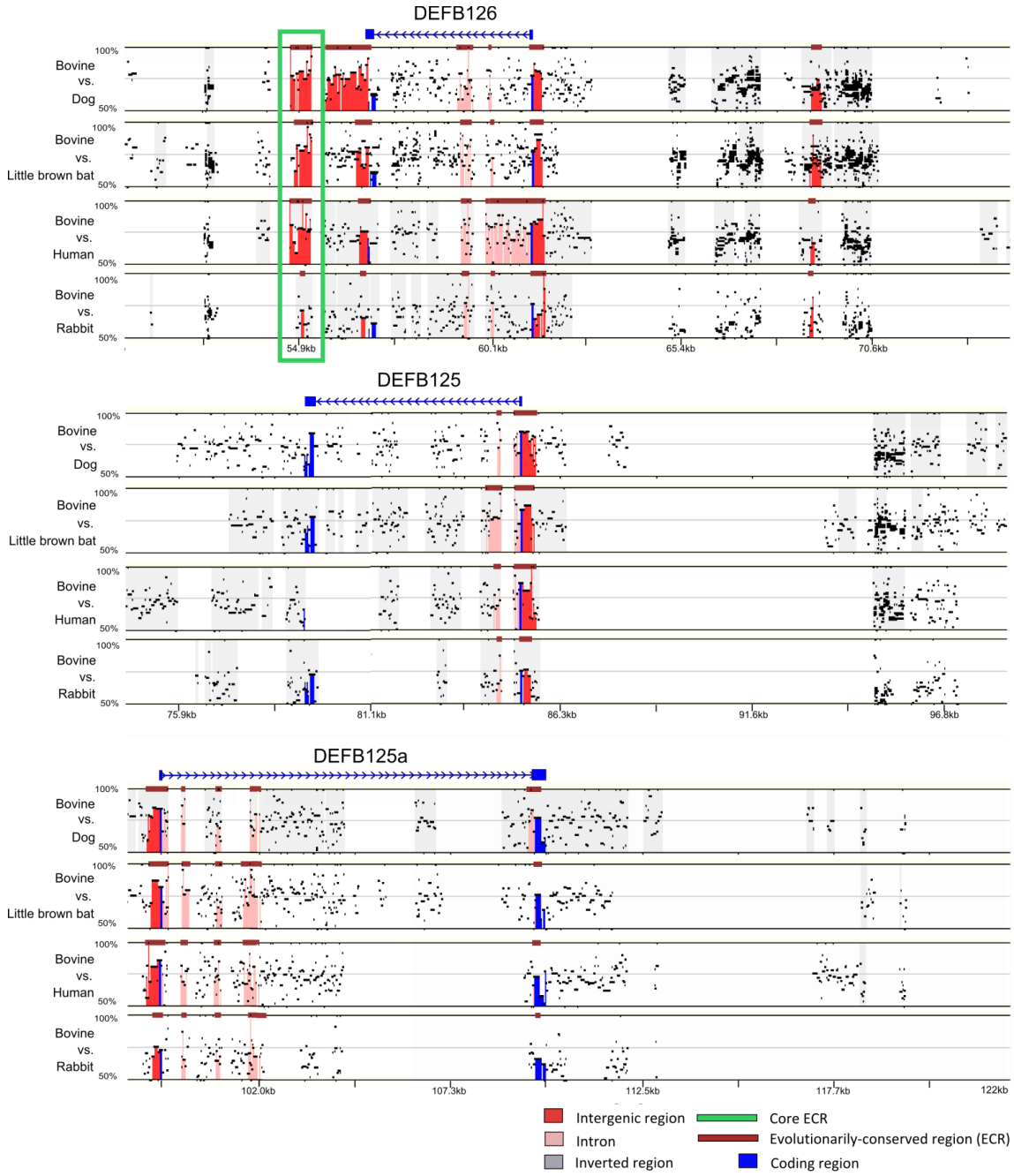
DEFB126
Bovine vs. Dog
Bovine vs. Little brown bat
Bovine vs. Human
Bovine vs. Rabbit
100%
50%
54.9kb
60.1kb
65.4kb
70.6kb
DEFB125
75.9kb
81.1kb
86.3kb
91.6kb
96.8kb
DEFB125a
102.0kb
107.3kb
112.5kb
117.7kb
122kb
Intergenic region
Intron
Inverted region
Core ECR
Evolutionarily-conserved region (ECR)
Coding region

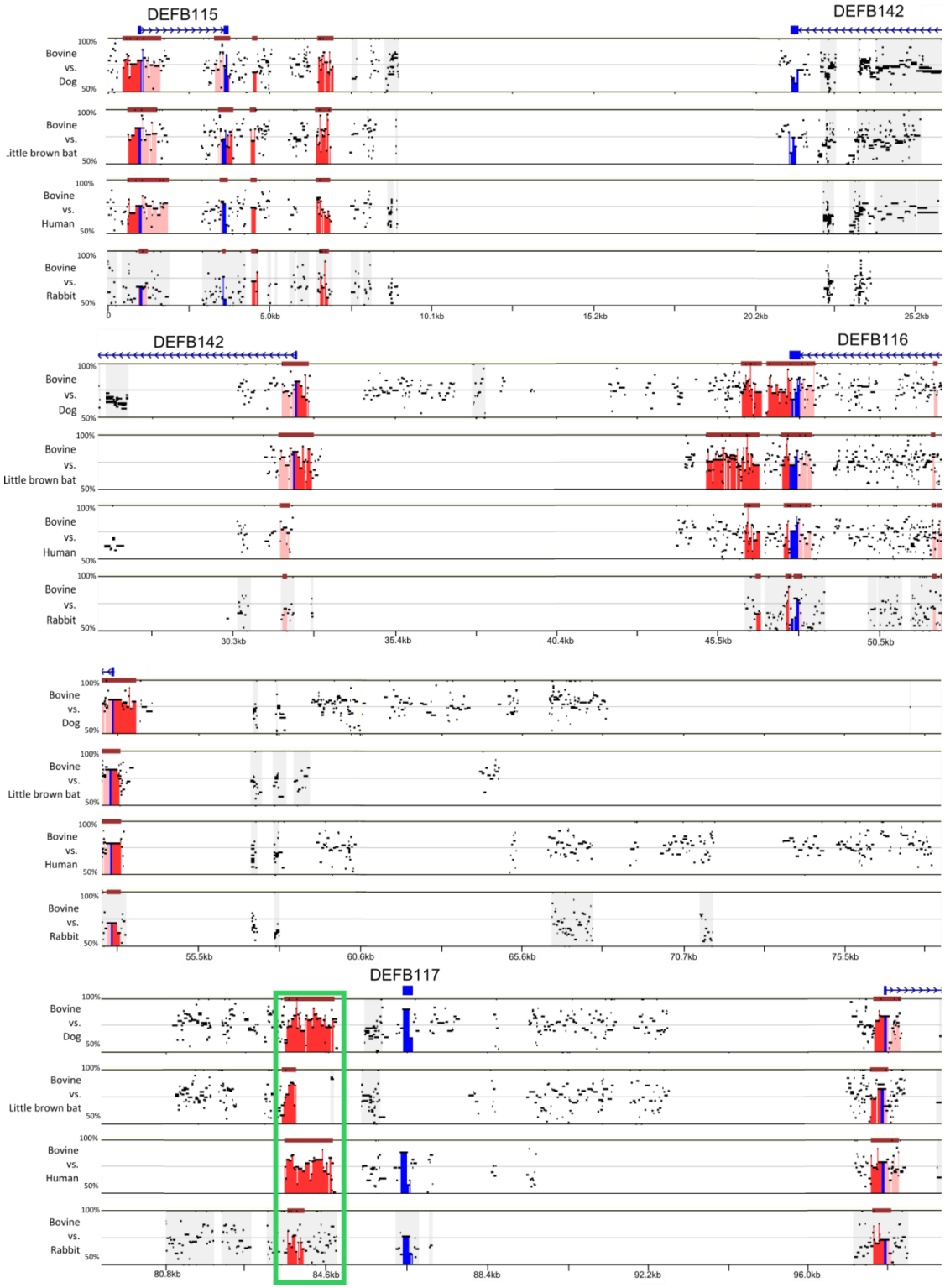


**Figure A.2 Stacked pairwise alignment of β-defensin syntenic cluster B, genes DEFB115 to DEFB124 between bovine and each of dog, little brown bat, human and rabbit**

Genomic sequences were downloaded from the UCSC browser and aligned using a threaded blockset algorithm within the online MULAN software tool. The ECRs shown are regions of at least 100bp with a minimum of 70% conservation among the 5 species. Following Ovcharenko et al. (2004), an increased threshold of 350bp with >77% similarity was taken to be indicative of a core enhancer. Core enhancers have been shown to be highly conserved among vertebrates and are more likely to be functional. Intergenic regions with this level of conservation among 4 species are indicated with a green box.

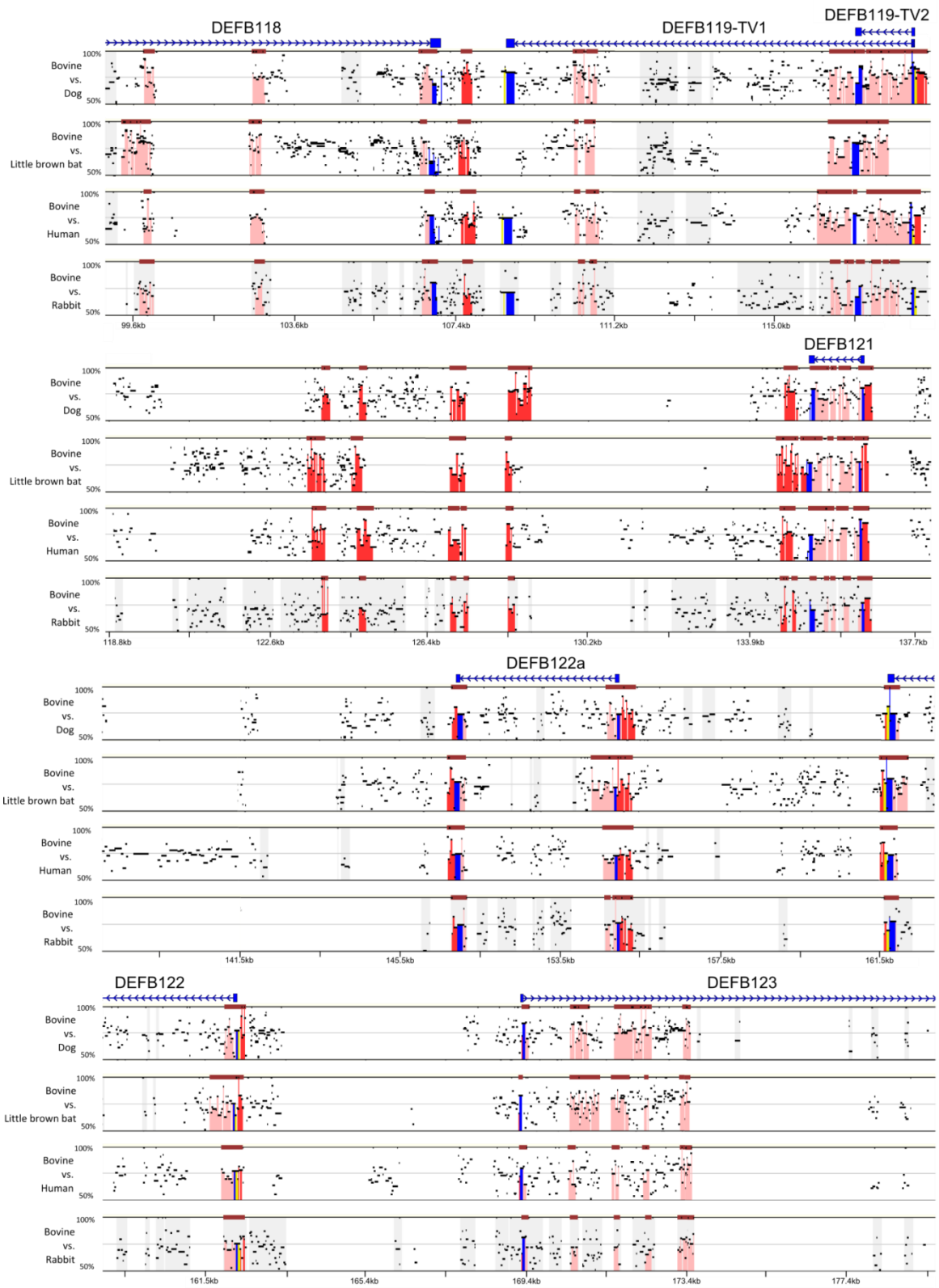
DEFB118
DEFB119-TV1
DEFB119-TV2
Bovine vs. Dog
Bovine vs. Little brown bat
Bovine vs. Human
Bovine vs. Rabbit
100%
50%
99.6kb
103.6kb
107.4kb
111.2kb
115.0kb
DEFB121
118.8kb
122.6kb
126.4kb
130.2kb
133.9kb
137.7kb
DEFB122a
141.5kb
145.5kb
153.5kb
157.5kb
161.5kb
DEFB122
DEFB123
161.5kb
165.4kb
169.4kb
173.4kb
177.4kb

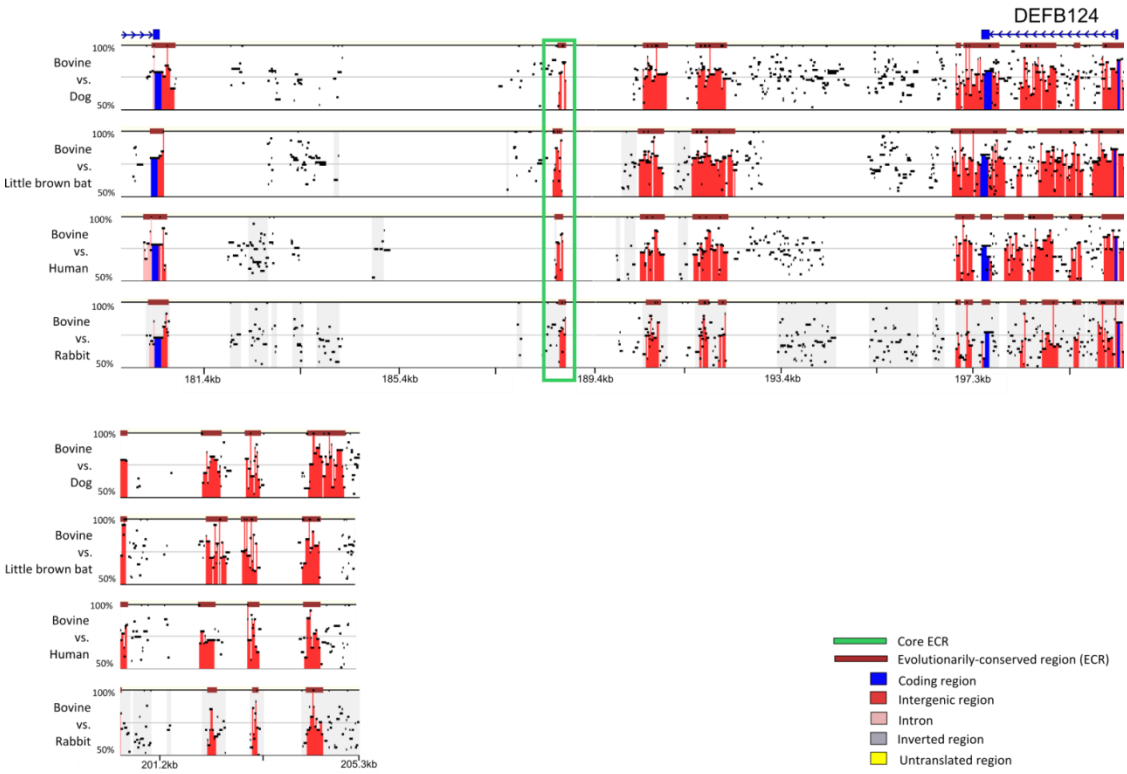


**Table A.5 Accession numbers of peptides/proteins used for alignments in this thesis**

| Peptide/Protein Name | Species | Accession Number |
|---|---|---|
| β-defensin 103A precursor | *Bos taurus* | XP_002698677.1 |
| | *Equus caballus* | XP_003364293.1 |
| | *Pan troglodytes* | NP_001123222.1 |
| β-defensin 103B precursor | *Bos taurus* | NP_001108334.1 |
| β-defensin 103 precursor | *Homo sapiens* | NP_001075020.1 |
| | *Capra hircus* | AHX83361.1 |
| | *Sus scrofa* | NP_999609.1 |
| | *Canis lupus familiaris* | NP_001123452.1 |
| β-defensin 106 precursor | *Homo sapiens* | NP_689464.1 |
| | *Pan troglodytes* | NP_001123228.1 |
| | *Canis lupus familiaris* | DQ011975.1 |
| IL-17A precursor | *Bos taurus* | NP_001008412.1 |
| | *Homo sapiens* | NP_002181.1 |
| IL-22 precursor | *Bos taurus* | NP_001091849.1 |
| | *Homo sapiens* | NP_065386.1 |

**Table A.6 Accession numbers of genes used for alignments in this thesis**

| Gene Name | Gene Symbol | Species | Accession Number |
|---|---|---|---|
| β-defensin 1/enteric β-defensin | *DEFB1 /EBD* | *Bos taurus* | NM_175703 |
| β-defensin 3/bovine neutrophil β-defensin 3 | *DEFB3 /BNBD3* | *Bos taurus* | NM_001282581.1 |
| β-defensin 4a/bovine neutrophil β-defensin 4 | *DEFB4A /BNBD4* | *Bos taurus* | NM_174775.1 |
| β-defensin 5/bovine neutrophil β-defensin 5 | *DEFB5 /BNBD5* | *Bos taurus* | NM_001115084.1 |
| β-defensin 7/bovine neutrophil β-defensin 7 | *DEFB7 /BNBD7* | *Bos taurus* | NM_001102362.2 |
| β-defensin 10/bovine neutrophil β-defensin 10 | *DEFB10 /BNBD10* | *Bos taurus* | NM_001130761.1 |
| Lingual antimicrobial peptide | *LAP* | *Bos taurus* | S76297.1 |
| Tracheal antimicrobial peptide | *TAP* | *Bos taurus* | NM_174776.1 |
| β-defensin 103A | *DEFB103A* | *Bos taurus* | XM_002698631.3 |
| β-defensin 103B | *DEFB103B* | *Bos taurus* | NM_001114862.1 |

**Table A.7 Primer sequences and conditions for qPCR analysis of FRT samples using GoTaq master mix**

| Gene Symbol | Gene Name | Accession Number | | Primer Sequence | Amplicon length (bp) | Annealing temp. (°C) | Primer conc. (nM) | Efficiency (%) |
|---|---|---|---|---|---|---|---|---|
| *DEFB103* | β-defensin 103 | NM_001114862 | F- | TGTTCCAGGCAACGGCG | 91 | 60 | 300 | 96 |
| | | | R- | TGGAAGGCAGCCAATCAGAG | | | | |
| *DEFB106* | β-defensin 106 | | F- | CCCCAGCCAGGAGTGGATT | 125 | 58 | 100 | 100 |
| | | | R- | TGCCACACAGCATTTCAGAGACTT | | | | |
| e*DEFB4A* | β-defensin genes representing *DEFB4A* expansion | | F- | AGGCTCCATCACCTGCTCCTC | 156 | 65 | 100 | 100 |
| | | | R- | ACAGGTGCCAATCTGTCTCATGC | | | | |
| *MRPS6* | Mitochondrial ribosomal protein S6 | NM_001040584.2 | F- | CGCACGCTTCCCTATAAGAT | 176 | 60 | 800 | 91 |
| | | | R- | TTCACTTCCTGGGTCAGAGG | | | | |
| *RPL13A* | Ribosomal protein L13A | NM_001076998.2 | F- | CACCACCCTATGACAAGAAAAAG | 222 | 60 | 500 | 98 |
| | | | R- | TTTCGGCCTGCTTCCGTA | | | | |
| *RPS9* | Ribosomal protein S9 | NM_001101152.2 | F- | GCGTCTGTTCGAAGGTAATGC | 161 | 60 | 800 | 93 |
| | | | R- | AAGTCGATGTGCTTCTGCGA | | | | |
| *SF3A1* | Splicing factor 3A, subunit 1 | NM_001081510.1 | F- | CAGGTCTCCGTCATCAAGGT | 89 | 60 | 600 | 92 |
| | | | R- | TTGATGAAAATGCCCTCGTACTG | | | | |
| *TUBA1B* | Tubulin, alpha1b | NM_001114856.1 | F- | GCTTGTCGGGGACAGTAACC | 79 | 60 | 300 | 93 |
| | | | R- | ACTCACGCATGGTGGCTACG | | | | |

**Table A.8 Primer sequences and conditions for qPCR analysis of endometrial stromal cell samples using PowerUp Master Mix**

| Gene Symbol | Gene Name | Gene Accession Number | | Primer Sequence | Amplicon length (bp) | Annealing temp. (°C) | Primer Conc. (nM) | Efficiency (%) |
|---|---|---|---|---|---|---|---|---|
| *CYP24A1* | Cytochrome P450, family 24, subfamily A, polypeptide 1 | NM_001191417.1 | F- | GAAGACTGGCAGAGGGTCAG | 97 | 60 | 300 | 98 |
| | | | R- | CAGCCAAGACCTCGTTGATT | | | | |
| *DDX58* | DExD/H-Box Helicase 58 | XM_580928.8 | F- | TCCCAGCAATGAGAACGCTA | 219 | 60 | 400 | 106 |
| | | | R- | GGGAGCGTCATTCCCATTGT | | | | |
| *DEFB103* | β-defensin 103 | NM_001114862 | F- | TGTTCCAGGCAACGGCG | 91 | 65 | 400 | 109 |
| | | | R- | TGGAAGGCAGCCAATCAGAG | | | | |
| *eDEFB4A* | β-defensin genes representing *DEFB4A* expansion | | F- | AGGCTCCATCACCTGCTCCTC | 156 | 64 | 400 | 103 |
| | | | R- | ACAGGTGCCAATCTGTCTCATGC | | | | |
| *IFIH1* | Interferon Induced With Helicase C Domain 1 | XM_010826464.2 | F- | AGCCCATGACACAGAATGAACA | 191 | 69 | 400 | 96 |
| | | | R- | CTCATCAGCTCTGGCTCGAC | | | | |
| *IFNB1* | Interferon-beta | NM_174350.1 | F- | AGAAGCAAAACTCCACTACGGA | 106 | 60 | 300 | 101 |
| | | | R- | CAGGCACACCTGTCGTACTC | | | | |
| *IL8* | Interleukin 8 | NM_173925.2 | F- | TGCTCTCTGCAGCTCTGTGT | 139 | 60 | 300 | 97 |
| | | | R- | TGTGGCCCACTCTCAATAACT | | | | |
| *IL22RA1* | IL-22 receptor, subunit alpha 1 | NM_001034311.2 | F- | CTCCCAGCTCCCTGAATGTC | 331 | 60 | 700 | 92 |
| | | | R- | AGAGCTCCCTGAGGTGCATA | | | | |
| *MB21D1* | Mab-21 Domain Containing 1 | XM_001251098.6 | F- | ACTTCTGATTAGAAAACCTAGAGAAATATCTGTGG | 207 | 60 | 400 | 103 |
| | | | R- | CGCCATGTTTCTTCTTGGAAAAGACT | | | | |
| *MRPS6* | Mitochondrial ribosomal protein S6 | NM_001040584.2 | F- | CGCACGCTTCCCTATAAGAT | 176 | 61 | 400 | 95 |
| | | | R- | TTCACTTCCTGGGTCAGAGG | | | | |
| *RPL13A* | Ribosomal protein L13A | NM_001076998.2 | F- | CACCACCCTATGACAAGAAAAAG | 222 | 61 | 400 | 92 |
| | | | R- | TTTCGGCCTGCTTCCGTA | | | | |
| *RPS9* | Ribosomal protein S9 | NM_001101152.2 | F- | GCGTCTGTTCGAAGGTAATGC | 161 | 61 | 400 | 91 |
| | | | R- | AAGTCGATGTGCTTCTGCGA | | | | |
| *SF3A1* | | NM_001081510.1 | F- | CAGGTCTCCGTCATCAAGGT | 89 | 61 | 400 | 103 |

| | | | | | | | | |
|---|---|---|---|---|---|---|---|---|
| | Splicing factor 3A, subunit 1 | | R- | TTGATGAAAATGCCCTCGTACTG | | | | |
| *TMEM173* | Transmembrane protein 173 | NM_001046357 | F-<br>R- | AGGTAGAAGATGCCTCACTCCA<br>CACCAGACAGGCACTTAGCA | 102 | 61 | 300 | 101 |
| *TLR3* | Toll-like receptor 3 | NM_001008664.1 | F-<br>R- | CAGCTCCAACTGGAGAACCT<br>ACCCAGGAGAGAACTCTTTGATT | 148 | 63 | 400 | 102 |
| *TUBA1B* | Tubulin, alpha1b | NM_001114856.1 | F-<br>R- | GCTTGTCGGGGACAGTAACC<br>ACTCACGCATGGTGGCTACG | 79 | 61 | 400 | 105 |